

71-9197

SAFETY ANALYSIS REPORT

FOR THE

NUPAC 10/140MB SHIPPING CASK

AUGUST, 1985

Prepared by: Nuclear Packaging, Inc.  
1010 South 336th Street  
Federal Way, WA 98003

25625

## NOTICE

This Safety Analysis Report for the NuPac Model 10/140MB Shipping Cask and all associated drawings including amendments thereto are the property of Nuclear Packaging, Inc., Federal, Washington. This material is being made available for the purpose of obtaining required certifications from the U. S. Nuclear Regulatory Commission and to enable others to register with the U.S.N.R.C. as a user of this package. No other use of this material is authorized unless by written consent of Nuclear Packaging, Inc. Parties who may come into possession of this material are cautioned that the information is not to be reproduced in any form without the prior written consent of Nuclear Packaging, Inc.

Unpublished - All rights reserved under law.



## TABLE OF CONTENTS

	<u>Page</u>
1.0 GENERAL INFORMATION	1-1
1.1 Introduction	1-1
1.2 Package Description	1-1
1.2.1 Packaging	1-1
1.2.1.1 General Description	1-1
1.2.1.2 Materials of Construction, Dimensions and Fabricating Methods	1-2
1.2.1.3 Containment Vessel	1-2
1.2.1.4 Neutron Absorbers	1-3
1.2.1.5 Package Weight	1-3
1.2.1.6 Receptacles	1-3
1.2.1.7 Containment Penetrations	1-3
1.2.1.8 Tiedowns	1-4
1.2.1.9 Lifting Devices	1-4
1.2.1.10 Pressure Relief System	1-4
1.2.1.11 Heat Dissipation	1-4
1.2.1.12 Coolants	1-4
1.2.1.13 Protrusions	1-4
1.2.1.14 Shielding	1-5
1.2.2 Operational Features	1-5
1.2.3 Contents of Packaging	1-5
APPENDIX 1.3.1	1-3-1-i

	<u>Page</u>
2.0 STRUCTURAL EVALUATION	2-1
2.1 Structural Design	2-1
2.1.1 Discussion	2-1
2.1.2 Design Criteria	2-1
2.1.2.1 Basic Design Criteria	2-1
2.1.2.2 Miscellaneous Structural Failure Modes	2-5
2.1.2.3 Overpack Design Criteria	2-26
2.2 Weights and Centers of Gravity	2-32
2.3 Mechanical Properties of Materials	2-32
2.4 General Standards for All Packages	2-37
2.4.1 Minimum Package Size	2-37
2.4.2 Tamper-proof Feature	2-37
2.4.3 Positive Closure	2-37
2.4.4. Chemical and Galvanic Reactions	2-37
2.5 Lifting and Tie-Down Standards for All Packages	2-38
2.5.1 Lifting Devices	2-38
2.5.1.1 Primary Lid Lifting Lugs	2-38
2.5.1.2 Secondary Lid Lifting Lug	2-42
2.5.2 Tie-down Devices	2-45

	<u>Page</u>
2.6 Normal Conditions of Transport	2-55
2.6.1 Heat	2-55
2.6.2 Cold	2-55
2.6.3 Reduced External Pressure	2-70
2.6.4 Increased External Pressure	2-73
2.6.5 Vibration	2-73
2.6.6 Water Spray	2-73
2.6.7 Free Drop	2-73
2.6.7.1 Flat End Drop	2-74
2.6.7.2 Oblique Impact	2-100
2.6.7.3 Flat Side Impact	2-111
2.6.8 Corner Drop	2-118
2.6.9 Compression	2-118
2.6.10 Penetration	2-118
2.7 Hypothetical Accident Conditions	2-119
2.7.1 Free Drop	2-119
2.7.1.1 Flat End Drop	2-120
2.7.1.2 Oblique Impact	2-144
2.7.1.3 Flat Side Impact	2-165
2.7.2 Puncture	2-183
2.7.2.1 Side Wall Puncture Resistance	2-184
2.7.2.2 Cask Lid Puncture Resistance	2-186
2.7.2.3 Overpack Puncture Resistance	2-187

	<u>Page</u>
2.7.3 Thermal	2-190
2.7.3.1 Summary of Pressures and Temperatures	2-190
2.7.3.2 Differential Thermal Expansion	2-190
2.7.3.3 Stress Calculations	2-190
2.7.3.4 Comparison with Allowable Stresses	2-190
2.7.4 Immersion - Fissile Material	2-191
2.7.5 Immersion - All Packages	2-191
2.7.6 Summary of Damage	2-192
APPENDIX 2.10.1 Stability and Buckling Design Criteria	2-10-1-i
2.10.1 Stability and Buckling Design Criteria	2-10-1-1
2.10.1.1 Criteria Definition	2-10-1-2
2.10.1.2 Background	2-10-1-5
2.10.1.3 Criteria Rationale	2-10-1-9
2.10.1.4 Safety Analysis	2-10-1-11
2.10.1.5 Reference	2-10-1-21
APPENDIX 2.10.2 ANSYS Program Description	2-10-2-i

	<u>Page</u>
APPENDIX 2.10.3      Tiedown Lug Loads and Stress Analysis	2-10-3-i
2.10.3.1      Tiedown Loads Analysis	2-10-3-1
2.10.3.2      Finite Element Analysis	2-10-3-3
2.10.3.3      Tiedown Lug Weld Stress Calculations	2-10-3-12
2.10.3.4      Tiedown Lug Weld Ultimate Strength	2-10-3-15
APPENDIX 2.10.4      EnviroLock <sup>tm</sup> Structural Analysis	2-10-4-i
2.10.4.1      Body Section	2-10-4-1
2.10.4.2      Lid Structure	2-10-4-7
2.10.4.3      Clamping Bolt	2-10-4-11
APPENDIX 2.10.5      Description of NuPac Proprietary Drop Programs	2-10-5-i
2.10.5.1      Overpack Deformation Behavior	2-10-5-1
2.10.5.2      Oblique Impact Dynamic Analysis	2-10-5-10
2.10.5.3      Sample Program Input and Output	2-10-5-28
2.10.5.4      NuPac Computer Code Quality Assurance	2-10-5-46

	<u>Page</u>
APPENDIX 2.10.6      Cask Wall Buckling Analysis	2-10-6-i
2.10.6.1    Finite Element Analysis	2-10-6-1
2.10.6.2    Normal Condition Stress Results	2-10-6-5
2.10.6.3    Accident Condition Stress Results	2-10-6-6
2.10.6.4    Normal Condition Buckling Consideration	2-10-6-7
2.10.6.5    Hypothetical Accident Condition Buckling Considerations	2-10-6-7
2.10.6.6    Lead Slump	2-10-6-8
 APPENDIX 2.10.7      End Drop Lid Analysis	 2-10-7-i
 APPENDIX 2.10.8      Lid Puncture Analysis	 2-10-8-i
 APPENDIX 2.10.9      ANSYS ANALYSIS OUTPUT (Microfiche)	 2-10-9-i
 3.0    THERMAL EVALUATION	 3-1
3.1    Discussion	3-1
3.2    Summary of Thermal Properties of Materials	3-2
3.3    Technical Specifications of Components	3-4
3.4    Thermal Evaluation For Normal Conditions of Transport	3-5
3.4.1    Thermal Model	3-6

	<u>Page</u>
3.4.1.1 Analytical Model	3-6
3.4.1.2 Test Model	3-8
3.4.2 Maximum Temperatures	3-9
3.4.3 Minimum Temperatures	3-11
3.4.4 Maximum Normal Condition	
Internal Pressure	3-11
3.4.5 Thermal Stresses	3-14
3.4.6 Evaluation of Package Performance	
For Normal Conditions of Transport	3-14
3.5 Hypothetical Accident Thermal Evaluation	3-15
3.5.1 Thermal Model	3-15
3.5.1.1 Analytical Model	3-15
3.5.1.2 Test Model	3-16
3.5.2 Package Conditions and Environment	3-16
3.5.3 Package Temperatures	3-17
3.5.4 Maximum Internal Pressure	3-19
3.5.5 Maximum Thermal Stresses	3-19
3.5.6 Evaluation of Package Performance	
for the Hypothetical Accident	
Thermal Conditions	3-20
APPENDIX 3.6	3-6-i
3.7 References	3-28

	<u>Page</u>
4.0 CONTAINMENT	4-1
4.1 Containment Boundary	4-1
4.1.1 Containment Vessel	4-1
4.1.2 Containment Penetrations	4-1
4.1.3 Seals and Welds	4-1
4.1.4 Closure	4-2
4.2 Requirements for Normal Conditions of Transport	4-2
4.2.1 Release of Radioactive Material	4-3
4.2.2 Pressurization of Containment Vessel	4-3
4.2.3 Coolant Contamination	4-3
4.2.4 Coolant Loss	4-3
4.3 Containment Requirements for the Hypothetical Accident Conditions	4-3
4.3.1 Fission Gas Products	4-4
4.3.2 Releases of Contents	4-4
5.0 SHIELDING EVALUATION	5-1
5.1 Discussion and Results	5-1
5.2 Source Specification	5-3
5.2.1 Gamma Source	5-3
5.2.2 Neutron Source	5-3



	<u>Page</u>
5.3 Model Specifications	5-3
5.3.1 Description of the Radial and Axial Shielding Configuration	5-3
5.3.1.1 Radial Shielding	5-3
5.3.2 Package Regional Densities	5-5
5.4 Shielding Evaluation	5-6
6.0 CRITICALITY	6-1
6.1 Discussion and Results	6-1
7.0 OPERATING PROCEDURES	7-1
7.1 Procedures for Loading the Package	7-1
7.2 Procedures for Unloading the Package	7-4
8.0 ACCEPTANCE TESTS AND MAINTENANCE PROGRAM	8-1
8.1 Acceptance Tests	8-1
8.2 Maintenance Program	8-2
APPENDIX 8.3.1 Gamma Scan	8-3-1-1
APPENDIX 8.3.2 Helium Leak Testing	8-2-2-i

	<u>Page</u>
9.0 QUALITY ASSURANCE	9-1
9.1 Introduction	9-1
9.2 Description of the PNSI, 10 CFR 71, Subpart H Quality Program	9-2
9.2.1 Organization	9-2
9.2.2 Quality Assurance Program	9-4
9.2.3 Design Control	9-4
9.2.4 Procurement Document Control	9-5
9.2.5 Instruction, Procedures and Drawings	9-6
9.2.6 Document Control	9-7
9.2.7 Control of Purchased Materials, Parts and Components	9-8
9.2.8 Identification and Control of Materials, Parts and Components	9-9
9.2.9 Control of Special Processes	9-10
9.2.10 Inspection	9-11
9.2.11 Test Control	9-11
9.2.12 Control of Measuring and Testing Equipment	9-12
9.2.13 Handling, Storage, and Shipping	9-13
9.2.14 Inspection, Test and Operating Status	9-13
9.2.15 Non-conforming Material, Parts, or Components	9-14
9.2.16 Corrective Action	9-14
9.2.17 Quality Assurance Records	9-15
9.2.18 Audits	9-16
9.2.19 References	9-16

## 1.0 GENERAL INFORMATION

### 1.1 Introduction

The NuPac 10/140MB Cask has been developed for the purpose of safely transporting Type B quantities of radioactive material. The purpose of this Safety Analysis Report is to demonstrate compliance of the package with 10 CFR 71 regulatory requirements. The package is capable of safely transporting Type B quantities of radioactive materials, including quantities greater than Type B meeting the definition of LSA. Authorization is sought for shipment by cargo vessel, motor vehicle and rail.

### 1.2 Package Description

#### 1.2.1 Packaging

##### 1.2.1.1 General Description

The NuPac 10/140MB reusable shipping packages designed to protect radioactive material from normal and hypothetical accident conditions of transport.

The NuPac 10/140MB Cask is a top and (optionally) bottom loading transport shield designed specifically for the safe transport of Type B levels of radioactive materials. The shields can accommodate full capacity liners, or miscellaneous form cargo such as 55 gallon drums, irradiated hardware, etc.

#### 1.2.1.2 Materials of Construction, Dimensions and Fabricating Methods

General arrangement drawings of the NuPac 10/140MB is included in Appendix 1.3.1. These show the overall dimensions as well as materials of construction.

The cask body consists of external and internal steel shells separated by a lead biological shield in the annular space between these two shells. The top and bottom ends of the cylindrical cask are constructed of stainless steel castings or forgings. The inner steel shell is constructed of 304 stainless steel plate.

The top (and as an option, the bottom) serves as a removable cask lid and is secured to the cylindrical cask body by eight, high strength, 'EnviroLock<sup>tm</sup>' binders. A 29 inch diameter secondary cask lid is located in the center of the top primary lid and is secured to the primary lid by eight 1-1/4 inch studs. Lifting lugs and tiedowns are a structural part of the package.

#### 1.2.1.3 Containment Vessel

The inner shell together with the top and bottom end plates of the cask serve as the containment vessel. Its mechanical configuration is described in the foregoing paragraph.

Two pairs of neoprene O-ring seals are employed in both the primary and secondary lid interfaces. These 'EnviroSeals<sup>tm</sup>', are of a unique design, affording an unprecedented level of containment to the contents of the 10/140MB.

Waste products will be contained in 55 gallon drums, in heavy gauge disposable steel liners, in crates or other suitable palletized forms.

1.2.1.4 Neutron Absorbers

There are no materials used as neutron absorbers or moderators in the NuPac 10/140MB package.

1.2.1.5 Package Weight

The gross, net and payload weights of the NuPac 10/140MB Package are as follows:

Gross Empty Weight	50,000
Payload Weight	<u>15,000</u>
Total Weight	65,000 (approx.)

1.2.1.6 Receptacles

There are no internal or external structures supporting or protecting receptacles, except as described in 1.2.1.7 below regarding the optional drain port.

1.2.1.7 Containment Penetrations

The casks are provided with a 0.44 inch diameter drain port in the bottom plate, suitably counter-drilled and tapped to accept an o-ring sealed pipe plug. The drain port is used for removal of entrapped liquids, such as rain or decontamination fluids. If a cask is configured to bottom-load, then no drain port is provided into containment.

1.2.1.8 Tiedowns

Tiedowns are a structural part of the package. From the attached general arrangement drawing, it can be seen that four reinforced tiedown locations are provided. Refer to Section 2.5.2 for a detailed analysis of their structural integrity.

1.2.1.9 Lifting Devices

Lifting devices are a structural part of the package. From the general arrangement drawing, it can be seen that three reinforced lifting locations are provided. Refer to Section 2.5.1 for a detailed analysis of their structural integrity.

1.2.1.10 Pressure Relief System

There are no pressure relief valves in the design of the NuPac 10/140MB packaging.

1.2.1.11 Heat Dissipation

There are no special devices used for the transfer or dissipation of heat. The package internal decay heat used for design is 95 watts.

1.2.1.12 Coolants

There are no coolants utilized in the package.

1.2.1.13 Protrusions

There are no outer or inner protrusions, except for the lifting and tiedown lugs described above.

#### 1.2.1.14 Shielding

The contents will be limited such that the radiological shielding provided will assure compliance with DOT and IAEA regulatory requirements. Should lead slump occur, as the result of a flat end drop, the deeply stepped lid will provide full shielding protection.

#### 1.2.2 Operational Features

Refer to the General Arrangement drawing of the packaging, in Appendix 1.10.1. There are no complex operational requirements connected with the packages and none that have any transport significance. The top primary lid and optional bottom lid are both readily removable with NuPac's rapid action EnviroLocks<sup>tm</sup> which, when not in use, are completely recessed beneath the protective over-pack to prevent inadvertent damage during normal or accident conditions of transport. Full and reliable containment is provided by NuPac's EnviroSeals<sup>tm</sup> providing an unprecedented level of containment to the package. These devices provide sealing surface protection during operational activities, and are themselves easily and quickly replaceable to maintain a sure and complete seal under all conditions. Full patent protection for both the Envirolocks<sup>tm</sup> and the EnviroSeals<sup>tm</sup> is being sought.

#### 1.2.3 Contents of Packaging

This application is for transporting the following radioactive materials as defined in U.S.A. and IAEA regulations:

- o Contents include less than 2,000 times the Type A quantity of radioisotopes as defined in 10CFR71, Table A.
- o Contents may be Type A or B quantities, including Low Specific Activity (LSA) in normal or special form.
- o Contents total less than 95 watts of internal decay heat.

- o Contents may be in dispersible or non-dispersible form (e.g., activated hardware) and may be contained within an internal liner not considered part of this application or solidified in a stabilizing media or both. The containment ability of any internal liner is not considered in this application.
  
- o Contents shall be so limited that the external radiation dose rates are within the limits specified in 10 CFR 71. This shall be verified by pre-shipment inspection.



APPENDIX 1.3.1

THIS SECTION IS PROPRIETARY

## 2.0 STRUCTURAL EVALUATION

This section identifies and describes the principal structural engineering design of the NuPac 10/140MB packaging, components, and systems important to safety and to compliance with the performance requirements of 10 CFR 71.

### 2.1 Structural Design

#### 2.1.1. Discussion

The principal structural member of the NuPac 10/140MB package is the containment vessel described in Section 1.2.1. The above component is identified on the drawing as noted in Appendix 1.3.1. A detailed discussion of the structural design and performance of all cask components is provided below.

#### 2.1.2 Design Criteria

##### 2.1.2.1 Basic Design Criteria (Allowable Stresses)

This section defines the stress allowables for primary membrane, primary bending, secondary, bearing, shear, and buckling stresses for containment structures and fasteners, and non-containment structures and fasteners.

Regulatory Guide 7.6, Design Criteria for Structural Analysis of Shipping Cask Containment Vessels is used in conjunction with Regulatory Guide 7.8, Load Combinations for the Structural Analysis of Shipping Casks to evaluate the integrity of the NuPac 10/140MB. Where the loads specified by Regulatory Guide 7.8 conflict with those given in the current version of 10 CFR 71, the latter is used. Material properties and design stress intensity values,  $S_m$ , used in the analyses can be found in Table 2.3-1.

#### 2.1.2.1.1 Containment Structures

Regulatory Guide 7.6 was used for all package containment boundaries for both the normal conditions of transport and the hypothetical accident conditions. Material data used in the evaluation correspond to the design stress values,  $S_m$ , yield strengths,  $S_y$ , and ultimate strengths,  $S_u$ , given in the ASME Code, Section III, Class I. The containment vessel is considered to be the 66.0 inch inside diameter, .75 inch thick inner shell of the cask, the castings or forgings at the top and bottom ends of the cask, the bolted secondary closure lid, and the drain port in fixed bottom modules. A summary of allowable stresses used for containment structures, non-containment structures, and fasteners is presented in Table 2.1.2-1. These data are consistent with Regulatory Guide 7.6 and Sections NB-3000 and Appendix F of ASME Section III.

#### 2.1.2.1.2 Non-Containment Structures

Structural evaluations of non-containment boundaries, such as tie down and lifting devices, and the cask outer shell use allowable stresses for normal and accident conditions as presented in Table 2.1.2-1. The overpack is allowed to exceed yield for all conditions. The acceptance criterion for all impact related loads within the overpacks is that no cask 'hard points' directly come into contact with the impact surface. For lifting and handling loads, the 'non-containment' allowables of Table 2.1.2-1 are utilized in conjunction with a load factor of three (3), per 10 CFR 71.45. These lifting and handling allowables are applicable to all package components, including the overpack lift lugs.

TABLE 2.1.2-1  
Allowable Stress Limits  
(Table 1 of 2)

	CONTAINMENT STRUCTURE ALLOWABLE STRESSES	
Stress Category		
	Normal Conditions	Accident Conditions
Primary Membrane Stress Intensity	$S_m$	Lesser of: $2.4S_m$ $0.7S_u$
Primary Membrane + Bending Stress Intensity	$1.5S_m$	Lesser of: $3.6S_m$ $S_u$
Range of Primary + Secondary Stress Intensity	$3.0S_m$	Not Applicable
Bearing Stress	$S_y$	$S_y$ for seal surfaces $S_u$ elsewhere
Pure Shear Stress	$0.6S_m$	Lesser of: $1.20S_m$ $0.35S_u$
Buckling	Per Section 2.1.2.2.3	
	CONTAINMENT FASTENER ALLOWABLE STRESSES	
Stress Category		
	Normal Conditions	Accident Conditions
Membrane Stress *	$2.0S_m$	Lesser of: $S_y$ $0.7S_u$
Membrane + Bending Stress *	$3.0S_m$	$S_u$

\* Not Considering Stress Concentrations

TABLE 2.1.2-1  
Allowable Stress Limits  
(Table 2 of 2)

	NON-CONTAINMENT STRUCTURE ALLOWABLE STRESSES		
Stress Category			
	Normal Conditions	Accident Conditions	
Primary Membrane Stress Intensity	Greater of:	$S_m$ $S_y$	$0.7S_u$
Primary Membrane + Bending Stress Intensity	Greater of:	$1.5S_m$ $S_y$	$S_u$
Range of Primary + Secondary Stress Intensity	Greater of:	$3.0S_m$ $S_y$	Not Applicable
Bearing Stress		$S_y$	$S_u$
Pure Shear Stress	Greater of:	$0.6S_m$ $0.6S_y$	$0.35S_u$
Buckling	Per Section 2.1.2.2.3		
	NON-CONTAINMENT FASTENER ALLOWABLE STRESSES		
Stress Category			
	Normal Conditions	Accident Conditions	
Membrane Stress	Greater of:	$2.0S_m$ $S_y$	Greater of: $S_y$ $0.7S_u$
Membrane + Bending Stress	Greater of:	$3.0S_m$ $S_y$	$S_u$

\* Not Considering Stress Concentrations

2.1.2.2 Miscellaneous Structural Failure Modes2.1.2.2.1 Brittle Fracture

With exception of the closure bolts and EnviroLocks, all containment structural components are fabricated of Type 304 austenitic stainless steel. Since this material does not undergo a ductile-to-brittle transition in the temperature range of interest (down to  $-40^{\circ}\text{F}$ ), it is safe from brittle fracture.

The secondary lid closure bolts are fabricated of ASTM A-320, Grade L43, alloy steel. Per Section 5 of NUREG/CR-1815 bolts are generally not considered as fracture-critical components because multiple load paths exist and because bolted systems are designed to be redundant. However, for purposes of comparison, the nil-ductility transition (NDT) temperature of the closure bolts will be calculated and compared with the requirements of NUREG/CR-1815.

According to Section 6.2.1.1 of the ASTM A-320, Grade L43, specification, the minimum impact energy absorption is 20 ft-lbs at  $-150^{\circ}\text{F}$ . The Charpy impact measurement may be transformed into a fracture toughness value by using the empirical relation developed in Section 4.2 of NUREG/CR-1815, as follows:

$$K_{ID} = [5E(C_v)]^{0.5}$$

Where:

$K_{ID}$  = dynamic fracture toughness,  $\text{psi-in}^{0.5}$

$E$  = Modulus of Elasticity,  $\text{psi}$

=  $28.8(10)^6$   $\text{psi}$  at  $-150^{\circ}\text{F}$  (Table I-5.0 of the ASME B and PV code)

$C_v$  = Charpy impact measurement,  $\text{ft-lbs}$

= 20  $\text{ft-lbs}$

Then,

$$K_{ID} = \{5[28.8(10)^6](20)\}^{0.5} = 53,665 \text{ psi-in}^{0.5}$$

The dynamic fracture toughness is translated to an equivalent nil ductility transition (NDT) temperature by using the Pellini reference curve given as Figure 2 in NUREG/CR-1815.

By interpolation, the temperature relative to NDT is found as:

$$(T - \text{NDT}) = 30^{\circ}\text{F}$$

Accordingly, the nil-ductility transition temperature is:

$$\begin{aligned} \text{NDT} &= -150 - (+30) \\ &= -180^{\circ}\text{F} \end{aligned}$$

For Category I fracture critical components, and in section thicknesses of 1.5 inches (bolt diameter), Figure 3, NUREG/CR-1815, gives the minimum offset, 'A' as approximately  $60^{\circ}\text{F}$ . Thus, the maximum NDT temperature value is:

$$T_{\text{NDT}} = \text{LST} - A = -20 - 60 = -80^{\circ}\text{F}$$

Where:

$T_{\text{NDT}}$  = maximum NDT temperature per NUREG/CR-1815

LST = lowest service temperature

=  $-20^{\circ}\text{F}$  (Reg Guide 7.6)

A =  $60^{\circ}\text{F}$ , per Figure 3, NUREG/CR-1815

The ASTM A-320, Grade L43, closure bolts experience a ductile to brittle transition temperature at  $-180^{\circ}\text{F}$  whereas the criterion of NUREG/CR-1815 prescribes a maximum NDT temperature of  $-80^{\circ}\text{F}$ . The  $100^{\circ}\text{F}$  margin between criteria requirements and material capability provide conservative assurance that brittle fracture failures will not occur in these ferritic closure bolt materials. Since bolts are acceptable under Category I rules, they are also acceptable for the Category II NuPac 10/140MB.

The EnviroLock<sup>tm</sup> closure devices include ASTM A522 grade I material, two inches in diameter. The material has a minimum tensile yield of 75,000 psi. NUREG/CR-1815 states that for steels with yield strengths greater than 70,000 psi, the dynamic yield strength ( $\sigma_{yd}$ ) may be taken as 15,000 psi greater than the static yield for brittle fracture considerations. So, for A522 material,

$$\sigma_{yd} = 90,000 \text{ psi}$$

From Figure 7 of NUREG/CR-1815 for 2 inch material and taking advantage of the relief allowed for reduced loading rates for steels with yield strengths in excess of 70,000 psi, a required NDT offset (A) of 27°F is obtained. Since the lowest service temperature (LST) of the 10/140MB is -20°F, the maximum nil ductility transition temperature ( $T_{NDT}$ ) may be calculated:

$$T_{NDT} = LST - A = -20 - 27 = -47^\circ\text{F}$$

Using the same curve in Figure 7, the ratio of the stress intensity factor  $K_I$  to the dynamic yield required at the NDT temperature (when A equals zero) is:

$$K_I / \sigma_{yd} = .8$$

Since  $\sigma_{yd} = 90,000$ ,  $K_I$  at the NDT temperature is

$$K_I = .8(90,000) = 72,000 \text{ psi-in}^{0.5}$$

Therefore, the required fracture toughness at the NDT temperature (-47°F) may be demonstrated by Charpy V-notch measurements using the following relationship:

$$C_{v\text{-reqd}} = K_I^2 / 5E$$

$$\text{Where: } K_I = 72,000 \text{ psi-in}^{0.5}$$

$$E = \text{Young's modulus} = 28 \times 10^6 \text{ psi}$$



$C_{v\text{-reqd}}$  = Required Charpy V notch measurement in ft-lb.

$$C_{v\text{-reqd}} = 37.0 \text{ ft-lb}$$

Therefore, if the A522 Class I material has a measured Charpy toughness of 37 ft-lbs at  $-50^{\circ}\text{F}$ , it demonstrates the toughness required to meet the criteria for Category II packages per NUREG/CR-1815.

The 1.25 inch outer shell, as well as the EnviroLock<sup>tm</sup> support structure attached to the outer cask side wall are fabricated from ASTM A516 grade 70 material. Under Category II rules for qualification of 0.625 inch to 4.0 inch thick sections, Figure 6 of NUREG/CR-1815 may be used to determine the nil-ductility transition temperature. Since the 10/140MB will be subjected to reduced loading rates and because the yield strength of ASTM A516 grade 70 steel is less than 60 ksi (it is actually 38 ksi), curve no. 3 of that figure may be used. For the 1.25 inch maximum thickness of A516, grade 70, the NDT temperature  $T_{\text{NDT}}$  is given as:

$$T_{\text{NDT}} = \text{LST} - A$$

Where  $T_{\text{NDT}}$  = NDT temperature

LST = Lowest service temperature,  $-20^{\circ}\text{F}$

A = determined from Figure 6 of NUREG/CR-1815

$$T_{\text{NDT}} = -20 - (-20)$$

$$T_{\text{NDT}} = 0^{\circ}\text{F}$$

Therefore, all A516 Grade 70 components of the 10/140MB greater than 0.625 inches thick are required to have a tested nil-ductility transition less than  $0^{\circ}\text{F}$ . All A516 Grade 70 components less than 0.625 inches thick are required to be normalized only, consistent with the requirements of NUREG/CR-1815.

This NDT may be verified by noting that on Figure 2, the dynamic fracture toughness  $K_{ID}$  is defined as 40,000 psi-in<sup>0.5</sup> at the NDT temperature. The required Charpy V-notch measurement to demonstrate this fracture toughness can be calculated by the following equation from NUREG/CR-1815:

$$K_{ID}^2 = 5(C_V)E$$

Where  $K_{ID} = 40,000 \text{ psi-in}^{0.5}$

$$E = 30 \times 10^6 \text{ psi}$$

$$C_V = \text{Charpy V-notch measurement, ft-lb.}$$

So,

$$C_V = K_{ID}^2 / 5E$$

$$C_V = 11 \text{ ft-lb.}$$

Therefore, the requirement to have an NDT of less than 0°F may be demonstrated by showing that the Charpy measurement of 0°F or lower is at least 11 ft-lbs. in the A516 Grade 70 1.25 inch (or thinner) plate. All A516, Grade 70 material greater than 0.625 inches thick used in the design of the NuPac 10/140MB possess Charpy values in excess of 15 ft-lbs. as shown on the drawings in Appendix 1.3.1.

#### 2.1.2.2.2 Fatigue

Normal operating cycles do not present a fatigue concern for the NuPac 10/140MB cask components which have no stress concentrations. This is because the highest allowable stress for normal conditions ( $3S_m$ ) is less than the allowable fatigue stress limit for the steels used in the 10/140MB design. For example,  $S_m$  for 304 stainless components is 20,000 psi in the temperature range of concern. Thus, assuming that the normal operating cycle stress

actually equals the allowable ( $3S_m$ ), Figure I-9.2.1 may be used to determine the number of cycles which would be allowed. From that figure, it can be seen that over 10,000 cycles are allowed. For the A516 grade 70 material,  $S_m$  is 23.3. Thus, for fatigue to become an important consideration, the cask would be required to under go at least 1600 cycles at or near its normal stress allowable. Since under the most severe usage the cask might under go 50 normal shipments per year, or 1000 cycles in 20 years of constant use, it seems clear that fatigue is not a problem for the cask components with no stress concentrations.

Fatigue considerations in the secondary lid bolts and EnviroLocks<sup>tm</sup> follow a similar logic. The torque requirements in the bolts are 375 ft-lbs and in the EnviroLocks<sup>tm</sup> it is 500 ft-lbs. Using the simple torque to preload relationship and a torque coefficient of 0.20, the axial force in both fasteners may be determined:

$$P = T/KD$$

where  $P$  = bolt load, lbs.

$T$  = torque, in-lb

$$K = 0.20$$

So for the lid bolts:

$$P = (375)(12)/(.20)(1.5) = 15,000 \text{ lbs}$$

For The EnviroLocks<sup>tm</sup>:

$$P = (500)(12)/(.20)(2.0) = 15,000 \text{ lbs}$$

The stress area for the bolt is  $1.405 \text{ in}^2$ . Since the EnviroLock<sup>tm</sup> has the same load as the bolt and the bolt has a smaller cross-section, the normal stress in the bolt is the worst case. The normal stress is:

$$15,000/1.405 = 10,700 \text{ lbs}$$

The fatigue alternating stress amplitude is then 5,350 psi.

This stress should be multiplied by the fatigue strength reduction factor (taken to be 4.0 per ASME NB-3232.3(c)) and using Figure I-9.4 from ASME Section III, Appendix I, the allowable number of cycles determined.

$$S_{\text{range}} = 4(5350) = 21,400 \text{ psi}$$

Note that since  $S_{\text{range}}$  is very much less than  $2.7 S_m$  for the bolt ( $2.7 \times 35,000 = 94,500 \text{ psi}$ ) the upper curve from Figure I-9.4 may be used. From that curve, it can be seen that the bolts may experience over 40,000 cycles before exceeding the ASME fatigue criteria for the bolts. Clearly fatigue is not a serious consideration in the design of the NuPac 10/140MB cask.

#### 2.1.2.2.3 Buckling

Buckling, per Regulatory Guide 7.6, is an unacceptable failure mode for containment vessels. The intent of this provision is to preclude large deformations which would compromise the validity of linear analysis assumptions and quasi-linear stress allowables, as given in Paragraph C.6 of Regulatory Guide 7.6.

There are three sets of forces that can potentially cause buckling instabilities in cylindrical vessels. These are axial compression forces, bending moments, and external pressure. The remainder of this subsection defines techniques and criteria used in subsequent segments of this Safety Analysis Report to demonstrate that containment vessel buckling, and non-containment vessel buckling, does not occur.

There are two shells within the NuPac 10/140MB Cask where buckling prevention criteria are applicable - i.e., the inner and outer shells of the cask. For reference purposes the principal geometric features of these shells are as follows:

<u>Shell</u>	<u>Dimension (inches)</u>		
	Mean		
	Radius	Thickness	Length
	(R)	(t)	(L)
Inner Shell	33.375	.75	75.5
Outer Shell	36.625	1.25	75.5

#### 1. Elastic Buckling

Representative elastic buckling stress estimates for the shells and applicable loading modes are as follows:

<u>Shell</u>	<u>Elastic Buckling Stresses (ksi)</u>		
	(at 212°F)		
	Axial	Bending	External
	<u>Compression</u>		<u>Pressure</u>
Inner Shell (304 SST)	261.7	280.4	177.5
Outer Shell (A516 Gr.70)	440.1	469.8	N/A

The above elastic buckling values are all based upon a temperature of 212°F, consistent with the stress-strain data for 304 stainless steel given in Figure 2.3-1. Calculations discussing these elastic buckling estimates are found in the following paragraphs. Equations are taken from Structural Analysis of Shells, by Baker, Kovalevsky and Rish.

- a) Crippling of Moderately Long Cylinders (Structural Analysis of Shells, p. 230) for the cask inner shell (containment vessel):

$$S_{cr}/\xi_a = (\gamma_a)CE(t/R)$$

Where:

$S_{cr}$  = buckling stress

$\xi_a$  = plasticity coefficient

$\gamma_a$  = a factor which accounts for the difference  
between theoretical and experimental results

$$= 0.70 \text{ (at } R/t = 44.5)$$

$$C = [3(1 - \mu^2)]^{-0.5} = 0.605$$

$$E = 27.5(10)^6 \text{ psi (at } 212^\circ \text{ F)}$$

$$t = 0.75 \text{ in}$$

$$R = 33.375 \text{ in}$$

$$\mu = 0.3$$

Then,

$$\begin{aligned} S_{cr}/\xi_a &= (0.70)(0.605)[27.5(10)^6](0.75/33.375) \\ &= 261,700 \text{ psi} \end{aligned}$$

Likewise, for the cask outer shell (non-containment):

$$S_{cr}/\xi_a = (\gamma_a)CE(t/R)$$

Where:

$$\gamma_a = 0.74 \text{ (at } R/t = 29.3)$$

$$t = 1.25 \text{ in}$$

$$R = 36.625 \text{ in}$$

$$E = 28.8 \times 10^6 \text{ psi (A516 at } 200^\circ\text{F)}$$

Then,

$$\begin{aligned} S_{cr}/\xi_a &= (0.74)(0.605)[28.8(10)^6](1.25/36.625) \\ &= 440,100 \text{ psi} \end{aligned}$$

- (b) Euler Column Buckling - The cask inner shell (containment) is laterally restrained and supported by the outer shell of the outer cask. Thus, Euler column buckling is governed by the geometric properties of the cask outer shell. The applied axial forces are distributed 'self weight' loads, thus buckling stresses are found as (per Theory of Elastic Stability by Timoshenko p. 118, Eq. 83):

$$S_{cr}/\xi_a = (qL)_{cr}/A = \pi^2 EI / (1.122L)^2 A$$

Where:

$$q = \text{load per unit length (lb/in)}$$

$$L' = \text{column length} = 75.5 \text{ in}$$

$$L = L'/2 = 37.75 \text{ in}$$

$$R = \text{mean radius} = 36.625 \text{ in}$$

$$t = 1.25 \text{ in}$$

$$A = 2\pi R t \text{ in}^2 = 287.65 \text{ in}^2$$

$$I = \pi R^3 t \text{ in}^4 = 192,900 \text{ in}^4$$

$$E = 28.8(10)^6 \text{ psi } (200^\circ \text{ F})$$

Then,

$$\begin{aligned} S_{cr}/\xi_a &= (E/2) [\pi R / (1.122) L]^2 \\ &= [28.8(10)^6 / 2] [\pi (36.625) / (1.122) (37.75)]^2 \\ &= 1.063 \times 10^8 \text{ psi} \end{aligned}$$

Thus, crippling is more critical for the outer cask shells than gross columnar instability.

c) Bending Moments (Structural Analysis of Shells pp. 234-235) for the cask inner shell (containment vessel):

$$S_{cr}/\xi_a = (\gamma_b) CE(t/R)$$

Where:

$$\gamma_b = 0.75 \text{ (at } R/t = 44.5)$$

$$t = 0.75 \text{ in}$$

$$R = 33.375 \text{ in}$$

Then,

$$\begin{aligned} S_{cr}/\xi_a &= (0.75) (.605) [27.5(10)^6] (0.75/33.375) \\ &= 280,400 \text{ psi} \end{aligned}$$

Likewise, for the cask outer shell (non-containment):

$$S_{cr}/\xi_a = (\gamma_b) CE(t/R)$$



Where:

$$\gamma_b = 0.79 \text{ (at } R/t = 29.3)$$

$$t = 1.25 \text{ in}$$

$$R = 36.625 \text{ in}$$

$$E = 28.8 \times 10^6$$

Then,

$$\begin{aligned} S_{cr}/\xi_a &= (0.79)(.605)[28.8(10)^6](1.25/36.625) \\ &= 469,800 \text{ psi} \end{aligned}$$

d) External Pressure, with external constraint. The case of a shell encased in a cavity is discussed in Pressure Buckling of Ring Incased in a Cavity James A. Cheney, ASCE EM Journal, April 1971, Vol. 97. Upon buckling, the shell can only move inward. This case corresponds to the cask inner shell where external constraint is provided by the lead biological shield. From Equation 47 of the referred document, the critical buckling pressure is:

$$q_{cr} = (k^2 - 1)E(t/R)^3/12(1 - \mu^2)$$

Utilizing thin-walled pressure vessel theory, the critical buckling stress may be written as:

$$S_{cr} = q_{cr}R/t$$

Then,

$$S_{cr}/\xi_p = (k^2 - 1)E(t/R)^2/12(1 - \mu^2)$$

For the cask inner shell (containment)

$$\begin{aligned} k &= 1.57(R/\rho)^{0.4} \text{ (Equation 29)} \\ &= 11.78 \end{aligned}$$

$$\begin{aligned} R/\rho &= R(12)^{0.5}/t \quad (\text{Equation 48}) \\ &= 154.2 \end{aligned}$$

$$t = 0.625 \text{ in}$$

$$R = 33.3125 \text{ in}$$

$$E = 27.5(10)^6 \text{ psi (at } 212^\circ \text{ F)}$$

$$\mu = 0.3$$

Then,

$$\begin{aligned} S_{cr}/\xi_p &= [(11.78)^2 - 1][27.5(10)^6](0.75/33.375)^2/12[1 - (0.3)^2] \\ &= 177,500 \text{ psi} \end{aligned}$$

## 2. Buckling Criteria

The high elastic buckling stress limits estimated for the cask shells within the previous paragraph (177.5 to 469.8 ksi) provide solid generalized assurance that instability failure modes do not exist for compressively loaded components of the NuPac 10/140MB Cask. To quantify this assertion, all compressively loaded states of stress are tested versus the stability and buckling criteria set forth within Section 2.10.1. These criteria recognize that compressively loaded structures behave in different fashions depending upon the geometric aspect ratio of the structure. The nature of the criteria is such that the factors of safety vary with this geometric aspect ratio up to asymptotic values of 5 and 7.5, versus elastic buckling stresses, for accident and normal conditions of transport, respectively. These asymptotic factors of safety may be considered conservative for general use as radioactive materials package design criteria.

Appendix 2.10.1 defines both the rationale and the specifics of the applicable criteria. Briefly, the criteria are as follows:

Direct primary compressive membrane stresses,  $S$ , in containment vessels shall be less than the lesser of  $S_e/R_d$  or  $S_j$ .  $S_e$  is defined as the appropriate elastic buckling stress limit considering adjustments resolving theoretical and experimental results, but neglecting plasticity corrections. The reduction coefficient  $R_d$  is to be taken as 7.5 for normal conditions of transport and 5 for accident conditions of transport. This reduction coefficient,  $R_d$ , corresponds to the intended factor of safety of the method at high aspect ratios of the structure.  $S_j$  is a generalized 'Johnson' parabolic transition curve having a value of  $S_s$  at an aspect ratio,  $G$ , of zero. This parabolic transition curve is also tangent to the expression  $S_e/R_d$  at a stress level of  $2/3 S_s$ . The term  $S_s$  denotes the applicable strength limit of the material --  $S_m$  for normal conditions of transport and  $S_y$  for hypothetical accident conditions, both as defined within Reg Guide 7.6. The details of the criteria, in symbolic form are as follows:

Where  $G$  is less than  $G^*$ :

$$S \leq S_j,$$

Where  $G$  is greater than or equal to  $G^*$ :

$$S \leq S_e/R_d.$$

Where:  $S_e$  = The classical elastic buckling stress expression (including adjustments for theory versus tests) cast in the generalized form:

$$= K/G.$$

$K$  = A numerical constant unique to each compressive loading mechanism reflecting materials properties (Young's Modulus, Poisson's ratio) and empirical or theoretical coefficients. See Table 2.10.1.1-1 for a summary versus typical loading mechanisms.

$G$  = A non-dimensionalized geometric aspect ratio unique to each loading mechanism. See Table 2.10.1.1-1 for a summary versus typical loading mechanisms. For example:

$G$  =  $(L/\rho)^2$ , for column type loadings [Note:  $\rho = (I/A)^{1/2}$ ],

$G$  =  $(R/t)$ , for external pressures on long cylinders and axial compression loadings of cylinders.

$R_d$  = 7.5, for Normal Conditions,  
= 5.0, for Accident Conditions.

$S_j$  = The parabolic transition from  $S_s$  to  $(S_e/R_d)$   
=  $S_s - [4S_s^3 G^2 / [27(K/R_d)^2]]$ .

$G^*$  = The aspect ratio,  $G$ , where the parabola defined by  $S_j$  intercepts and is tangent to the curve defined by  $(S_e/R_d)$ ; in other words,  $G^*$  corresponds to the aspect ratio where  $S_j = (S_e/R_d)$ , or:  
=  $(3/2)(K/R_d)/S_s$ .

$S_s$  =  $S_m$ , for Normal Conditions,  
=  $S_y$ , for Accident Conditions.

$S_m$  = Design Stress Intensity as used within Section III, ASME Boiler and Pressure Vessel Code.

$S_y$  = Minimum Yield Stress per Section III, ASME Boiler and Pressure Vessel Code.

### 3. Specific Buckling Limits

Application of these criteria to the specific shell geometries of the NuPac 10/140 MB Cask are presented in Tables 2.1-1 thru 2.1-4 for normal and accident conditions, respectively. The allowable stresses based on the buckling criteria have been derived using a combination of the shell geometries introduced at the beginning of this Section and the criteria described immediately above. A single example serves to demonstrate the method for calculation of these allowables. For this example, consider normal conditions of transport and axial compression of the Cask Inner Shell at 250°F.

The parameters, K and G, are evaluated as follows:

$$K = \gamma_a C E, \text{ see preceding 'Elastic Buckling' discussion}$$

$$= (.70)(.605)(27.3 \times 10^6) = 1.156 \times 10^7$$

$$G = R/t = 33.375/0.75 = 44.5$$

Elastic Buckling stress,  $S_e$ , is:

$$S_e = K/G = 259,800 \text{ psi}$$

For normal conditions

$$R_d = 7.5$$

$$S_s = S_m = 20,000 \text{ psi}$$

The intercept tangent point  $G^*$  is:

$$G^* = (3/2) (K/R_d) / S_s$$

$$= (1.5)(1.156 \times 10^7 / 7.5) / 20000 = 115.6$$

Since  $G \ll G^*$ , the allowable stress is given by:

$$\begin{aligned} S_j &= S_s - \left[ 4S_s^3 G^2 / \left[ 27(K/R_d)^2 \right] \right] \\ &= (20000) - 4(20000)^3 (44.5)^2 / \left[ 27(1.156 \times 10^7 / 7.5)^2 \right] \\ &= 19,012 \text{ psi} \end{aligned}$$

Table 2.1-1

NORMAL CONDITIONS OF TRANSPORT  
Crippling and Buckling Allowables  
for Inner Shell

Loading Condition and Shell	*****		TEMPERATURE (Deg-F)				*****
	-20	70	100	150	200	250	
<hr/>							
Material Properties (psi):							
E	2870000*	28300000	281000000*	27900000*	27600000	27300000*	
Sy	34100**	30000	30000	27500*	25000	23750*	
Sm	20000**	20000**	20000	20000*	20000	20000*	
Ss	20000	20000	20000	20000	20000	20000	
 <u>Axial Compression Buckling Allowables (psi):</u>							
	19106	19081	19068	19054	19034	19012	
 <u>Bending Buckling Allowables (psi):</u>							
	19222	19199	19188	19176	19158	19140	
 <u>External Pressure Buckling Allowables (psi):</u>							
	18004	17948	17919	17889	17843	17794	

\* Interpolated from ASME Code, Section III Appendix Data (See Table 2.3-1)

\*\* Extrapolated from ASME Code, Section III Appendix Data (See Table 2.3-1)

Table 2.1-2

NORMAL CONDITIONS OF TRANSPORT  
Crippling and Buckling Allowables  
for Outer Shell

Loading Condition and Shell	*****	TEMPERATURE (Deg-F)					*****
	-20	70	100	150	200	250	

## Material Properties (psi):

E	2990000*	2950000	2930000*	2910000*	2880000	2860000*
Sy	40200**	38000	38000	36300*	34600	34200*
Sm	23800**	23500**	23300	23200*	23100	22800*
Ss	23800	23500	23300	23200	23100	22800

Axial Compression Buckling Allowables (psi):

23262	22968	22774	22674	22570	22283
-------	-------	-------	-------	-------	-------

Bending Buckling Allowables (psi):

23328	23033	22839	22738	22635	22346
-------	-------	-------	-------	-------	-------

\* Interpolated from ASME Code, Section III Appendix Data (See Table 2.3-1)

\*\* Extrapolated from ASME Code, Section III Appendix Data (See Table 2.3-1)



Table 2.1-3

ACCIDENT CONDITIONS OF TRANSPORT  
Crippling and Buckling Allowables  
for Inner Shell

Loading Condition and Shell	*****	TEMPERATURE (Deg-F)					*****
	-20	70	100	150	200	250	

## Material Properties (psi):

E	2870000*	28300000	28100000*	27900000*	27600000	27300000*
Sy	34100**	30000	30000	27500*	25000	23750*
Sm	20000**	20000**	20000	20000*	20000	20000*
Ss	34100	30000	30000	27500	25000	23750

Internal Compression Buckling Allowables (psi):

32131	28621	28602	26408	24161	23015
-------	-------	-------	-------	-------	-------

Bending Buckling Allowables (psi):

32385	28799	28782	26548	24269	23110
-------	-------	-------	-------	-------	-------

External Pressure Buckling Allowables (psi):

29704	26923	26877	25061	23200	22109
-------	-------	-------	-------	-------	-------

\* Interpolated from ASME Code, Section III Appendix Data (See Table 2.3-1)

\*\* Extrapolated from ASME Code, Section III Appendix Data (See Table 2.3-1)

Table 2.1-4

ACCIDENT CONDITIONS OF TRANSPORT  
Crippling and Buckling Allowables  
for Outer Shell

Loading Condition and Shell	*****	TEMPERATURE (Deg-F)					*****
	-20	70	100	150	200	250	

## Material Properties (psi):

E	2990000*	2950000	2930000*	2910000*	2880000	2860000*
Sy	40200**	38000	38000	36300*	34600	34200*
Sm	23800**	23500**	23300	23200*	23100	22800*
Ss	40200	38000	38000	36300*	34600	34200*

axial Compression Buckling Allowables (psi):

39047	37000	36986	35404	33808	33424
-------	-------	-------	-------	-------	-------

Bending Buckling Allowables (psi):

39189	37122	37110	35514	33905	33519
-------	-------	-------	-------	-------	-------

\* Interpolated from ASME Code, Section III Appendix Data (See Table 2.3-1)

\*\* Extrapolated from ASME Code, Section III Appendix Data (See Table 2.3-1)

4. Combined Buckling Stresses are treated in the following fashion:

- (a) Stress ratios are calculated for each stress component at any point where compressive principal stresses exist:

$$R = S/S_{cr}$$

Where:

S = stress component under consideration

$S_{cr}$  = buckling stress allowable for the  
stress component under consideration

- (b) The stress ratios are summed linearly and compared with unity (Structural Analysis of Shells pp. 240-241):

$$M.S. = [1/(R_a + R_b + R_p)] - 1$$

Where:

$R_a$  = stress ratio for axial stress

$R_b$  = stress ratio for bending stress

$R_p$  = stress ratio for external pressure stress

2.1.2.3 Overpack Design Criteria

The NuPac 10/140MB package design incorporates impact-absorbing polyurethane foam filled overpacks to mitigate the consequences of many of the regulatory events. The properties of the closed-cell rigid polyurethane foam used in the NuPac 10/140MB design have been studied at great length in preparation for

this application. The foam was studied with regard to the effects of variations in as-poured density, temperature, and direction of load application on the stress-strain relationship of the foam. From this study, enveloping stress-strain relationships were developed for design. The logic used in constructing these relationships is presented below.

First, while samples of foam of exactly the same density exhibit an extremely consistent stress-strain curve, it is difficult to reproduce that density to within better than five percent. The resulting variation in the stress-strain relationship can easily exceed the density variation. It was determined that foam placement techniques could not consistently hold the as-placed stress-strain relationship better than within plus or minus 15% of the mean value.

Second, it was found that the stress-strain relationship of the foam varies with the temperature of the tested specimen. Tests were performed on many samples at temperatures of  $-20^{\circ}\text{F}$ ,  $75^{\circ}\text{F}$ , and  $180^{\circ}\text{F}$ . Interestingly, the properties of the foam at  $-20^{\circ}\text{F}$  were very much stiffer and stronger than at the higher temperatures. At  $180^{\circ}\text{F}$ , the foam was considerably softer than at room temperature. However, it is important to note that the foam reacted to temperature in a very consistent manner—that is, the stress-strain properties in all specimens tested were very consistent at a given temperature.

Finally, samples were tested to determine the variation of properties with respect to the orientation of the applied stress in relation to the direction of foam rise. While this is an important concern for some rigid foams, it was found that the foam used in the NuPac 10/140MB has little or no discernible directionality.

Figure 2.1.2-1 presents the average stress-strain behavior expected at the three temperatures studied. To determine the behavior of the foam at an intermediate temperature, the stress at a given strain is linearly interpolated between the curves. In order to envelope the behavior variations due to the slight variations in density, the resulting curve is scaled by plus or minus 15%, depending on whether stiff or soft foam is more detrimental.

In general, at higher temperatures, the softer the foam, the greater the potential for 'bottoming out', or the case where the foam does not remove enough energy to avoid a large acceleration spike at the end of the impact stroke. Since the foam properties at low temperatures are much stiffer, the highest impact accelerations will be imparted to the package during hypothetical impacts at  $-20^{\circ}\text{F}$ . Therefore, the design stress-strain curve at upper temperature extremes are degraded 15% from the mean curve estimated for that temperature from interpolation, while the mean stress-strain curve at  $-20^{\circ}\text{F}$  is scaled up 15% to get the design stress strain curve. The resulting stress-strain curves used for design are presented in Figure 2.1.2-2.

FIGURE 2.1.2-1

THIS FIGURE IS PROPRIETARY

FIGURE 2.1.2-2

THIS FIGURE IS PROPRIETARY

During fabrication, the stress-strain properties of the foam are controlled by pouring samples of each batch in a special box. Test specimens are then prepared from each box and tested to determine their stress-strain characteristics at 75°F. The overpack is regarded as acceptable if the average stress-strain properties from all pours are within 10 percent of the mean curve at 75°F shown in Figure 2.1.2-1. Thus, the use of a 15% possible variation in properties is conservative, allowing for the occasional pour slightly further away from the mean. Batches of foam exhibiting properties more than 20% from the required mean curve will be rejected.

The impact analyses presented in this application are similar to those presented in other applications. Notably, the analysis techniques and assumptions are very similar to those used to analyze the performance of the NuPac 125B Fuel Shipping Cask (Docket No. 9200). An extensive drop test program was performed on that cask, showing that the assumptions and analytic techniques used on both that cask and the NuPac 10/140MB are both reasonably accurate and slightly conservative.

Because the force required to strain a sample of this foam much beyond 70% is greater than the capacity of the instrument used to measure it, the behavior of the foam beyond this point is not well defined. It is clear, however, that the foam neither disappears nor becomes perfectly rigid. In analyses where deflections are critical (such as when clearance between hard spots on the package and the essentially unyielding surface is required to maintain the integrity of the analysis), predicted strains may exceed 70%, but the force from foam strained beyond 70% is conservatively (for deflection prediction) linearly extrapolated from the stress-strain states at 65% and 70%. This is automatically done by the programs EYDROP, SYDROP, and CYDROP. In such situations, the force of impact is slightly underpredicted. However, the highest impact forces occur when the foam is assumed to exhibit its stiffest stress-strain relationship. For EYDROP, SYDROP, and CYDROP analyses performed to determine the greatest forces on the package, the foam strain is not permitted to exceed 70%, thereby insuring a high degree of accuracy for the prediction of impact forces.



As stated above, the integrity of the analysis method used to evaluate the impact forces requires that none of the protrusions on the side of the cask or the cylindrical edge of the lead and steel shield actually strike the unyielding surface. While such an impact would not necessarily cause a loss of packaging effectiveness, the loads output from the various impact analysis programs used to verify the design would not be correct. A determination of the actual loads would involve a fairly complicated analysis for which there is little experimental data to verify the results. Therefore, the overpack has been designed to insure that package 'hard spots' do not strike the impact surface.

The NuPac 10/140MB employs a very efficient overpack design, which insures that protuberances such as the tie-down lugs and EnviroLocks are adequately protected during the impact events, yet the sides of the cask are not protected more than required where there are no such protuberances. Such a design makes for a lighter overpack than might otherwise be required, but forces certain bounding calculations since the impact analysis programs are written for a more simple design. These bounding calculations are described in detail in Sections 2.6.7 and 2.7.1.

### 2.2 Weights and Centers of Gravity

The weight of the cask and payload is approximately 65,000 lb. The center of gravity for the assembled package is located at the approximate geometric center of the assembly.

### 2.3 Mechanical Properties of Materials

The cask outer shell, tiedown lug gussets and some EnviroLock<sup>tm</sup> binder components are fabricated from ASTM A516 Grade 70 carbon steel. The tiedown lugs are constructed of ASTM A517 Grade P alloy steel plate. The inner shell is constructed of ASTM A240 Type 304 stainless steel, and the top and bottom lids are ASTM A351 Grade CF8A Type 304 stainless steel castings. Studs are

ASTM A320, Grade L43. Figures 2.3-1 and 2.3-2 show the tensile and compressive stress-strain curves for lead at various temperatures. EnviroLock<sup>tm</sup> binder threaded components are ASTM A522, Grade I. Properties of these structural components are delineated in Table 2.3-1.

TABLE 2.3-1  
Mechanical Properties of Materials Used in the NuPac 10/140MB Cask

Steel Material Specification	Type or Grade	Temperature (°F)	Strength (ksi)			Elastic Modulus* (10 <sup>6</sup> psi)	Coefficient* of Thermal Expansion <sup>†</sup> (10 <sup>-6</sup> in/in/°F)
			Yield <sup>1</sup> S <sub>y</sub>	Ultimate <sup>2</sup> S <sub>u</sub>	Allowable <sup>3</sup> S <sub>m</sub>		
ASTM A-240 (Inner Shell)	304	-100	-	-	-	29.1	-
		70	30.0**	75.0**	-	28.3	8.46
		100	30.0	75.0	20.0	-	8.55
		200	25.0	71.0	20.0	17.6	8.79
		300	22.5	66.0	20.0	27.0	9.00
		400	20.7	64.4	18.7	26.5	9.19
		500	19.4	63.5	17.5	25.8	9.37
		600	18.2	63.5	16.4	25.3	9.53
700	17.7	63.5	16.0	24.8	9.69		
ASTM A-320 (Studs)	L43	-100	-	-	-	28.5	-
		70	105.0**	125.0**	-	27.8	6.20
		100	105.0	-	35.0	-	6.27
		200	99.0	-	33.0	27.1	6.54
		300	95.7	-	31.9	26.7	6.78
ASTM A-351 (Lids)	CF8A/304	-100	-	-	-	29.1	-
		70	35.0**	77.0**	-	28.3	8.46
		100	35.0	77.0	23.3	-	8.55
		200	29.1	72.8	23.3	27.6	8.79
		300	26.3	67.8	22.6	27.0	9.00
ASTM A-182 (Lids - Alternate Mat'l)	F304	-100	-	-	-	29.1	-
		70	30.0**	70.0****	-	28.3	8.46
		100	30.0	70.0	20.0	-	8.55
		200	25.0	66.2	20.0	27.6	8.79
300	22.5	61.5	20.0	27.0	9.00		
ASTM A-351 (Lids - Alternate Mat'l)	CF8/304	-100	-	-	-	29.1	-
		70	30.0**	70.0**	-	28.3	8.46
		100	30.0	70.0	20.0	-	8.55
		200	25.0	66.2	20.0	27.6	8.79
		300	22.5	61.5	20.0	27.0	9.00
ASTM A-516 (Outer Shell)	70	-100	-	-	-	30.2	-
		70	38.0**	70.0***	-	29.5	5.42
		100	38.0	70.0	23.3	-	5.53
		200	34.6	70.0	23.1	28.8	5.89
		300	33.7	70.0	22.5	28.3	6.26
		400	32.6	70.0	21.7	27.7	6.61
		500	30.7	70.0	20.5	27.3	6.91
		600	28.1	70.0	18.7	26.7	7.17
700	27.4	70.0	18.3	25.5	7.41		
ASTM A-517 (Tiedown Lugs)	P	-100	-	-	-	30.4	-
		70	100.0**	115.0***	-	29.7	6.20
		100	100.0	-	38.3	-	6.27
		200	95.8	-	38.3	29.0	6.54
		300	93.0	-	38.3	28.5	6.78
ASTM A-522 (EnviroLocks)	I	-100	-	-	-	28.5	-
		70	75.0**	100.0**	-	27.8	6.60
		100	-	-	-	-	-
		200	-	-	-	27.1	7.20
		300	-	-	-	26.7	7.60

Lead Material Specification	Type of Grade	Temperature (°F)	Strength (ksi)				Elastic Modulus* (10 <sup>6</sup> psi)	Coefficient* of Thermal Expansion* (10 <sup>-6</sup> in/in/°F)
			Proportional <sup>4</sup> S <sub>p</sub> (Tens)	Yield <sup>5</sup> S <sub>y</sub> (Comp)	Ultimate <sup>6</sup> S <sub>u</sub> (Tens)			
QQ-L-171e	A or C	-99	-----	-----	-----	-----	2.50	15.28
		70	-----	-----	-----	-----	2.34	16.07
		100	0.276	0.215	0.584	0.490	2.30	16.21
		175	0.293	0.107	0.509	0.428	1.62	16.58
		250	0.277	0.107	0.498	0.391	0.844	16.95
		325	0.189	0.093	0.311	0.320	0.642	17.54
		440	-----	-----	-----	-----	1.74	18.50
		620	-----	-----	-----	-----	1.36	20.39

References:

1. ASME Boiler and Pressure Vessel Code, Sect. III, Nuclear Power Plant Components, Division 1, 1983 Edition, Tables I-2.1, I-2.2, I-13.1 and I-13.3, except as noted.
2. Ibid, Tables I-3.1 and I-3.2, except as noted.
3. Ibid, Tables I-1.1, I-1.2, I-1.3 and I-11.1
4. Ibid, Table I-6.0
5. Ibid, Table I-5.0
6. WADC Technical Report 57-695, ASTIA Document No. 151165, Determination of the Mechanical Properties of a High Purity Lead and a 0.058% Copper-Lead Alloy, April 1958, by Thomas Tietz, Stanford Research Center, pp. 21,26
7. Ibid
8. Ibid, p.14
9. NUREG/CR-0481, SAND77-1872, An Assessment of Stress-Strain Data Suitable for Finite Element Elastic - Plastic Analysis of Shipping Containers, H. J. Rack and G. A. Knorovsky, Sept. 1978, p.66
10. Ibid, p. 56

\* Mean from 70°F

\*\* ASME Boiler and Pressure Vessel Code, Sect. II, Material Specifications, Part A, 1983 Edition

\*\*\* Ibid, minimum of specified range

\*\*\*\* Ibid, derated from 75 ksi for sections greater than 5.0 in. thick

Notes: Steel density taken at 0.283 lb/in<sup>3</sup>, Poisson's Ratio = 0.3  
Lead density taken at 0.41 lb/in<sup>3</sup>, Poisson's Ratio = 0.45, melting point = 620°F.

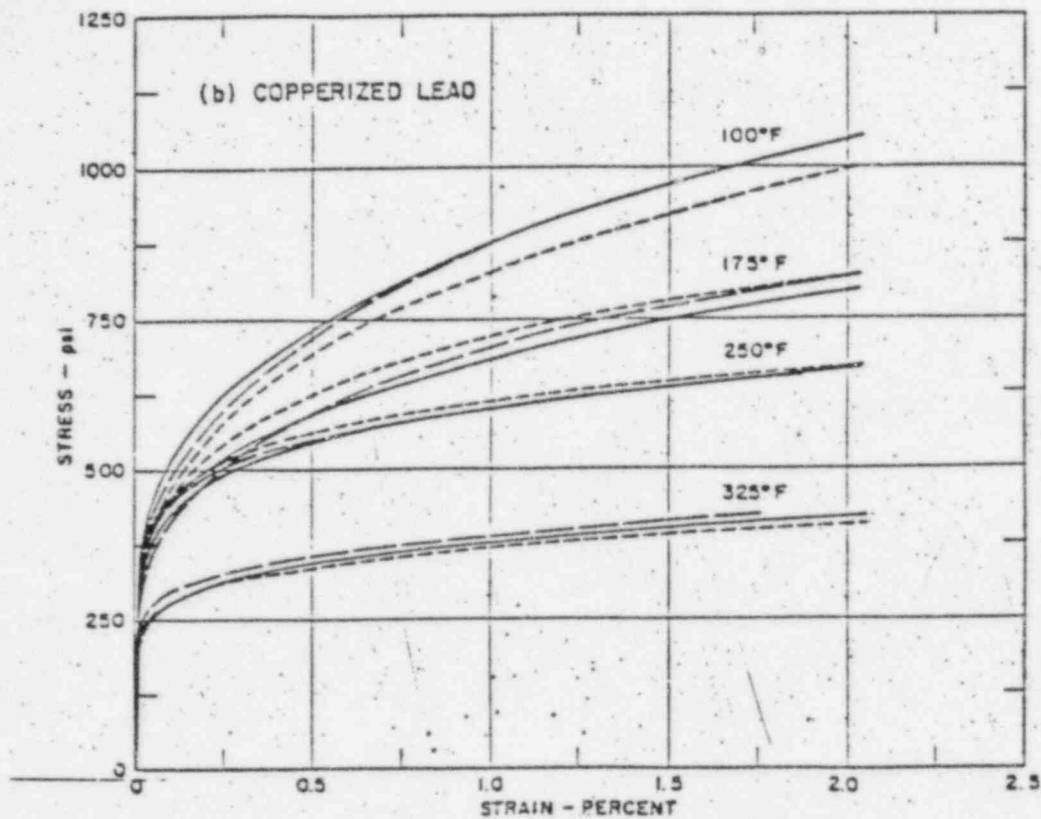


FIGURE 2.3-1

Tensile Stress-Strain Curves to 2% Strain At a Strain Rate of 0.005 In/In/Min

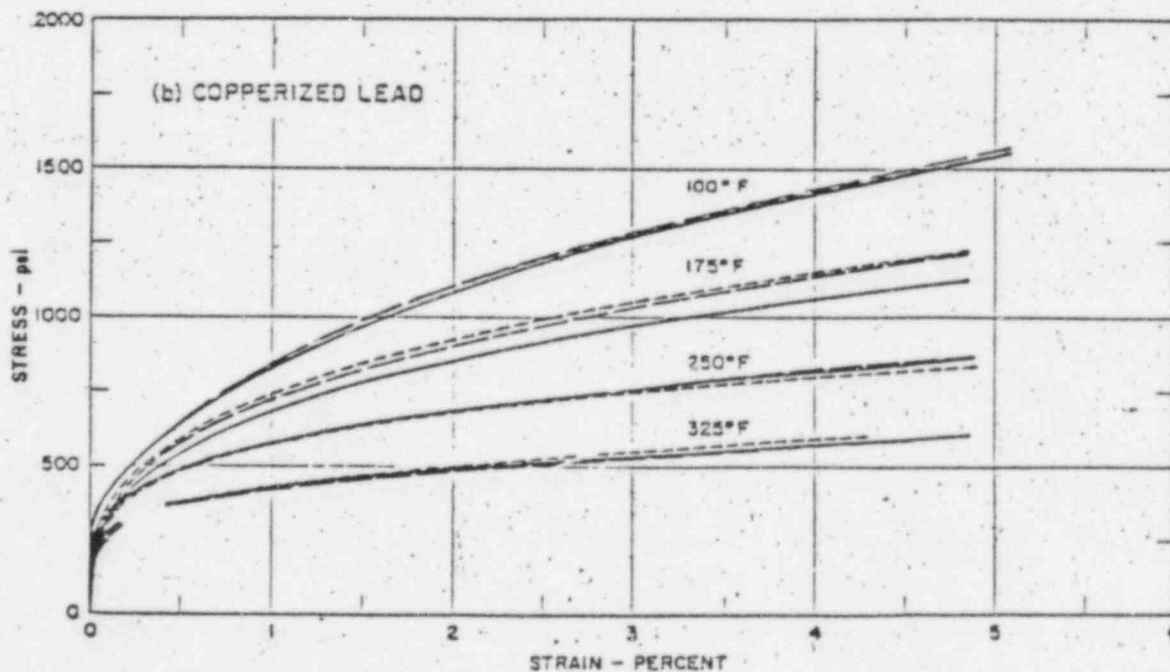


FIGURE 2.3-2

Compression Stress-Strain Curves to 5% Strain At a Strain Rate of 0.005 In/In/Min

The lead shielding will possess those properties referenced in WADC Technical Report 57-695, ASTIA Document No. 151165, Determination of the Mechanical Properties of a High-Purity Lead and a 0.058% Copper-Lead Alloy, April 1958, by Thomas Tietz, Stanford Research Institute, pp. 14, 21 and 26.

#### 2.4 General Standards for All Packages

This section demonstrates that the general standards for all packages are met.

##### 2.4.1 Minimum Package Size

The NuPac 10/140MB package does not have any overall dimension less than 4 inches.

##### 2.4.2 Tamper-proof Feature

The NuPac 10/140MB cask will be sealed with an approved tamper indicating seal and suitable locks to prevent inadvertent and undetected opening.

##### 2.4.3. Positive Closure

As described in Section 1.2.1, the positive closure system consists of a primary lid secured by eight high strength EnviroLock<sup>tm</sup> binders and a secondary lid affixed with eight 1-1/4 inch diameter studs.

##### 2.4.4. Chemical and Galvanic Reactions

The materials from which this package is fabricated (carbon, alloy and stainless steel, lead and polyurethane foam) will not cause significant chemical, galvanic, or other reaction in air, nitrogen, or water atmosphere. The technical basis for this fact is that all metallic materials of construction are essentially of equal potential in the Galvanic Series of Metals and Alloys.

## 2.5 Lifting and Tie-Down Standards for All Packages

### 2.5.1. Lifting Devices

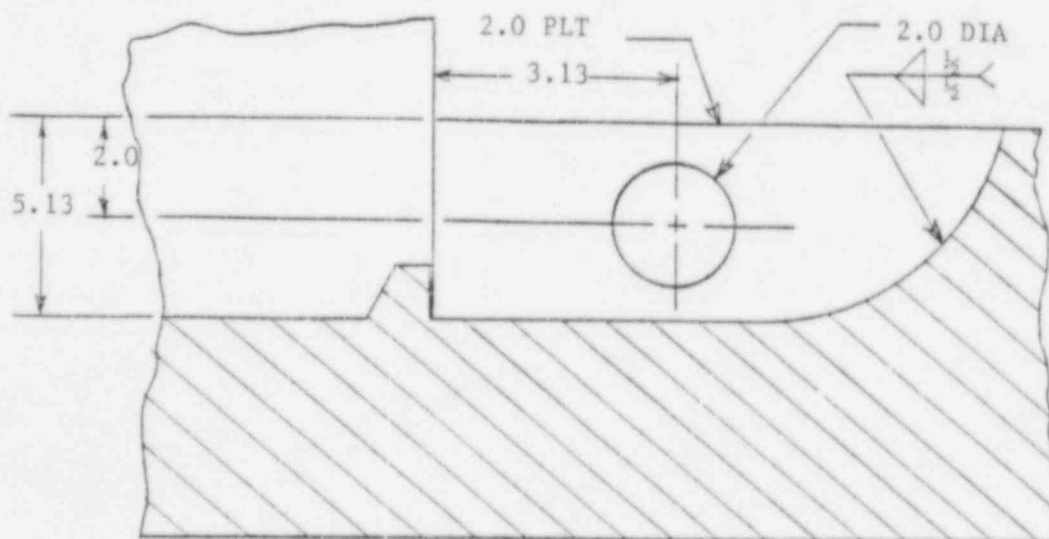
There are three lifting lugs for the lid assembly (primary and secondary lids), and there is a single lifting lug for the secondary lid. All lifting lugs are evaluated per the requirements of 10 CFR 71, Section 71.45(a).

#### 2.5.1.1. Primary Lid Lifting Lugs

The three primary lid lifting lugs will be utilized in handling both the entire cask as well as the primary lid assembly. For this reason, the following analysis will consider loads due to the maximum loaded cask weight. The net weight of the cask is 50,000 lb., and the maximum payload weight is 15,000 lb., for a combined gross weight of 65,000 lbs. 10 CFR 71 Para. 45(a) states that lifting attachments must be designed with a minimum safety factor of three against yielding. For three lifting lugs and a minimum lifting cable angle of  $60^\circ$  from the horizontal, the load per lug is:

$$P_L = (65,000 \text{ lbs} / \sin 60^\circ)(3) / (3 \text{ lugs})$$

$$P_L = 75,056 \text{ lbs/lug}$$



Using the conventional  $40^\circ$  shear-out equation, the yield capacity is:

$$P_s = F_{sy} 2t (e_d - d/2 \cos 40^\circ)$$

Where:  $F_{sy} = (.6)(30,000) \text{ psi (yield)}$   
 $= 18,000 \text{ psi}$

$$t = 2.0 \text{ in.}$$

$$d = 2.00 \text{ in.}$$

$$e_d = 2.00 \text{ in.}$$

$$P_s = (18,000)(2)(2.0 \text{ in.})[2.00 - (2.00 \text{ in.}/2) \cos 40^\circ]$$

$$P_s = 88,844 \text{ lbs}$$

The yield Margin of Safety, using the maximum lug load, is:

$$M.S. = P_s / P_L - 1 = (88,844) / (75,056) - 1$$

$$M.S. = + 0.18$$

The yield capacity of the lug-to-lid weld may be estimated as:

$$P_a = F_{sy} t_w$$

Where:  $F_{sy} = 18,000 \text{ psi (E308 Weld Rod)}$

$$A_w = L_w t_w$$

$$L_w = 2[3.69 + \pi (5.13)/4] = 23.4 \text{ in.}$$

$$t_w = (0.707)(50 \text{ in.}) = 0.35 \text{ in.}$$

$$A_w = (23.4)(0.35)(0.85) = 8.3 \text{ in.}^2$$



Then:  $P_a = (18,000)(8.3) = 149,400 \text{ lbs.}$

The lug-to-lid weld Margin of Safety is:

$$M.S. = P_a / P_L - 1 = (149,400) / (75,056) - 1$$

$$M.S. = + 0.99$$

It can therefore be concluded that the primary lid lifting lugs are more than adequate to resist a load equal to three times the maximum weight of the fully loaded cask.

To evaluate the effect of lifting lug loads on the primary containment system, consider stress levels in the primary lid and EnviroLock<sup>tm</sup> binders. To conservatively analyze the lid structure, assume a flat circular plate of 5.25 in. constant thickness. Ignoring inner and outer edge 'lips', outside diameter is 65.75 in. and inner diameter is 33.25 in. Also assume lug load is uniformly distributed around the inner edge, and is:

$$w = P_v / \pi D_i$$

Where

$P_v$  = Vertical Component of Lifting Lug Load

$$= (3)(65,000) = 195,000 \text{ lb.}$$

$$w = 195,000 / \pi(33.25) = 1,867 \text{ lb./in.}$$

From Roark and Young, Formulas for Stress and Strain, 5th ed., Table 24, case 1a, maximum bending moment is:

$$M_{max} = M_{tb}$$

Where:

$$M_{tb} = K_{Mtb} w a$$

$$a = \text{Outside Radius} = 65.75/2 = 32.88 \text{ in.}$$

$$b = \text{Inside Radius} = 33.25/2 = 16.63 \text{ in.}$$

$$b/a = 16.63/32.88 = 0.506$$

Therefore:

$$K_{Mtb} = 0.778$$

and:

$$M_{tb} = (0.778)(1,867)(32.88) = 47,810 \text{ in.-lb./in.}$$

Maximum bending stress thus becomes:

$$S_{\max} = 6M_{tb}/t^2$$

Where:

$$t = \text{Plate Thickness} = 5.25 \text{ in.}$$

$$S_{\max} = (6)(47,810)/(5.25)^2 = 10,406 \text{ psi}$$

Note that the horizontal component of the lifting load will tend to induce a bending moment of opposite sign as that resulting from the vertical component. This will act to reduce maximum bending stress. Therefore, the above stress value is the maximum possible bending stress that could result from the regulatory lifting requirements.

Maximum anticipated lid temperature at the inner edge (point of maximum stress) for normal conditions of transport will be 130°F (refer to Section 3.0, Thermal Evaluation for details). Interpolating Table 2.3-1 for this temperature results in a material yield strength of 28,500 psi. The Margin of Safety for 1/3 yield then becomes:

$$M.S. = 28,500/10,406 - 1 = + 1.74$$

The maximum EnviroLock<sup>tm</sup> binder load that can be anticipated from lifting lug loads is:

$$P_B = (3)(65,000)/8 = 28,146 \text{ lb./binder}$$

Tensile yield strength of the EnviroLock<sup>tm</sup> is given in Section 2.10.4 as 187,500, so the binder Margin of Safety is thus:

$$M.S. = 187,500/28,146 - 1 = +5.66$$

All the margins of safety for all components are larger than the 0.17 margin for the tear out of the eye of the lug indicating that its failure would not affect the integrity of the cask.

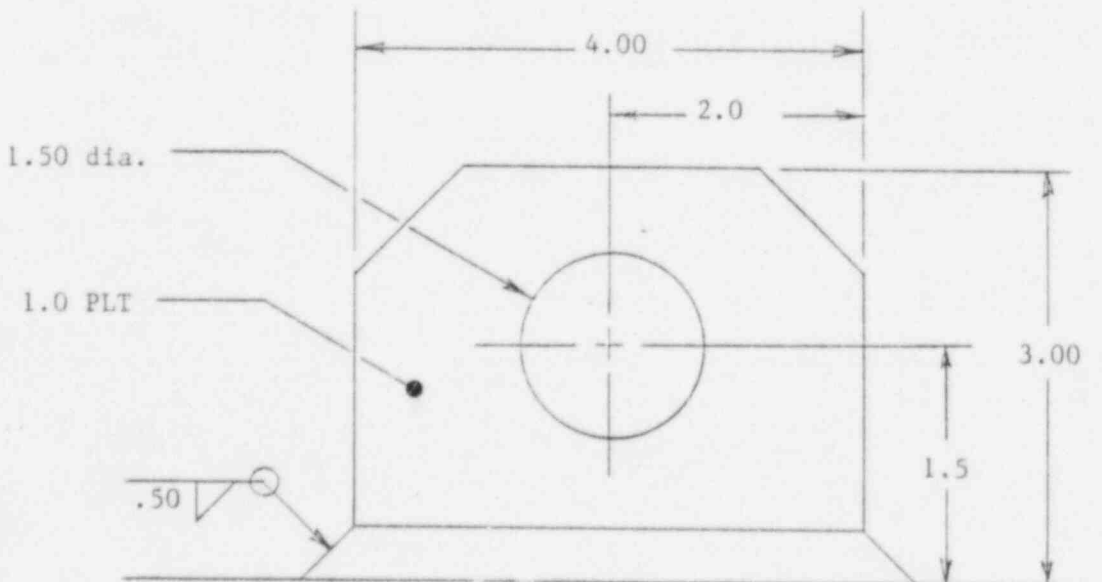
Thus, lifting forces will not significantly affect the containment capability of the cask.

#### 2.5.1.2. Secondary Lid Lifting Lug

The secondary lid weight will be 1,660 lbs. The total lug load is then:

$$P_L = (1660 \text{ lbs})(3)$$

$$P_L = 4,980 \text{ lbs}$$



Using the conventional  $40^\circ$  shear-out equation, the yield capacity is:

$$P_s = F_{sy} 2t (e_d - d/2 \cos 40^\circ)$$

Where:  $F_{sy} = 18,000$  psi (yield)

$$t = 1.0 \text{ in.}$$

$$d = 1.5 \text{ in.}$$

$$E_d = 1.5 \text{ in.}$$

$$P_s = (18,000)(2)(1.0)[1.5 - (1.5/2) \cos 40^\circ]$$

$$P_s = 33,317 \text{ lbs}$$

The yield Margin of Safety, using the maximum lug load, is:

$$M.S. = P_s / P_L - 1 = (33,317) / (4,980)$$

$$M.S. = + 5.69$$

The yield capacity of the lug-to-lid weld may be estimated as:

$$P_a = F_{sy} t_w$$

Where:  $F_{sy} = 18,000$  psi (E308 Weld Rod)

$$A_w = L_w t_w$$

$$L_w = 2(4.0 \text{ in.} + 1.0 \text{ in.}) = 10.0 \text{ in.}$$

$$t_w = (0.707)(.50 \text{ in.}) = 0.35 \text{ in.}$$

$$A_w = (10.0)(.35) = 3.5 \text{ in.}^2$$

Then:  $P_a = (18,000)(3.5) = 63,000 \text{ lbs.}$

The lug-to-lid weld Margin of Safety is:

$$M.S. = P_a/P_L - 1 = (63,000)/(4,980) - 1$$

$$M.S. = + \text{Large}$$

The secondary lid is held on by the use of eight 1-1/2 inch ASTM 320 L43 bolts.

They have a yield load of:

$$P_y = 1.4041 (105,000) = 147,430 \text{ lbs/bolt}$$

or

$$\begin{aligned} P_{y\text{-total}} &= 8 (147,430) \\ &= 1,179,444 \text{ lbs} \end{aligned}$$

This gives a yield margin of safety of:

$$M.S. = P_{y\text{-total}}/P_L - 1 = 1,179,444/4,980 - 1 + \text{Large}$$

Therefore, by comparing the margins of safety it can be concluded that the secondary lid lift eye will fail prior to any of the containment boundary components.

It can therefore be concluded that the secondary lid lifting lug is more than adequate to resist a load equal to three times its normal maximum load. Since the secondary lid lifting lug is not designed to react the full package load, it will be covered during transit.

2.5.2. Tie-down Devices

Four tie-down lugs are provided to resist transportation induced loads. From 10 CFR 71, Para. 71.45(b)(1), the required load factors are:

$$A_x = 10g \text{ (longitudinal)}$$

$$A_y = 5g \text{ (lateral)}$$

$$A_z = 2g \text{ (vertical)}$$

The four tie-down lugs are located with their lug-eyes at  $90^\circ$  intervals around the package side wall. The lugs are positioned at an angle of  $38^\circ$  with respect to the horizontal, with their end tips just below the lower surface of the upper overpack. To evenly distribute the tie-down cable load from the lug into the cask outer shell, two pairs of gussets were added to the lug, as shown in Figure 2.5.2-1. The general tie-down arrangement for the NuPac 10/140MB Cask is shown in Figure 2.5.2-2.

From the geometry given in Figure 2.5.2-2, the cable tension due to horizontal accelerations can be determined by summing moments about the bottom corner of the package opposite the reacting cables. Conservatively ignoring the weight of the cask itself, the longitudinal acceleration case can be derived as follows:

$$(A_x c)W = 2 (P_v d' + P_h h)$$

But,

$$(A_x c)W = 2P_C (B_z d' + B_x h)$$

Where:  $B_x$  = Cable Direction Cosine with Respect to the X-axis  
 $= x/\text{Cable Length } L$

$$B_z = z/L$$

$$L = (x^2 + y^2 + z^2)^{1/2}$$

FIGURE 2.5.2-1  
TIE-DOWN LUG GEOMETRY

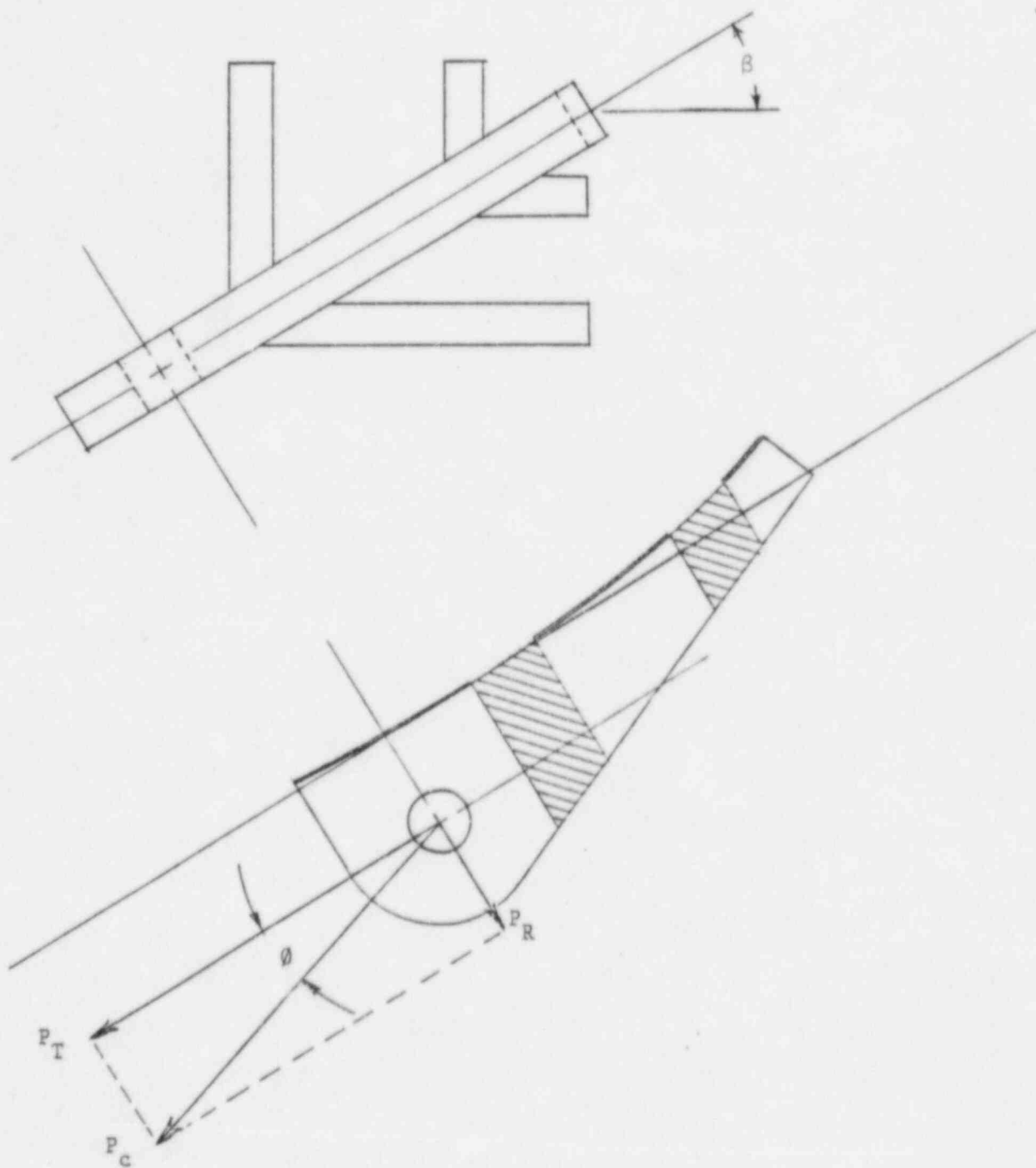
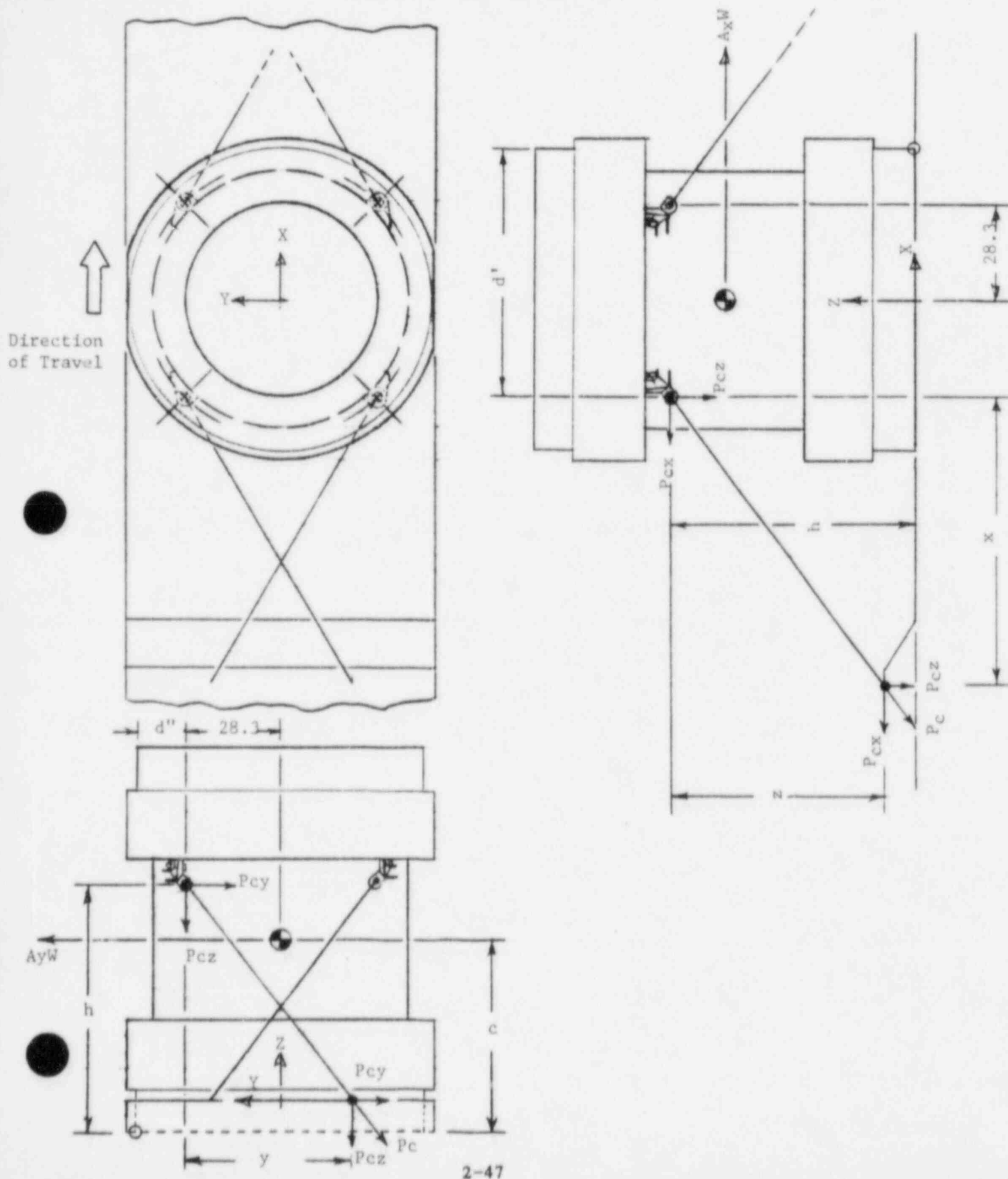


FIGURE 2.5.2-2  
TIE-DOWN CABLE ARRANGEMENT





Solving for  $P_C$ :

$$P_{C \text{ long}} = W/2 [(A_x c)/(B_z d' + B_x h)]$$

Similarly, the cable tension due to the lateral acceleration is:

$$P_{C \text{ lat}} = W/2 [(A_y c)/(B_z d'' + B_y h)]$$

Where:  $B_y = y/L$

The cable tension due to the vertical acceleration is simply:

$$4P_v = A_z W = 4B_z P_C$$

Solving for  $P_C$ :

$$P_{C \text{ vert}} = A_z W / 4B_z$$

These three loads will coincide for the most severely loaded cable:

$$P_C = W/2 [A_x c / (B_z d' + B_x h) + A_y c / (B_z d'' + B_y h) + A_z / 2B_z]$$

Where, for the NuPac 10/140MB Cask:

$$W = \text{Cask Gross Weight} = 65,000 \text{ lb.}$$

$$c = 59.75 \text{ in.}$$

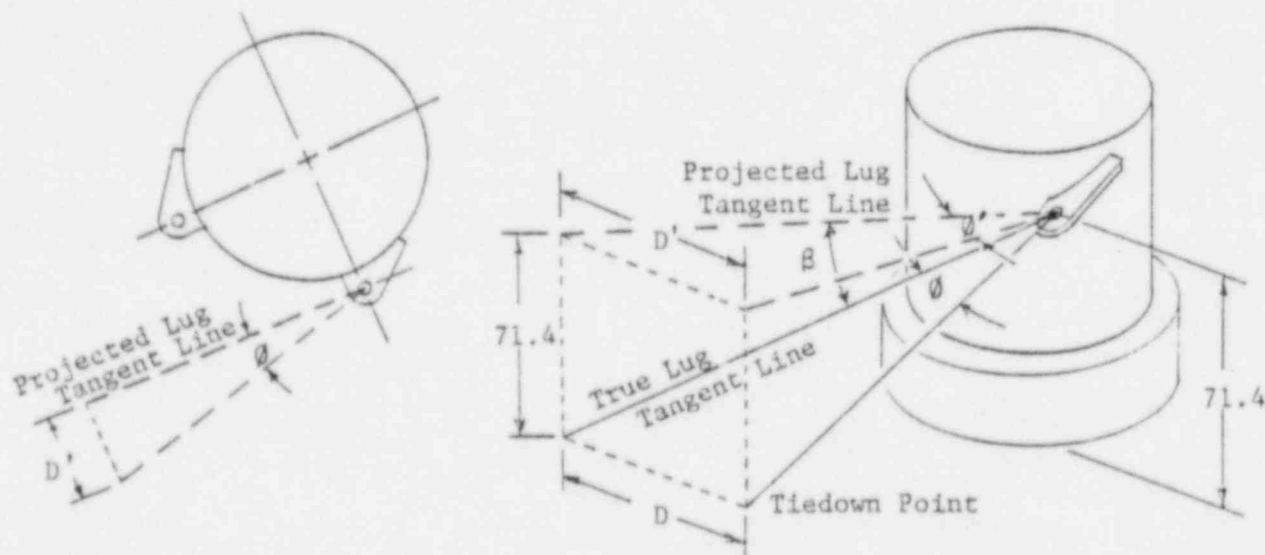
$$d' = 73.78 \text{ in.}$$

$$d'' = 19.72 \text{ in.}$$

$$h = 71.40 \text{ in.}$$

To obtain the tie-down loads, the direction cosines of the tie-down cable must be defined. Since the cable will always lie in the plane of the tie-down lug, whose angle  $\beta$  is constant, the cable direction cosines will be entirely dependent on the cable angle  $\theta$ . Cable angle is defined as the true angle which the tie-down cable makes with respect to the tangent line of the tie-down lug (refer to Figure 2.5.2-1).

Cable direction cosines can be determined as a function of lug angle  $\beta$  and cable angle  $\theta$  in the following manner:



$$\text{True Lug Tangent Line Length } T = h / \sin \beta$$

$$\text{True Deviation Distance } D = \text{Projected Deviation Distance } D' = T \tan \theta$$

$$\text{Projected Lug Tangent Line Length } T' = h / \tan \beta$$

To allow some flexibility in the tie-down arrangement, two cable angles were investigated. One angle,  $18^\circ$ , corresponds to the angle at which the line of action of the cable describes a tangent with the centroid of the cask outer wall. This is considered to be the optimum configuration for obtaining the most uniform load distribution from the tie-down lug into the cask outer wall. Thus, tie-down location is:

$$\text{True Lug Tangent Line Length } T = 71.40 / \sin 38^\circ = 115.97 \text{ in.}$$

$$\text{Deviation Distance } D = (115.97)(\tan 18^\circ) = 37.68 \text{ in.}$$

$$\text{Projected Lug Tangent Line Length } T' = 71.40 / \tan 38^\circ = 91.38 \text{ in.}$$

These dimensions were used to locate the trailer tie-down point, shown in Appendix 2.10.3. The coordinates of this location were then utilized in calculating direction cosines, as defined above (refer to Figure 2.5.2-2), with which the corresponding maximum tie-down load could be determined. This load, calculated in Appendix 2.10.3, was found to be 537,464 lb.

In order to obtain greater lateral support for the cask in its tied down position (refer to Figure 2.5.2-2), a smaller cable angle,  $14^\circ$ , was also selected for evaluation. In an analysis similar to that above and detailed in Appendix 2.10.3, the tie-down cable load for this angle was found to be 508,265 lb.

To ensure that lug and cask outer shell stresses did not exceed the regulatory limitation (material yield strength) under these tie-down loads, a detailed computer analysis was undertaken. This analysis was performed utilizing the finite element program ANSYS, Revision 4.1c, available on the Boeing Computer Services (BCS) National Network, MAINSTREAM - EKS. The capabilities of ANSYS

are outlined in Appendix 2.10.2, and details of the analysis are given in Appendix 2.10.3.

From the above tie-down loads analysis, it is apparent that cable direction cosines, and thus loads, will change with varying cable angle. Since the finite element analysis is based entirely on elastic material properties, element stresses can be varied in direct proportion to the changing cable load. For analysis purposes, a 500,000 lb. cable load was applied to the lug eye. Adjusted stress levels for the varying cable loads are calculated in Appendix 2.10.2 and summarized in Table 2.5.2-1. Resulting stress Margins of Safety are also given in Table 2.5.2-1.

Each tie-down lug is made of 2.5 inch thick ASTM A-517 steel plate welded to the cask outer skin. The lug is designed and positioned so that the tie-down cable lies in the plane of lug, and there are no twisting moments induced in the lug. The finite element analysis results for the lug are outlined in Appendix 2.10.2 and summarized in Table 2.5.2-1.

To check lug shear yield capacity, the conventional  $40^\circ$  shear-out equation was utilized:

$$P_{sy} = F_{sy} 2t [e_d - (d/2) \cos 40^\circ]$$

Where:  $F_{sy} = (.6)(100,000 \text{ psi}) = 60,000 \text{ psi}$

$$t = 2.5 \text{ in.}$$

$$e_d = 3.0 \text{ in.}$$

$$d = 2.25 \text{ in.}$$

Then:  $P_{sy} = (60,000)(2)(2.5)[(3.0) - (2.25/2) \cos 40^\circ]$

$$= 641,460 \text{ lb.}$$

TABLE 2.5.2.-1

## Tie-Down Lug Analysis Stress Levels and Margins of Safety

Structural Component	Tie-Down Cable Angle	
	18°	14°
Maximum Outer Skin Stress	35,719 psi	33,418 psi
Margin of Safety	+0.05	+0.12
Maximum Tie-Down Lug Stress	88,398 psi	78,772 psi
Margin of Safety	+0.13	+0.27
Maximum Tie-Down Lug Weld Stress	31,927 psi	32,796 psi
Margin of Safety	+0.26	+0.23

Shear yield margin of safety is:

$$M.S. = (641,460/537,464) - 1 = +0.19$$

For shackle pin bearing stress, assume cable load is evenly distributed around one-half of the lug-eye diameter. The maximum cable load then becomes:

$$\begin{aligned} F_b &= (100,000 \text{ psi})(2.25 \text{ in})(2.50 \text{ in}) \\ &= 562,500 \text{ lb.} \end{aligned}$$

$$\text{Then: } M.S. = (562,500/537,464) - 1 = +0.05$$

The cable load consists of both radial and tangential (to the cask wall) components, introducing both a bending moment and a shear load into the outer shell through the lug-to-shell weld. The weld stresses in the lug-to-shell weld are thus composed of pure shear and tension/compression due to the moments (refer to Figure 2.5.2-1).

With the tie-down cable acting in the plane of the lug, and assuming weld load components parallel to the lug tangent line, the lug weld stress components can be determined. Results are given in Appendix 2.10.2 and summarized in Table 2.5.2-1.

To ensure that excessive cable loads will not result in damage to the cask, the lug ultimate shear-out capacity was evaluated:

$$P_{su} = 2F_{su}t[e_d - (d/2)\cos 40^\circ]$$

$$\begin{aligned} \text{Where: } F_{su} &= \text{Maximum Shear Strength of Lug Material} \\ &= (.6)(135,000) = 81,000 \text{ psi} \end{aligned}$$

$$\begin{aligned} P_{su} &= (2)(81,000)(2.5)[3.0 - (2.25/2)\cos 40^\circ] \\ &= 865,971 \text{ lb.} \end{aligned}$$

Likewise, ultimate strength of the lug welds was checked for the two extreme cable angles, as shown in Appendix 2.10.3. The results indicated that the controlling failure load would be lug shear-out at 865,971 lb. Applying this load at the maximum cable angle of  $18^{\circ}$  (worst case load condition) and directly ratioing maximum stress obtained from the finite element analysis yields a cask outer shell stress of:

$$P_{\text{shell}} = (865,971/500,000)(33,229) = 57,551 \text{ psi}$$

Specified minimum ultimate strength of the A-516 Gr. 70 material comprising the cask outer shell is 70,000 psi. Failure margin of safety for the cask is thus:

$$\text{M.S.} = 70,000/57,551 - 1 = +0.22$$

It can therefore be concluded that the tie-down lug is more than adequate to resist the loads specified in 10 CFR 71 Para. 45(b)(1), and yet not compromise the structural integrity of the cask under more extreme loading conditions.

## 2.6 Normal Conditions of Transport

The NuPac 10/140MB cask has been designed and the contents are so limited (as described in Section 1.2.3 above) that the performance requirements specified in 10 CFR 71.71 will be met when the package is subjected to the normal conditions of transport specified therein. The ability of the NuPac 10/140MB to satisfactorily withstand the normal conditions of transport has been assessed as described on the following pages.

### 2.6.1 Heat

A detailed thermal analysis can be found in Section 3.4 wherein the package was exposed to a combination of solar heating, internal decay heat and 100°F ambient air. The steady state analysis conservatively assumed a 24-hour day as maximum solar heat load. The maximum steady state temperature was found to be 160°F. This temperature will have no detrimental effect on the package.

### 2.6.2 Cold

For the cold condition, a -40°F steady state ambient temperature is assumed as is no internal heat generation. This will result in a uniform temperature throughout the cask of -40°F. The materials of construction for the cask are not adversely affected by the -40°F condition. In particular, brittle fracture is not a concern, as discussed in Section 2.1.2.2.1.

The only concern identified with the cold condition is with shrinkage of the lead onto the inner shell of the outer cask. As shown by the following calculations, a hoop stress of -2,914 psi and an axial stress of -2,820 psi can develop in the inner shell when cooled to -40°F. This case is independent of other load cases and will not, therefore, limit the cask design. However, a -20°F case must be considered as a possible initial condition for other load cases per 10 CFR 71.71(b). The hoop stress will be approximately -2,462 psi



and the axial stress approximately -2,705 psi at -20°F. These stresses are determined by conservatively neglecting creep effects.

#### Fabrication Stresses Due to Lead Pour:

Assume a uniform steel and lead temperature of 620°F. The static head (pressure) due to a column of lead is simply:

$$p = \rho h$$

Where:

$$\rho = 0.386 \text{ lb/in}^3 \quad (\text{liquid lead})$$

$$h = 77.5 + 10.0 = 87.5 \text{ in} \quad (10.0 \text{ inches for overflow pipe})$$

Then,

$$p = (0.386)(87.5) = 33.78 \text{ psi}$$

The physical properties of ASTM A-240, Type 304, stainless steel used for the cask inner shell are extracted from Section 2.3, are:

Temperature (°F)	E (10 <sup>6</sup> psi)	$\alpha$ (10 <sup>-6</sup> in/in/°F)	$\mu$
70	28.3	8.46	0.3
100	28.1	8.55	0.3
200	27.6	8.79	0.3
300	27.0	9.00	0.3
400	26.5	9.19	0.3
500	25.8	9.37	0.3
600	25.3	9.53	0.3
620	25.2	9.56	0.3

The physical properties of ASTM A-516, Grade 70 carbon steel used for the cask outer shell are:

Temperature (°F)	E ( $10^6$ psi)	$\alpha$ ( $10^{-6}$ in/in/°F)	$\mu$
70	29.5	5.42	0.3
100	29.3	5.53	0.3
200	28.8	5.89	0.3
300	28.3	6.26	0.3
400	27.7	6.61	0.3
500	27.3	6.91	0.3
600	26.7	7.17	0.3
620	26.5	7.22	0.3

The physical properties of lead (copperized) are also taken from Section 2:3, as follows:

Temperature (°F)	E ( $10^6$ psi)	$\alpha$ ( $10^{-6}$ in/in/°F)	$\mu$
70	2.34	16.07	0.45
100	2.30	16.22	0.45
200	2.17	16.70	0.45
300	2.00	17.33	0.45
400	1.82	18.16	0.45
500	1.61	19.12	0.45
600	1.40	20.17	0.45
620	1.36	20.38	0.45

Where:

E = Young's (Elastic) Modulus

$\alpha$  = coefficient of thermal expansion (mean from 70 ° F)

$\mu$  = Poisson's Ratio

At 70° F, the steel shell geometry is as follows:

Geometry (at 70° F)	Inner Shell (in)	Outer Shell (in)
Inside Diameter, $D_i$	66.00	72.00
Outside Diameter, $D_o$	67.50	74.50
Shell Thickness, $t$	0.75	1.25
Mean Shell Radius, $R$	33.375	36.625

At 620° F, without lead, the shells will grow as follows:

$$R' = R(1 + \alpha \Delta T)$$

$$t' = t(1 + \alpha \Delta T)$$

$$\Delta T = 620 - 70 = 550^\circ \text{ F}$$

$$\alpha_s = 9.56(10)^{-6} \text{ in/in/}^\circ\text{F (304 Stainless Steel)}$$

$$\alpha_c = 7.20(10)^{-6} \text{ in/in/}^\circ\text{F (A-516 Carbon Steel)}$$

Then,

$$R'_i = 33.375[1 + 9.56(10)^{-6}(550)] = 33.5505 \text{ in}$$

$$t'_i = 0.75[1 + 9.56(10)^{-6}(550)] = 0.7539 \text{ in}$$

$$R'_o = 36.625[1 + 7.20(10)^{-6}(550)] = 36.7701 \text{ in}$$

$$t'_o = 1.25[1 + 7.20(10)^{-6}(550)] = 1.2550 \text{ in}$$

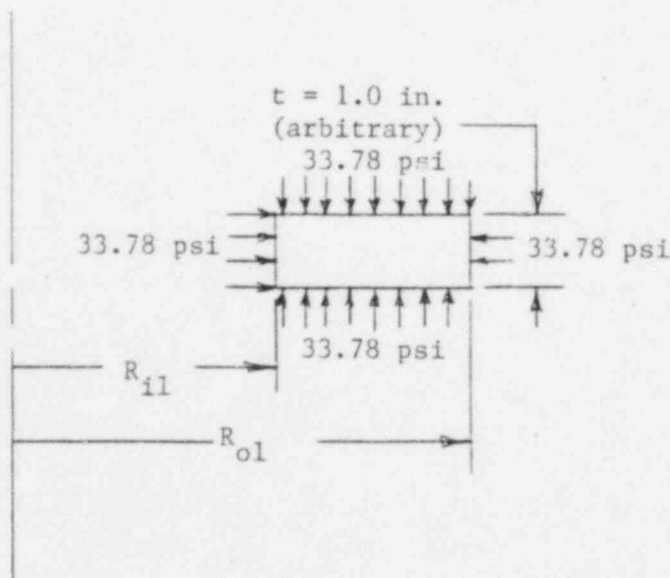
When filled with molten lead, the inner and outer shells of the outer cask will be subjected to the 33.78 psi pressure head. This will decrease the radius of the inner shell and increase the radius of outer shell. Utilizing Roark, Raymond J., and Young, Warren C., Formulas For Stress and Strain, 5th ed., Table 29, Case 1b, the change in radius for each shell is:

$$\begin{aligned}\Delta R'_i &= q(R'_i)^2/Et'_i \\ &= (-33.78)(33.5505)^2/25.2(10^6)(0.7539) = -0.0020 \text{ in.} \\ \Delta R'_o &= q(R'_o)^2/Et'_o \\ &= (33.78)(36.7701)^2/25.5(10^6)(1.2550) = 0.0014 \text{ in.}\end{aligned}$$

In summary, the initial condition of the steel shells just before lead solidification at 620° F,  $(R' + \Delta R' \pm t'/2)$  is:

Shell	Inner Radius (in)	Outer Radius (in)
Inner	33.1716	33.9255
Outer	36.1440	37.3990

Lead experiences a decrease in volume of approximately 3.85% upon solidification. As the lead solidifies, it will shrink and liquid lead from above will fill in between the solidifying lead and the outer cask inner and outer shells, thus maintaining a 33.78 psi pressure on the shells. Eventually, the full annular region between the shells will be filled with lead, subjected to a loading as illustrated below:



Note: the 33.78 psi pressure actually only exists at the base of the lead column and will linearly decrease toward the top of the column.

Under this loading,  $R_{i1} = 33.9255$  inches and  $R_{o1} = 36.1440$  inches, the outer radius of the inner shell and inner radius of the outer shell, respectively. Geometry of the unloaded lead shell is determined as follows:

$$R_{o1} = a + \Delta a$$

$$R_{i1} = b + \Delta b$$

$a$  = outer radius

$b$  = inner radius

Solve for  $a$  and  $b$  by superimposing Cases 1b and 1d, Table 32, of the Reference above with  $q = 33.78$  psi:

$$\begin{aligned}\Delta a &= qab^2(2 - \mu)/E(a^2 - b^2) - qa[a^2(1 - 2\mu) + b^2(1 + \mu)]/E(a^2 - b^2) \\ &= R_{o1} - a\end{aligned}$$

$$\begin{aligned}\Delta b &= qb[a^2(1 + \mu) + b^2(1 - 2\mu)]/E(a^2 - b^2) - qba^2(2 - \mu)/E(a^2 - b^2) \\ &= R_{i1} - b\end{aligned}$$

Simplifying the two equations yields:

$$[1] \quad \Delta a = -qa(1-2\mu)/E$$

$$[2] \quad \Delta b = -qb(1-2\mu)/E$$

$$\text{For } q(1-2\mu)/E = (33.78)[1-2(.45)]/1.36(10)^6 = 2.484(10)^{-6},$$

$$[1] \quad [1-2.484(10)^{-6}]a = R_{o1}$$

$$[2] \quad [1-2.484(10)^{-6}]b = R_{i1}$$

Where:

$$E = 1.36(10)^6 \text{ psi}$$

$$\mu = 0.45$$

$$R_{o1} = 36.1440 \text{ in}$$

$$R_{i1} = 33.9255 \text{ in}$$

Then, solving for a and b:

$$a = 36.14409 \text{ in.}$$

$$b = 33.92558 \text{ in.}$$

At this point, the hoop stress in the inner and outer steel shells of the outer cask is:

$$\begin{aligned} \sigma_i &= pR_i/t_i \\ &= (-33.78) \left[ (33.9255 + 33.1716)/2 \right] / (33.9255 - 33.1716) = -1,503 \text{ psi} \end{aligned}$$

$$\begin{aligned} \sigma_o &= pR_o/t_o \\ &= (33.78) \left[ (37.399 + 36.144)/2 \right] / (37.399 - 36.144) = 990 \text{ psi} \end{aligned}$$

Again, utilizing Table 32, Cases 1b and 1d, of the Reference, the stress in the lead shell,  $\sigma_1$  = axial,  $\sigma_2$  = hoop,  $\sigma_3$  = radial, upon solidification, may be determined as:

$$\sigma_1 = \sigma_2 = \sigma_3 = -33.78 \text{ psi}$$

Determine the temperature at which lead will separate from the outer shell,  $T_{sep}$ . Separation initiates when the lead outer radius,  $R_{o1}$ , and outer steel shell inner radius,  $R_{os}$ , become equal. The unrestrained state of each of the above shells, at  $620^\circ \text{ F}$ , is:

$$R_{os} = R'_o - t'_o/2 = 36.1426 \text{ in}$$

$$R_{ol} = a = 36.14409 \text{ in}$$

At 70° F, the lead outer radius, R, is such that  $R + R\alpha\Delta T = 36.14409$  inches at 620° F. Then, solving for R:

$$\begin{aligned} R &= 36.14409 / (1 + \alpha\Delta T) \\ &= 36.14409 / [1 + 20.38(10)^{-6}(550)] = 35.7434 \text{ in} \end{aligned}$$

At 70° F, the outer steel shell inner radius is 36.0 inches. At the temperature of separation,  $T_{sep}$ , the following relationship is true:

$$35.7434(1 + \alpha_1\Delta T) = 36.0(1 + \alpha_c\Delta T)$$

A solution for  $T_{sep}$  is achieved by trial and error. At approximately 600° F:

$$\Delta T = 600 - 70 = 530^\circ \text{ F}$$

$$\alpha_1 = 20.17(10)^{-6} \text{ in/in/}^\circ\text{F}$$

$$\alpha_c = 7.42 \times 10^{-6} \text{ in/in/}^\circ\text{F}$$

and,

$$36.1255 \neq 36.1415$$

At 600°F, lead shell outer radius has decreased to less than the outer shell inner radius, e.g., separation has taken place between 620°F and 600°F.

$$\text{At } 620^\circ\text{F, } \Delta R = R_{os} - R_{oa} = -0.001465 \text{ in.}$$

$$\text{At } 600^\circ\text{F, } \Delta R = R_{os} - R_{oa} = 0.01610 \text{ in.}$$

Linearly interpolating for the temperature at  $\Delta R = 0$ :

$$(620 - T_{sep}) / (620 - 600) = (-0.001465 - 0) / (-0.001465 - 0.01610)$$

Or:

$$T_{\text{sep}} = 618.3^{\circ}\text{F}$$

That is, lead separation from the outer shell commences almost immediately when cool-down begins.

At  $618.3^{\circ}\text{F}$ , check press fit of the lead onto the inner steel shell. At  $70^{\circ}\text{F}$ , lead inner radius,  $R$ , is such that  $R + R \alpha \Delta T = 33.92558$  inches at  $620^{\circ}\text{F}$ . Then, solving for  $R$ :

$$\begin{aligned} R &= 33.92558 / (1 + \alpha \Delta T) \\ &= 33.92558 / [1 + 20.38(10)^{-6}(550)] = 33.550 \text{ in} \end{aligned}$$

At  $70^{\circ}\text{F}$ , the steel inner shell outer radius is 33.75 inches. At  $618.3^{\circ}\text{F}$ , the interference is calculated as:

$$\begin{aligned} \delta &= -33.550[1 + 20.362(10)^{-6}(548.33)] + 33.75[1 \\ &\quad + 9.56(10)^{-6}(548.33)] \\ &= +0.002829 \text{ in} \end{aligned}$$

Utilizing the press fit equation (2-63) from Shigley, Joseph E., Mechanical Engineering Design, 3rd ed., McGraw-Hill, the interface pressure,  $p$ , at a temperature of  $618.3^{\circ}\text{F}$ , is:

$$\begin{aligned} \delta &= b_1 p [ [(c^2 + b_1^2) / (c^2 - b_1^2)] + \mu_1 ] / E_1 \\ &\quad + b_s p [ [(b_s^2 + a^2) / (b_s^2 - a^2)] - \mu_s ] / E_s \end{aligned}$$

Where, from previous calculational techniques:

$$a = \text{inner radius of inner steel shell} = 33.1729 \text{ in}$$

$$b_s = \text{outer radius of inner steel shell} = 33.9268 \text{ in}$$

$$b_1 = \text{inner radius of lead shell} = 33.92542 \text{ in}$$

$$c = \text{outer radius of lead shell} = 36.14392 \text{ in}$$



$$E_s = 25.2(10)^6 \text{ psi}$$

$$\mu_s = 0.3$$

$$E_l = 1.36(10)^6 \text{ psi}$$

$$\mu_l = 0.45$$

Thus,

$$\delta = p[4.04545(10)^{-4} + 5.94949(10)^{-5}] = 0.002829 \text{ in}$$

$$p = 47.6 \text{ psi interface pressure}$$

Using thick-walled pressure vessel theory, the inner shell hoop stress is:

$$\begin{aligned}\sigma_s &= -p[(b_s^2 + a^2)/(b_s^2 - a^2)] \\ &= -2,116 \text{ psi}\end{aligned}$$

Likewise, the lead shell hoop stress is:

$$\begin{aligned}\sigma_l &= p[(c^2 + b_l^2)/(c^2 - b_l^2)] \\ &= 752 \text{ psi}\end{aligned}$$

Note that at 325° F, the proportional limit of the lead is 189 psi, or with an offset of 0.2% strain, yield is 311 psi which indicates the lead will yield under such a pressure. To fully accommodate the 0.002829 inch interference, the lead would be required to see a strain of  $0.002829/33.92542 = 0.000083$  in/in, or 0.0083%. Utilizing Figure 2.3-1 from Section 2.3, the corresponding lead stress for a strain of 0.0083% would be approximately 270 psi. The interface pressure would then be:

$$p = \sigma_l / [(c^2 + b_l^2)/(c^2 - b_l^2)]$$

$$p = 17.1 \text{ psi interface pressure}$$

Now, cool to 70° F and summarize the steel and lead shell, stress-free dimensions from the analyses performed above. The geometry and properties are, at 70° F, as follows:

$$a = 33.00 \text{ in}$$

$$b_s = 33.75 \text{ in}$$

$$b_l = 33.550 \text{ in}$$

$$c = 35.7434 \text{ in}$$

$$E_s = 28.3(10)^6 \text{ psi}$$

$$\mu_s = 0.3$$

$$E_l = 2.34(10)^6 \text{ psi}$$

$$\mu_l = 0.45$$

and,

$$\delta = b_s - b_l = 0.200 \text{ in}$$

Utilizing the same press-fit equation as above, the interface pressure is:

$$\delta = b_l p \left\{ \left[ \frac{c^2 + b_l^2}{c^2 - b_l^2} \right] + \mu_l \right\} / E_l + b_s p \left\{ \left[ \frac{b_s^2 + a^2}{b_s^2 - a^2} \right] - \mu_s \right\} / E_s$$

$$\delta = [2.8587(10)^{-4}] p$$

Then,

$$p = 0.200 / 2.8587(10)^{-4} = 700 \text{ psi interface pressure}$$

This corresponds to a lead shell hoop stress of:

$$\begin{aligned} \sigma_l &= p \left[ \frac{c^2 + b_l^2}{c^2 - b_l^2} \right] \\ &= 11,090 \text{ psi} \end{aligned}$$

which, obviously, cannot be sustained.

To fully accommodate the 0.200 inch interference, the lead would be required to see a strain of  $0.200/33.55 = 0.00596$  in/in, or 0.60%. Extrapolating lead stress-strain data from Section 2.3, a hoop stress of approximately 725 psi will exist in the lead for this strain. The effective interface pressure would be:

$$p = \sigma_1 / [(c^2 + b_1^2) / (c^2 - b_1^2)]$$

$$= 45.85 \text{ psi interface pressure}$$

[NOTE:  $\delta$  of inner shell for  $-45.85 \text{ psi} = 2.43(10)^{-5}(-45.85) = -0.0011$  inches, which can be conservatively neglected.]

The hoop stress in the inner steel shell would be:

$$\sigma_s = p[(b_s^2 + a^2) / (b_s^2 - a^2)]$$

$$= -2,041 \text{ psi}$$

Next, consider cooling to  $-20^\circ \text{ F}$  ( $-90 \text{ }^\circ \text{F}$ ) for the worst hoop stress on the inner steel shell during all hypothetical accident drop events. The steel and lead properties may be extrapolated from Table 2.3-1 as:

$$\alpha_s = 8.21(10)^{-6} \text{ in/in/}^\circ \text{F}$$

$$E_s = 29.0(10)^6 \text{ psi}$$

$$\alpha_l = 15.7(10)^{-6} \text{ in/in/}^\circ \text{F}$$

$$E_l = 2.43(10)^6 \text{ psi}$$

The steel and lead shell initial shell conditions are determined as:

$$a = (33.00)[1 + 8.21(10)^{-6}(-90)] = 32.9756 \text{ in}$$

$$b_s = (33.75)[1 + 8.21(10)^{-6}(-90)] = 33.7251 \text{ in}$$

$$b_1 = (33.550) [1 + 15.7(10)^{-6}(-90)] = 33.5026 \text{ in}$$

$$c = (35.7434) [1 + 15.7(10)^{-6}(-90)] = 35.6929 \text{ in}$$

and,

$$\delta = b_s - b_1 = 0.2225 \text{ in}$$

To fully accommodate the 0.2225 inch interference, the lead would be required to see a strain of  $0.2225/33.5026 = 0.0064 \text{ in/in}$ , or 0.64%. Extrapolating from data given in Section 2.3, a hoop stress of approximately 875 psi will exist in the lead for this strain. The effective interface pressure would be:

$$\begin{aligned} p &= \sigma_1 / [(c^2 + b_1^2) / (c^2 - b_1^2)] \\ &= 55.3 \text{ psi interface pressure} \end{aligned}$$

The hoop stress in the inner steel shell, conservatively neglecting the beneficial effects of lead creep, would be:

$$\begin{aligned} \sigma_s &= p[(b_s^2 + a^2) / (b_s^2 - a^2)] \\ &= -2,462 \text{ psi} \end{aligned}$$

Finally, consider cooling to  $-40^\circ \text{ F}$  ( $-110 \text{ AT}$ ) for the worst hoop stress on the inner steel shell. The steel and lead properties, extrapolated from Table 2.3-1, are:

$$\alpha_s = 8.15(10)^{-6} \text{ in/in/}^\circ\text{F}$$

$$E_s = 29.0(10)^6 \text{ psi}$$

$$\alpha_1 = 15.6(10)^{-6} \text{ in/in/}^\circ\text{F}$$

$$E_1 = 2.43(10)^6 \text{ psi}$$

The steel and lead shell initial shell conditions are determined as:

$$a = (33.00) [1 + 8.15(10)^{-6}(-110)] = 32.9704 \text{ in}$$

$$b_s = (33.75)[1 + 8.15(10)^{-6}(-110)] = 33.7197 \text{ in}$$

$$b_1 = (33.550)[1 + 15.6(10)^{-6}(-110)] = 33.4724 \text{ in}$$

$$c = (35.7434)[1 + 15.6(10)^{-6}(-110)] = 35.6821 \text{ in}$$

and,

$$\delta = b_s - b_1 = 0.227 \text{ in}$$

To fully accommodate the 0.227 inch interference, the lead would be required to see a strain of  $0.227/33.4924 = 0.00679$  in/in, or 0.68%. Extrapolating from the data given in Section 2.3, a hoop stress of approximately 1,035 psi will exist in the lead for this strain. The effective interface pressure would be:

$$\begin{aligned} p &= \sigma_1 / [(c^2 + b_1^2) / (c^2 - b_1^2)] \\ &= 65.5 \text{ psi interface pressure} \end{aligned}$$

The hoop stress in the inner steel shell, conservatively neglecting the beneficial effects of lead creep, would be:

$$\begin{aligned} \sigma_s &= p[(b_s^2 + a^2) / (b_s^2 - a^2)] \\ &= -2,915 \text{ psi} \end{aligned}$$

The preceding calculations deal only with the calculation of hoop stresses. Axial stress will also develop in the inner steel and lead shells due to axial shrinkage of the lead. In cooling to  $-20^\circ\text{F}$ , axial strain in the lead, assuming bonding of the lead to the inner steel shell, is:

$$\begin{aligned} \epsilon_a &= [(\alpha_1 - \alpha_s)\Delta T]_{620} + [(\alpha_1 - \alpha_s)\Delta T]_{-20} \\ &= [(20.38 - 9.56)(10)^{-6}(620 - 70)] - [(15.7 - 8.21)(10)^{-6}(-20 - 70)] \\ &= 0.0663 = 0.663\% \text{ strain (tensile)} \end{aligned}$$

Extrapolating from the data in Section 2.3, an axial stress of approximately 990 psi will exist in the lead for this strain. The effective force in the lead shell would be:

$$\begin{aligned} P_a &= pA_1 \\ &= 990\pi[(36.6929)^2 - (33.7251)^2] = 424,854 \text{ lbs} \end{aligned}$$

From equilibrium, this same force can develop in the inner steel shell. Thus, the compressive axial stress in the inner steel shell is:

$$\begin{aligned} \sigma_a &= P/A_i \\ &= -424,854/\pi[(33.7251)^2 - (32.9756)^2] = -2,705 \text{ psi} \end{aligned}$$

This is a conservative estimate in that it assumes the ends of the outer cask inner shell are free and that no load develops in the outer shell.

In cooling to  $-40^\circ\text{F}$ , axial strain in the lead, assuming bonding of the lead to the inner steel shell, is:

$$\begin{aligned} \epsilon_a &= [(\alpha_1 - \alpha_s)\Delta T]_{620} + [(\alpha_1 - \alpha_s)\Delta T]_{-40} \\ &= [(20.38 - 9.56)(10)^{-6}(620 - 70)] + [(15.6 - 8.15)(10)^{-6}(-40 - 70)] \\ &= 0.00677 = 0.677\% \text{ strain (tensile)} \end{aligned}$$

Extrapolating from the data in Section 2.3, an axial stress of approximately 1,035 psi will exist in the lead for this strain. The effective force in the lead shell would be:

$$\begin{aligned} P_a &= pA_1 \\ &= 1,035\pi[(35.6820)^2 - (33.7197)^2] = 442,820 \text{ lbs} \end{aligned}$$

From equilibrium, this same force can develop in the inner steel shell. Thus, the compressive axial stress in the inner steel shell is:

$$\begin{aligned}\sigma_a &= P/A_i \\ &= -442,820/\pi[(33.1797)^2 - (32.9704)^2] = -2,820 \text{ psi}\end{aligned}$$

Again, this calculation conservatively assumed that the ends of the outer cask inner shell are free and that no load develops in the outer shell.

### 2.6.3 Reduced External Pressure

An external pressure of 3.5 psia will result in a cask internal pressure of 11.2 psig, which will be reacted by the lid and its associated closures comprised of 'Enviro-Lock' binders for the primary lid and studs for the secondary lid. Loads on the primary lid 'Enviro-Locks' are calculated as:

$$P_s = Ap/N$$

Where:  $A = \pi D^2/4$

$$p = 11.2 \text{ psi}$$

$$N = 8$$

For the worst case loading:

$$\begin{aligned}P_s &= [\pi(76.15)^2/4](11.2)(1/8) \\ &= 6,376 \text{ lbs.}\end{aligned}$$

The rated load of the NuPac 'EnviroLock'<sup>tm</sup> binder is 250,000 lbs. (see Appendix 2.10.3). Thus, the Margin of Safety is:

$$M.S. = (.7)(250,000)/6,376 - 1 = + \text{Large}$$

For the secondary lid studs, the load is:

$$P_s = \left[ \pi (29.0)^2 / 4 \right] (11.2) (1/8)$$

$$= 925 \text{ lbs.}$$

The stress in the stud is then:

$$\sigma = 925 / (1.407) = 657 \text{ psi}$$

and the Margin of Safety is:

$$M.S. = (105,000/657) - 1 = + \text{Large}$$

Stresses induced in the cylindrical portion of the cask are conservatively estimated by assuming the pressure differential is totally borne by the 0.75 in. thick inner shell. The hoop, longitudinal and radial stresses are:

$$f_h = PR/T = (11.2)(33.375/0.75) = 500 \text{ psi}$$

$$f_l = PR/2T = (11.2)(33.375/0.75)(1/2) = 250 \text{ psi}$$

$$f_r = -P = -11.2 \text{ psi}$$



By the maximum distortion energy theorem, the resulting equivalent stress in the inner shell is:

$$\begin{aligned} f_e &= \{[(f_h - f_l)^2 + (f_l - f_r)^2 + (f_r - f_h)^2]/2\}^{1/2} \\ &= \{[(500 - 250)^2 + (250 + 11.2)^2 + (-11.2 - 500)^2]/2\}^{1/2} \\ &= 442 \text{ psi} \end{aligned}$$

The margin of safety is:

$$M.S. = 30,000/442 - 1 = + \text{ Large}$$

Pressure across the lids is carried in plate bending by the 5.25 in. (minimum) thick steel plates top and bottom. Assuming a circular plate, uniformly loaded and with edges simply supported, the maximum stress can be calculated as follows (ref. Roark, Formulas for Stress and Strain, 4th ed.):

$$f_r = 3W(3M+1)/8\pi Mt^2$$

Where:  $W = (11.2)\pi(66.0)^2/4 = 38,317 \text{ lbs.}$

$$t = 5.25 \text{ in.}$$

$$M = 1/.33 = 3.0$$

$$f_r = (3)(38,317)(10)/[(8\pi)(3)(5.25)]$$

$$f_r = 2,904 \text{ psi}$$

Margin of Safety is:

$$M.S. = 30,000/2,904 - 1 = + \text{ Large}$$

It can therefore be concluded that the packaging can safely react a reduced external pressure of 3.5 psia.

#### 2.6.4 Increased External Pressure

An external pressure of 20 psia will result in a cask internal pressure of -5.3 psig. The magnitude of this pressure is less than for Section 2.6.3 above, so margins of safety for this condition will be even larger than those calculated above.

#### 2.6.5 Vibration

Shock and vibration normally incident to transport are considered to have negligible effects on the NuPac Type B packages.

#### 2.6.6 Water Spray

Since the package exterior is constructed of steel, this test is not required.

#### 2.6.7 Free Drop

The NuPac 10/140MB Shipping Cask weighs approximately 65,000 pounds. Subpart F of 10 CFR 71 requires that a package in excess of 33,000 pounds be capable of resisting the effects of a one foot drop onto a flat, essentially unyielding, horizontal surface striking the surface in a position for which maximum damage is expected. The following subsections address free drops in any orientation, and show that the requirements of 10 CFR 71 are met.

For end and side impact events, the package is analyzed using Nuclear Packaging's EYDROP and SYDROP programs, respectively. These programs are described in detail in Appendix 2.10.5. The programs predict a maximum acceleration imparted to the cask during the event, which is then applied statically

to the package as a whole. Since the overpack foam stress-strain curve is dependent on temperature, the foam performance at the extreme temperatures predicted for the foam under normal conditions ( $-20^{\circ}$  to  $157^{\circ}\text{F}$ ) is assumed as a means of bounding the performance of the overpack. Additionally, since the programs assume a relatively simple cylindrical overpack surrounding a smaller cylinder, additional bounding analyses have been performed to account for the flat sections of the overpack, as well as the 'notch' in the side of the overpack.

For oblique impacts, the package was analyzed using Nuclear Packaging's CYDROP and OBLIQUE computer programs. These programs are also detailed in Appendix 2.10.5. Again, bounding calculations were performed to insure adequate consideration was taken with respect to the somewhat unconventional shape of the overpack and the temperature variation of the polyurethane foam.

Polyurethane overpack behavior is becoming more and more understood, due to the many drop test programs that have been undertaken in the past few years. Notable among these programs are the tests performed in support of the 1-13C II package, and most recently, the NuPac 125-B Fuel Shipping Cask (Docket Number 71-9200). These tests indicate that analysis methods and assumptions used in this application are reasonable and conservative.

#### 2.6.7.1 Flat End Drop

Analysis of the NuPac 10/140MB Cask behavior during the end drop impact is performed in the following steps:

- (1) Analyze the impact force using the EYDROP computer program.
- (2) Analyze the cask lid for bending assuming the payload acts as a uniform load on the inside surface of the lid with the overpack foam pressure acting in the opposite direction in the appropriate place on the outside of the lid.

- (3) Analyze the stresses in the secondary lid bolts.
- (4) Analyze the axial and hoop stresses in the cask shells and lead.

Material properties are available from Table 2.3-1.

#### 2.6.7.1.1 Impact Forces

Tables 2.6.7-1 and 2.6.7-2 present the results from the EYDROP program for an overpack at -20 degrees Fahrenheit and 157 degrees Fahrenheit, corresponding to the temperature extremes the polyurethane foam in the package might experience under normal conditions as described in 10 CFR 71 (see section 3.0). It should be noted that the foam properties assumed for 157°F were taken at the lower bound that might be expected, while those at -20°F were taken at the upper bound that might be expected at that temperature. In this manner, the full range of overpack behavior is taken into account.

The overpack is modeled as having an outside diameter of 100.34 inches, corresponding to the diameter of a circle with the same area as a 101 inch diameter circle flattened to 96 inches on each side. As a result, the impacted area calculated by EYDROP is exactly equivalent to the end contact area of the overpack. Tests performed on a variety of packages indicate that loads calculated in this manner are slightly conservative (over predicted).

Table 2.6.7-1

EYDROP(ENB)

NUPAC 10/140M COLD FOAM (-20 DEG)

PACKAGE WEIGHT = 65000. (LBS)  
 PACKAGE DIAMETER = 100.34 (IN)  
 HOLE DIAMETER = 55.00 (IN)  
 OVERPACK DEPTH = 18.00 (IN)  
 DROP HEIGHT = 1.00 (FT)

CRUSH DEPTH (IN)	STRAIN	**** IMPACT ****		***** ENERGY *****		
		FORCE (LBS)	ACCEL. (G)	KINETIC (IN-LB)	STRAIN (IN-LB)	RATIO (SE/KE)
.05	.003	491702.	7.6	783250.	12293.	.016
.10	.006	983404.	15.1	786500.	49170.	.063
.15	.008	1475107.	22.7	789750.	110633.	.140
.20	.011	1966809.	30.3	793000.	196681.	.248
.25	.014	2458511.	37.8	796250.	307314.	.386
.30	.017	2950213.	45.4	799500.	442532.	.554
.35	.019	3441916.	53.0	802750.	602335.	.750
.40	.022	3933618.	60.5	806000.	786724.	.976
.45	.025	4425320.	68.1	809250.	995697.	1.230
.50	.028	4917022.	75.6	812500.	1229256.	1.513
.55	.031	5388817.	82.9	815750.	1486902.	1.823
.60	.033	5773813.	88.8	819000.	1765967.	2.156
.65	.036	6146858.	94.6	822250.	2063984.	2.510
.70	.039	6507952.	100.1	825500.	2380354.	2.884
.75	.042	6857095.	105.3	828750.	2714481.	3.275
.80	.044	7194287.	110.7	832000.	3065765.	3.685
.85	.047	7519527.	115.7	835250.	3433610.	4.111
.90	.050	7832816.	120.5	838500.	3817419.	4.553
.95	.053	8142192.	125.3	841750.	4216794.	5.010
1.00	.056	8438667.	129.8	845000.	4631316.	5.481
1.05	.058	8721295.	134.2	848250.	5060315.	5.966
1.10	.061	8989126.	138.3	851500.	5503075.	6.463
1.15	.064	9241212.	142.2	854750.	5958834.	6.971
1.20	.067	9476604.	145.8	858000.	6426779.	7.490
1.25	.069	9694355.	149.1	861250.	6906053.	8.019
1.30	.072	9895639.	152.2	864500.	7395803.	8.555
1.35	.075	10076592.	155.0	867750.	7895109.	9.098
1.40	.078	10234924.	157.5	871000.	8402897.	9.647
1.45	.081	10365297.	159.5	874250.	8917902.	10.201
1.50	.083	10457414.	160.9	877500.	9438470.	10.756

ACC = 6/2  
 STRAIN RATIO = 1.000

Table 2.6.7-2

EYDROP(END)

NUPAC 10/140M HOT FOAM (161 DEG)

PACKAGE HEIGHT = 65000 (LBS)  
 PACKAGE DIAMETER = 100.34 (IN)  
 HOLE DIAMETER = 55.00 (IN)  
 OVERPACK DEPTH = 18.00 (IN)  
 DROP HEIGHT = 1.00 (FT)

CRUSH DEPTH (IN)	STRAIN	**** IMPACT ****			***** ENERGY *****		
		FORCE (LBS)	ACCEL. (G)	KINETIC (IN-LB)	STRAIN (IN-LB)	RATIO (SE/KE)	
.25	.014	1049989.	16.2	796250.	131249.	.165	
.50	.028	2099978.	32.3	812500.	524995.	.646	
.75	.042	3030038.	46.6	828750.	1146247.	1.407	
1.00	.056	3491273.	53.7	845000.	1981411.	2.345	
1.25	.069	3592948.	55.3	861250.	2866938.	3.329	
1.50	.083	3704293.	57.0	877500.	3779093.	4.307	
1.75	.097	3788315.	58.3	893750.	4715669.	5.276	
2.00	.111	3833886.	59.0	910000.	5668445.	6.229	
2.25	.125	3861783.	59.4	926250.	6630403.	7.158	
2.50	.139	3902942.	60.0	942500.	7600994.	8.065	
2.75	.153	3953311.	60.8	958750.	8585026.	8.952	
3.00	.167	3997645.	61.3	975000.	9576895.	9.822	
3.25	.181	4039994.	62.2	991250.	10581600.	10.675	
3.50	.194	4081936.	62.6	1007500.	11596841.	11.511	
3.75	.208	4128426.	63.5	1023750.	12623136.	12.330	
4.00	.222	4180371.	64.3	1040000.	13661736.	13.156	
4.25	.236	4236161.	65.2	1056250.	14713803.	13.950	
4.50	.250	4296156.	66.1	1072500.	15780342.	14.714	
4.75	.264	4360718.	67.1	1088750.	16862452.	15.488	
5.00	.278	4430209.	68.2	1105000.	17961317.	16.255	

ACC = 29.0 (1000)  
 RATIO = 1000

From the tables, the acceleration at which all the impact energy is absorbed by the overpack may be calculated by interpolation. For the 157°F case the acceleration is 39.0 g's and for the -20°F case, the acceleration would be 61.2 g's. These loads are well below those reported in section 2.7.1 for the hypothetical accident free drop event.

Importantly, the tables show that a very little overpack deflection would be expected from this event. The impact energy is such that the foam would be expected to perform nearly elastically.

#### 2.6.7.1.2 Lid Stresses

The lid analyses performed in Section 2.7.1 for the hypothetical accident 30 foot drop may be used to determine stresses during the normal condition drop event, since that analysis was based on a linear analysis. Because the worst case impact under normal conditions is only 35.8% of the worst case accident conditions, and the allowable membrane stresses for normal conditions are 41.7% of the accident allowables ( $S_m$  verses  $2.4S_m$ ), and allowable bending stresses are 43.0% ( $1.5 S_m$  versus  $S_u$ ), then clearly the normal condition margins of safety are larger than the accident margins of safety for the lid during end impact.

A summary of the lid margins of safety during the normal condition 1 foot end drop is given below as Table 2.6.7-3. The table is derived by scaling the stresses determined for the hypothetical accident condition reported in Section 2.7.1 by 35.8% and comparing them with the allowable normal stresses per Table 2.3-1.

#### 2.6.7.1.3 Secondary Lid Bolts

The stresses in the ASTM A320 L43 secondary lid bolts may also be scaled from the accident condition stresses. In section 2.7.1, the stresses in a bolt from a 170.8 g impact acceleration was determined to be 72,200 psi. The stress during normal conditions is then

$$(61.2/170.8)72,200 = 25,870 \text{ psi}$$

TABLE 2.6.7-3

## NORMAL CONDITION LID STRESSES

Lid	Max. Bending Stress (psi) (Margin of Safety)	Max. Membrane Stress (psi) (Margin of Safety)
Bottom	10,016 (M.S. = +2.00)	1,630 (M.S. = + Large)
Top	12,371 (M.S. = +1.42)	5,057 (M.S. = +2.96)



The stress in the bolts from the normal condition maximum pressure may be conservatively added to this stress (this is conservative because the maximum internal pressure occur at a temperature for which the impact accelerations are considerably lower) to get the maximum stress in the bolt:

$$(6.8 \text{ psi})(\pi)(29/2)^2 8(1.405) = 400 \text{ psi}$$

Therefore, the maximum normal condition tensile stress in the bolts is

$$25,870 + 400 = 26,270 \text{ psi}$$

The margin of safety taking  $S_m$  as 35,000 psi for ASTM 320 L43 at  $-20^\circ\text{F}$ :

$$\text{M.S.} = 35,000/26,270 - 1 = +0.33$$

#### 2.6.7.1.4 Axial and Hoop Stresses in the Shells

Stresses in the Cask Shells and Lead (Maximum Fabrication Stress Condition Assumed)

The response of the cask steel shells and lead shielding to the normal end drop event is determined using both hand calculations and finite element analyses. The principal concern for the cask is with buckling of the inner shell. As shown by the following calculations, buckling will not occur as the result of the hoop and axial compressive stresses which develop in the cask inner shell under normal end drop conditions.

Various initial conditions can be assumed for the normal drop event. In particular, a temperature must be assumed in order to establish an initial fabrication stress for the inner shell. A lower assumed temperature will result in a higher initial hoop stress on the inner shell (see Section 2.6.2) but higher allowable stresses. For purposes of this analysis, drops at  $123^\circ\text{F}$  (maximum lead normal temperature per Section 3.4.2),  $70^\circ\text{F}$ , and  $-20^\circ\text{F}$  are considered.

To adequately bound the consequences of the drop event at a given temperature, two initial lead conditions are also considered. The first assumes that the lead has shrunk onto the inner shell and away from the outer shell. In addition, due to the combined effects of friction between the lead and inner shell, and axial shrinkage of the lead relative to the inner and outer shells, axial gaps will develop between the lead and the steel structures at the top and bottom end of the lead column. These axial gaps are important in that, until friction is overcome, under increased axial loading, the lead will impose a direct axial load on the inner shell. Once friction is overcome, the lead will become supported at its base (the bottom of the lead column) and will grow radially outward due to the 'Poisson Effect' under increased axial loading. This radial growth will tend to relieve the initial fabrication hoop stress as the lead separates from the inner shell. If sufficient axial load develops, the lead would grow out to the outer shell creating tensile hoop stresses therein, and under further loading would eventually flow back inward into the inner shell, thereby developing compressive hoop stresses in the inner shell. Since the primary mechanism of this load case would be to relieve stresses on the critical inner shell, it is not considered to be worst-case condition.

From Section 2.6.2, hoop stress in the inner shell due to fabrication is as follows:

Temperature (°F)	Inner Shell Hoop Stress (psi)
123	-1,793 (extrapolated)
70	-2,041
-20	-2,642

Note:

The outer shell hoop stress is considered negligible since the lead separates from the outer shell upon cooling.

The equivalent pressure at the lead/inner shell interface is as follows:

$$p = \sigma t / r$$

Where:

$$t = 0.75 \text{ in}$$

$$r = 33.375 \text{ in}$$

Thus, the interface pressures at the different temperatures are:

Temperature (°F)	Interface Pressure, p (psi)
123	40.3
70	45.9
-20	59.4

With a coefficient of friction,  $f$ , for lead on stainless steel assumed to fall in the 0.5 to 1.0 range (Refer to Mark's Standard Handbook for Mechanical Engineers, 8th ed., 1978, pp. 3-26), the load,  $P$ , which can be supported by friction at the lead/inner shell interface, may be determined as follows:

$$P = \pi DLpf$$

Where:

$$D = 67.5 \text{ in (inner shell outside diameter)}$$

$$L = 77.5 \text{ in (lead column height)}$$

$$p = \text{interface pressure, psi}$$

$$f = 0.5 \text{ to } 1.0 \text{ (coefficient of friction)}$$

Applying the interface pressures determined earlier, the total load which may be supported is:

<u>Temperature</u> <u>(°F)</u>	<u>Coefficient</u> <u>of Friction</u>	<u>Load Supported</u> <u>(lbs)</u>
123	0.5	331,090
	1.0	662,179
70	0.5	376,885
	1.0	753,769
-20	0.5	487,863
	1.0	975,727

Total lead weight can be calculated as:

$$W_L = \pi(R_{Oi}^2 - R_{Io}^2)L_C\rho_L$$

Where:

$$R_{Oi} = \text{Outer Shell Inside Radius} = 36.0 \text{ in.}$$

$$R_{Io} = \text{Inner Shell Outside Radius} = 33.75 \text{ in.}$$

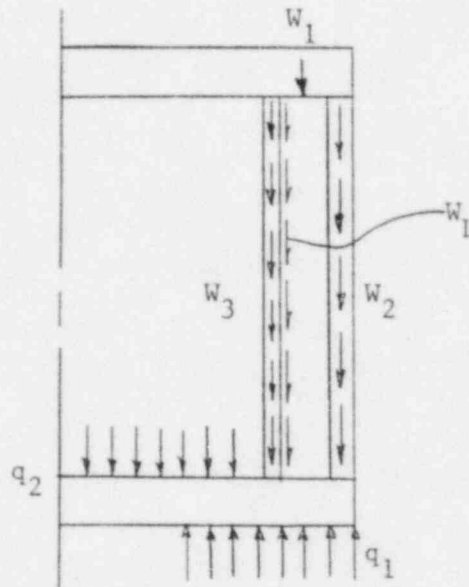
$$L_C = \text{Height of Lead Column,} - 77.5 \text{ in.}$$

$$\rho_L = \text{Lead Density} = 0.41 \text{ lb./in.}^3$$

$$W_L = \pi[(36.0)^2 - (33.75)^2](77.5)(0.41) = 15,666 \text{ lb.}$$

At the Normal Conditions of Transport maximum lead temperature of 123°F, the maximum g-load which can be supported by friction is  $(662,179/15,666) = 42.3$  g's. Since this exceeds the 123°F Normal Condition end drop load of 39.0 g's, it is possible that the entire lead weight would cling to the inner shell during the drop event at 123°F. Likewise, at the minimum temperature of -20°F, maximum sustainable g-load is  $(975,727/15,666) = 62.3$  g's. End drop acceleration at this temperature condition is only 61.2 g's. It is clear, therefore, that lead cling is a possible load condition across the entire anticipated Normal Condition temperature range.

To conservatively bound the end drop event, the maximum g-load of 61.2 g's (derived at  $-20^{\circ}\text{F}$ ) will be used to calculate shell stresses, while the minimum applicable buckling allowables (derived at  $123^{\circ}\text{F}$ ) will be used to evaluate Margins of Safety.



For calculating structural deflections, refer to Pilkey, Walter A., and Pin, Yu Chang, Modern Formulas for Statics and Dynamics, McGraw-Hill, Tables 11-1 and 11-2. Relevant structural weight components are:

$$\begin{aligned} W_1 &= (\text{Weight of top overpack, cask lid and top ring}) (61.2 \text{ g's}) \\ &= (10,440)(61.2) = 638,930 \text{ lbs} \end{aligned}$$

$$\begin{aligned} W_2 &= (\text{Weight of cask outer shell, thermal shield, etc.}) (61.2 \text{ g's}) \\ &= (9,290)(61.2) = 568,550 \text{ lbs} \end{aligned}$$

$$\begin{aligned} W_3 &= (\text{Weight of cask inner shell}) (61.2 \text{ g's}) \\ &= (3,560)(61.2) = 217,870 \text{ lbs} \end{aligned}$$

$$\begin{aligned} W_L &= (\text{Weight of lead}) (61.2 \text{ g's}) \\ &= (15,666)(61.2) = 958,760 \text{ lbs} \end{aligned}$$

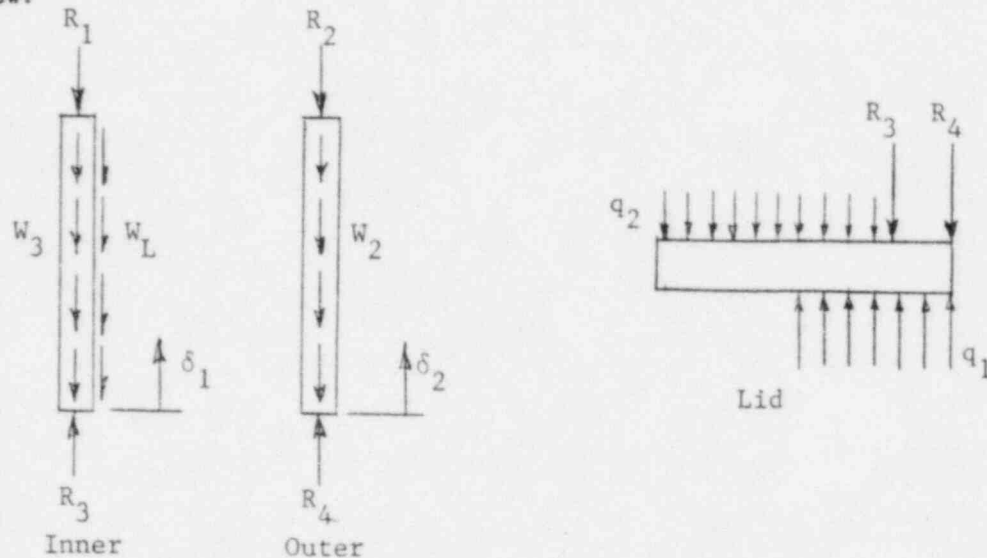
$$q_2 = (\text{Weight of payload}) / (61.2 \text{ g's}) \pi (33.0)^2$$

$$= (15,000)(61.2) / 3,421.2 = 268.3 \text{ lb/in}^2$$

$$q_1 = [W_1 + W_2 + W_3 + W_L + q_2 \pi (33.0)^2] / \pi (37.25^2 - 27.5^2)$$

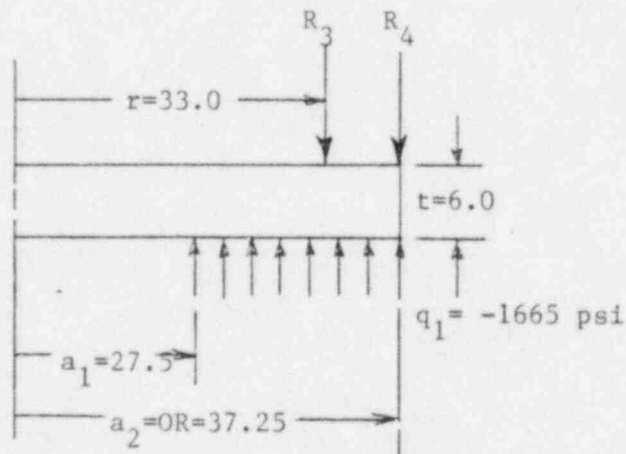
$$= 1,206 \text{ lb/in}^2$$

Free-body diagrams of the outer cask inner and outer shells, and end plate are illustrated below:



Assuming reaction  $R_3$  does not affect the deflection of the lower end plate (conservative for maximum  $R_3$ ), the differential deflection,  $\delta_1 - \delta_2$ , may be calculated. The analysis requires superposition of two pressure loads -  $q_1$ , due to the reaction force of the bottom overpack, and  $q_2$ , due to the package payload. For the first case, the differential deflection is:

$$\delta_1 - \delta_2 = y_c - M_c r^2 / 2D(1 + \mu) + F_v$$



Where:

$$y_c = -[OR^2/2D(1 + \mu)] F_M|_{r=OR} - F_v|_{r=OR}$$

$$D = Et^3/[12(1-\mu^2)]$$

$$E = 28.0(10)^6 \text{ psi (at } 123^\circ\text{F)}$$

$$t = 6.0 \text{ in. (average lid thickness)}$$

$$\mu = 0.3$$

$$D = 553.85 \times 10^6$$

$$F_M|_{r=OR} = -(q_1/4) [F_{Mw1}(OR, a_1) - F_{Mw1}(OR, a_2)]$$

$$F_{Mw1}(OR, a_1) = \langle OR - a_1 \rangle^0 \left[ (3 + \mu)OR^2/4 - a_1^2 + (1 - \mu)a_1^4/4OR^2 - (1 + \mu)a_1^2 \ln(OR/a_1) \right]$$

$$OR = 37.25 \text{ in.}$$

$$a_1 = 27.5 \text{ in.}$$

$$F_{Mw1}(OR, a_1) = 162.27$$

Similarly:

$$F_{Mw1}(OR, a_2) = 0$$

Therefore:

$$F_M|_{r=OR} = 48,926$$

$$F_v|_{r=OR} = (q_1/8D) [F_{vw1}(OR, a_1) - F_{vw1}(OR, a_2)]$$

$$F_{vw1}(OR, a_1) = \langle OR - a_1 \rangle^0 \left[ OR^4/8 - 5a_1^4/8 + a_1^2OR^2/2 - a_1^2(OR^2 + a_1^2/2) \ln(OR/a_1) \right]$$

$$F_{vw1}(OR, a_1) = 2,673.57$$

Similarly:

$$F_{vw2}(OR, a_2) = 0$$

$$F_v|_{r=OR} = -7.277(10)^{-4}$$

Then:

$$y_c = -0.0464 \text{ in. (positive downward)}$$

$$M_c = -F_m|_{r=OR} = -48,926$$

$$F_v = (q_1/8D) [F_{vw1}(r, a_1) - F_{vw2}(r, a_2)]$$

$$F_{vw1}(r, a_1) = \langle r - a_1 \rangle^0 \left[ r^4/8 - 5a_1^4/8 + a_1^2 r^2/2 - a_1^2 (r^2 + a_1^2/2) \ln(r/a_1) \right]$$

$$r = 33.0 \text{ in.}$$

$$\langle r - a_1 \rangle^0 = 1 \text{ when } a_1 < r$$

$$= 0 \text{ when } a_1 \geq r$$

$$F_{vw1}(r, a_1) = 283.77$$

Since  $r < a_2$ ,  $\langle r - a_2 \rangle^0 = 0$  and  $F_{rw2} = 0$

$$F_v = -7.724(10)^{-5}$$

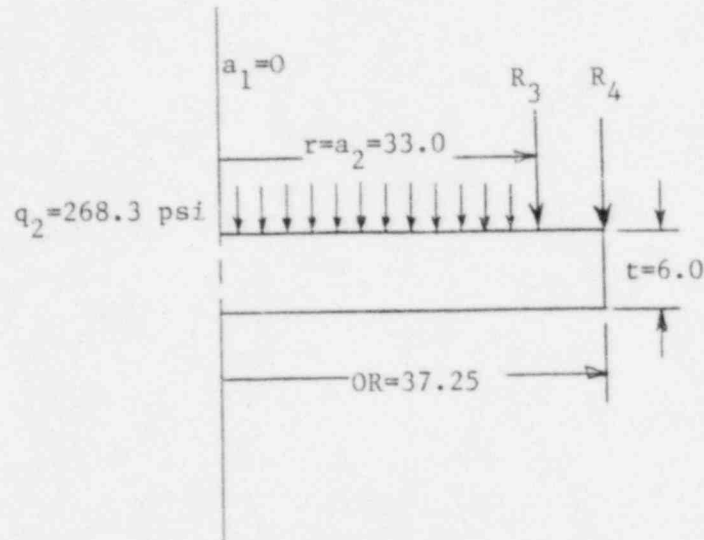
Then:

$$\delta_1 - \delta_2 = -0.0464 - (-48,926)(33.0)^2/(2)(553.85(10)^6)(1.3) + (-7.724(10)^{-5})$$

$$\delta_1 - \delta_2 = -0.009494 \text{ in. (positive downward)}$$

The second load case represents the differential deflection due to the distributed payload pressure  $q_2$ .





An analysis similar to that above yields a deflection of:

$$\delta_1 - \delta_2 = 0.009859 \text{ in. (positive downward)}$$

Superposition of results yields:

$$\delta_1 - \delta_2 = 3.658(10)^{-4} \text{ in. (positive downward)}$$

Also, from the free-body diagrams for the cask inner and outer shells, and axial stiffness relations for the shells ( $\delta = PL/AE$  for an end load, and  $\delta = PL/2AE$  for self-weight, i.e., distributed load), the deflections,  $\delta_1$  and  $\delta_2$ , and reactions,  $R_3$  and  $R_4$ , may be found:

$$\delta_1 = R_3 L / A_1 E_1 - (W_3 + W_L) L / 2 A_1 E_1$$

$$\delta_2 = R_4 L / A_2 E_2 - W_2 L / 2 A_2 E_2$$

Where:

$$L = 77.5 \text{ in}$$

$$\begin{aligned} A_1 &= \pi[(33.75)^2 - (33.0)^2] \\ &= 157.28 \text{ in}^2 \end{aligned}$$

$$A_2 = \pi[(37.25)^2 - (36.0)^2] \\ = 287.65 \text{ in}^2$$

$$E_1 = 28.0(10)^6 \text{ psi (at } 123^\circ\text{F)}$$

$$E_2 = 29.2(10)^6 \text{ psi (at } 123^\circ\text{F)}$$

Then,

$$\delta_1 = (1.760(10)^{-8})R_3 - 0.01035$$

$$\delta_2 = (9.227(10)^{-9})R_4 - 0.00260$$

and,

$$R_3 + R_4 = W_1 + W_2 + W_3 + W_L = 2,384,110 \text{ lbs}$$

or,

$$R_4 = 2,384,110 - R_3$$

Solving simultaneously,

$$R_3 = 1,122,525 \text{ lbs}$$

$$R_4 = 2,384,110 - 1,122,525 = 1,261,585$$

Therefore, the axial compressive stress in the cask inner shell,  $\sigma_1$ , and outer shell,  $\sigma_2$ , is:

$$\sigma_1 = R_3/A_1 = 7,137 \text{ psi}$$

$$\sigma_2 = R_4/A_2 = 4,386 \text{ psi}$$

From Section 2.6.2, worst-case inner shell hoop stress for Normal Condition of Transport temperatures is -2,462 psi at  $-20^\circ\text{F}$ . Conservatively taking radial stress (pressure) as zero, inner shell stress intensity becomes:

$$S.I._1 = 0 - (-7,137) = 7,137 \text{ psi}$$

From Table 2.1.2-1, the allowable stress limit for the inner shell material is  $S_m = 20,000$  psi at  $123^\circ\text{F}$ . Stress Margin of Safety is therefore:

$$\text{M.S.} = 20,000/7,137 - 1 = +1.80$$

From Table 2.1-1, at  $123^\circ\text{F}$ , inner shell buckling allowables are 19,062 psi (axial) and 17,905 psi (hoop). Buckling Margin of Safety is thus:

$$\begin{aligned}\text{M.S.} &= 1/\left[(7,137/19,062) + (2,462/17,905)\right] - 1 \\ &= +0.95\end{aligned}$$

From Section 2.6.2, the outer shell will not be in contact with the lead, and will, therefore, undergo axial stress only.

$$S_{I_2} = 0 - (-4,386) = 4,386 \text{ psi}$$

Table 2.1.2-1 yields an allowable stress of  $S_y = 37,200$  psi (greater than  $S_m = 23,250$ ) at  $123^\circ\text{F}$ . Stress Margin of Safety is thus:

$$\text{M.S.} = 37,200/4,386 - 1 = +7.49$$

Table 2.1-2 yields an axial compression buckling allowable of 22,728 psi at  $123^\circ\text{F}$ , for a Margin of Safety of:

$$\text{M.S.} = 1/(4,386/22,728) - 1 = +4.18$$

Therefore, the cask inner and outer shell structures are both well in excess of regulatory requirements for the Normal Conditions of Transport end drop event when the lead shielding is completely supported by the inner shell.

# Stresses in the Outer Cask Shells and Lead (Zero Fabrication Stress Condition Assumed)

The second initial lead condition assumes that the fabrication stress has fully crept away resulting in a stress free column of lead just in contact with the inner and outer shells. This is a potential worst case since any axial load imposed on the lead will directly load, radially, both the inner and outer shells (i.e., the lead need not flow away from the inner shell, into the outer shell and back into the inner shell to develop a compressive hoop stress in the inner shell).

For this condition, initial stresses in the lead and the steel shells are taken as zero. As axial load is applied to the lead and shells, the lead will attempt to move downward and outward and develop pressures on both the inner and outer shells.

Under acceleration, the lead column will experience a linearly increasing axial stress distribution from top to bottom:

$$\sigma_z = \gamma \rho_L L$$

Where:

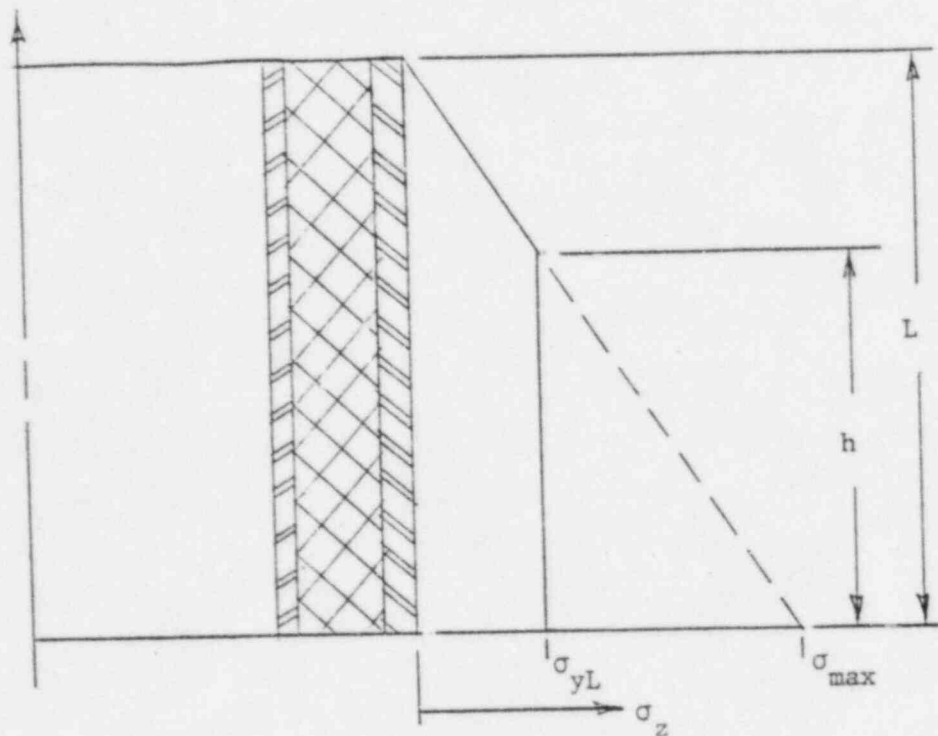
$\sigma_z$  = Lead Axial Stress

$\gamma$  = Acceleration

$\rho_L$  = Lead Density = 0.41 lb./in.<sup>3</sup>

$L$  = Lead Column Height = 77.5 in.

However, from the lead stress-strain curves shown in Figures 2.3-1 and 2.3-2, it is apparent that, as the lead reaches a stress level around its yield point, the stress will tend to remain fairly uniform under continued loading. The resulting axial stress distribution can thus be illustrated as follows:



Where:

$\sigma_{yL}$  = Yield Strength of Lead

$\sigma_{max}$  = Maximum Stress at Applied Acceleration for Fully Elastic Material

The height  $h$  at which the lead reaches its yield point can be found by:

$$L - h = \sigma_{yL} / \gamma \rho_L$$

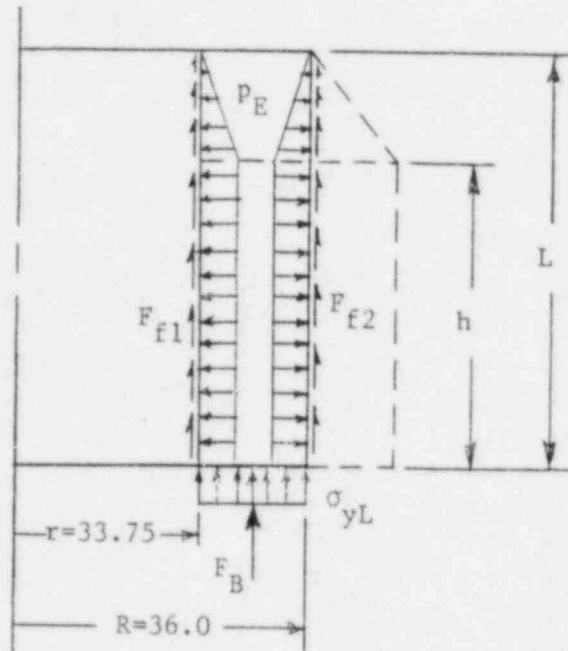
Or:

$$h = L - \sigma_{yL} / \gamma \rho_L$$

For the maximum Normal Condition of Transport and drop acceleration of 61.2 g's,  $h$  becomes:

$$h = 77.5 - 600 / (61.2)(0.41) = 53.6 \text{ in.}$$

Where  $\sigma_{yL}$  is conservatively taken as 600 psi, the approximate yield strength of lead at 123°F.



The sum of the forces acting on the lead column may now be expressed as:

$$W_L = F_B + F_{f1} + F_{f2}$$

Where:

$$W_L = (15,666)(61.2) = 958,760 \text{ lb.}$$

$$F_B = (600) \pi (36.0^2 - 33.75^2) = 295,820 \text{ lb.}$$

$$F_{f1} = \text{Frictional Reaction Force of Inner Shell}$$

$$F_{f2} = \text{Frictional Reaction Force of Outer Shell}$$

The above frictional forces result from radial forces exerted by the lead column onto the steel shells. These radial forces will be a function of the lead-to-steel coefficient of friction. Conservatively assuming the minimum friction coefficient of 0.5, the net radial forces become:

$$F_{R1} = F_{f1}/0.5, \text{ or } F_{f1} = 0.5 F_{R1}$$

$$F_{R2} = F_{f2}/0.5, \text{ or } F_{f2} = 0.5 F_{R2}$$

These radial forces can then be expressed in terms of a lead maximum radial pressure,  $p_E$ , which is assumed to be equal on both shells. For uniform pressure  $p_E$  in the lead yield region and linearly varying pressure in the lead elastic region, the radial force on the inner shell may be expressed as:

$$F_{R1} = p_E \mu D_1 h + 0.5 p_E \mu D_1 (L-h)$$

Or:

$$F_{R1} = 0.5 p_E \mu D_1 (L+h)$$

From which:

$$F_{f1} = 0.25 p_E \mu D_1 (L+h)$$

Likewise, for the outer shell:

$$F_{f2} = 0.25 p_E \mu D_2 (L+h)$$

The lead equilibrium equation may now be re-written as:

$$W_L - F_B = 0.25 \mu p_E (D_1 + D_2) (L+h)$$

or:

$$p_E = 4(W_L - F_B) / \mu(D_1 + D_2) (L+h)$$

Substituting in the proper terms, the equivalent shell pressure becomes:

$$p_E = 46.15 \text{ psi}$$

Therefore, the inner shell compressive hoop stress is:

$$\begin{aligned} \sigma_1 &= -p_E R_1 / t_1 \\ &= -(46.15)(33.75) / (0.75) = -2,077 \text{ psi} \end{aligned}$$

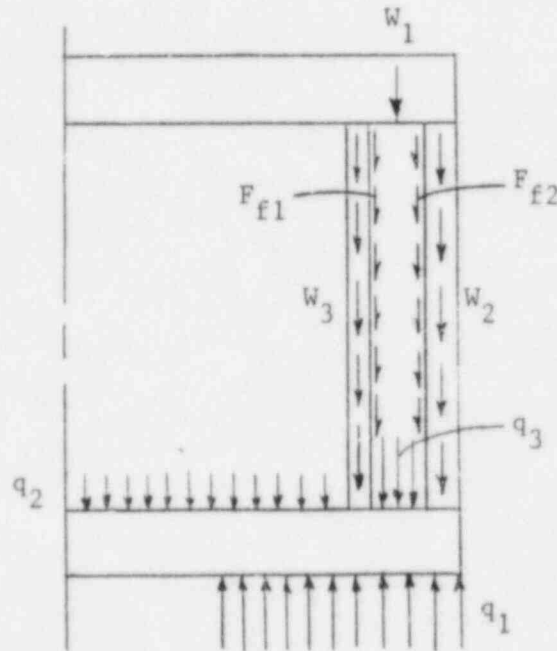
The outer shell tensile hoop stress is:

$$\begin{aligned} \sigma_2 &= p_E R_2 / t_2 \\ &= (46.15)(36.0) / (1.25) = 1,330 \text{ psi} \end{aligned}$$

To evaluate axial stresses, a similar approach to the previous analysis is utilized. Appropriate frictional forces are added to the inner and outer shells, and an applied pressure load  $q_3$ , representing the yield stress of the lead column, is added to the bottom plate between the inner and outer shells. From the above analysis, shell frictional forces may be calculated:

$$F_{f1} = 320,778 \text{ lbs.}$$

$$F_{f2} = 342,163 \text{ lbs.}$$



$$q_3 = 600 \text{ psi}$$

Repeating the previous calculational approach, and taking  $q_3$  into account:

$$\delta_1 - \delta_2 = -0.002628 \text{ in. (positive downward)}$$

$$\delta_1 = R_3 L / A_1 E_1 - (W_3 + F_{f1}) L / 2 A_1 E_1$$

$$\delta_2 = R_4 L / A_2 E_2 - (W_2 + F_{f2}) L / 2 A_2 E_2$$

$$R_4 = 2,384,110 - R_3$$



Solving simultaneously, inner shell reaction load becomes:

$$R_3 = 743,092 \text{ lbs.}$$

Thus, outer shell reaction is:

$$R_4 = 1,642,018 \text{ lbs.}$$

Therefore, compressive axial stresses on the inner and outer shell are:

$$\sigma_1 = R_3/A_1 = -4,718 \text{ psi}$$

$$\sigma_2 = R_4/A_2 = -5,708 \text{ psi}$$

Conservatively ignoring shell radial loading, inner shell stress intensity is:

$$S.I._1 = 0 - (-4,718) = 4,718 \text{ psi}$$

From the previous section, the stress allowable for the inner shell is  $S_m = 20,000$  psi. The stress Margin of Safety is thus:

$$M.S. = 20,000/4,718 - 1 = +3.24$$

Buckling allowables are 19,062 psi (axial) and 17,905 psi (hoop). Buckling Margin of Safety is then:

$$\begin{aligned} M.S. &= 1/[(4,718/19,062) + (2,077/17,905)] - 1 \\ &= +1.75 \end{aligned}$$

Stress intensity of the outer shell is:

$$S.I._2 = 1,330 - (-5,708) = 7,038 \text{ psi}$$

With an allowable stress intensity of 37,200 psi, the Margin of Safety becomes:

$$M.S. = 37,200/7,038 - 1 = +4.29$$

Axial buckling allowable is 22,728 psi, and the buckling Margin of Safety is thus:

$$M.S. = 1/(5,708/22,728) - 1 = +2.98$$

This analysis indicates that the cask inner and outer shells will not be adversely affected by the Normal Conditions of Transport end drop event with no fabrication stresses present in the lead shielding. However, to more accurately analyze the complex interaction of lead shielding with inner and outer steel shells during the end drop event, a finite element analysis was conducted with the ANSYS program. Details of this program are given in Appendix 2.10.2, the analysis results are shown in Appendix 2.10.6 and these results are summarized below.

While the minimum temperature condition for the drop event ( $-20^{\circ}\text{C}$ ) induces the highest acceleration loading (61.2 g's), the material properties and buckling and stress intensity allowables are also at a maximum (refer to Sections 2.1 and 2.3 for details). Likewise, though the maximum temperature case results in lower impact loads (a maximum of 39.0 g's), material properties and buckling and stress intensity allowables are also reduced at the higher temperature condition. Refer to Section 2.1.2.2, Overpack Design Criteria, as well as Section 2.6.7.1.1 above for details of the effects of temperature variation on drop loads.

To conservatively bound the buckling and stress allowable calculations, the maximum g-load (obtained at the minimum temperature condition) was applied to the analysis while utilizing reduced strength material properties (found at the higher temperature), which will tend to maximize stresses. Therefore, the analysis utilized material properties based on a maximum expected normal condition of transport temperature of  $121^{\circ}\text{F}$  at the inner shell.

The smaller buckling and stress allowable values found at the higher temperature were then used to derive Margins of Safety. Thus, maximum possible loads were combined with minimum possible material strength conditions for a worst-case analysis and minimum possible Margins of Safety.

The results of the stress analysis for Normal Conditions of Transport, detailed in Appendix 2.10.6, are summarized below:

Drop Load = 65 g's  
Drop Temperature = 121°F

Maximum Inner Shell Stress Intensities (Elem. 33)		Maximum Outer Shell Stress Intensities (Elem. 36)	
<u>Surface</u>	<u>Membrane</u>	<u>Surface</u>	<u>Membrane</u>
7,752 psi	6,639 psi	11,463 psi	7,906 psi
Stress Intensity Allowables*		Stress Intensity Allowables*	
30,000 psi	20,000 psi	37,300 psi	37,300 psi
Margins of Safety		Margins of Safety	
+ 2.87	+ 2.01	+ 2.25	+ 3.72

\* Interpolated from Table 2.1.2-1

The results of the buckling analysis for Normal Conditions of Transport, detailed in Appendix 2.10.6, are summarized below:

Drop Load = 65 g's  
Drop Temperature = 121°F

Maximum Inner Shell Stresses (Elem. 33)		Maximum Outer Shell Stress (Elem. 36)
<u>Axial</u>	<u>Hoop</u>	<u>Axial</u>
-6,639 psi	-2,381 psi	-3,557 psi
Buckling Allowables *		Buckling Allowable **
19,062 psi	17,906 psi	22,630 psi
Margin of Safety		Margin of Safety
+ 1.08		+ 5.36

\* Interpolated from Table 2.1-3

\*\* Interpolated from Table 2.1-4

Thermal analysis of the cask resulted in an actual inner shell temperature of 123°F at the critical area (e.g., the portion where end drop-induced stresses are maximum). However, in light of the conservatism of the analysis and magnitude of the Margins of Safety derived therefrom, it can be reasonably assumed that this small temperature difference will not significantly affect the final results.

#### 2.6.7.2 Oblique Impact

Analysis of the NuPac 10/140MB package behavior during normal condition drops from 1 foot proceeds in the following steps, using the same conservative assumptions made in the analysis of the hypothetical accident 30 foot drop event discussed in Section 2.7.1.2 below.

1. Use CYDROP to determine worst case overpack deformations for minimum foam properties.
2. Use CYDROP with the highest (coldest) foam stress-strain data to determine a conservative estimate of the force-deflection relationship of the 10/140MB overpack design at various impact angles. This force deflection relationship is identical to the one used (and discussed in detail) for the analysis of the hypothetical 30 foot drop (see Section 2.7.1.2.2).
3. Use the OBLIQUE program to determine internal forces in the cask body.
4. Determine the worst case stress state from internal forces in the cask body.
5. Determine lid attachment forces in EnviroLocks<sup>tm</sup> under worst conditions.

##### 2.6.7.2.1 Worst Case Corner Deformations

Under normal conditions as defined by 10 CFR 71, the polyurethane foam-filled overpacks may range in temperature from -20°F to approximately 160°F during normal operations. It is clear from an examination of the stress-strain properties of the polyurethane foam at various temperatures that the highest overpack deformations will occur at the highest temperature extreme and that the highest impact forces would develop at the lowest temperature extreme.

Tables 2.6.7-4 and 2.6.7-5 present the output from NuPac's CYDROP energy balance program for overpacks of 96- and 101-inch diameters assuming an impact angle corresponding to the c.g. over struck corner cask. The two overpack diameters chosen for analysis provide a conservative estimate of the deformation which would occur in the actual overpack should it be subjected to this event. A more complete discussion of the conservative nature of these analyses appears in Section 2.7.1.2.1.

The tables show that a normal condition drop event would be expected to result in less than 8 inches of deformation under the worst conditions.

#### 2.6.7.2.2 Force - Deflection Relationship

As stated above, the conservative force-deflection relationship for normal conditions is identical to the the hypothetical accident force-deflection relation, since the relationship is a function of overpack geometry, not drop height. A complete discussion on the conservative and reasonable nature of the force-deflection relationship used for the 10/140MB oblique impact analysis is presented in Section 2.7.1.2.2.

#### 2.6.7.2.3 Internal Forces During Oblique Impact

Cask internal forces are calculated by NuPac's OBLIQUE computer program discussed in Appendix 2.10.5. The force-deflection relationship calculated using the assumptions presented in Section 2.7.1.2.2 was used in conjunction with the physical properties of the package calculated in Section 2.7.1.2.3 by OBLIQUE to determine a conservative estimate of cask internal forces.

Table 2.6.7-6 presents a summary of these internal forces calculated by OBLIQUE for a drop of 1 ft. The forces and moments are presented graphically in Figures 2.6.7-1 and 2.6.7-2.

TABLE 2.6.7-4

CYDROP(CORNER)

NUCLEAR PACKAGING PROPRIETARY

17.21.29

85/06/27

PAGE 14

## NUPAC-B 10/140M CRUSH DEPTH CHECK (161 DEG)

PACKAGE WEIGHT = 65000. (LBS)  
 PACKAGE EXTERNAL LENGTH = 119.50 (IN)  
 PACKAGE EXTERNAL DIAMETER = 96.00 (IN)  
 PACKAGE EXTERNAL HOLE DIA = 55.00 (IN)  
 PAYLOAD ENVELOPE LENGTH = 83.50 (IN)  
 PAYLOAD ENVELOPE DIAMETER = 75.00 (IN)  
 OVERPACK LENGTH = 40.00 (IN)

DROP HEIGHT = 1.00 (FT)  
 ORIENTATION ANGLE = 38.660 (DEGREES WRT TO VERTICAL)

PLATEAU CRUSH STRESS = 687.00 (PSI)  
 (DEFAULT TAKEN AT 10 PCT STRAIN)

STRESS/STRAIN EVALUATED IN 1/2 CRUSH PLANE ELLIPSE AT:  
 NX = 25 POINTS PARALLEL TO SEMI-MINOR ELLIPSE AXIS  
 NY = 25 POINTS PARALLEL TO SEMI-MAJOR ELLIPSE AXIS

EXPERIMENTAL STRAIN VS. STRESS VALUES

CYDROP(CORNER)

NUCLEAR PACKAGING PROPRIETARY

17.21.29

85/06/27

PAGE 15

## NUPAC-B 10/140M CRUSH DEPTH CHECK (161 DEG)

CRUSH DEPTH (IN)	** CRUSH PLANE **		**** IMPACT ****		***** ENERGY *****			DISTRIBUTION OF STRAIN RATIOS BY PERCENT OF CONTACT AREA				
	AREA (IN2)	VOLUME (IN3)	FORCE (LBS)	ACCEL. (G)	KINETIC (IN-LB)	STRAIN (IN-LB)	RATIO (SE/KE)	LE.70	GT.70	GT.80	GT.90	GT.95
.50	11.9	3.	1424.	.0	812500.	386.	.000	100.00	0.00	0.00	0.00	0.00
1.00	33.6	14.	8043.	.1	845000.	2723.	.003	100.00	0.00	0.00	0.00	0.00
1.50	61.5	38.	20988.	.3	877500.	9981.	.011	100.00	0.00	0.00	0.00	0.00
2.00	96.2	77.	38811.	.6	910000.	24931.	.027	100.00	0.00	0.00	0.00	0.00
2.50	131.1	133.	60633.	.9	942500.	49792.	.053	100.00	0.00	0.00	0.00	0.00
3.00	171.6	209.	85885.	1.3	975000.	86421.	.089	100.00	0.00	0.00	0.00	0.00
3.50	215.3	306.	114180.	1.8	1007500.	136437.	.135	100.00	0.00	0.00	0.00	0.00
4.00	261.9	425.	146116.	2.2	1040000.	201511.	.194	100.00	0.00	0.00	0.00	0.00
4.50	311.1	568.	183803.	2.8	1072500.	283991.	.265	100.00	0.00	0.00	0.00	0.00
5.00	362.7	737.	223820.	3.4	1105000.	385897.	.349	100.00	0.00	0.00	0.00	0.00
5.50	416.5	932.	264672.	4.1	1137500.	508620.	.447	100.00	0.00	0.00	0.00	0.00
6.00	472.4	1154.	307663.	4.7	1170000.	651103.	.556	100.00	0.00	0.00	0.00	0.00
6.50	530.2	1404.	352854.	5.4	1202500.	816232.	.679	100.00	0.00	0.00	0.00	0.00
7.00	589.8	1684.	400399.	6.2	1235000.	1004545.	.813	100.00	0.00	0.00	0.00	0.00
7.50	651.0	1995.	449278.	6.9	1267500.	1216965.	.960	100.00	0.00	0.00	0.00	0.00
8.00	713.7	2336.	501298.	7.7	1300000.	1454608.	1.119	100.00	0.00	0.00	0.00	0.00
8.50	777.9	2709.	555128.	8.5	1332500.	1718735.	1.290	100.00	0.00	0.00	0.00	0.00
9.00	843.4	3114.	611580.	9.4	1365000.	2010392.	1.473	100.00	0.00	0.00	0.00	0.00
9.50	910.2	3552.	670612.	10.3	1397500.	2330940.	1.668	100.00	0.00	0.00	0.00	0.00
10.00	978.1	4025.	733781.	11.3	1430000.	2682038.	1.876	100.00	0.00	0.00	0.00	0.00
10.50	1047.1	4531.	798202.	12.3	1462500.	3065034.	2.096	100.00	0.00	0.00	0.00	0.00
11.00	1117.1	5072.	866345.	13.3	1495000.	3481171.	2.329	100.00	0.00	0.00	0.00	0.00
11.50	1188.0	5648.	939692.	14.3	1527500.	3932680.	2.575	100.00	0.00	0.00	0.00	0.00
12.00	1259.7	6260.	1020332.	15.7	1560000.	4422886.	2.835	100.00	0.00	0.00	0.00	0.00
12.50	1332.3	6908.	1103244.	17.0	1592500.	4953580.	3.111	100.00	0.00	0.00	0.00	0.00
13.00	1405.6	7593.	1194597.	18.4	1625000.	5528041.	3.402	100.00	0.00	0.00	0.00	0.00
13.50	1479.3	8314.	1293681.	19.9	1657500.	6150110.	3.710	100.00	0.00	0.00	0.00	0.00
14.00	1554.0	9072.	1404565.	21.6	1690000.	6824672.	4.038	100.00	0.00	0.00	0.00	0.00
14.50	1629.1	9868.	1522536.	23.4	1722500.	7556447.	4.387	100.00	0.00	0.00	0.00	0.00
15.00	1704.6	10701.	1664138.	25.6	1755000.	8355115.	4.760	100.00	0.00	0.00	0.00	0.00



TABLE 2.6.7-5

CYDROP(CORNER)

NUCLEAR PACKAGING PROPRIETARY

17.19.16

85/06/27

PAGE 11

NUPAC-B 10/140M CRUSH DEPTH CHECK (161 DEG)

PACKAGE WEIGHT \* 65000. (LBS)  
 PACKAGE EXTERNAL LENGTH \* 117.50 (IN)  
 PACKAGE EXTERNAL DIAMETER \* 101.00 (IN)  
 PACKAGE EXTERNAL HOLE DIA \* 55.00 (IN)  
 PAYLOAD ENVELOPE LENGTH \* 63.50 (IN)  
 PAYLOAD ENVELOPE DIAMETER \* 75.00 (IN)  
 OVERPACK LENGTH \* 40.00 (IN)

DROP HEIGHT \* 1.00 (FT)  
 ORIENTATION ANGLE \* 40.090 (DEGREES HRT TO VERTICAL)

PLATEAU CRUSH STRESS \* 687.00 (PSI)  
 (DEFAULT TAKEN AT 10 PCT STRAIN)

STRESS/STRAIN EVALUATED IN 1/2 CRUSH PLANE ELLIPSE AT:  
 NX \* 25 POINTS PARALLEL TO SEMI-MINOR ELLIPSE AXIS  
 NY \* 25 POINTS PARALLEL TO SEMI-MAJOR ELLIPSE AXIS

EXPERIMENTAL STRAIN VS. STRESS VALUES

CYDROP(CORNER)

NUCLEAR PACKAGING PROPRIETARY

17.19.16

85/06/27

PAGE 12

NUPAC-B 10/140M CRUSH DEPTH CHECK (161 DEG)

CRUSH DEPTH (IN)	** CRUSH PLANE **		**** IMPACT ****		***** ENERGY *****			DISTRIBUTION OF STRAIN RATIOS BY PERCENT OF CONTACT AREA				
	AREA (IN <sup>2</sup> )	VOLUME (IN <sup>3</sup> )	FORCE (LBS)	ACCEL. (G)	KINETIC (IN-LB)	STRAIN (IN-LB)	RATIO (SE/KE)	LE.70	GT.70 LE.80	GT.80 LE.90	GT.90 LE.95	GT.95
50	11.9	3.	1197.	.0	812500.	369.	.000	100.00	0.00	0.00	0.00	0.00
1.00	33.6	14.	7899.	.1	845000.	2673.	.003	100.00	0.00	0.00	0.00	0.00
1.50	61.5	38.	20711.	.3	877500.	9826.	.011	100.00	0.00	0.00	0.00	0.00
2.00	94.4	77.	38453.	.6	910000.	24617.	.027	100.00	0.00	0.00	0.00	0.00
2.50	131.4	134.	60201.	.9	942500.	49280.	.052	100.00	0.00	0.00	0.00	0.00
3.00	172.0	209.	85305.	1.3	975000.	85657.	.088	100.00	0.00	0.00	0.00	0.00
3.50	215.9	306.	113275.	1.7	1007500.	135302.	.134	100.00	0.00	0.00	0.00	0.00
4.00	262.7	426.	141962.	2.2	1040000.	199611.	.192	100.00	0.00	0.00	0.00	0.00
4.50	312.1	570.	177224.	2.7	1072500.	279908.	.261	100.00	0.00	0.00	0.00	0.00
5.00	360.1	739.	212967.	3.3	1105000.	377436.	.342	100.00	0.00	0.00	0.00	0.00
5.50	418.3	934.	253368.	3.9	1137500.	494039.	.434	100.00	0.00	0.00	0.00	0.00
6.00	474.6	1158.	297843.	4.6	1170000.	631842.	.540	100.00	0.00	0.00	0.00	0.00
6.50	532.9	1409.	343278.	5.3	1202500.	792122.	.659	100.00	0.00	0.00	0.00	0.00
7.00	593.0	1691.	390554.	6.0	1235000.	975580.	.790	100.00	0.00	0.00	0.00	0.00
7.50	654.8	2003.	440023.	6.8	1267500.	1183224.	.934	100.00	0.00	0.00	0.00	0.00
8.00	718.2	2346.	491850.	7.6	1300000.	1416193.	1.089	100.00	0.00	0.00	0.00	0.00
8.50	783.1	2721.	546081.	8.4	1332500.	1675676.	1.258	100.00	0.00	0.00	0.00	0.00
9.00	849.4	3130.	601557.	9.3	1365000.	1962585.	1.438	100.00	0.00	0.00	0.00	0.00
9.50	917.1	3571.	659861.	10.2	1397500.	2277940.	1.630	100.00	0.00	0.00	0.00	0.00
10.00	985.9	4047.	721543.	11.1	1430000.	2625291.	1.834	100.00	0.00	0.00	0.00	0.00
10.50	1056.0	4557.	784864.	12.1	1462500.	2999892.	2.051	100.00	0.00	0.00	0.00	0.00
11.00	1127.1	5105.	851459.	13.1	1495000.	3408973.	2.280	100.00	0.00	0.00	0.00	0.00
11.50	1199.2	5645.	924755.	14.2	1527500.	3853027.	2.522	100.00	0.00	0.00	0.00	0.00
12.00	1272.3	6303.	999382.	15.4	1560000.	4334062.	2.778	100.00	0.00	0.00	0.00	0.00
12.50	1346.2	6957.	1077273.	16.6	1592500.	4853228.	3.048	100.00	0.00	0.00	0.00	0.00
13.00	1421.0	7649.	1168390.	18.0	1625000.	5414621.	3.332	100.00	0.00	0.00	0.00	0.00
13.50	1496.5	8378.	1260384.	19.4	1657500.	6021792.	3.633	100.00	0.00	0.00	0.00	0.00
14.00	1572.8	9146.	1362910.	21.0	1690000.	6677616.	3.951	100.00	0.00	0.00	0.00	0.00
14.50	1649.6	9951.	1478454.	22.7	1722500.	7387957.	4.289	100.00	0.00	0.00	0.00	0.00
15.00	1727.1	10795.	1601697.	24.6	1755000.	8157995.	4.648	100.00	0.00	0.00	0.00	0.00



TABLE 2.6.7-6

HUPAC OBLIQUE ANALYSIS-HUPAC 10/140MB SHIPPING CASE ENVELOPE DIMENSIONS, COLD FOAM IFT

PACKAGE GEOMETRY-						
	LENGTH	=	83.500			
	RADIUS	=	37.250			
	OVERPACK LENGTH	=	55.000			
	OVERPACK SIDE THICKNESS	=	14.750			
	OVERPACK BOTTOM THICKNESS	=	13.000			
PACKAGE MASS PROPERTIES-						
	MASS	=	168.220			
	MASS MOMENT OF INERTIA	=	241400.000			
	GRAVITATIONAL CONSTANT	=	386.400			
SOLUTION CHARACTERISTICS-						
	IMPACT VELOCITY (YDOT)	=	-96.300			
	(XDOT)	=	0.000			
	(THETADOT)	=	0.000			
	FRICTION COEFFICIENT	=	0.000			
	ESTIMATED CRUSH DEPTH	=	20.000			
THETA	FMAX	SHEAR	THRUST	MOMENT	DEFLECTION	CLEARANCE
88.0000	738005.	25204.	737574.	311788.	.47	13.03
86.0000	966104.	62179.	964130.	769171.	.95	12.96
84.0000	840277.	82575.	836239.	1021478.	1.18	13.19
82.0000	710683.	93255.	704600.	1153601.	1.47	13.33
80.0000	724882.	119940.	714982.	1483697.	1.59	13.65
78.0000	644165.	127698.	631515.	1579666.	1.83	13.81
76.0000	584882.	134942.	569248.	1669278.	2.05	13.98
74.0000	543097.	142611.	524182.	1764151.	2.29	14.10
72.0000	515050.	151371.	492523.	1872515.	2.61	14.13
70.0000	520163.	169353.	492069.	2096457.	2.96	14.11
68.0000	560841.	200813.	523946.	2484126.	3.40	14.01
66.0000	614211.	240424.	563627.	2974139.	3.80	13.92
64.0000	638864.	270634.	578937.	3347846.	4.11	13.91
62.0000	629186.	285958.	560449.	3537403.	4.35	13.93
60.0000	612879.	297545.	536246.	3680738.	4.55	13.97
58.0000	614589.	317222.	526408.	3924154.	4.71	14.04
56.0000	618211.	338386.	517378.	4185963.	4.84	14.11
54.0000	620688.	358872.	506423.	4439378.	4.95	14.18
52.0000	620949.	377935.	492741.	4675190.	5.06	14.24
50.0000	619957.	395857.	477120.	4896894.	5.14	14.28
48.0000	616228.	411653.	458561.	5092305.	5.20	14.33
46.0000	610222.	424972.	437916.	5257055.	5.23	14.37
44.0000	602201.	435824.	415576.	5391301.	5.23	14.42
42.0000	592518.	444320.	391991.	5496403.	5.21	14.45
40.0000	581620.	450688.	367643.	5575183.	5.16	14.48
38.0000	568624.	453628.	342863.	5611544.	5.10	14.51
36.0000	556499.	456474.	318405.	5646749.	5.01	14.52
34.0000	546928.	459694.	296620.	5686589.	4.90	14.54
32.0000	540240.	464349.	276770.	5744166.	4.77	14.56
30.0000	531240.	465550.	255888.	5759029.	4.61	14.58
28.0000	510045.	455598.	229677.	5635920.	4.41	14.61
26.0000	484206.	440159.	202370.	5444932.	4.18	14.65
24.0000	456626.	421442.	176350.	5213391.	3.91	14.71
22.0000	431942.	404230.	152917.	5000477.	3.62	14.77
20.0000	413434.	391389.	133334.	4841622.	3.33	14.82
18.0000	402681.	385439.	116926.	4768021.	3.07	14.80
16.0000	405227.	391667.	104847.	4845066.	2.84	14.75
14.0000	400896.	390530.	90877.	4830999.	2.57	14.73
12.0000	407982.	400349.	79183.	4952471.	2.34	14.64
10.0000	427929.	422107.	70296.	5221618.	2.12	14.56
8.0000	308598.	305808.	41401.	3782961.	1.56	14.80
6.0000	389873.	388091.	37240.	4800826.	1.59	14.33
4.0000	336337.	335605.	22183.	4151555.	1.18	14.40
2.0000	433078.	432840.	14363.	5354393.	.99	14.18

FIGURE 2.6.7-1

## IMPACT FORCES (LBS)

NUPAC 10/140MB SHIPPING CASK ENVELOPE DIMENSIONS. INITIAL VELOCITY = -96.300

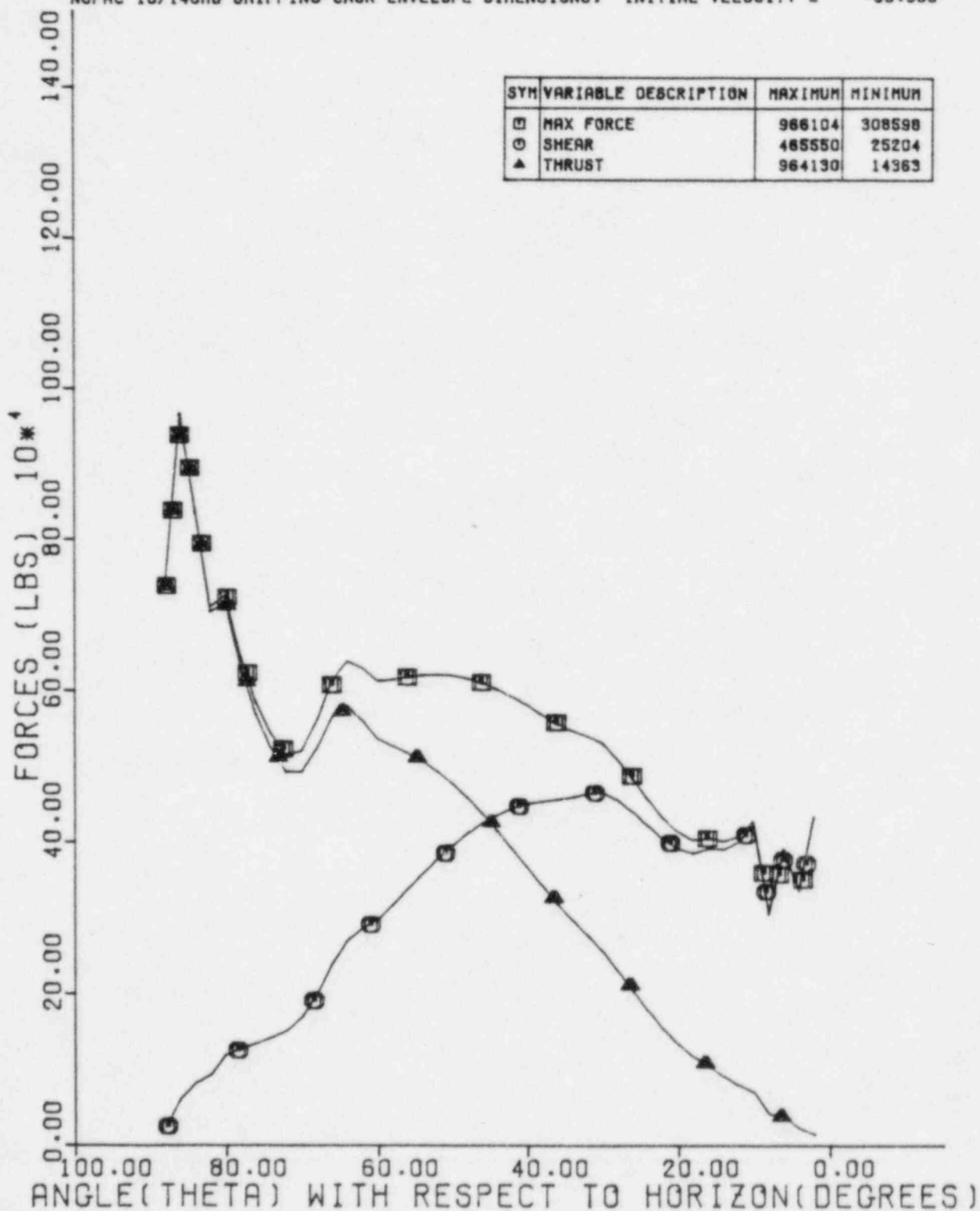
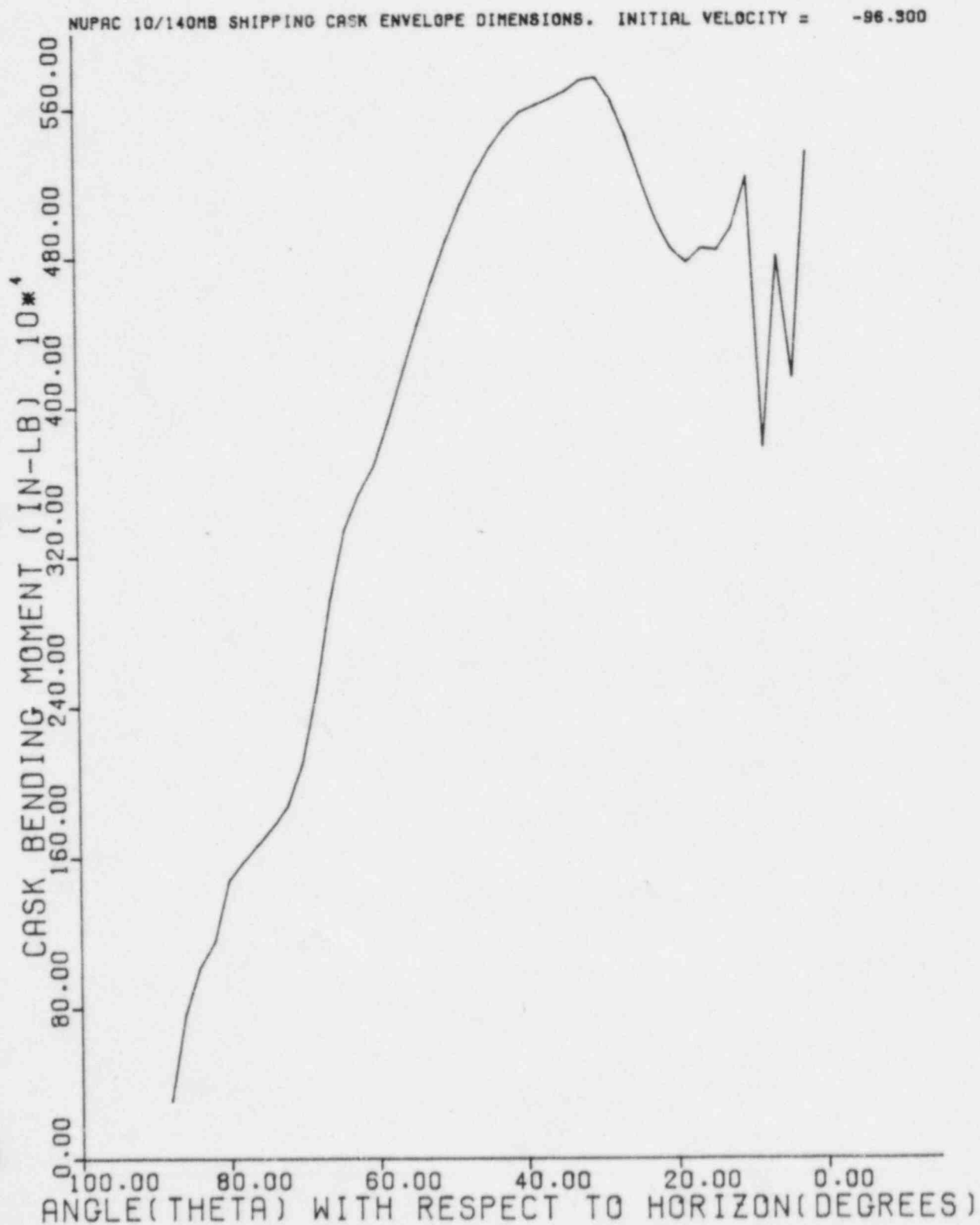


FIGURE 2.6.7-2

## CASK BENDING MOMENT (IN-LB)



Not surprisingly, the internal forces for a drop from one foot are very much less than for a drop from 30 feet.

As in the case of the hypothetical accident 30 foot oblique impact, the separation moment at the cask lid interface is calculated using the OBLIQUE post processor POSTOB. Input data for POSTOB for normal conditions is identical to the accident condition input data presented in Section 2.7.1.2.3.

The worst case separation moment occurs in the c.g. over struck corner orientation, just as in the 30 foot impact case. POSTOB predicts a moment of  $8.51 \times 10^6$  lb-in. The OBLIQUE time history results for this case (approximately  $50^\circ$  from horizontal impact) is presented in Table 2.6.7-7 and the POSTOB analysis of the case is shown in Table 2.6.7-8.

TABLE 2.6.7-7

NUPAC OBLIQUE ANALYSIS-NUPAC 10/140MB SHIPPING CASK ENVELOPE DIMENSIONS, COLD FOAM 1FT

PACKAGE GEOMETRY-						
LENGTH	*	83.500				
RADIUS	*	37.250				
OVERPACK LENGTH	*	40.000				
OVERPACK SIDE THICKNESS	*	16.500				
OVERPACK BOTTOM THICKNESS	*	18.000				
PACKAGE MASS PROPERTIES-						
MASS	*	168.220				
MASS MOMENT OF INERTIA	*	241400.000				
GRAVITATIONAL CONSTANT	*	386.400				
SOLUTION CHARACTERISTICS-						
IMPACT VELOCITY (YDOT)	*	-96.300				
(XDOT)	*	0.000				
(THETADOT)	*	0.000				
FRICTION COEFFICIENT	*	0.000				
ESTIMATED CRUSH DEPTH	*	20.000				
THETA0	FMAX	SHEAR	THRUST	MOMENT	DEFLECTION	CLEARANCE
50.0000	623157.	599464.	478282.	4941513.	5.15	19.24

TIME	X	XDOT	Y	YDOT	THETA	THETADOT	F	SHEAR	THRUST	DELTA(-Y AND X)
0.	0.	0.	0.	-9630E+02	8727E+00	0.	0.	3545E+06	5183E+06	1608E+00
1.664E-02	0.	0.	-1608E+00	-9694E+02	8727E+00	1016E-04	1082E+04	6952E+03	8285E+03	1608E+00
3.328E-02	0.	0.	-3226E+00	-9756E+02	8727E+00	4010E-04	2170E+04	1395E+04	1662E+04	3226E+00
4.991E-02	0.	0.	-4854E+00	-9818E+02	8727E+00	8904E-04	3266E+04	2099E+04	2502E+04	4854E+00
6.655E-02	0.	0.	-6493E+00	-9878E+02	8727E+00	1715E-03	6529E+04	4197E+04	5002E+04	6493E+00
8.319E-02	0.	0.	-8141E+00	-9935E+02	8727E+00	3253E-03	1144E+05	7352E+04	8762E+04	8141E+00
9.983E-02	0.	0.	-9798E+00	-9983E+02	8727E+00	5664E-03	1798E+05	1156E+05	1377E+05	9797E+00
1.165E-01	0.	0.	-1146E+01	-1003E+03	8727E+00	9251E-03	2627E+05	1689E+05	2013E+05	1146E+01
1.331E-01	0.	0.	-1315E+01	-1008E+03	8727E+00	1420E-02	3636E+05	2537E+05	2785E+05	1315E+01
1.497E-01	0.	0.	-1481E+01	-1008E+03	8727E+00	2070E-02	4826E+05	3102E+05	3697E+05	1481E+01
1.664E-01	0.	0.	-1649E+01	-1009E+03	8727E+00	2895E-02	6200E+05	3985E+05	4750E+05	1649E+01
1.830E-01	0.	0.	-1817E+01	-1009E+03	8727E+00	3909E-02	7745E+05	4979E+05	5933E+05	1817E+01
1.997E-01	0.	0.	-1984E+01	-1007E+03	8727E+00	5123E-02	9451E+05	6075E+05	7240E+05	1984E+01
2.163E-01	0.	0.	-2151E+01	-1003E+03	8727E+00	6544E-02	1151E+06	7267E+05	8661E+05	2151E+01
2.329E-01	0.	0.	-2318E+01	-9971E+02	8727E+00	8177E-02	1330E+06	8546E+05	1019E+06	2318E+01
2.496E-01	0.	0.	-2485E+01	-9895E+02	8727E+00	1002E-01	1541E+06	9902E+05	1180E+06	2485E+01
2.662E-01	0.	0.	-2647E+01	-9794E+02	8727E+00	1208E-01	1762E+06	1135E+06	1350E+06	2647E+01
2.828E-01	0.	0.	-2809E+01	-9675E+02	8728E+00	1434E-01	1992E+06	1281E+06	1526E+06	2809E+01
2.995E-01	0.	0.	-2969E+01	-9529E+02	8728E+00	1679E-01	2230E+06	1433E+06	1708E+06	2969E+01
3.161E-01	0.	0.	-3126E+01	-9360E+02	8728E+00	1944E-01	2472E+06	1589E+06	1894E+06	3126E+01
3.328E-01	0.	0.	-3280E+01	-9168E+02	8729E+00	2226E-01	2718E+06	1747E+06	2082E+06	3280E+01
3.494E-01	0.	0.	-3431E+01	-8951E+02	8729E+00	2524E-01	2965E+06	1906E+06	2272E+06	3430E+01
3.660E-01	0.	0.	-3578E+01	-8644E+02	8730E+00	2837E-01	3213E+06	2065E+06	2462E+06	3577E+01
3.827E-01	0.	0.	-3721E+01	-8244E+02	8730E+00	3163E-01	3460E+06	2232E+06	2651E+06	3720E+01
3.993E-01	0.	0.	-3859E+01	-7740E+02	8730E+00	3502E-01	3704E+06	2380E+06	2838E+06	3858E+01
4.159E-01	0.	0.	-3992E+01	-7143E+02	8731E+00	3851E-01	3946E+06	2534E+06	3022E+06	3990E+01
4.325E-01	0.	0.	-4119E+01	-6460E+02	8732E+00	4209E-01	4179E+06	2684E+06	3202E+06	4118E+01
4.492E-01	0.	0.	-4241E+01	-5556E+02	8732E+00	4576E-01	4406E+06	2830E+06	3377E+06	4240E+01
4.658E-01	0.	0.	-4357E+01	-4556E+02	8733E+00	4950E-01	4626E+06	2971E+06	3545E+06	4355E+01
4.823E-01	0.	0.	-4466E+01	-3535E+02	8734E+00	5330E-01	4836E+06	3105E+06	3707E+06	4464E+01
4.991E-01	0.	0.	-4568E+01	-2506E+02	8735E+00	5715E-01	5035E+06	3233E+06	3859E+06	4566E+01
5.158E-01	0.	0.	-4618E+01	-1426E+02	8736E+00	5913E-01	5131E+06	3295E+06	3954E+06	4615E+01
5.324E-01	0.	0.	-4715E+01	-264E+02	8737E+00	6099E-01	5396E+06	3464E+06	4137E+06	4748E+01
5.490E-01	0.	0.	-4796E+01	-4767E+02	8738E+00	6717E-01	5686E+06	3522E+06	4206E+06	4795E+01
5.657E-01	0.	0.	-4902E+01	-4059E+02	8739E+00	7297E-01	5701E+06	3659E+06	4372E+06	4999E+01
5.823E-01	0.	0.	-4946E+01	-3553E+02	8741E+00	7701E-01	5830E+06	3741E+06	4471E+06	4962E+01
5.990E-01	0.	0.	-5020E+01	-3035E+02	8742E+00	8108E-01	5942E+06	3813E+06	4558E+06	5016E+01
6.156E-01	0.	0.	-5067E+01	-2506E+02	8743E+00	8518E-01	6037E+06	3873E+06	4631E+06	5062E+01
6.322E-01	0.	0.	-5084E+01	-2264E+02	8744E+00	8705E-01	6074E+06	3896E+06	4660E+06	5080E+01
6.489E-01	0.	0.	-5132E+01	-1426E+02	8746E+00	9350E-01	6172E+06	3958E+06	4736E+06	5126E+01
6.655E-01	0.	0.	-5151E+01	-8778E+01	8748E+00	9772E-01	6212E+06	3983E+06	4767E+06	5145E+01
6.822E-01	0.	0.	-5161E+01	-3266E+01	8750E+00	1020E+00	6232E+06	3995E+06	4783E+06	5155E+01

MAX= .62316E+06 FMIN= 0.

TABLE 2.6.7-8

PROGRAM POSTOB, VERSION 0, DATE 7/12/85

CENTER OF GRAVITY OFFSET \* 8.50  
 MOMENT OF INERTIA OF UPPER PART \* 166100.00  
 MASS OF UPPER PART (INCL. P/L) \* 139.20  
 MASS OF PAYLOAD \* 38.80  
 LID FLANGE THICKNESS \* 2.25  
 PACKAGE LENGTH (W/O OVERPACK) \* 83.50  
 PACKAGE RADIUS (W/O OVERPACK) \* 37.25  
 ACCELERATION OF GRAVITY \* 386.40

ANGLE	TIME	LAT. ACCEL	AX. ACCEL	X ACCEL	Y ACCEL	TH ACCEL	MOMENT ADJACENT	MOMENT OPPOSITE	MAX ADJ. MOMENT	MAX OPP. MOMENT
50.00	.1664E-02	-1.199	1.367	-3976E-01	1.818	.6106E-02	3912.	-.1414E+05	3912.	-.1414E+05
50.00	.3328E-02	-9.026	10.57	-1172	13.90	.1799E-01	.2375E+05	-.1028E+06	.2375E+05	-.1414E+05
50.00	.4991E-02	-8.979	10.40	-1916	13.74	.2943E-01	.2597E+05	-.1038E+06	.2597E+05	-.1414E+05
50.00	.6655E-02	-17.02	19.78	-3227	26.09	.4956E-01	.4796E+05	-.1959E+06	.4796E+05	-.1414E+05
50.00	.8319E-02	-36.69	42.80	-5940	56.57	.9123E-01	.1002E+06	-.4204E+06	.1002E+06	-.1414E+05
50.00	.9983E-02	-56.47	65.82	-9553	86.72	.1464	.1555E+06	-.6478E+06	.1555E+06	-.1414E+05
50.00	.1163E-01	-68.97	80.02	-1399	105.6	.2149	.1972E+06	-.7958E+06	.1972E+06	-.1414E+05
50.00	.1331E-01	-134.7	157.6	-1941	207.3	.2981	.3605E+06	-.1539E+07	.3605E+06	-.1414E+05
50.00	.1497E-01	-174.2	203.7	-2550	268.1	.3916	.4674E+06	-.1991E+07	.4674E+06	-.1414E+05
50.00	.1664E-01	-214.1	250.1	-3217	329.2	.4940	.5769E+06	-.2448E+07	.5769E+06	-.1414E+05
50.00	.1830E-01	-253.6	296.0	-3978	389.7	.6108	.6886E+06	-.2903E+07	.6886E+06	-.1414E+05
50.00	.1997E-01	-331.5	387.8	-4734	510.1	.7269	.8857E+06	-.3786E+07	.8857E+06	-.1414E+05
50.00	.2163E-01	-410.5	480.6	-5574	632.0	.8560	.1088E+07	-.4683E+07	.1088E+07	-.1414E+05
50.00	.2329E-01	-485.2	568.3	-6406	747.2	.9837	.1280E+07	-.5530E+07	.1280E+07	-.1414E+05
50.00	.2496E-01	-558.0	653.8	-7186	859.5	1.104	.1466E+07	-.6357E+07	.1466E+07	-.1414E+05
50.00	.2662E-01	-642.2	752.9	-8081	989.6	1.241	.1682E+07	-.7315E+07	.1682E+07	-.1414E+05
50.00	.2828E-01	-728.4	854.4	-8866	1125.	1.361	.1898E+07	-.8289E+07	.1898E+07	-.1414E+05
50.01	.2995E-01	-815.0	956.6	-9554	1257.	1.467	.2111E+07	-.9267E+07	.2111E+07	-.1414E+05
50.01	.3161E-01	-916.2	1076.	-1040	1413.	1.596	.2363E+07	-.1041E+08	.2363E+07	-.1414E+05
50.01	.3328E-01	-1002.	1177.	-1180	1545.	1.689	.2571E+07	-.1137E+08	.2571E+07	-.1414E+05
50.01	.3494E-01	-1104.	1298.	-1169	1703.	1.795	.2819E+07	-.1253E+08	.2819E+07	-.1414E+05
50.01	.3660E-01	-1197.	1408.	-1228	1849.	1.886	.3046E+07	-.1358E+08	.3046E+07	-.1414E+05
50.02	.3827E-01	-1288.	1517.	-1271	1990.	1.952	.3261E+07	-.1460E+08	.3261E+07	-.1414E+05
50.02	.3995E-01	-1388.	1635.	-1330	2145.	2.042	.3500E+07	-.1575E+08	.3500E+07	-.1414E+05
50.02	.4159E-01	-1481.	1746.	-1369	2289.	2.102	.3719E+07	-.1678E+08	.3719E+07	-.1414E+05
50.03	.4326E-01	-1563.	1843.	-1396	2416.	2.144	.3907E+07	-.1769E+08	.3907E+07	-.1414E+05
50.03	.4492E-01	-1660.	1958.	-1440	2567.	2.211	.4136E+07	-.1878E+08	.4136E+07	-.1414E+05
50.03	.4659E-01	-1740.	2054.	-1459	2692.	2.240	.4319E+07	-.1968E+08	.4319E+07	-.1414E+05
50.04	.4825E-01	-1831.	2162.	-1491	2833.	2.289	.4528E+07	-.2070E+08	.4528E+07	-.1414E+05
50.04	.4991E-01	-1904.	2250.	-1511	2947.	2.319	.4696E+07	-.2152E+08	.4696E+07	-.1414E+05
50.05	.5158E-01	-1116.	1320.	-7.726	1728.	1.186	.2715E+07	-.1259E+08	.4696E+07	-.1414E+05
50.06	.5324E-01	-2912.	3441.	-23.00	4508.	3.530	.7172E+07	-.3291E+08	.7172E+07	-.1414E+05
50.06	.5490E-01	-1272.	1506.	-8.559	1972.	1.313	.3086E+07	-.1435E+08	.7172E+07	-.1414E+05
50.07	.5657E-01	-2995.	3547.	-22.64	4645.	3.473	.7348E+07	-.3388E+08	.7348E+07	-.1414E+05
50.08	.5823E-01	-2225.	2634.	-15.86	3948.	2.454	.5419E+07	-.2512E+08	.7348E+07	-.1414E+05
50.09	.5990E-01	-2259.	2675.	-15.89	3501.	2.437	.5492E+07	-.2550E+08	.7348E+07	-.1414E+05
50.09	.6156E-01	-2313.	2741.	-16.10	3587.	2.470	.5617E+07	-.2612E+08	.7348E+07	-.1414E+05
50.10	.6322E-01	-1193.	1415.	-7.345	1850.	1.127	.2865E+07	-.1345E+08	.7348E+07	-.1414E+05
50.11	.6489E-01	-3499.	4146.	-25.19	5425.	3.862	.8514E+07	-.3953E+08	.8514E+07	-.1414E+05
50.12	.6655E-01	-2387.	2831.	-16.58	3703.	2.542	.5785E+07	-.2694E+08	.8514E+07	-.1414E+05
50.13	.6822E-01	-2385.	2830.	-16.72	3701.	2.563	.5781E+07	-.2695E+08	.8514E+07	-.1414E+05

2.6.7.2.4 Stress Calculations in Cask Body

From the summary of internal forces in Table 2.6.7-6 above, the worst case state of compressive stress may be found. From that table, it is clear that the worst stress state will occur during drops from angles between 64 and 30 degrees from horizontal. Using the standard formula for combined axial and bending stress

$$\sigma = P/A + Mc/I$$

and conservatively assuming all stress is carried by the outer shell, the following table may be constructed:

<u>Impact Angle</u>	<u>Thrust</u> (10 <sup>6</sup> lbs)	<u>Moment</u> (10 <sup>6</sup> lb-in)	<u>Stress</u> (psi)
64	.5790	3.348	2659
62	.5604	3.537	2631
60	.5362	3.681	2575
58	.5264	3.924	2587
56	.5174	4.186	2607
54	.5064	4.439	2617
52	.4927	4.675	2615
50	.4771	4.897	2604
48	.4586	5.092	2577
46	.4379	5.257	2537
44	.4156	5.391	2485
42	.3920	5.496	2424
40	.3676	5.575	2354
38	.3429	5.612	2275
36	.3184	5.647	2197
34	.2966	5.687	2129
32	.2768	5.744	2071
30	.2559	5.759	2001

The stresses above were calculated assuming that all of the bending and axial forces are carried by the outer shell, which has a cross section area of 287.6 in<sup>2</sup> and moment of inertia of  $1.93 \times 10^5$  in<sup>4</sup> (see Section 2.7.1.2.4). These stresses have been derived using extremely conservative techniques. In addition, the stress maximum for the package for 1 foot oblique impacts occurs at the point of local peak in thrust load, 64°. Thrust loads are clearly highest during end impacts, and moments are clearly higher in side impacts, so it seems clear that oblique corner impacts from 1 foot are very much less severe than end or side impacts. Margins of Safety during oblique impacts from 1 foot are large.

#### 2.6.7.2.5 Lid Attachment Forces

The maximum lid separation moment calculated by POSTOB is  $8.51 \times 10^6$  lb-in. Using the formula relating the moment to the maximum EnviroLock<sup>tm</sup> force given in Section 2.7.1.2.5, the maximum force the EnviroLock would be:

$$f_M = 4(8.51 \times 10^6) / 3(40.5)8 = 35,000 \text{ lbs.}$$

The yield strength of the EnviroLocks<sup>tm</sup> is 184,500 lbs, so the Margin of Safety is

$$184,500 / 35,000 - 1 = +4.27$$

which is very large.

#### 2.6.7.3 Flat Side Impact

Analysis of the 10/140MB cask behavior during side impact from one foot follows the same approach described in Section 2.7.1.3 for the hypothetical accident impact event. Because the normal condition impact is much less severe than the accident condition impact, the evaluation of the event is somewhat less complicated.



The analysis presented here follows these steps:

- 1.) Determine the impact forces using the SYDROP computer program as well as some hand analyses.
- 2.) Determine stresses in the outer shell assuming it reacts the entire impact bending load.
- 3.) Determine stresses in the inner shell assuming it reacts the payload weight and half the lead weight in bending.

#### 2.6.7.3.1 Side Impact Forces and Deflections

Side impact forces from impact on the cylindrical sides of the overpack were determined using the SYDROP energy balance program. Analyses were performed assuming foam properties at  $-20^{\circ}\text{F}$  increased 15% and at  $157^{\circ}\text{F}$  decreased 15% to envelope the full range of normal condition foam response. The full 30 inches of 108 inches dia. overpack length on each end is assumed effective. This has been shown by test to be the most realistic model and results in higher loads. The additional 10 inches of overpack length at 101 inches in diameter is not modeled since the SYDROP analysis shows that during one foot drops, the overpack does not deflect enough to mobilize this part of the foam. Tables 2.6.7-9 and 2.6.7-10 are the results of the SYDROP analyses at  $-20^{\circ}\text{F}$  and  $157^{\circ}\text{F}$  respectively. They show that the highest acceleration on side impact is 25.8 g's (at  $-20^{\circ}\text{F}$ ), and the largest deflection occurs at  $157^{\circ}\text{F}$ , 1.80 inches.

The analysis of impacts on the flat sides of the overpacks may proceed as in the hypothetical accident analysis, see section 2.7.1.3 for an explanation of the necessity and conservative nature of the following analysis.

The highest impact accelerations will clearly occur at  $-20^{\circ}\text{F}$ . The overpack response may be conservatively assumed to act as a pad of foam of uniform thickness equal to the narrowest thickness of the overpack, 10.75 inches. The pad may be conservatively assumed to have the same impact footprint area as the flat sides of the overpack. The impact footprint is diagrammed below:

TABLE 2.6.7-9

SYDROP(SIDE)	NUCLEAR PACKAGING PROPRIETARY	17.47.20	85/06/26	PAGE 9
	HUPAC 10/140M COLD FOAM (-20 DEG)			
	PACKAGE WEIGHT	=	65000. (LBS)	
	PACKAGE EXTERNAL LENGTH	=	60.00 (IN)	
	PACKAGE EXTERNAL DIAMETER	=	108.00 (IN)	
	PAYLOAD DIAMETER	=	75.00 (IN)	
	DROP HEIGHT	=	1.00 (FT)	

## STRAIN VS STRESS TABLE

SYDROP(SIDE)	NUCLEAR PACKAGING PROPRIETARY						17.47.20	85/06/26	PAGE 10			
HUPAC 10/140M COLD FOAM (-20 DEG)												
	** CRUSH PLANE **		**** IMPACT ****		***** ENERGY *****		DISTRIBUTION OF STRAIN RATIOS BY PERCENT OF CONTACT AREA					
CRUSH DEPTH (IN)	AREA (IN2)	VOLUME (IN3)	FORCE (LBS)	ACCEL. (G)	POTENTIAL (IN-LB)	STRAIN (IN-LB)	RATIO (SE/PE)	LE.70	GT.70	GT.80	GT.90	GT.95
.25	622.8	104.	201140.	5.1	796250.	25143.	.032	100.00	0.00	0.00	0.00	0.00
.50	879.8	294.	567642.	8.7	812500.	121240.	.149	100.00	0.00	0.00	0.00	0.00
.75	1076.2	539.	988617.	15.2	828750.	315773.	.381	100.00	0.00	0.00	0.00	0.00
1.00	1241.3	829.	1425121.	21.9	845000.	617490.	.731	100.00	0.00	0.00	0.00	0.00
1.15	1325.7	1021.	1674891.	25.8	854468.	856294.	1.000	100.00	0.00	0.00	0.00	0.00
1.25	1386.2	1158.	1853808.	28.5	861250.	1027356.	1.193	100.00	0.00	0.00	0.00	0.00
1.50	1516.7	1521.	2234554.	34.4	877500.	1538401.	1.753	100.00	0.00	0.00	0.00	0.00
1.75	1636.3	1915.	2570213.	39.5	893750.	2138997.	2.393	100.00	0.00	0.00	0.00	0.00
2.00	1747.2	2338.	2863236.	44.0	910000.	2818178.	3.097	100.00	0.00	0.00	0.00	0.00
2.25	1851.0	2788.	3120708.	48.0	926250.	3566171.	3.850	100.00	0.00	0.00	0.00	0.00
2.50	1948.8	3263.	3356182.	51.6	942500.	4375782.	4.643	100.00	0.00	0.00	0.00	0.00
2.75	2041.5	3762.	3574521.	55.0	958750.	5242120.	5.468	100.00	0.00	0.00	0.00	0.00
3.00	2129.8	4284.	3779292.	58.1	975000.	6161346.	6.319	100.00	0.00	0.00	0.00	0.00
3.25	2214.1	4827.	3973051.	61.1	991250.	7130389.	7.193	100.00	0.00	0.00	0.00	0.00
3.50	2295.0	5391.	4158308.	64.0	1007500.	8146809.	8.086	100.00	0.00	0.00	0.00	0.00
3.75	2372.7	5974.	4337166.	66.7	1023750.	9208743.	8.995	100.00	0.00	0.00	0.00	0.00
4.00	2447.5	6577.	4511114.	69.4	1040000.	10314778.	9.918	100.00	0.00	0.00	0.00	0.00
4.25	2519.8	7198.	4681531.	72.0	1056250.	11463859.	10.853	100.00	0.00	0.00	0.00	0.00
4.50	2589.7	7836.	4849708.	74.6	1072500.	12655264.	11.800	100.00	0.00	0.00	0.00	0.00
4.75	2657.5	8492.	5016875.	77.2	1088750.	13885587.	12.756	100.00	0.00	0.00	0.00	0.00
5.00	2723.2	9165.	5184126.	79.8	1105000.	15163712.	13.723	100.00	0.00	0.00	0.00	0.00
5.25	2787.1	9854.	5351775.	82.3	1121250.	16480699.	14.699	100.00	0.00	0.00	0.00	0.00
5.50	2849.2	10558.	5521436.	84.9	1137500.	17839851.	15.683	100.00	0.00	0.00	0.00	0.00
5.75	2909.7	11278.	5694426.	87.6	1153750.	19241834.	16.678	100.00	0.00	0.00	0.00	0.00
6.00	2968.6	12013.	5872159.	90.3	1170000.	20687657.	17.682	100.00	0.00	0.00	0.00	0.00
6.25	3026.1	12762.	6056045.	93.2	1186250.	22178682.	18.696	100.00	0.00	0.00	0.00	0.00
6.50	3082.3	13526.	6247452.	96.1	1202500.	23716619.	19.723	100.00	0.00	0.00	0.00	0.00
6.75	3137.1	14303.	6446321.	99.2	1218750.	25303341.	20.762	100.00	0.00	0.00	0.00	0.00
7.00	3190.7	15095.	6652470.	102.3	1235000.	26940690.	21.814	100.00	0.00	0.00	0.00	0.00
7.25	3243.2	15899.	6864976.	105.7	1251250.	28633933.	22.882	100.00	0.00	0.00	0.00	0.00
7.50	3294.5	16716.	7109119.	109.2	1267500.	30377132.	23.966	100.00	0.00	0.00	0.00	0.00
7.75	3344.8	17546.	7347186.	113.0	1283750.	32183046.	25.070	100.00	0.00	0.00	0.00	0.00
8.00	3394.1	18388.	7613574.	117.1	1300000.	34053144.	26.195	100.00	0.00	0.00	0.00	0.00
8.25	3442.4	19243.	7902202.	121.6	1316250.	35992613.	27.345	100.00	0.00	0.00	0.00	0.00
8.50	3489.8	20109.	8206739.	126.3	1332500.	38006231.	28.522	100.00	0.00	0.00	0.00	0.00
8.75	3536.3	20988.	8533378.	131.3	1348750.	40098745.	29.730	100.00	0.00	0.00	0.00	0.00
9.00	3582.0	21878.	8890727.	136.8	1365000.	42276758.	30.972	100.00	0.00	0.00	0.00	0.00
9.25	3626.8	22779.	9286188.	142.9	1381250.	44548873.	32.253	100.00	0.00	0.00	0.00	0.00
9.50	3670.8	23691.	9727536.	149.7	1397500.	46925588.	33.578	100.00	0.00	0.00	0.00	0.00
9.75	3714.1	24614.	10222921.	157.3	1413750.	49419395.	34.956	100.00	0.00	0.00	0.00	0.00
10.00	3756.6	25548.	10781992.	165.9	1430000.	52045010.	36.393	100.00	0.00	0.00	0.00	0.00

TABLE 2.6.7-10

SYDROP(SIDE)

NUCLEAR PACKAGING PROPRIETARY

17.47.20

85/06/26

PAGE 11

NUPAC 10/140M HOT FOAM (161 DEG)

PACKAGE WEIGHT = 65000. (LBS)  
 PACKAGE EXTERNAL LENGTH = 60.00 (IN)  
 PACKAGE EXTERNAL DIAMETER = 108.00 (IN)  
 PAYLOAD DIAMETER = 75.00 (IN)  
 DROP HEIGHT = 1.00 (FT)

## STRAIN VS STRESS TABLE

SYDROP(SIDE)

NUCLEAR PACKAGING PROPRIETARY

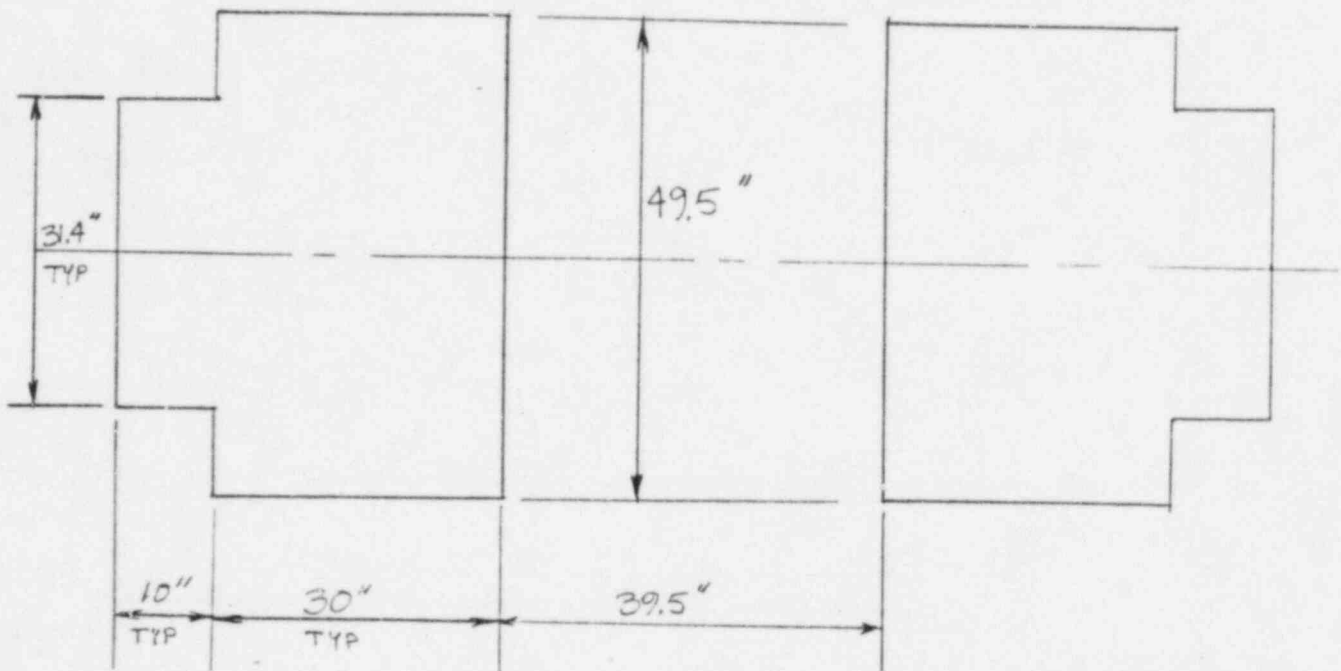
17.47.20

85/06/26

PAGE 12

NUPAC 10/140M HOT FOAM (161 DEG)

CRUSH DEPTH (IN)	** CRUSH PLANE **		**** IMPACT ****		***** ENERGY *****			DISTRIBUTION OF STRAIN RATIOS BY PERCENT OF CONTACT AREA				
	AREA (IN <sup>2</sup> )	VOLUME (IN <sup>3</sup> )	FORCE (LBS)	ACCEL. (G)	POTENTIAL (IN-LB)	STRAIN (IN-LB)	RATIO (SE/PE)	LE.70	GT.70	GT.80	GT.90	GT.95
.25	622.8	104.	85904.	1.3	796250.	10738.	.013	100.00	0.00	0.00	0.00	0.00
.50	879.8	294.	242488.	5.7	812500.	51787.	.064	100.00	0.00	0.00	0.00	0.00
.75	1076.2	539.	431691.	6.4	828750.	136059.	.164	100.00	0.00	0.00	0.00	0.00
1.00	1241.3	829.	598346.	9.2	845000.	264814.	.313	100.00	0.00	0.00	0.00	0.00
1.25	1386.2	1158.	728984.	11.2	861250.	430730.	.500	100.00	0.00	0.00	0.00	0.00
1.50	1518.7	1521.	846035.	13.0	877500.	627607.	.715	100.00	0.00	0.00	0.00	0.00
1.75	1636.3	1915.	951593.	14.6	893750.	852311.	.954	100.00	0.00	0.00	0.00	0.00
1.80	1656.3	1991.	968703.	14.9	896677.	897294.	1.000	100.00	0.00	0.00	0.00	0.00
2.00	1747.2	2338.	1046596.	16.1	910000.	1102085.	1.211	100.00	0.00	0.00	0.00	0.00
2.25	1851.0	2788.	1134448.	17.5	926250.	1374715.	1.484	100.00	0.00	0.00	0.00	0.00
2.50	1948.8	3263.	1218953.	18.8	942500.	1668890.	1.771	100.00	0.00	0.00	0.00	0.00
2.75	2041.5	3762.	1299943.	20.0	958750.	1983752.	2.069	100.00	0.00	0.00	0.00	0.00
3.00	2129.6	4284.	1377735.	21.2	975000.	2318462.	2.378	100.00	0.00	0.00	0.00	0.00
3.25	2214.1	4827.	1452919.	22.4	991250.	2672294.	2.696	100.00	0.00	0.00	0.00	0.00
3.50	2295.0	5391.	1526359.	23.5	1007500.	3044703.	3.022	100.00	0.00	0.00	0.00	0.00
3.75	2372.7	5974.	1598803.	24.6	1023750.	3435349.	3.356	100.00	0.00	0.00	0.00	0.00
4.00	2447.5	6577.	1670544.	25.7	1040000.	3844017.	3.696	100.00	0.00	0.00	0.00	0.00
4.25	2519.8	7198.	1741934.	26.8	1056250.	4270577.	4.043	100.00	0.00	0.00	0.00	0.00
4.50	2589.7	7836.	1813321.	27.9	1072500.	4714984.	4.396	100.00	0.00	0.00	0.00	0.00
4.75	2657.5	8492.	1884990.	29.0	1088750.	5177273.	4.755	100.00	0.00	0.00	0.00	0.00
5.00	2723.2	9145.	1957222.	30.1	1105000.	5657549.	5.120	100.00	0.00	0.00	0.00	0.00
5.25	2787.1	9854.	2029921.	31.2	1121250.	6135942.	5.490	100.00	0.00	0.00	0.00	0.00
5.50	2849.2	10558.	2103544.	32.4	1137500.	6672625.	5.866	100.00	0.00	0.00	0.00	0.00
5.75	2909.7	11278.	2178572.	33.5	1153750.	7207889.	6.247	100.00	0.00	0.00	0.00	0.00
6.00	2968.6	12013.	2255412.	34.7	1170000.	7762137.	6.634	100.00	0.00	0.00	0.00	0.00
6.25	3026.1	12762.	2334498.	35.9	1186250.	8335876.	7.027	100.00	0.00	0.00	0.00	0.00
6.50	3082.3	13526.	2416219.	37.2	1202500.	8929716.	7.426	100.00	0.00	0.00	0.00	0.00
6.75	3137.1	14303.	2499790.	38.5	1218750.	9544217.	7.831	100.00	0.00	0.00	0.00	0.00
7.00	3190.7	15095.	2584052.	39.8	1235000.	10179697.	8.243	100.00	0.00	0.00	0.00	0.00
7.25	3243.2	15899.	2671446.	41.1	1251250.	10836634.	8.661	100.00	0.00	0.00	0.00	0.00
7.50	3294.5	16716.	2763660.	42.5	1267500.	11516022.	9.086	100.00	0.00	0.00	0.00	0.00
7.75	3344.8	17546.	2862384.	44.0	1283750.	12219278.	9.518	100.00	0.00	0.00	0.00	0.00
8.00	3394.1	18388.	2969344.	45.7	1300000.	12948244.	9.960	100.00	0.00	0.00	0.00	0.00
8.25	3442.4	19243.	3086424.	47.5	1316250.	13705215.	10.412	100.00	0.00	0.00	0.00	0.00
8.50	3489.8	20109.	3213883.	49.4	1332500.	14492753.	10.876	100.00	0.00	0.00	0.00	0.00
8.75	3536.3	20988.	3354280.	51.6	1348750.	15313774.	11.354	100.00	0.00	0.00	0.00	0.00
9.00	3582.0	21878.	3510652.	54.0	1365000.	16171890.	11.848	100.00	0.00	0.00	0.00	0.00
9.25	3626.8	22779.	3685927.	56.7	1381250.	17071462.	12.359	100.00	0.00	0.00	0.00	0.00
9.50	3670.8	23691.	3883223.	59.7	1397500.	18017606.	12.893	100.00	0.00	0.00	0.00	0.00
9.75	3714.1	24614.	4105651.	63.2	1413750.	19016215.	13.451	100.00	0.00	0.00	0.00	0.00
10.00	3756.6	25548.	4354171.	67.0	1430000.	20073693.	14.038	100.00	0.00	0.00	0.00	0.00



## OVERPACK FLAT FOOT PRINT GEOMETRY

The footprint area is given by:

$$2(49.5)(30) + 2(31.4)(10) = 3598 \text{ in.}^2 - \text{say } 3600 \text{ in.}^2$$

Using this cross-sectional area and the stress strain relationship for 20 lb. foam at  $-20^{\circ}\text{F}$  increased 15%, the following table may be constructed.

DEFLECTION (in)	STRAIN	STRESS (psi)	FORCE (lbs)	TOTAL STRAIN ENERGY (in lbs.)
0	0	0	0	0
0.323	3%	960	3456000	558144
0.538	5%	1416	5097600	1477656

The energy that must be dissipated assuming .323 inches of overpack deflection is

$$(12.323 \text{ in})(65000) = 800995 \text{ in-lb.}$$

so the ratio of strain energy to energy from the drop at .323 inches of deflection is

$$558144/800995 = .697$$

At .538 inches of deflection, the drop energy to dissipate is

$$(12.538)(65000) = 814970 \text{ in-lb.}$$

so the energy ratio is

$$1477656/814970 = 1.813$$

The maximum force from the impact may be determined by interpolation:

$$((1-.697)/(1.813-.697)) (5097600 - 3456000) + 3456000 = 3901700 \text{ lb.}$$

The maximum acceleration on impact may be estimated as:

$$3901700/65000 = 60.0 \text{ g's}$$

The maximum acceleration during a normal condition side impact would not exceed 60.0 g's.

2.6.7.3.2 Outer Shell Bending Stresses

The outer shell bending stresses for the hypothetical accident 30 foot side impact were determined using a linear analysis (see section 2.7.1.3.2). Therefore, the stresses derived from that analysis may be factored by the ratio of the normal condition impact acceleration to the hypothetical accident impact acceleration. The maximum stress intensity from hoop and longitudinal bending during the accident event is given in Section 2.7.1.3.2 as 11512 psi. Therefore, during normal conditions, the stress would be:

$$(60/141.9) (11512) = 4868 \text{ psi}$$

The allowable membrane stress under normal conditions for A516 grade 70 steel is 23,200 psi ( $S_m$ ) so the margin of safety is

$$M.S. = 23200/4868 - 1 = + \text{ Large}$$

The normal condition bending buckling allowable is 22,660 so the Margin of Safety on bending buckling is

$$M.S. = 22,660/4868 - 1 = + \text{ Large}$$

2.6.7.3.3 Inner Shell Stresses

The inner shell stresses may be factored from the hypothetical accident conditions in the same manner that outer shell stresses were. Thus, the 14925 psi maximum stress in the inner shell during the hypothetical accident side impact event becomes:

$$(60.0/141.9) (15043) = 6361 \text{ psi}$$

The margin of safety is then (using the membrane stress allowable):

$$M.S. = 20,000/6361 - 1 = +2.17$$

The buckling bending allowable is 19,173 psi so the margin of safety on bending buckling is then:

$$M.S. = 19,173/6361 - 1 = + 2.01$$

#### 2.6.8 Corner Drop

This requirement is not applicable since the NuPac 10/140MB is constructed primarily of steel and lead, and exceeds 220 pounds gross weight.

#### 2.6.9 Compression

This requirement is not applicable since the NuPac 10/140MB exceeds 10,000 pounds weight.

#### 2.6.10 Penetration

From previous container tests, as well as engineering judgement, it can be concluded that a 13 pound rod would have a negligible effect on the heavy gauge steel sheet overpack or cask.

As the result of the above assessment, it is concluded that in normal conditions of transport:

1. There will be no release of radioactive material from the package;
2. The effectiveness of the packaging will not be substantially reduced;
3. There will be no mixture of gases or vapors in the package which could, through any credible increase in pressure or an explosion, significantly reduce the effectiveness of the package.



## 2.7 Hypothetical Accident Conditions

The NuPac 10/140MB Cask, when subjected to hypothetical accident conditions as specified in 10 CFR 71.73, meets the performance requirements specified in Subpart E of 10 CFR 71. This is demonstrated in the following subsections where each accident condition is addressed and shown to meet the applicable design criteria previously discussed in Section 2.1.2.

### 2.7.1 Free Drop

Subpart F of 10 CFR 71 requires that a 30 foot free drop be considered for the NuPac 10/140MB Cask. The drop is to be onto a flat, essentially unyielding, horizontal surface, and the cask is to strike the surface in a position for which maximum damage is expected. Per 10 CFR 71.73(b) the initial temperature for the drop is to be the worst case constant ambient air temperature between -20°F and 100°F. Internal heat generation from the payload (95 watts) is also considered when it is conservative to do so. (Note: 10 CFR 71 does not require consideration of insolation as an initial condition for accident conditions). Regarding initial internal pressure, the maximum normal operating pressure must be considered unless a lower internal pressure consistent with the ambient temperature assumed to precede and follow the drop is more unfavorable.

The analyses in this section extract accelerations from NuPac's impact analyses programs (EYDROP, SYDROP, CYDROP, and OBLIQUE) and statically apply them to the package. Static application is justified since the natural frequencies of the cask are relatively high and the duration of the impact loadings relatively long. The cask frequencies are high as the result of using relatively thick, stiff shells in the cask design. The duration of impact loadings are relatively long as the result of using soft (relative to the steel structures) energy absorbing overpacks to protect the cask during free drop events. In addition, inspection of accelerometer data available from the other drop tests indicates that casks such as the 10/140MB respond essentially as a rigid body. This observation further justifies static application of g loads.



2.7.1.1 Flat End Drop

Analysis of the NuPac 10/140MB Cask behavior during the end drop impact is performed in the following steps:

- (1) Analyze the impact force using the EYDROP computer program.
- (2) Analyze the cask lid for bending assuming the payload acts as a uniform load on a plate supported by the overpack exerting a uniform pressure in the opposite direction.
- (3) Analyze the stresses in the cask secondary lid bolts.
- (4) Analyze the axial and hoop stresses in the outer cask shells and lead.
- (5) Determine the amount of lead slump.

2.7.1.1.1 End Impact Force Determination

The acceleration imparted to the 10/140MB cask during a flat end impact from 30 feet is calculated using the energy balance program EYDROP. Three bounding cases were performed, assuming the softest polyurethane foam properties possible (15% less than the average for foam at 109°F) the hardest foam possible (15% greater than the average for foam at -20°F) and the hardest foam possible at the upper temperature limit at the start of the hypothetical accident (15% greater than the average for foam at 109°F).

The overpack is conservatively assumed to resist the impact over its entire footprint area. Tests performed on a variety of packages indicate that loads calculated in this manner are over predicted. The overpack diameter used for input to EYDROP is adjusted to account for the overpack 'flats', which reduce the impact - resisting area of the overpack. The equivalent diameter may be calculated as follows:

$$D_e = [D^2 - D^2(2/\pi)(\alpha - \sin\alpha\cos\alpha)]^{0.5}$$

where  $D_e$  = equivalent diameter

$D$  = major diameter (101.0 in. in this case)

$\alpha = \cos^{-1}(\text{Flat width}/D) = \cos^{-1}(96/101) = .316 \text{ radians}$

$$D_e = [101^2 - 101^2(2/\pi)(.316)\cos(.316)]^{0.5}$$

$$= 100.34 \text{ inches}$$

The results of the EYDROP analyses are presented in Tables 2.7.1-1, 2.7.1-2 and 2.7.1-3. The accelerations for each case can be interpolated from the appropriate lines of output on each of the tables. The results are summarized below:

<u>Case</u>	<u>Acceleration, g's</u>
-20°F Foam + 15%	170.8
109°F Foam - 15%	82.9
109°F Foam + 15%	105.2

Table 2.7.1-1

EYDROF (END)

NUPAC 10/140M COLD FOAM (-23 DEG)

PACKAGE HEIGHT \* 45000 (LBS)  
 PACKAGE DIAMETER \* 100.34 (IN)  
 HOLE DIAMETER \* 55.00 (IN)  
 OVERPACK DEPTH \* 18.00 (IN)  
 DROP HEIGHT \* 30.00 (FT)

CRUSH DEPTH (IN)	STRAIN	**** IMPACT ****		***** ENERGY *****		
		FORCE (LBS)	ACCEL. (G)	KINETIC (IN-LB)	STRAIN (IN-LB)	RATIO (SE/AE)
.25	.014	2458511.	37.8	23416250.	307314.	.013
.50	.028	4917022.	75.6	23432500.	1229256.	.052
.75	.042	6857095.	105.5	23448750.	2701020.	.115
1.00	.056	8438667.	129.8	23465000.	4612991.	.197
1.25	.069	9694355.	149.1	23481250.	6879618.	.293
1.50	.083	10457414.	160.9	23497500.	9398589.	.400
1.75	.097	10816827.	166.4	23513750.	12057869.	.513
2.00	.111	11028751.	169.7	23530000.	14788567.	.626
2.25	.125	11067276.	170.3	23546250.	17550570.	.745
2.50	.139	11081198.	170.5	23562500.	20319129.	.862
2.75	.153	11094007.	170.7	23578750.	23091030.	.979
3.00	.167	11107893.	170.9	23595000.	25866267.	1.096
3.25	.181	11121656.	171.1	23611250.	28644961.	1.213
3.50	.194	11138215.	171.4	23627500.	31427445.	1.330
3.75	.208	11164062.	171.8	23643750.	34215229.	1.447
4.00	.222	11201407.	172.3	23660000.	37010913.	1.564
4.25	.236	11249790.	173.1	23676250.	39817312.	1.682
4.50	.250	11310841.	174.0	23692500.	42637391.	1.800
4.75	.264	11386192.	175.2	23708750.	45474520.	1.918
5.00	.278	11477471.	176.6	23725000.	48332478.	2.037

ACCEL. = 170.8  
 WHIM RATIO = 1.000

Table 2.7.1-2

EYDROP(END)

NUPAC 10/140M HARM FOAM (109 DEG)

PACKAGE HEIGHT \* 65000. (LBS)  
 PACKAGE DIAMETER \* 100.34 (IN)  
 HOLE DIAMETER \* 55.00 (IN)  
 OVERPACK DEPTH \* 18.00 (IN)  
 DROP HEIGHT \* 30.00 (FT)

CRUSH DEPTH (IN)	STRAIN	**** IMPACT ****		***** ENERGY *****		
		FORCE (LBS)	ACCEL. (G)	KINETIC (IN-LB)	STRAIN (IN-LB)	RATIO (SE/KE)
.25	.014	1306084.	20.1	23416250.	163261.	.007
.50	.028	2612168.	40.2	23432500.	653042.	.028
.75	.042	3615740.	55.6	23448750.	1431531.	.061
1.00	.056	4164249.	64.1	23465000.	2404029.	.102
1.25	.069	4365131.	67.2	23481250.	3470202.	.148
1.50	.083	4480910.	68.9	23497500.	4575957.	.195
1.75	.097	4591076.	70.7	23513750.	5710205.	.25
2.00	.111	4662752.	71.7	2353	6867183.	.32
2.25	.125	4693663.	72.2	2354	8036735.	.41
2.50	.139	4726407.	72.7	23562500.	9214244.	.51
2.75	.153	4765385.	73.3	23578750.	10400718.	.64
3.00	.167	4808032.	74.0	23595000.	11597395.	.80
3.25	.181	4853770.	74.7	23611250.	12805120.	.94
3.50	.194	4902690.	75.4	23627500.	14024678.	1.10
3.75	.208	4953552.	76.2	23643750.	15256708.	1.28
4.00	.222	5006709.	77.0	23660000.	16501741.	1.47
4.25	.236	5063509.	77.9	23676250.	17760518.	1.67
4.50	.250	5124521.	78.8	23692500.	19034022.	1.89
4.75	.264	5190312.	79.9	23708750.	20323376.	2.12
5.00	.278	5261454.	80.9	23725000.	21629847.	2.37
5.25	.292	5338514.	82.1	23741250.	22954842.	2.64
5.50	.306	5418712.	83.4	23757500.	24299496.	2.92
5.75	.319	5501350.	84.6	23773750.	25664503.	3.22
6.00	.333	5592976.	86.0	23790000.	27051294.	3.54
6.25	.347	5695130.	87.6	23806250.	28462507.	3.88
6.50	.361	5809354.	89.4	23822500.	29900568.	4.24
6.75	.375	5937189.	91.3	23838750.	31368686.	4.62
7.00	.389	6080176.	93.5	23855000.	32870857.	5.01
7.25	.403	6234995.	95.9	23871250.	34410253.	5.42
7.50	.417	6389389.	98.3	23887500.	35988101.	5.85
7.75	.431	6566938.	101.0	23903750.	37607842.	6.30
8.00	.444	6771999.	104.2	23920000.	39275209.	6.77

ACCEL = 82.9  
 WHEN RATIO = 1.000

Table 2.7.1-3

EYDROP(END)		NUPAC 10/140M WARM FOAM (109 DEG) MAXIMUM PROPERTIES AT TE				
		PACKAGE HEIGHT = 65000. (LBS) PACKAGE DIAMETER = 100.34 (IN) HOLE DIAMETER = 55.00 (IN) OVERPACK DEPTH = 18.00 (IN) DROP HEIGHT = 30.00 (FT)				
CRUSH DEPTH (IN)	STRAIN	**** IMPACT ****		***** ENERGY *****		
		FORCE (LBS)	ACCEL. (G)	KINETIC (IN-LB)	STRAIN (IN-LB)	RATIO (SE/KE)
.25	.014	1767055.	27.2	23416250.	220882.	.009
.50	.028	3534110.	54.4	23432500.	883527.	.038
.75	.042	4892303.	75.3	23448750.	1936829.	.083
1.00	.056	5634985.	86.7	23465000.	3252740.	.139
1.25	.069	5906784.	90.9	23481250.	4695461.	.200
1.50	.083	6061118.	93.2	23497500.	6191449.	.263
1.75	.097	6211985.	95.6	23513750.	7725587.	.329
2.00	.111	6307402.	97.0	23530000.	9290510.	.395
2.25	.125	6350190.	97.7	23546250.	10872709.	.462
2.50	.139	6393399.	98.4	23562500.	12465658.	.529
2.75	.153	6444175.	99.1	23578750.	14070355.	.597
3.00	.167	6501641.	100.0	23595000.	15688582.	.665
3.25	.181	6564215.	101.0	23611250.	17321814.	.734
3.50	.194	6631743.	102.0	23627500.	18971308.	.803
3.75	.208	6701556.	103.1	23643750.	20637970.	.873
4.00	.222	6773999.	104.2	23660000.	22322415.	.943
4.25	.236	6851296.	105.4	23676250.	24025577.	1.015
4.50	.250	6934200.	106.7	23692500.	25748764.	1.087
4.75	.264	7023464.	108.1	23708750.	27493472.	1.160
5.00	.278	7119840.	109.5	23725000.	29261385.	1.233
5.25	.292	7224081.	111.1	23741250.	31054375.	1.308
5.50	.306	7332182.	112.8	23757500.	32873908.	1.384
5.75	.319	7443096.	114.5	23773750.	34720817.	1.460
6.00	.333	7566068.	116.4	23790000.	36596963.	1.538
6.25	.347	7703232.	118.5	23806250.	38505625.	1.617
6.50	.361	7856722.	120.9	23822500.	40450620.	1.698
6.75	.375	8028671.	123.5	23838750.	42436294.	1.780
7.00	.389	8221216.	126.5	23855000.	44467530.	1.864
7.25	.403	8430040.	129.7	23871250.	46548937.	1.950
7.50	.417	8638978.	132.9	23887500.	48682564.	2.038
7.75	.431	8879394.	136.6	23903750.	50872360.	2.128
8.00	.444	9157157.	140.9	23920000.	53126929.	2.221

2.7.1.1.2 Lid Stress Analysis

Because the end drop impact acceleration at  $-20^{\circ}\text{F}$  (170.8 g's) is very much higher than that at the upper temperature bound ( $105.2^{\circ}\text{F}$ ), margins of safety in the lid will be conservatively calculated using the acceleration expected at  $-20^{\circ}\text{F}$  and material properties taken at a temperature of  $200^{\circ}\text{F}$ . Stress allowables are derived at the maximum temperature for the lids at the start of the accident which is  $106^{\circ}\text{F}$ .

To accurately predict stress levels under end drop impact conditions for the rather complex lid configurations utilized in the 10/140MB cask, a finite element analysis was undertaken using the ANSYS program described in Appendix 2.10.2. Both the top lid assembly (primary and secondary lids) as well as the bottom lid for the optional bottom loading configuration were evaluated.

Details of this analysis are given in Appendix 2.10.7, and are summarized in Table 2.7.1-4 below.

The EnviroLock<sup>tm</sup> closure binders will tend to unload their tensile prestress during the end impact event, and since their design will prevent them from carrying comparison loads, the EnviroLock<sup>tm</sup> binder loads will not be a consideration for this load configuration. The binders will, however, be subjected to a preload of 11,380 lb. each to ensure proper initial seating of EnviroSeal<sup>tm</sup> O-rings.

From Section 2.1.2, maximum allowable fastener membrane load under accident conditions is the smaller of the material's specified minimum yield load  $S_y$  or 0.7 times the ultimate tensile load  $S_u$ . From Appendix 2.10.4, these values for the EnviroLock<sup>tm</sup> binder are:

$$S_y = 184,500 \text{ lbs.}$$

$$S_u = 250,000 \text{ lbs.}$$

Therefore, the allowable stress is  $(0.7)(250,000) = 175,000$  lbs. which is less than 184,500 lbs. The resulting Margin of Safety is:

$$M.S. = 175,000/11,380 - 1 = + \text{ Large}$$

Since the bottom plate of the fixed bottom version of the 10/140MB cask has the same basic dimensions as the bottom lid on the bottom loading version, yet is more rigidly fixed to the cask body, it will exhibit no excessive stress levels during the end drop event either. It is therefore apparent that the cask bottom of either version of the 10/140MB cask is suitably designed to withstand the regulatory drop requirement on the end of the bottom overpack.

As with the bottom lid, EnviroLock<sup>tm</sup> binder stresses will not be a consideration for the end drop event. Secondary lid bolt prestress results from a preload of 12,000 lb. per bolt required to properly seat the EnviroSeal<sup>tm</sup> O-ring seals. The resulting prestress on the bolt's 1.405 tensile stress area is:

$$S_B = 12,000/1.405 = 8,540 \text{ psi}$$

Mechanical properties of the A320 Grade L43 bolt material are:

$$S_y = 105,000 \text{ psi}$$

$$S_u = 125,000 \text{ psi}$$

resulting in a maximum allowable membrane stress of  $(0.7)(125,000) = 87,500$  psi. The bolt preload Margin of Safety is thus:

$$M.S. = 87,500/8,540 - 1 = + \text{ Large}$$

Bolt stress under end impact load is calculated in Section 2.7.1.1.3 below, and a positive Margin of Safety is derived. A drop on the bottom overpack will not load the secondary lid bolts. Therefore, the bolts are adequate to meet the regulatory requirements for a 30 foot drop on either end of the cask.

Thus it is obvious that the primary lid assembly is more than adequate to meet the regulatory requirements for end drop on the top overpack.



TABLE 2.7.1-4

## SUMMARY OF LID ANALYSIS RESULTS

Lid	Max. Bending Stress (psi) (Margin of Safety)	Max. Membrane Stress (psi) (Margin of Safety)	Min. O-ring Compression- Primary Seal	Min. O-ring Compression- Secondary Seal	Max. Bolt Stress (psi) (Margin of Safety)
Bottom	27,977 (M.S. = +1.79)	4,553 (M.S. = +Large)	21.3%	-	-
Top	34,557 (M.S. = +1.02)	14,125 (M.S. = +2.40)	15.9%	20.1%	72,260* (M.S. = +0.21)

\*From Section 2.7.1.1.3 below

2.7.1.1.3 Secondary Lid Bolt Stresses

The secondary lid bolts are 1.50 dia. ASTM A320 L43 high strength steel. The loads may be calculated by multiplying the weight of the lid and portion of the payload reacted by the lid by the maximum impact acceleration. It is clear that the smallest margin of safety for the bolts will occur during impacts at  $-20^{\circ}\text{F}$ , since the acceleration at that temperature limit, and the allowable at  $-20^{\circ}\text{F}$  is only slightly greater than at the maximum temperature.

The portion of the payload reacted by the secondary lid bolts may be calculated as follows:

$$29^2/66^2 (15,000) = 2900 \text{ lbs.}$$

The secondary lid weighs approximately 1850 lbs. Therefore, the total weight of the secondary lid bolts must resist is:

$$2900 + 1850 = 4750 \text{ lbs.}$$

The force in each bolt is:

$$4750(170.8 \text{ g's})/8 = 101,430 \text{ lbs./bolts}$$

The effective tensile stress area in the 1.5 inch diameter bolts is 1.405 in.<sup>2</sup>, so the stress in the bolt is:

$$101,430/1.405 = 72,200 \text{ psi}$$

The secondary lid bolts secure part of the containment boundary, so the tensile (membrane) allowable is the lesser of  $S_y$  or  $0.7S_u$ . From Table 2.3-1,  $S_y = 100,000 \text{ psi}$  and  $S_u = 125,000 \text{ psi}$  at  $-20^{\circ}\text{F}$ . The allowable is then:

$$\text{min. } ((100,000), (0.7)(125,000)) = 87,500 \text{ psi}$$

The margin of safety is then

$$M.S. = 87,500/72,200 - 1 = +0.21$$

This stress should be combined with the maximum normal internal pressure of 6.8 psi from section 3.4.4. That pressure may be converted to stress in the bolts as follows:

$$(6.8 \text{ psi})(\pi)(29/2)^2/(8)(1.405) = 400 \text{ psi}$$

The combined margin of safety in the bolts is then

$$M.S. = 87,500/(72,200+400) - 1 = +0.20$$

#### 2.7.1.1.4 Axial and Hoop Stresses in the Shells

Of all impact orientations, the flat end impact causes the greatest acceleration to be imparted to the cask. This acceleration creates a significant compression load to be carried by the inner and outer shells of the package. The lead between the two shells complicates the state of stress, since it is much softer than the steel. As the acceleration increases, the lead expands radially at a different rate than the steel, and when the lead actually yields, both inner and outer shells support and contain the lead.

Stresses in the Cask Shells and Lead Shielding (Maximum Fabrication Stress Condition Assumed)

The response of the cask steel shells and lead shielding to the accident end drop event is determined using both hand calculations and finite element analyses. The principal concern for the outer cask is with buckling of the inner shell. As shown by the following calculations, buckling will not occur as the result of the hoop and axial compressive stresses which develop in the cask inner shell under accident end drop conditions.

Various initial conditions can be assumed for the accident drop event. In particular, a temperature must be assumed in order to establish an initial fabrication stress for the inner shell. A lower assumed temperature will result in a higher initial hoop stress on the inner shell (see Section 2.6.2) but higher allowable stresses. For purposes of this analysis, drops at 123°F (maximum lead normal temperature per Section 3.4.2) and -20°F are considered.

To adequately analyze the full consequences of the drop event at the given temperatures, two initial lead conditions are also considered. The first assumes that the lead has shrunk onto the inner shell and away from the outer shell. In addition, due to the combined effects of friction between the lead and inner shell, and axial shrinkage of the lead relative to the shells, axial gaps will develop between the lead and the steel structures at the top and bottom end of the lead column. These axial gaps are important in that, until friction is overcome, under increased axial loading, the lead will impose a direct axial load on the inner shell. Once friction is overcome, the lead will become supported at its base (the bottom of the lead column) and will grow radially outward due to the 'Poisson Effect' under increased axial loading. This radial growth will tend to relieve the initial fabrication hoop stress as the lead separates from the inner shell. If sufficient axial load develops, the lead would grow out to the outer shell creating tensile hoop stresses therein, and under further loading would eventually flow back inward into the inner shell, thereby developing compressive hoop stresses in the inner shell. Since the primary mechanism of this load case would be to relieve stresses on the critical inner shell, it is not considered to be a worst-case condition.

From Section 2.7.1.1.4, hoop stress in the inner shell due to fabrication is as follows:

Temperature (°F)	Inner Shell Hoop Stress (psi)
123	-1,793 (extrapolated)
70	-2,041
-20	-2,642

Note: The outer shell hoop stress is considered negligible since the lead separates from the outer shell upon cooling.

The equivalent pressure at the lead/inner shell interface is as follows:

$$p = \sigma t / r$$

$$t = 0.75 \text{ in}$$

$$r = 33.375 \text{ in}$$

Thus, the interface pressures at the different temperatures are:

Temperature (°F)	Interface Pressure, p (psi)
123	40.3
70	45.9
-20	59.4

With a coefficient of friction,  $f$ , for lead on stainless steel assumed to fall in the 0.5 to 1.0 range (Refer to Mark's Standard Handbook for Mechanical Engineers, 8th ed., 1978, p. 3-26), the load,  $P$ , which can be supported by friction at the lead/inner shell interface, may be determined as follows:

$$P = \pi DLpf$$

Where:

$D = 67.5$  in (inner shell outside diameter)

$L = 7.5$  in (lead column height)

$p =$  interface pressure, psi

$f = 0.5$  to  $1.0$  (coefficient of friction)

Apply the interfaces pressures determined earlier, the total load which may be supported is:

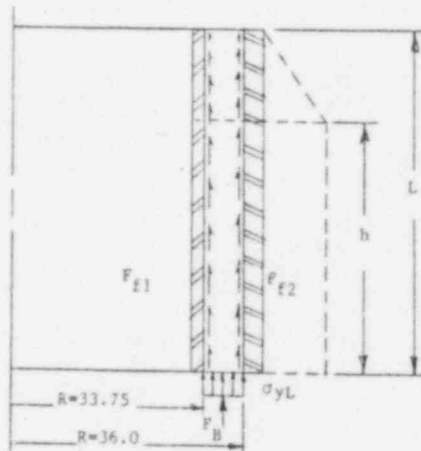
Temperature (°F)	Coefficient of Friction	Load Supported (lbs)
123	0.5	331,090
	1.0	662,179
70	0.5	376,885
	1.0	753,769
-20	0.5	487,863
	1.0	975,727

With the total lead weight equal to 15,666 lb., as calculated in Section 2.6.7.1.4, the maximum g-load which can be supported by friction is  $975,727/15,666 = 62.3$  g's. The Hypothetical Accident Condition g-load's range from 105.2 g's at 123°F to 170.8 g's at -20°F. Since all possible accident condition g-loads are greater than the maximum at which the lead can be supported by friction, the lead will always slip, and this load case will not be of concern here.

# Stresses in the Outer Cask Shells and Lead (Zero Fabrication Stress Condition Assumed)

The second initial lead condition assumes that the fabrication stress has fully crept away resulting in a stress free column of lead just in contact with the inner and outer shells. This is a potential worst case since any axial load imposed on the lead will directly load, radially, both the inner and outer shells (i.e., the lead need not flow away from the inner shell, into the outer shell and back into the inner shell to develop a compressive hoop stress in the inner shell).

For this condition, initial stresses in the lead and the steel shells are taken as zero. As axial load is applied to the lead and shells, the lead will attempt to move downward and outward and develop pressures on both the inner and outer shells.



Utilizing the analytical technique developed in Section 2.6.7.1.4, inner and outer shell hoop and axial stresses can be calculated.

The height  $h$  at which the lead reaches its yield point is:

$$\begin{aligned} h &= L - \sigma_{yL} / \gamma \rho_L \\ &= 77.5 - 600 / (170.8)(0.41) = 68.9 \text{ in.} \end{aligned}$$

Static equilibrium of the lead column yields:

$$W_L = F_B + F_{f1} + F_{f2}$$

Where:

$$W_L = (15,666)(170.8) = 2,675,750 \text{ lb.}$$

$$F_B = (600)\pi(36.0^2 - 33.75^2) = 295,820 \text{ lb.}$$

$$F_{f1} = \text{Frictional Reaction Force of Inner Shell}$$

$$F_{f2} = \text{Frictional Reaction Force of Outer Shell}$$

Inner and outer shell radial forces are:

$$F_{R1} = F_{f1} / 0.5, \text{ or } F_{f1} = 0.5 F_{R1}$$

$$F_{R2} = F_{f2} / 0.5, \text{ or } F_{f2} = 0.5 F_{R2}$$

Also:

$$F_{R1} = 0.5 p_E \pi D_1 (L+h)$$

and:

$$F_{R2} = 0.5 p_E \pi D_2 (L+h)$$

Solving for  $F_{R1}$  and  $F_{R2}$  in terms of  $p_E$  and substituting back into the lead equilibrium equation yields:

$$W_L - F_B = 0.25 \pi p_E (D_1 + D_2) (L+h)$$



or:

$$p_E = 4 (W_L - F_B) / \pi (D_1 + D_2) (L + h)$$

From which:

$$p_E = 148.37 \text{ psi}$$

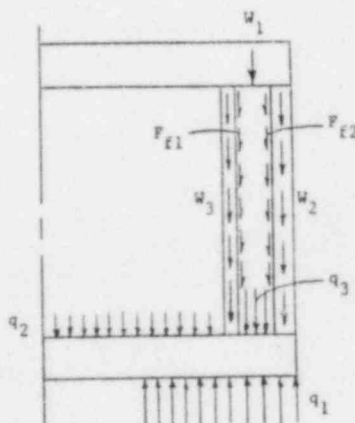
Therefore, the inner shell compressive hoop stress is:

$$\begin{aligned} \sigma_1 &= -p_E R_1 / t_1 \\ &= -(148.37)(33.75) / (0.75) = -6,677 \text{ psi} \end{aligned}$$

The outer shell, tensile hoop stress is:

$$\begin{aligned} \sigma_2 &= p_E R_2 / t_2 \\ &= (148.37)(36.0) / (1.25) = 4,273 \text{ psi} \end{aligned}$$

To evaluate axial stresses, a similar approach to that detailed in Section 2.6.7.1.4 is utilized.



$$F_{f1} = 0.25 \pi D_1 p_E (L+h)$$

$$F_{f1} = 1,151,579 \text{ lb.}$$

$$F_{f2} = 0.25 \pi D_2 p_E (L+h)$$

$$F_{f2} = 1,228,351$$

$$W_1 = (\text{Weight of top overpack, cask lid and top ring})(170.8 \text{ g's})$$

$$= (10,440)(170.8) = 1,783,150 \text{ lb.}$$

$$W_2 = (\text{Weight of cask outer shell, thermal shield, etc})(170.8 \text{ g's})$$

$$= (9,290)(170.8) = 1,586,730 \text{ lb.}$$

$$W_3 = (\text{Weight of cask inner shell})(170.8 \text{ g's})$$

$$= (3,560)(170.8) = 608,050 \text{ lb.}$$

$$W_L = (\text{Weight of lead})(170.8 \text{ g's})$$

$$= (15,666)(170.8) = 2,675,750 \text{ lb.}$$

$$q_2 = (\text{Weight of payload})(170.8 \text{ g's})/\pi(33.0)^2$$

$$= (15,000)(170.8)/\pi(33.0)^2 = 748.9 \text{ lb./in.}^2$$

$$q_1 = [W_1 + W_2 + W_3 + W_L + q_2\pi(33.0)^2]/\pi(37.25^2 - 27.5^2)$$

$$= 4,647 \text{ lb./in.}^2$$

$$q_3 = \text{Yield stress of lead (at } 123^\circ\text{F)} = 600 \text{ lb./in.}^2$$

From the computational technique used in Section 2.6.7.1.4, relative deflection due to the pressure loads is:

$$\delta_1 - \delta_2 = -0.008441 \text{ (positive downward)}$$

$$\delta_1 = R_3 L / A_1 E_1 - (W_3 + F_{f1}) L / 2 A_1 E_1$$

$$\delta_2 = R_4 L / A_2 E_2 - (W_2 + F_{f2}) L / 2 A_2 E_2$$

$$R_4 = W_1 + W_2 + W_3 + W_L - R_3$$

$$= 6,653,680 - R_3$$

Solving simultaneously, the inner shell reaction load becomes:

$$R_3 = 2,696,064 \text{ lb.}$$

$$R_4 = 3,957,616$$

Therefore, compressive axial stress on the inner and outer shell is:

$$\sigma_1 = -R_3 / A_1 = -17,141 \text{ psi}$$

$$\sigma_2 = -R_4 / A_2 = -13,758 \text{ psi}$$

Conservatively ignoring inner shell radial loading, stress intensity in the shell is:

$$S.I._1 = 0 - (-17,141) = 17,141 \text{ psi}$$

From Table 2.1.2-1, the stress allowable for the inner shell is the lesser of  $2.4 S_m$  or  $0.7 S_u$ , where  $S_m = 20,000 \text{ psi}$  and  $S_u = 75,000 \text{ psi}$  at  $-20^\circ\text{F}$ . For the inner shell material, the allowable is thus  $(2.4)(20,000) = 48,000 \text{ psi}$  (which is less than  $(0.7)(75,000) = 52,500 \text{ psi}$ ).

The stress Margin of Safety for the inner shell is thus:

$$M.S. = 48,000/17,141 - 1 = +1.80$$

From Table 2.1-3, buckling allowables at  $-20^{\circ}\text{F}$  are 32,131 psi (axial) and 29,704 psi (hoop). Buckling Margin of Safety is thus:

$$\begin{aligned} M.S. &= 1/[(17,141/32,131) + (6,677/29,704)] - 1 \\ &= +0.32 \end{aligned}$$

Stress intensity of the outer shell is:

$$S.I._2 = 4,273 - (-13,758) = 18,031 \text{ psi}$$

From Table 2.1.2-1, allowable stress for this structure is  $0.7 S_u$ , where  $S_u = 70,000$  psi at  $-20^{\circ}\text{F}$ . Thus the stress Margin of Safety is:

$$M.S. = (0.7)(70,000)/18,031 - 1 = +1.72$$

From Table 2.1-4, the axial buckling allowable at  $123^{\circ}\text{F}$  is 39,89 The buckling Margin of Safety is therefore:

$$M.S. = 1/(13,758/39,189) - 1 = +1.85$$

In addition to the hand analysis developed above, a finite element model was developed to analyze this phenomenon using the common ANSYS structural analysis code. A description of ANSYS is given in Appendix 2.10.2, and details of the analysis are shown in Appendix 2.10.6.

While the minimum temperature condition for the drop event ( $-20^{\circ}\text{F}$ ) induces the highest acceleration loading (170.8 g's), the material properties are also at a maximum (refer to Sections 2.1 and 2.3 for details). Likewise, though the maximum temperature case results in lower impact loads (a maximum 105.2 g's),

material properties are also reduced at the higher temperature condition. Refer to Section 2.1.2.2, Overpack Design Criteria, as well as Section 2.7.1.1.1 above for details of the effects of temperature variation on drop loads.

Thus, to conservatively bound the buckling and stress allowable calculations, the maximum g-load (obtained at the minimum temperature condition) was applied to the analysis while utilizing reduced strength material properties (found at the higher temperature), which will tend to maximize stresses. Therefore the analysis utilized material properties based on an expected normal condition of transport temperature of 121°F at the inner shell. Refer to Section 3.0, Thermal Evaluation, for details of this temperature condition.

The finite element analysis was run beyond its theoretical maximum acceleration of 105.2 g's (accident condition end drop load at the upper temperature limit) up to 170.0 g's, to investigate accident condition stresses at normal condition temperature material properties. Further conservatism is induced in the analysis since the hypothetical accident condition drop, whose maximum anticipated temperature at the critical area during the drop event is only 105°F, was analyzed at the higher normal condition temperature of 121°F, where material properties will be lower and resulting stresses higher. Buckling and stress allowables were taken at the drop temperature of -20°F.

The results of the stress analysis for Hypothetical Accident Conditions, detailed in Appendix 2.10.6, are summarized below:

Drop Load = 170 g's

Material Properties Temperature = 121°F

(Actual Temperature During Drop is 105°F)

Maximum Inner Shell Stress Intensities (Elem. 33)		Maximum Outer Shell Stress Intensities (Elem. 36)	
<u>Surface</u>	<u>Membrane</u>	<u>Surface</u>	<u>Membrane</u>
21,287 psi	19,242 psi	30,744 psi	21,138 psi
Stress Intensity Allowables*		Stress Intensity Allowables*	
72,000 psi	48,000 psi	70,000 psi	49,000 psi
Margins of Safety		Margins of Safety	
+ 2.38	+ 1.49	+ 1.28	+ 1.32

\* See Table 2.1.2-1

The results of the buckling analysis for Hypothetical Accident Conditions, detailed in Appendix 2.10.6, are summarized below:

Drop Load = 170 g's (load at $-20^{\circ}\text{F}$ )			
Material Properties Temperature = $121^{\circ}\text{F}$			
(Actual Temperature During Drop is $105^{\circ}\text{F}$ )			
Maximum Inner Shell Stresses (Elem. 33)		Maximum Outer Shell Stress (Elem. 36)	
Axial	Hoop	Axial	
-19,242 psi	-6,642 psi	-9,606 psi	
Buckling Allowables*		Buckling Allowable**	
32,131 psi	29,204 psi	39,047 psi	
Margin of Safety		Margin of Safety	
+ 0.21		+ 3.06	

\* See Table 2.1-3

\*\* See Table 2.1-4

Though the actual cold condition drop load was 170.8 g's and not 170 g's, the high of conservatism of the analysis assures that this small difference in drop load (0.5%) will not significantly affect the final results.

In addition to the above, positive margins of safety against buckling can be calculated using loads from a drop at  $-20^{\circ}\text{F}$  and allowables derived at  $121^{\circ}\text{F}$ . Since the analysis also used material properties at the upper temperature extreme, which conservatively over-estimates the buckling stresses at the cold temperature, these margins of safety, then, demonstrate that the shells will not buckle at any temperature in the range of interest.

A comparison of hand calculations and finite element analysis results is presented below. As can be seen, very good correlation is achieved for the more critical hoop stress components on both shells, while axial stress hand analysis results are conservative for the outer shell and slightly non-conservative for the inner shell. The difference in results can most likely be attributed to end constraint effects in the finite model which were not taken into account in the hand analysis.

Stress Component	Hand Analysis	F.E. Analysis
Inner Shell Axial Stress (psi)	-17,141	-19,242
Inner Shell Hoop Stress (psi)	-6,677	-6,742
Inner Shell Buckling M.S.	+0.32	+0.21
Outer Shell Axial Stress (psi)	-13,758	-9,606
Outer Shell Hoop Stress (psi)	4,273	4,123
Outer Shell Buckling M.S.	+1.85	+3.06

From this analysis, it is thus apparent that the cask inner and outer shells will withstand the regulatory Hypothetical Accident Condition end drop event for all applicable temperatures.



2.7.1.1.5 Lead Slump

The analyses performed in Section 2.7.1.1.5 above demonstrates that the lead might be expected to slump during end impact 0.305 inches at the maximum drop temperature. Refer to Appendix 2.10.6 for analysis results. Due to the deeply stepped configuration of the primary lids, this small amount of lead settlement will not adversely affect the ability of the package to meet the shielding requirements of 10 CFR 71.

2.7.1.2 Oblique Impact

Analysis of the NuPac 10/140MB package behavior during hypothetical impacts from drops of 30 feet has been performed in the following steps:

1. Use CYDROP to determine worst case overpack deformation to insure that the package will not 'bottom out'.
2. Use CYDROP with highest crush strength foam data to determine a conservative estimate of the force-deflection relationship of the 10/140MB overpack design at various impact angles.
3. Use OBLIQUE program to determine internal forces in the 10/140MB during impact.
4. Determine worst case stress state from internal forces in cask body.
5. Determine lid attachment forces in EnviroLocks<sup>tm</sup> under worst conditions.

2.7.1.2.1 Worst Case Corner Deformations

Because the containment and shielding structure of the 10/140MB is many times harder than the polyurethane overpacks, it is essential that it may be demonstrated that the cask shield and associated hardware will not actually strike the impact surface. Therefore, the energy balance program CYDROP was used in

conjunction with the minimum polyurethane foam stress-strain properties to determine a conservative estimate of the maximum deflection. Because CYDROP is written for simple cylindrical cylinders, two bounding cases were run. The first case ignores the contribution of the overpack beyond the 101 inch diameter base of the overpack. This will conservatively over estimate the amount of deflection required to generate enough strain energy to balance the energy of impact. The second case assumes a 96 inch overpack diameter corresponding to the width of the overpack flats. This is even more conservative, since larger volumes of crushed foam are ignored.

The results of the 101 inch diameter case impacting with the package c.g. over the struck corner is presented in Table 2.7.1-5 and the 96 inch case in Table 2.7.1-6. The results show that the 101 inch overpack would deflect 19.92 inches while the 96 inch case would deflect 19.55 inches.

TABLE 2.7.1-5

CYDROP(CORNER)

NUCLEAR PACKAGING PROPRIETARY

17.15.32

85/06/27

PAGE 1

NUPAC-B 10/140M CRUSH DEPTH CHECK (109 DEG)

PACKAGE WEIGHT = 45000. (LBS)  
 PACKAGE EXTERNAL LENGTH = 119.50 (IN)  
 PACKAGE EXTERNAL DIAMETER = 101.00 (IN)  
 PACKAGE EXTERNAL HOLE DIA = 55.00 (IN)  
 PAYLOAD ENVELOPE LENGTH = 83.50 (IN)  
 PAYLOAD ENVELOPE DIAMETER = 75.00 (IN)  
 OVERPACK LENGTH = 40.00 (IN)

DROP HEIGHT = 30.00 (FT)  
 ORIENTATION ANGLE = 40.090 (DEGREES HRT TO VERTICAL)

PLATEAU CRUSH STRESS = 834.00 (PSI)  
 (DEFAULT TAKEN AT 10 PCT STRAIN)

STRESS/STRAIN EVALUATED IN 1/2 CRUSH PLANE ELLIPSE AT:  
 NX = 25 POINTS PARALLEL TO SEMI-MINOR ELLIPSE AXIS  
 NY = 25 POINTS PARALLEL TO SEMI-MAJOR ELLIPSE AXIS

EXPERIMENTAL STRAIN VS. STRESS VALUES

CYDROP(CORNER)

NUCLEAR PACKAGING PROPRIETARY

17.15.32

85/06/27

PAGE 2

NUPAC-B 10/140M CRUSH DEPTH CHECK (109 DEG)

CRUSH DEPTH (IN)	** CRUSH PLANE **		**** IMPACT ****		***** ENERGY *****			DISTRIBUTION OF STRAIN RATIOS BY PERCENT OF CONTACT AREA					
	AREA (IN2)	VOLUME (IN3)	FORCE (LBS)	ACCEL. (G)	KINETIC (IN-LB)	STRAIN (IN-LB)	RATIO (SE/KE)	LE.70	GT.70	LE.80	GT.80	LE.90	GT.95
.50	11.9	3.	1738.	.0	23432500.	434.	.000	100.00	0.00	0.00	0.00	0.00	0.00
1.00	33.6	14.	9751.	.2	23465000.	3307.	.000	100.00	0.00	0.00	0.00	0.00	0.00
1.50	61.5	38.	25170.	.4	23497500.	12037.	.001	100.00	0.00	0.00	0.00	0.00	0.00
2.00	94.4	77.	46611.	.7	23530000.	29983.	.001	100.00	0.00	0.00	0.00	0.00	0.00
2.50	131.4	134.	72927.	1.1	23562500.	59867.	.003	100.00	0.00	0.00	0.00	0.00	0.00
3.00	172.0	209.	103369.	1.6	23595000.	103941.	.004	100.00	0.00	0.00	0.00	0.00	0.00
3.50	215.9	306.	137278.	2.1	23627500.	164103.	.007	100.00	0.00	0.00	0.00	0.00	0.00
4.00	262.7	426.	174411.	2.7	23660000.	242025.	.010	100.00	0.00	0.00	0.00	0.00	0.00
4.50	312.1	570.	214567.	3.3	23692500.	339269.	.014	100.00	0.00	0.00	0.00	0.00	0.00
5.00	364.1	739.	257604.	4.0	23725000.	457313.	.019	100.00	0.00	0.00	0.00	0.00	0.00
5.50	418.3	934.	306253.	4.7	23757500.	598273.	.025	100.00	0.00	0.00	0.00	0.00	0.00
6.00	474.6	1158.	359641.	5.5	23790000.	764741.	.032	100.00	0.00	0.00	0.00	0.00	0.00
6.50	532.9	1409.	414189.	6.4	23822500.	958198.	.040	100.00	0.00	0.00	0.00	0.00	0.00
7.00	593.0	1691.	470773.	7.2	23855000.	1179439.	.049	100.00	0.00	0.00	0.00	0.00	0.00
7.50	654.8	2003.	529851.	8.2	23887500.	1429595.	.060	100.00	0.00	0.00	0.00	0.00	0.00
8.00	718.2	2346.	591615.	9.1	23920000.	1709961.	.071	100.00	0.00	0.00	0.00	0.00	0.00
8.50	783.1	2721.	656110.	10.1	23952500.	2021892.	.084	100.00	0.00	0.00	0.00	0.00	0.30
9.00	849.4	3110.	721929.	11.1	23985000.	2366402.	.099	100.00	0.00	0.00	0.00	0.00	0.00
9.50	917.1	3571.	791111.	12.2	24017500.	2746662.	.114	100.00	0.00	0.00	0.00	0.00	0.00
10.00	985.9	4047.	864239.	13.3	24050000.	3158500.	.131	100.00	0.00	0.00	0.00	0.00	0.00
10.50	1056.0	4557.	939460.	14.5	24082500.	3609424.	.150	100.00	0.00	0.00	0.00	0.00	0.00
11.00	1127.1	5103.	1018675.	15.7	24115000.	4098958.	.170	100.00	0.00	0.00	0.00	0.00	0.00
11.50	1199.2	5685.	1105928.	17.0	24147500.	4630109.	.192	100.00	0.00	0.00	0.00	0.00	0.00
12.00	1272.3	6303.	1194676.	18.4	24180000.	5205260.	.215	100.00	0.00	0.00	0.00	0.00	0.00
12.50	1346.2	6957.	1287131.	19.8	24212500.	5825711.	.241	100.00	0.00	0.00	0.00	0.00	0.00
13.00	1421.0	7649.	1394545.	21.5	24245000.	6496130.	.268	100.00	0.00	0.00	0.00	0.00	0.00
13.50	1496.5	8378.	1502587.	23.1	24277500.	7220413.	.297	100.00	0.00	0.00	0.00	0.00	0.00
14.00	1572.8	9146.	1622227.	25.0	24310000.	8001617.	.329	100.00	0.00	0.00	0.00	0.00	0.00
14.50	1649.6	9951.	1756877.	27.0	24342500.	8846393.	.363	100.00	0.00	0.00	0.00	0.00	0.00
15.00	1727.1	10795.	1899645.	29.2	24375000.	9760523.	.400	100.00	0.00	0.00	0.00	0.00	0.00
15.50	1805.0	11679.	2054267.	31.6	24407500.	10749000.	.440	100.00	0.00	0.00	0.00	0.00	0.00
16.00	1883.5	12691.	2234753.	34.4	24440000.	11821255.	.484	100.00	0.00	0.00	0.00	0.00	0.00
16.50	1962.4	13562.	2448818.	37.7	24472500.	12992148.	.531	99.09	.91	0.00	0.00	0.00	0.00
17.00	2041.7	14543.	2673386.	41.1	24505000.	14272699.	.582	97.72	2.28	0.00	0.00	0.00	0.00
17.50	2121.3	15604.	2945400.	45.3	24537500.	15677395.	.639	95.93	4.07	0.00	0.00	0.00	0.00
18.00	2201.2	16685.	3224785.	49.6	24570000.	17219941.	.701	94.54	5.46	0.00	0.00	0.00	0.00
18.50	2281.3	17895.	3529984.	54.3	24602500.	18908634.	.769	93.17	6.13	.70	0.00	0.00	0.00
19.00	2361.6	18966.	3885243.	59.8	24635000.	20762440.	.843	92.31	6.07	1.61	0.00	0.00	0.00
19.50	2442.1	20167.	4271388.	65.7	24667500.	22801598.	.924	90.72	6.51	2.77	0.00	0.00	0.00
20.00	2522.7	21408.	4675357.	71.9	24700000.	25038284.	1.014	88.62	7.20	4.17	0.00	0.00	0.00

TABLE 2.7.1-6

CYDROP(CORNER)

NUCLEAR PACKAGING PROPRIETARY

17.17.15

85/06/27

PAGE 6

NUPAC-B 10/140M CRUSH DEPTH CHECK (109 DEG)

PACKAGE WEIGHT = 65000. (LBS)  
 PACKAGE EXTERNAL LENGTH = 119.50 (IN)  
 PACKAGE EXTERNAL DIAMETER = 96.00 (IN)  
 PACKAGE EXTERNAL HOLE DIA = 55.00 (IN)  
 PAYLOAD ENVELOPE LENGTH = 83.50 (IN)  
 PAYLOAD ENVELOPE DIAMETER = 75.00 (IN)  
 OVERPACK LENGTH = 40.00 (IN)

DROP HEIGHT = 50.00 (FT)  
 ORIENTATION ANGLE = 38.660 (DEGREES WRT TO VERTICAL)

PLATEAU CRUSH STRESS = 834.00 (PSI)  
 (DEFAULT TAKEN AT 10 PCT STRAIN)

STRESS/STRAIN EVALUATED IN 1/2 CRUSH PLANE ELLIPSE AT:  
 NX = 25 POINTS PARALLEL TO SEMI-MINOR ELLIPSE AXIS  
 NY = 25 POINTS PARALLEL TO SEMI-MAJOR ELLIPSE AXIS

EXPERIMENTAL STRAIN VS. STRESS VALUES

CYDROP(CORNER)

NUCLEAR PACKAGING PROPRIETARY

17.17.15

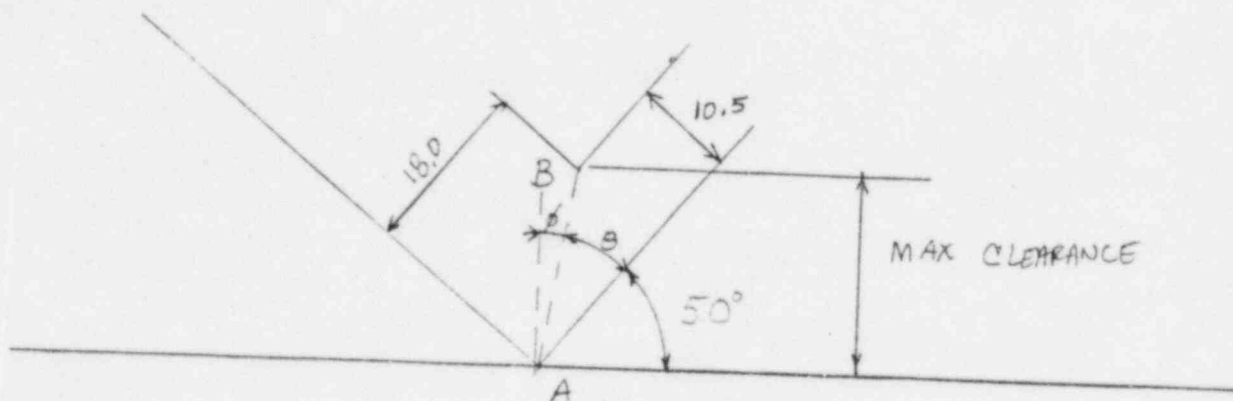
85/06/27

PAGE 7

NUPAC-B 10/140M CRUSH DEPTH CHECK (109 DEG)

CRUSH DEPTH (IN)	** CRUSH PLANE **		**** IMPACT ****		***** ENERGY *****			DISTRIBUTION OF STRAIN RATIOS BY PERCENT OF CONTACT AREA				
	AREA (IN <sup>2</sup> )	VOLUME (IN <sup>3</sup> )	FORCE (LBS)	ACCEL. (G)	KINETIC (IN-LB)	STRAIN (IN-LB)	RATIO (SE/KE)	LE.70	GT.70	GT.80	GT.90	GT.95
.50	11.9	3.	1772.	.0	23432500.	443.	.000	100.00	0.00	0.00	0.00	0.00
1.00	33.6	14.	9921.	.2	23465000.	3566.	.000	100.00	0.00	0.00	0.00	0.00
1.50	61.5	38.	25498.	.4	23497500.	12221.	.001	100.00	0.00	0.00	0.00	0.00
2.00	98.2	77.	47041.	.7	23530000.	30356.	.001	100.00	0.00	0.00	0.00	0.00
2.50	131.1	133.	73453.	1.1	23562500.	40979.	.003	100.00	0.00	0.00	0.00	0.00
3.00	171.6	209.	104072.	1.6	23595000.	104860.	.004	100.00	0.00	0.00	0.00	0.00
3.50	215.3	306.	138376.	2.1	23627500.	165472.	.007	100.00	0.00	0.00	0.00	0.00
4.00	261.9	425.	176984.	2.7	23660000.	244312.	.010	100.00	0.00	0.00	0.00	0.00
4.50	311.1	568.	222444.	3.4	23692500.	344169.	.015	100.00	0.00	0.00	0.00	0.00
5.00	362.7	737.	270664.	4.2	23725000.	467447.	.020	100.00	0.00	0.00	0.00	0.00
5.50	416.5	932.	319864.	4.9	23757500.	615079.	.026	100.00	0.00	0.00	0.00	0.00
6.00	472.4	1154.	371511.	5.7	23790000.	787923.	.033	100.00	0.00	0.00	0.00	0.00
6.50	530.2	1404.	425707.	6.5	23822500.	987227.	.041	100.00	0.00	0.00	0.00	0.00
7.00	589.8	1684.	482605.	7.4	23855000.	1214305.	.051	100.00	0.00	0.00	0.00	0.00
7.50	651.0	1995.	540964.	8.3	23887500.	1470198.	.062	100.00	0.00	0.00	0.00	0.00
8.00	713.7	2336.	602922.	9.3	23920000.	1756169.	.073	100.00	0.00	0.00	0.00	0.00
8.50	777.9	2709.	666850.	10.3	23952500.	2073612.	.087	100.00	0.00	0.00	0.00	0.00
9.00	843.4	3114.	733740.	11.3	23985000.	2423760.	.101	100.00	0.00	0.00	0.00	0.00
9.50	910.2	3552.	803580.	12.4	24017500.	2808090.	.117	100.00	0.00	0.00	0.00	0.00
10.00	978.1	4025.	878394.	13.5	24050000.	3228583.	.134	100.00	0.00	0.00	0.00	0.00
10.50	1047.1	4531.	954940.	14.7	24082500.	3686917.	.153	100.00	0.00	0.00	0.00	0.00
11.00	1117.1	5072.	1036134.	15.9	24115000.	4184685.	.174	100.00	0.00	0.00	0.00	0.00
11.50	1188.0	5648.	1123545.	17.3	24147500.	4724605.	.196	100.00	0.00	0.00	0.00	0.00
12.00	1259.7	6260.	1219408.	18.8	24180000.	5310343.	.220	100.00	0.00	0.00	0.00	0.00
12.50	1332.3	6908.	1317585.	20.3	24212500.	5944591.	.246	100.00	0.00	0.00	0.00	0.00
13.00	1405.6	7593.	1424846.	21.9	24245000.	6630199.	.273	100.00	0.00	0.00	0.00	0.00
13.50	1479.5	8314.	1540169.	23.7	24277500.	7371453.	.304	100.00	0.00	0.00	0.00	0.00
14.00	1554.0	9072.	1668082.	25.7	24310000.	8173516.	.336	100.00	0.00	0.00	0.00	0.00
14.50	1629.1	9868.	1803538.	27.7	24342500.	9041421.	.371	100.00	0.00	0.00	0.00	0.00
15.00	1704.6	10701.	1965341.	30.2	24375000.	9983641.	.410	100.00	0.00	0.00	0.00	0.00
15.50	1780.6	11573.	2165952.	33.3	24407500.	11016464.	.451	100.00	0.00	0.00	0.00	0.00
16.00	1856.9	12482.	2385621.	36.7	24440000.	12154357.	.497	98.14	1.86	0.00	0.00	0.00
16.50	1933.5	13430.	2641476.	40.6	24472500.	13411131.	.548	96.05	3.95	0.00	0.00	0.00
17.00	2010.4	14416.	2925148.	45.0	24505000.	14802787.	.604	94.64	5.36	0.00	0.00	0.00
17.50	2087.5	15440.	3251884.	50.0	24537500.	16347045.	.666	93.01	6.99	0.00	0.00	0.00
18.00	2164.7	16503.	3607792.	55.5	24570000.	18061965.	.735	90.92	7.17	1.91	0.00	0.00
18.50	2242.1	17605.	3988982.	61.4	24602500.	19961158.	.811	88.53	8.11	3.56	0.00	0.00
19.00	2319.5	18745.	4429382.	68.1	24635000.	22065749.	.896	86.99	8.26	4.75	0.00	0.00
19.50	2396.9	19924.	4883391.	75.1	24667500.	24393943.	.989	85.77	8.03	6.20	0.00	0.00
20.00	2474.2	21142.	5389131.	82.9	24700000.	26962073.	1.092	83.70	8.70	5.66	1.94	0.00

The impact orientation analyzed above, that where the center of gravity is directly over the impact point, in approximately  $40^\circ$  from vertical. The available crush depth on the overpack flat may be determined from the Figure below:



The distance from point A to point B in the figure is:

$$((10.5^2) + (18.0)^2)^{0.5} = 20.84 \text{ inches}$$

The maximum crush depth is equal to AB times cosine  $\theta$ , or:

$$20.84 \cos (40 - \tan^{-1}(10.5/18)) = 20.54 \text{ inches}$$

Since for the 96 inch diameter case only 19.55 inches of deflection is predicted, there remains approximately one inch of clearance between the cask hard point and the impacted surface even under this extremely conservative analysis approach. For the 101 inch diameter case, the maximum crush depth that could be allowed prior to 'bottoming out' is given by:

$$((13.0)^2 + (18.0)^2)^{0.5} \cos (40 - \tan^{-1}(13/18)) = 22.15 \text{ inches}$$

So, since CYDROP predicts 19.92 inches of deflection under a conservative analysis, there will be at least 2.23 inches of clearance remaining during impact on the 101 inch diameter portions of the overpack. These results indicate that under the most adverse conditions, the 10/140MB overpack is large enough and stiff enough to protect the shield and containment structures from impacting the hypothetical unyielding surface directly.

#### 2.7.1.2.2 Force-Deflection Relationship

In order to obtain a conservative estimate of the internal forces and stresses within the NuPac 10/140MB, assumptions were made regarding the overpack geometry input to both CYDROP and OBLIQUE (Nuclear Packaging's oblique impact analysis tools) to maximize both forces (in the CYDROP input) and lever arms (in the OBLIQUE input). These assumptions were required due to the somewhat complicated overpack profile used on the 10/140MB.

A conservatively high force-deflection relationship was obtained by assuming the overpack is only 13 inches thick on the end of the package and 14.75 inches thick on the side of the package. This corresponds to an overpack whose outer corner is halfway between the 101 inch diameter corner and the 108 inch diameter corner. Because this overpack is so much smaller than the actual overpack, and because the stress-strain properties of  $-20^{\circ}\text{F}$  foam increased 15% were used, the stresses in the crushed polyurethane are predicted to be much higher than one might expect in practice for an equivalent amount of deformation.

Table 2.7.1-7 below presents a summary of the amount of foam crushed beyond 70 percent strain when the strain energy of deformation is equal to the energy of impact for various impact angles:

Angles (From Horizontal)	Percent above 70% Strain (Footprint area basis)	(Strain Energy) Basis
85	0	0
80	0	0
75	0	0
70	0	0
65	0	0
60	0	0
55	0.45%	.07%
50	1.64%	.36%
45	3.33%	1.39%
40	3.32%	1.84%
35	2.98%	1.08%
30	1.81%	0.53%
25	0.76%	0.23%
20	0.08%	0.02%
15	0	0
10	0	0
5	0	0

TABLE 2.7.1-7



From the Table above, (derived from CYDROP data), it is clear that less than 2% of the strain energy required to absorb the impact of a 30 foot drop is derived from extrapolated stress-strain data. It is clear that this extrapolation has little effect on the overall results of the analyses. Because the overpack is actually much larger than the dimensions input to CYDROP, it is also clear that the actual maximum foam strain would not exceed 70% for the worst case foam properties.

#### 2.7.1.2.3 Internal Forces during Oblique Impact

Cask internal forces are calculated by NuPac's OBLIQUE computer program discussed in Appendix 2.10.5. OBLIQUE utilizes the force-deflection relationship calculated by CYDROP to determine the rigid-body kinematic response of the cask.

Required input to OBLIQUE includes the cask and overpack dimensions, the mass and mass moment of inertia, the acceleration of gravity, velocity of impact and the force-deflection relationship of the overpacks at various angles. For purposes of OBLIQUE input, the overpack was taken to be 108 inches in diameter, 40 inches long extending 18 inches beyond the ends of the lead and steel cask structure. This causes OBLIQUE to apply the impact forces farther from the cask center line, resulting in higher internal forces. The combination of a conservatively derived force-deflection relationship with conservatively simplified overpack dimensions makes for a very conservative estimate of cask internal forces.

OBLIQUE uses inches, pounds and seconds as its primary units of length, force and time. The acceleration of gravity is then  $386.4 \text{ in/sec}^2$  and the mass of the 10/140MB in consistent units is  $65,000/386.4 = 168.22 \text{ lb.-sec}^2/\text{in}$ .



The mass moment of inertia may be calculated in the following manner, utilizing the basic formula:

$$I = 0.25 M (R^2 + L^2/3)$$

Where  $I$  = mass moment of inertia of a cylinder of mass  $M$ , radius  $R$  and length  $L$

For simplicity, the moment of inertia calculations were performed by dividing the package into 3 parts: overpacks, containment shield and payload. The weight of these three parts were divided by their volume and the acceleration of gravity to obtain an equivalent mass density. This density was used to calculate the moment of inertia.

The 10/140MB weight may be broken out in the following manner:

	Weight	Mass	Eq. Mass Density
Shield	41,000	106.1	$9.287 \times 10^{-4}$
Overpacks	9,000	23.3	$6.454 \times 10^{-5}$
Payload	15,000	38.8	$1.554 \times 10^{-4}$

$$\begin{aligned}
 I_{\text{shield}} &= (\pi/4)(83.5)(74.5)^2(9.287 \times 10^{-4})(.25)((37.2)^2 + (83.5)^2/3) \\
 &- (\pi/4)(73)(66)^2(9.287 \times 10^{-4})(.25)((33)^2 + (73)^2/3) \\
 &= 313668 - 166147 = 147,500 \text{ lb sec}^2\text{-in}
 \end{aligned}$$

$$\begin{aligned}
 I_{\text{overpacks}} &= (\pi/4)(119.5)(101)^2(6.454 \times 10^{-5})(.25)(50.5^2 + (119.5)^2/3) \\
 &- (\pi/4)(119.5)(55)^2(6.454 \times 10^{-5})(.25)((27.5)^2 + (119.5)^2/3) \\
 &- (\pi/4)(83.5)(75)^2(6.454 \times 10^{-5})(.25)((37.5)^2 + (83.5)^2/3) \\
 &+ (\pi/4)(83.5)(55)^2(6.454 \times 10^{-5})(.25)((27.5)^2 + (83.5)^2/3)
 \end{aligned}$$

$$\begin{aligned}
& - (\pi/4)(39.5)(101)^2(6.454 \times 10^{-5})(.25)((50.5)^2 + (39.5)^2/3) \\
& + (\pi/4)(39.5)(75)^2(6.454 \times 10^{-5})(.25)((37.5)^2 + (39.5)^2/3) \\
& = 65,100 \text{ lb-sec}^2\text{-in}
\end{aligned}$$

$$\begin{aligned}
I_{\text{payload}} & = (\pi/4)(73)(66)^2(1.554 \times 10^{-4})(.25)((33)^2 + (73)^2/3) \\
& = 27,800 \text{ lb-sec}^2\text{-in}
\end{aligned}$$

The total mass moment of inertia is then

$$I_{\text{total}} = 147,500 + 65,100 + 27,800 = 240,400 \text{ lb-sec}^2\text{-in}$$

For OBLIQUE input, the mass moment of inertia is taken as  $241,400 \text{ lb-sec}^2\text{-in}$ , or less than one half percent greater than calculated above. This is well within the accuracy of the calculations.

The results from the OBLIQUE computer analysis is presented in the following table. These results are also presented on the following pages in graphical form. From the table, it can be seen that the maximum impact bending moment is  $45.3 \times 10^6 \text{ in-lb}$ , occurring at an impact angle of approximately  $42^\circ$  from horizontal. It should be noted that this moment is derived from slender rod dynamics ( $4/27 F \cos \theta$ ) and as such is fairly conservative for the short, squat 10/140MB. The peak thrust proximate to the peak moment impact angle is  $4.099 \times 10^6 \text{ lb}$  at  $56^\circ$  lb at an impact angle of  $42^\circ$  from horizontal.

TABLE 2.7.1-8

NUPAC OBLIQUE ANALYSIS-NUPAC 10/140MB SHIPPING CASE ENVELOPE DIMENSIONS, COLD FOAM

PACKAGE GEOMETRY-						
	LENGTH	=	83.500			
	RADIUS	=	37.250			
	OVERPACK LENGTH	=	40.000			
	OVERPACK SIDE THICKNESS	=	16.500			
	OVERPACK BOTTOM THICKNESS	=	18.000			
PACKAGE MASS PROPERTIES-						
	MASS	=	168.220			
	MASS MOMENT OF INERTIA	=	241400.000			
	GRAVITATIONAL CONSTANT	=	386.400			
SOLUTION CHARACTERISTICS-						
	IMPACT VELOCITY (YDOT)	=	-527.450			
	(XDOT)	=	0.000			
	(THETADOT)	=	0.000			
	FRICTION COEFFICIENT	=	0.000			
	ESTIMATED CRUSH DEPTH	=	20.000			
THETA0	FMAX	SHEAR	THRUST	MOMENT	DEFLECTION	CLEARANCE
88.0000	10187282.	236522.	10185424.	2925864.	3.15	15.14
86.0000	8511249.	417570.	8502751.	5165493.	4.31	14.40
84.0000	5297690.	430440.	5283575.	5324697.	5.09	14.04
82.0000	5031889.	564348.	5004840.	6981192.	6.03	13.56
80.0000	4607867.	674444.	4564216.	8343126.	6.49	13.58
78.0000	4337868.	769635.	4276542.	9520667.	7.32	13.16
76.0000	4186621.	878300.	4101544.	10864891.	8.08	12.82
74.0000	4186229.	1005941.	4072096.	12445865.	8.81	12.49
72.0000	4141492.	1126712.	3995108.	13937848.	9.58	12.11
70.0000	4143543.	1262804.	3956367.	15621352.	10.31	11.75
68.0000	4175966.	1405018.	3941169.	17380591.	11.05	11.38
66.0000	4230767.	1562814.	3939077.	19332592.	11.75	11.01
64.0000	4336173.	1745749.	3974915.	21595566.	12.41	10.67
62.0000	4442464.	1939871.	4001826.	23996926.	13.04	10.34
60.0000	4587644.	2162778.	4050285.	26754566.	13.60	10.04
58.0000	4727936.	2395652.	4080254.	29635106.	14.10	9.77
56.0000	4875491.	2643317.	4099431.	32698807.	14.54	9.53
54.0000	5002422.	2890185.	4083021.	35752653.	14.89	9.34
52.0000	5104568.	3127183.	4034518.	38684418.	15.16	9.17
50.0000	5147088.	3328233.	3926243.	41171470.	15.35	9.05
48.0000	5116108.	3474742.	3755094.	42983850.	15.45	8.97
46.0000	5032762.	3574617.	3542711.	44219341.	15.47	8.92
44.0000	4913212.	3635422.	3305050.	44971518.	15.43	8.89
42.0000	4766246.	3661034.	3052990.	45288350.	15.32	8.88
40.0000	4590635.	3637046.	2801040.	44991604.	15.14	8.92
38.0000	4421410.	3613616.	2553037.	44701773.	14.93	8.93
36.0000	4218937.	3547124.	2300754.	43879240.	14.67	8.95
34.0000	4010193.	3448864.	2058894.	42663720.	14.37	9.01
32.0000	3822467.	3357076.	1841077.	41528279.	14.02	9.05
30.0000	3639781.	3258504.	1637879.	40308898.	13.64	9.15
28.0000	3503535.	3189636.	1468328.	39456978.	13.22	9.22
26.0000	3384599.	3128318.	1311406.	38698447.	12.77	9.31
24.0000	3272762.	3068413.	1166240.	37957408.	12.27	9.43
22.0000	3211406.	3044009.	1043793.	37655524.	11.75	9.58
20.0000	3131285.	3001229.	920904.	37126314.	11.23	9.70
18.0000	3059301.	2960256.	805677.	36619463.	10.58	9.89
16.0000	3056718.	2978141.	715967.	36840792.	9.97	10.10
14.0000	2954616.	2900153.	596453.	35875962.	9.20	10.36
12.0000	2894927.	2855733.	495638.	35326475.	8.57	10.66
10.0000	2761231.	2731614.	40914.	33791074.	7.53	11.43
8.0000	2251324.	2236597.	2584.	27667533.	5.83	12.62
6.0000	2619108.	2607271.	21275.	32252906.	5.91	11.94
4.0000	2502005.	2500368.	128129.	30930473.	4.80	12.34
2.0000	1944444.	1943439.	62509.	24041058.	2.99	14.08

FIGURE 2.7.1-1

## IMPACT FORCES (LBS) -30 FT DROP

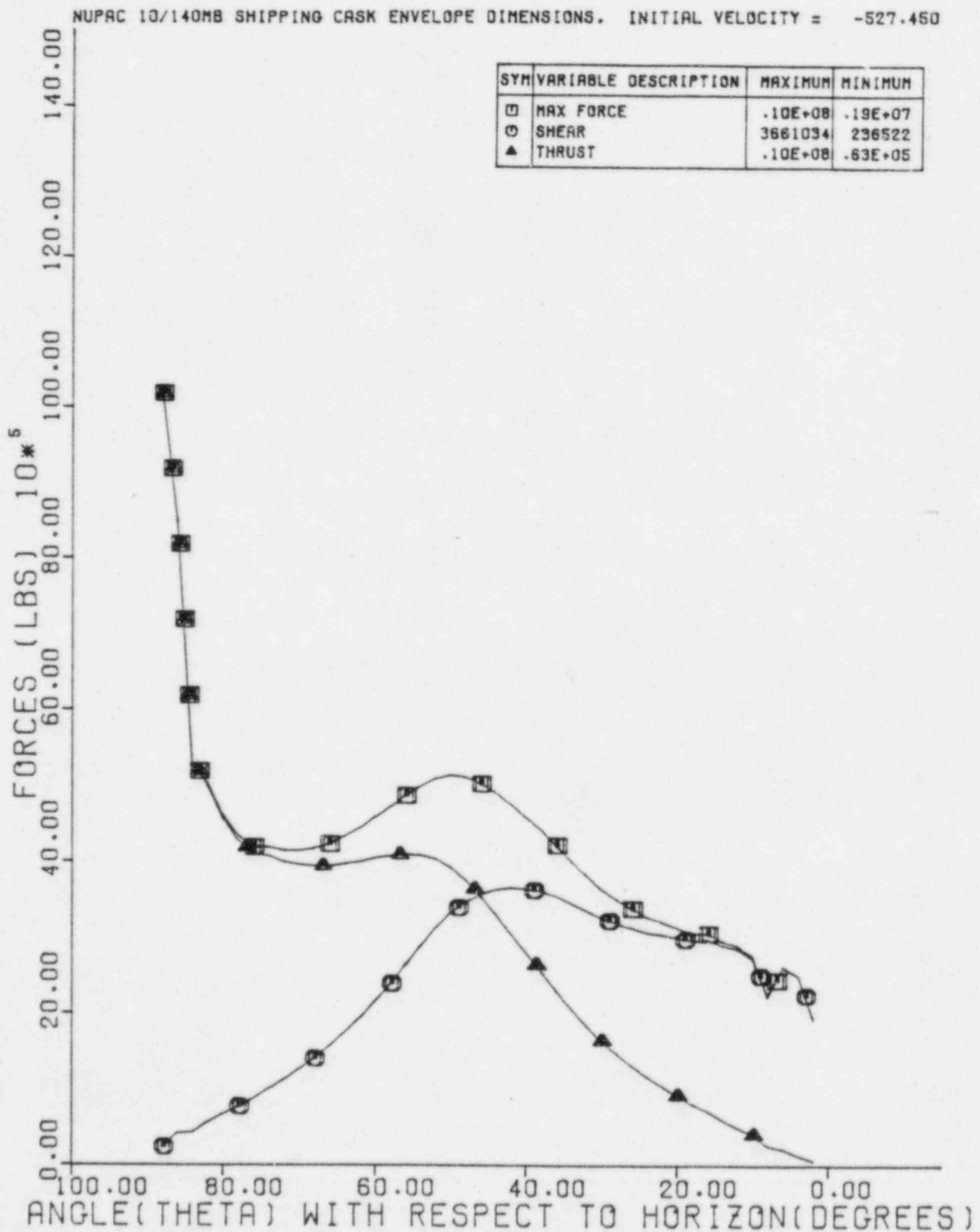
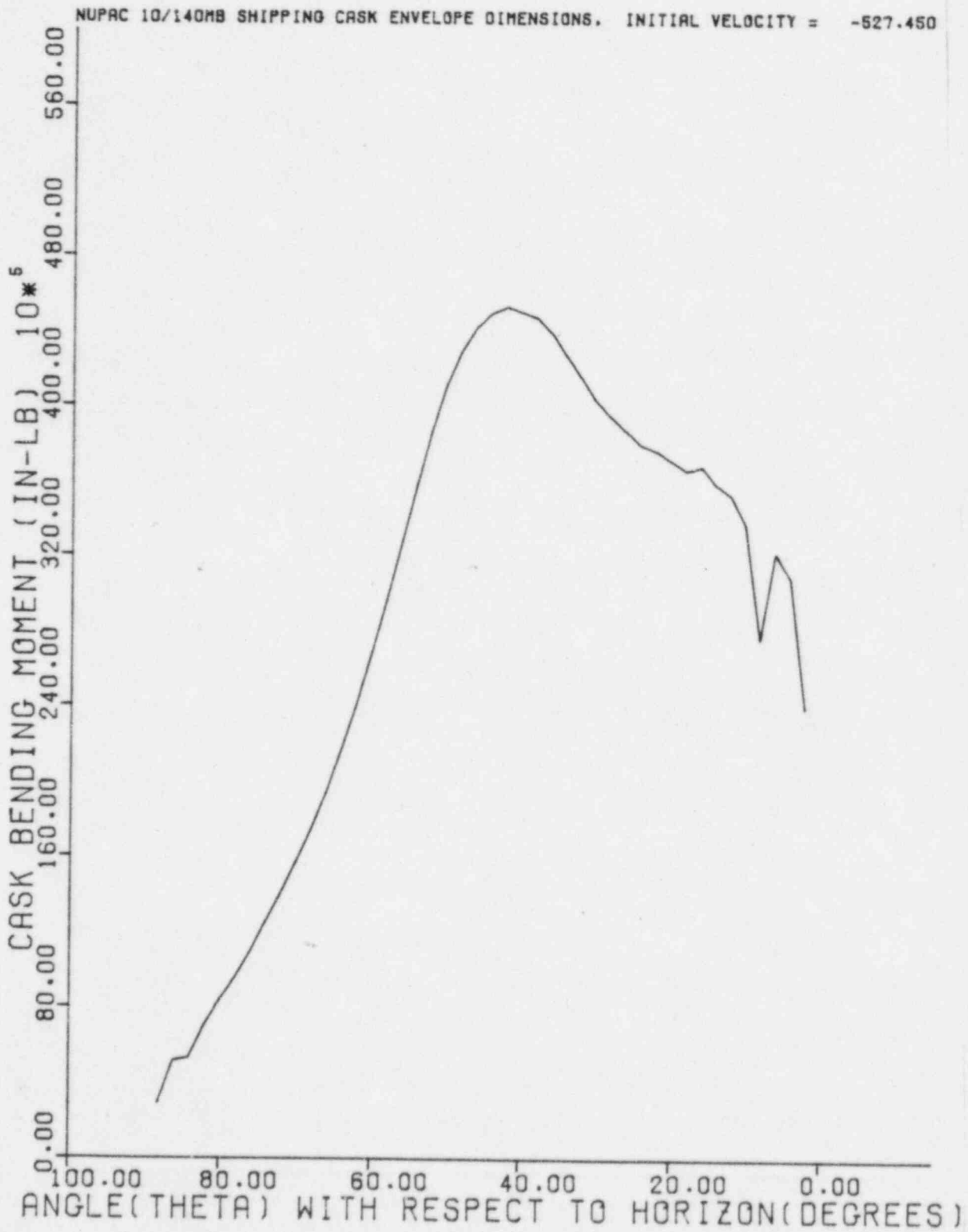


FIGURE 2.7.1-2

## CASK BENDING MOMENT (IN-LB) -30 FT DROP



Overpack separation moments were calculated using the OBLIQUE post processor POSTOB, which uses the linear and angular velocity history from OBLIQUE to derive the accelerations of the centroid of the 10/140MB package without the lid and impacted overpack. From this information the forces acting between the overpack/lid assembly and the rest of the package may be calculated. POSTOB represents these forces as a force and moment at the lid-body interface, either nearest the impact point or farthest from that point. The EnviroLocks<sup>tm</sup> act to counteract moments tending to open the package.

POSTOB requires that the mass moment of inertia for the package without the lid and overpack be calculated as well as the distance the c.g. of the entire loaded package is from the c.g. of the package without the lid and overpack. The mass of the payload as well as the mass of the entire loaded package without the lid and overpack is also required.

For the 10/140MB, the payload mass is

$$15,000/386.4 = 38.8 \text{ lb-sec}^2/\text{in.}$$

The weight of one overpack is approximately 4,500 lbs and the weight of a lid is approximately 6,700 lbs. Therefore, the mass of the package without the lid or overpack is:

$$(65,000 - (4,500 + 6,700))/386.4 = 139.2 \text{ lb-sec}^2/\text{in}$$

By inspection it can be seen that the center of gravity of the lid-overpack assembly is approximately 40.5 inches above the c.g. of the entire package. Since the mass of the package as a whole is 168.22 lb sec<sup>2</sup>/in, the location of the center of gravity of the package without the lid and overpack may be calculated:

$$139.2 x = (168.22 - 139.2) 40.5$$

$$x = 8.5$$

So the center of gravity of the 10/140MB without the lid and overpack is approximately 8.5 inches lower than the c.g. of the entire package.

The mass moment of inertia of the package without its lid and top overpack ( $I'$ ) may be calculated by solving the following equation:

$$I_{TOTAL} = I_{OPCG} + I_{LID} + M_{LID} d_{LID}^2 + I' + M' d'^2$$

Where  $I_{TOTAL}$  = mass moment of entire package = 241,400 lb-sec<sup>2</sup>-in

$I_{OPCG}$  = mass moment of overpack around package c.g.  
 = 65,100/2 = 32,550 lb-sec<sup>2</sup>-in (see calculation for total mass moment contribution of overpacks calculated above).

$I_{LID}$  = (6700/386.4) (.25) (37.5<sup>2</sup> + 5.25<sup>2</sup>/3)  
 = 6136 lb-sec<sup>2</sup>-in

$M_{LID}$  = 6700/386.4 = 17.34 lb-sec<sup>2</sup>/in

$d_{LID}$  = (83.5 - 5.25)/2 = 39.125

$I'$  = mass moment of inertia of package without lid or overpack on one end

$M'$  = mass of package without lid or overpack  
 = 139.2 lb-sec<sup>2</sup>/in

$d'$  = 8.5 (calculated above)

Solving for  $I'$ :

$$\begin{aligned} I' &= 241,400 - 32,550 - 6,136 - (17.34)(39.125)^2 - (139.2)(8.5)^2 \\ &= 166,100 \text{ lb-sec}^2\text{-in} \end{aligned}$$

This information was input to POSTOB with the time history results from the OBLIQUE analysis. The highest overpack separation moment calculated by POSTOB occurs during the c.g. over struck corner condition, or 50 degrees from a horizontal impact. At that impact angle, the separation moment calculated by POSTOB is approximately  $30.45 \times 10^6$  lb-in. The time history data from OBLIQUE as well as the moment calculation output from POSTOB for this impact angle are presented in Table 2.7.1-9 and 2.7.1-10 below.



TABLE 2.7.1-9

NUPAC OBLIQUE ANALYSIS-NUPAC 10/140MB SHIPPING CASK ENVELOPE DIMENSIONS, COLD FOAM

PACKAGE GEOMETRY-  
 LENGTH = 83.500  
 RADIUS = 37.250  
 OVERPACK LENGTH = 40.000  
 OVERPACK SIDE THICKNESS = 16.500  
 OVERPACK BOTTOM THICKNESS = 18.000  
 PACKAGE MASS PROPERTIES-  
 MASS = 168.220  
 MASS MOMENT OF INERTIA = 241400.000  
 GRAVITATIONAL CONSTANT = 386.400  
 SOLUTION CHARACTERISTICS-  
 IMPACT VELOCITY (YDOT) = -577.450  
 (XDOT) = 0.000  
 (THETADOT) = 0.000  
 FRICTION COEFFICIENT = 0.000  
 ESTIMATED CRUSH DEPTH = 20.000

THETA0	FMAX	SHEAR	THRUST	MOMENT	DEFLECTION	CLEARANCE
50.0000	5145562.	5325292.	3924112.	41135099.	15.35	9.05

TIME	X	XDOT	Y	YDOT	THETA	THETADOT	F	SHEAR	THRUST	DELTA(-Y AND X)
0.	0.	0.	0.	-5275E+03	.8727E+00	0.	0.	.2769E+07	.4097E+07	
.9893E-03	0.	0.	-5220E+00	-5278E+03	.8727E+00	.1914E-04	.3758E+04	.2416E+04	.2879E+04	.5220E+00
.1979E-02	0.	0.	-1044E+01	-5281E+03	.8727E+00	.1372E-03	.2099E+05	.1349E+05	.1608E+05	.1044E+01
.2968E-02	0.	0.	-1567E+01	-5283E+03	.8727E+00	.4663E-03	.5509E+05	.3541E+05	.4220E+05	.1567E+01
.3957E-02	0.	0.	-2090E+01	-5282E+03	.8727E+00	.1138E-02	.1060E+06	.6816E+05	.8123E+05	.2090E+01
.4947E-02	0.	0.	-2612E+01	-5278E+03	.8727E+00	.2195E-02	.1714E+06	.1102E+06	.1313E+06	.2612E+01
.5936E-02	0.	0.	-3134E+01	-5269E+03	.8727E+00	.3636E-02	.2485E+06	.1597E+06	.1904E+06	.3134E+01
.6925E-02	0.	0.	-3655E+01	-5256E+03	.8727E+00	.5410E-02	.3347E+06	.2151E+06	.2564E+06	.3654E+01
.7915E-02	0.	0.	-4174E+01	-5238E+03	.8727E+00	.7434E-02	.4282E+06	.2753E+06	.3280E+06	.4174E+01
.8904E-02	0.	0.	-4691E+01	-5213E+03	.8727E+00	.9598E-02	.5281E+06	.3394E+06	.4046E+06	.4691E+01
.9893E-02	0.	0.	-5205E+01	-5183E+03	.8727E+00	.1178E-01	.6337E+06	.4073E+06	.4855E+06	.5205E+01
.1088E-01	0.	0.	-5716E+01	-5146E+03	.8727E+00	.1383E-01	.7447E+06	.4786E+06	.5705E+06	.5716E+01
.1187E-01	0.	0.	-6223E+01	-5103E+03	.8727E+00	.1562E-01	.8604E+06	.5530E+06	.6591E+06	.6223E+01
.1286E-01	0.	0.	-6725E+01	-5053E+03	.8727E+00	.1697E-01	.9808E+06	.6304E+06	.7514E+06	.6725E+01
.1385E-01	0.	0.	-7223E+01	-4995E+03	.8728E+00	.1773E-01	.1106E+07	.7107E+06	.8472E+06	.7222E+01
.1484E-01	0.	0.	-7714E+01	-4930E+03	.8728E+00	.1773E-01	.1235E+07	.7938E+06	.9462E+06	.7713E+01
.1583E-01	0.	0.	-8079E+01	-4876E+03	.8728E+00	.1712E-01	.1335E+07	.8581E+06	.1023E+07	.8079E+01
.1682E-01	0.	0.	-8674E+01	-4777E+03	.8728E+00	.1475E-01	.1505E+07	.9670E+06	.1153E+07	.8674E+01
.1781E-01	0.	0.	-9052E+01	-4706E+03	.8728E+00	.1217E-01	.1620E+07	.1041E+07	.1241E+07	.9052E+01
.1880E-01	0.	0.	-9602E+01	-4590E+03	.8728E+00	.6577E-02	.1804E+07	.1159E+07	.1382E+07	.9601E+01
.1979E-01	0.	0.	-1005E+02	-4483E+03	.8728E+00	.5349E-04	.1965E+07	.1263E+07	.1505E+07	.1005E+02
.2078E-01	0.	0.	-1047E+02	-4367E+03	.8728E+00	.8356E-02	.2128E+07	.1368E+07	.1630E+07	.1047E+02
.2177E-01	0.	0.	-1091E+02	-4241E+03	.8728E+00	.1884E-01	.2295E+07	.1475E+07	.1758E+07	.1091E+02
.2276E-01	0.	0.	-1133E+02	-4104E+03	.8728E+00	.3159E-01	.2470E+07	.1587E+07	.1892E+07	.1133E+02
.2374E-01	0.	0.	-1173E+02	-3958E+03	.8728E+00	.4680E-01	.2644E+07	.1699E+07	.2025E+07	.1173E+02
.2473E-01	0.	0.	-1211E+02	-3801E+03	.8727E+00	.6462E-01	.2819E+07	.1812E+07	.2160E+07	.1211E+02
.2572E-01	0.	0.	-1248E+02	-3634E+03	.8726E+00	.8522E-01	.3002E+07	.1930E+07	.2300E+07	.1248E+02
.2671E-01	0.	0.	-1283E+02	-3455E+03	.8725E+00	.1088E+00	.3193E+07	.2053E+07	.2446E+07	.1283E+02
.2770E-01	0.	0.	-1316E+02	-3266E+03	.8724E+00	.1355E+00	.3380E+07	.2173E+07	.2589E+07	.1316E+02
.2869E-01	0.	0.	-1377E+02	-3053E+03	.8723E+00	.1654E+00	.3571E+07	.2296E+07	.2734E+07	.1377E+02
.2968E-01	0.	0.	-1429E+02	-2853E+03	.8721E+00	.1988E+00	.3772E+07	.2426E+07	.2888E+07	.1429E+02
.3067E-01	0.	0.	-1404E+02	-2629E+03	.8719E+00	.2356E+00	.3973E+07	.2556E+07	.3042E+07	.1404E+02
.3166E-01	0.	0.	-1429E+02	-2394E+03	.8716E+00	.2761E+00	.4169E+07	.2683E+07	.3191E+07	.1429E+02
.3265E-01	0.	0.	-1451E+02	-2147E+03	.8713E+00	.3201E+00	.4361E+07	.2807E+07	.3337E+07	.1452E+02
.3364E-01	0.	0.	-1471E+02	-1888E+03	.8710E+00	.3677E+00	.4546E+07	.2928E+07	.3477E+07	.1472E+02
.3463E-01	0.	0.	-1489E+02	-1620E+03	.8706E+00	.4188E+00	.4710E+07	.3035E+07	.3602E+07	.1489E+02
.3562E-01	0.	0.	-1503E+02	-1343E+03	.8702E+00	.4729E+00	.4850E+07	.3127E+07	.3707E+07	.1504E+02
.3661E-01	0.	0.	-1515E+02	-1058E+03	.8697E+00	.5299E+00	.4942E+07	.3201E+07	.3792E+07	.1516E+02
.3759E-01	0.	0.	-1524E+02	-7670E+02	.8691E+00	.5893E+00	.5050E+07	.3260E+07	.3857E+07	.1525E+02
.3858E-01	0.	0.	-1530E+02	-4719E+02	.8685E+00	.6507E+00	.5111E+07	.3301E+07	.3901E+07	.1531E+02
.3957E-01	0.	0.	-1533E+02	-1740E+02	.8678E+00	.7136E+00	.5144E+07	.3325E+07	.3924E+07	.1535E+02

FMAX= .51436E+07 FMIN= 0.

TABLE 2.7.1-10

CENTER OF GRAVITY OFFSET \* 8.50  
 MOMENT OF INERTIA OF UPPER PART \* 166100.00  
 MASS OF UPPER PART (INCL. P/L) \* 139.20  
 MASS OF PAYLOAD \* 38.80  
 LID FLANGE THICKNESS \* 2.25  
 PACKAGE LENGTH (W/O OVERPACK) \* 83.50  
 PACKAGE RADIUS (W/O OVERPACK) \* 37.25  
 ACCELERATION OF GRAVITY \* 386.40

ANGLE	TIME	LAT. ACCEL	AX. ACCEL	X ACCEL	Y ACCEL	TH ACCEL	MOMENT ADJACENT	MOMENT OPPOSITE	MAX ADJ. MOMENT	MAX OPP. MOMENT
50.00	9893E-03	-53.61	63.70	-1260	83.26	1935E-01	1232E+06	-5997E+06	1232E+06	-5997E+06
50.00	1979E-02	-54.50	63.80	-7439	83.70	1142	1445E+06	-6217E+06	1445E+06	-5997E+06
50.00	2968E-02	-121.3	141.1	2.200	186.0	3378	3386E+06	-1394E+07	3386E+06	-5997E+06
50.00	3957E-02	-319.1	373.5	-6.422	491.2	6792	8484E+06	-3642E+07	8484E+06	-5997E+06
50.00	4947E-02	-517.1	605.5	-6.952	796.3	1.068	1368E+07	-5897E+07	1368E+07	-5997E+06
50.00	5936E-02	-845.7	993.1	-9.488	1304.	1.457	2178E+07	-9607E+07	2178E+07	-5997E+06
50.00	6925E-02	-1108.	1303.	-11.68	1711.	1.794	2831E+07	-1258E+08	2831E+07	-5997E+06
50.00	7915E-02	-1434.	1689.	-13.31	2216.	2.044	3607E+07	-1624E+08	3607E+07	-5997E+06
50.00	8904E-02	-1892.	2232.	-14.25	2926.	2.188	4654E+07	-2135E+08	4654E+07	-5997E+06
50.00	9893E-02	-2217.	2620.	-14.37	3432.	2.204	5381E+07	-2498E+08	5381E+07	-5997E+06
50.00	1088E-01	-2676.	3168.	-13.52	4164.	2.077	6375E+07	-3007E+08	6375E+07	-5997E+06
50.00	1187E-01	-3056.	3623.	-11.77	4740.	1.608	7165E+07	-3627E+08	7165E+07	-5997E+06
50.00	1286E-01	-3506.	4165.	-8.879	5444.	1.364	8077E+07	-3923E+08	8077E+07	-5997E+06
50.00	1385E-01	-4020.	4784.	-4.999	6249.	7677	9097E+07	-4488E+08	9097E+07	-5997E+06
50.01	1484E-01	-4468.	5326.	0.	6952.	0.	9934E+07	-4977E+08	9934E+07	-5997E+06
50.01	1583E-01	-3749.	4475.	4.013	5835.	-6162	8209E+07	-4168E+08	9934E+07	-5997E+06
50.01	1682E-01	-6655.	7957.	15.59	1037E+05	-2.394	1431E+08	-7383E+08	1431E+08	-5997E+06
50.01	1781E-01	-4835.	5791.	16.97	7544.	-2.606	1022E+08	-5555E+08	1431E+08	-5997E+06
50.01	1880E-01	-7731.	9273.	36.79	1207E+05	-5.649	1604E+08	-8540E+08	1604E+08	-5997E+06
50.01	1979E-01	-7139.	8576.	42.91	1116E+05	-6.589	1453E+08	-7868E+08	1604E+08	-5997E+06
50.01	2078E-01	-7707.	9273.	55.32	1206E+05	-8.495	1540E+08	-8746E+08	1604E+08	-5997E+06
50.01	2177E-01	-8338.	1005E+05	68.96	1306E+05	-10.59	1638E+08	-9155E+08	1638E+08	-5997E+06
50.01	2275E-01	-9122.	1101E+05	84.72	1429E+05	-13.01	1743E+08	-9995E+08	1743E+08	-5997E+06
50.01	2374E-01	-9596.	1159E+05	100.0	1505E+05	-15.36	1820E+08	-1049E+09	1820E+08	-5997E+06
50.00	2473E-01	-1029E+05	1245E+05	117.2	1615E+05	-18.00	1921E+08	-1123E+09	1921E+08	-5997E+06
50.00	2572E-01	-1091E+05	1322E+05	135.5	1716E+05	-20.81	2004E+08	-1189E+09	2004E+08	-5997E+06
49.99	2671E-01	-1167E+05	1415E+05	155.1	1834E+05	-23.82	2111E+08	-1269E+09	2111E+08	-5997E+06
49.99	2770E-01	-1229E+05	1492E+05	175.6	1933E+05	-26.97	2187E+08	-1335E+09	2187E+08	-5997E+06
49.98	2869E-01	-1305E+05	1584E+05	196.6	2052E+05	-30.20	2290E+08	-1414E+09	2290E+08	-5997E+06
49.97	2968E-01	-1373E+05	1669E+05	219.6	2162E+05	-33.74	2373E+08	-1486E+09	2373E+08	-5997E+06
49.96	3067E-01	-1449E+05	1762E+05	241.9	2281E+05	-37.17	2474E+08	-1565E+09	2474E+08	-5997E+06
49.95	3166E-01	-1518E+05	1847E+05	266.2	2390E+05	-40.91	2554E+08	-1637E+09	2554E+08	-5997E+06
49.93	3265E-01	-1593E+05	1939E+05	289.1	2509E+05	-44.44	2655E+08	-1716E+09	2655E+08	-5997E+06
49.91	3364E-01	-1669E+05	2031E+05	312.7	2628E+05	-48.08	2755E+08	-1795E+09	2755E+08	-5997E+06
49.89	3463E-01	-1725E+05	2100E+05	335.6	2717E+05	-51.62	2814E+08	-1852E+09	2814E+08	-5997E+06
49.87	3562E-01	-1782E+05	2169E+05	355.1	2807E+05	-54.65	2886E+08	-1911E+09	2886E+08	-5997E+06
49.84	3661E-01	-1832E+05	2230E+05	374.0	2886E+05	-57.58	2948E+08	-1963E+09	2948E+08	-5997E+06
49.81	3759E-01	-1890E+05	2298E+05	393.6	2975E+05	-60.61	3024E+08	-2021E+09	3024E+08	-5997E+06
49.78	3858E-01	-1897E+05	2306E+05	402.5	2985E+05	-62.02	3023E+08	-2027E+09	3024E+08	-5997E+06
49.74	3957E-01	-1916E+05	2326E+05	412.1	3013E+05	-63.54	3045E+08	-2044E+09	3045E+08	-5997E+06

2.7.1.2.4 Stress Calculations in Cask Body

From the summary of internal forces in Table 2.7.1-8 above, the worst case state of compressive stress may be found. From that table it is clear that the worst stress state will occur during drops from angles between  $56^\circ$  and  $42^\circ$  from horizontal. Using the standard formula for combined axial and bending stress:

$$\sigma = P/A + Mc/I$$

and conservatively assuming all stress is carried by the outer shell, the following table may be constructed:

Impact Angle	Thrust ( $10^6$ lbs)	Moment ( $10^7$ lb-in)	Stress (psi)
56	4.10	3.270	20565
54	4.08	3.575	21084
52	4.03	3.868	21475
50	3.93	4.117	21608
48	3.76	4.298	21367
46	3.54	4.422	20841
44	3.31	4.497	20186
42	3.05	4.529	19344

The stresses above were calculated assuming that all of the bending and axial forces are carried by the outer shell. The outer shell compressive area is:

$$A = \pi(74.5^2 - 72^2)/4 = 287.65 \text{ in}^2$$

and the moment of inertia is  $1.93 \times 10^5 \text{ in}^4$  (see Section 2.7.1.3.2).

It is important to note that while the method of calculating the above stresses is very simple, the assumptions used are very conservative. First, the loads are developed using a conservative envelope of the 10/140MB cask overpack. Second, it is assumed that the maximum axial force acts at the same point on the package as the maximum bending moment for the impact angle. Since the maximum axial force is always at the end of the package and the moment acts at approximately the third point along the length of the package, the moment and axial force maxima never act simultaneously. As stated above and in the discussion of the OBLIQUE program, the moment is based on a slender beam impact, which greatly over predicts the moment in a short, large radius cylinder such as the 10/140MB. Finally, because the internal forces arise from inertial effects, it is conservative to assume that the stresses are entirely carried by the outer shell. If all these elements of conservatism were removed, the stresses calculated in the cask would be much less than predicted above.

The following margin of safety is calculated using the ASME membrane stress allowable even though the stresses calculated above include a small fraction which is properly a bending stress.

$$M.S. = (36,258/21,608) - 1 = +0.68$$

When the conservative nature of the stresses and allowables used for this analysis are considered, it is clear that oblique impacts from 30 feet will not severely affect the package's containment or shielding capability.

#### 2.7.1.2.5 Lid Attachment Loads

The eight EnviroLock<sup>tm</sup> lid hold down devices must be strong enough to remain intact during the impact. An analysis of the moment exerted on the package body by the lid and overpack interface was performed by POSTOB, a post processor written for the OBLIQUE program time history output. From that analysis, the maximum lid separation moment was found to be  $30.5 \times 10^6$  lb-in. at an impact angle of  $50^\circ$  from horizontal. The maximum force in the EnviroLock<sup>tm</sup> may be

estimated using the assumption that the force varies linearly from the point nearest the impact. The moment exerted by a set of discrete forces equally spaced around a circumference of radius  $R$ , where the force is proportional to its projected distance from the point of rotation nearest the impact point is given by the formula:

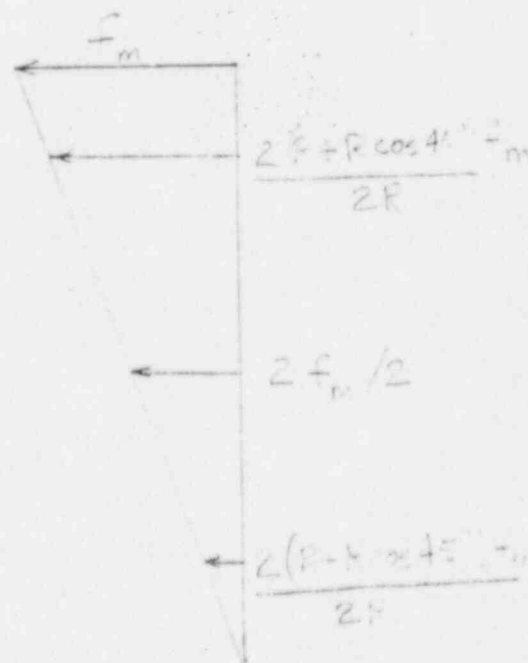
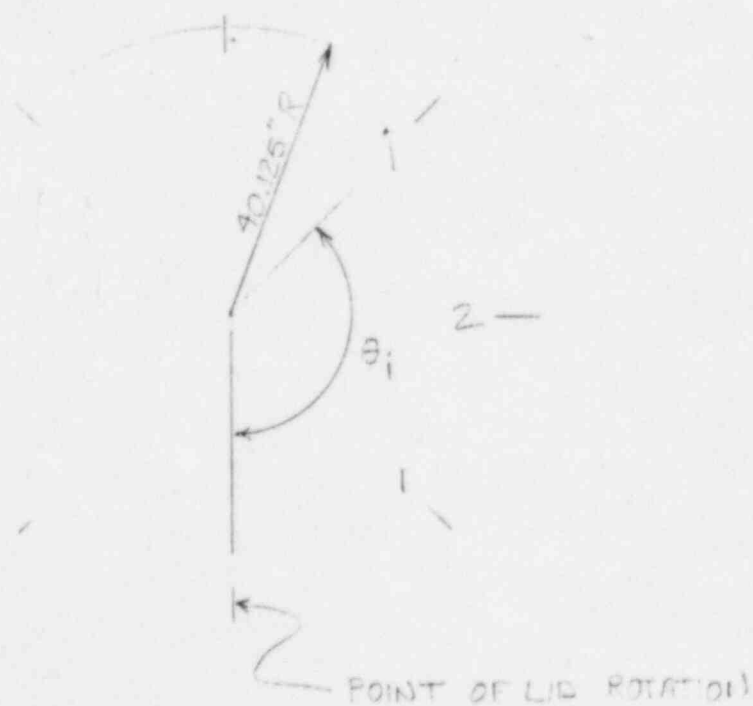
$$M = 0.5 f_m R \sum (1 - \cos \theta_i)^2$$

where  $M$  = moment to resist

$f_m$  = maximum force in the lid attachment

$R$  = lid attachment radius

$\theta_i$  = angle from point of rotation to attachment  $i$



This formula reduces to:

$$M = 3RNf_m/4$$

where  $N$  is the number of attachments. Therefore, the maximum force in the EnviroLocks<sup>tm</sup> will be:

$$f_m = 4(30.5 \times 10^6)/3(40.25)8 = 126,300 \text{ lb}$$

The ultimate strength of the EnviroLock<sup>tm</sup> is given in Appendix 2.10.4 as 250,000 lbs, while the yield strength is given as 184,500 lbs. For accident conditions, the allowable load in these fasteners is the lesser of the yield strength and 70% of the ultimate strength. Therefore, accident allowable load in the EnviroLock<sup>tm</sup> is:

$$(.7)(250,000) = 175,000 \text{ lbs}$$

The margin of safety is then:

$$175,000/126,300 - 1 = +0.39$$

#### 2.7.1.3 Flat Side Impact

Analysis of the NuPac 10/140MB package behavior during a hypothetical 30 foot side impact is performed in the following steps:

1. Determine the impact forces using the SYDROP computer program as well as hand analysis; and determine worst case deflections.
2. Determine stresses in the outer shell assuming it reacts the entire impact bending load. Include ovalty effects.
3. Determine stresses in the inner shell assuming it reacts the payload weight and half the load weight in bending. Include ovalty effects.

#### 2.7.1.3.1 Side Impact Forces and Deflection

Several bounding analyses were performed using the energy-balance program SYDROP to determine the behavior of the 10/140MB overpack system during side impact. The bounding analyses were performed to compensate for the unusual geometry of the 10/140MB overpack system. SYDROP was written assuming a simple rigid cylinder is protected by a simple cylindrical foam overpack around the sides of the rigid cylinder.

The actual geometry of the 10/140MB package differs from this assumption in three ways. First, the overpack extends beyond the end of the rigid cylinder. As a result, some assumptions must be made regarding the effect of the cantilevered foam. Many drop tests have been performed which indicate that the cantilevered foam contributes a significant part of the package's ability to resist impacts. In general, the effectiveness of the overhang in foam may be estimated by comparing the plateau crush strength of the impacted foam with the shear strength of the foam carrying the load back into the package. The shear strength of the foam in the 10/140MB is more than adequate to assure nearly complete involvement of the overpack length in resisting side impacts.

Second, the 10/140MB overpack employs a stepped design, such that 10 inches from the end of the overpack the radius of the overpack is reduced 3.5 inches. This step allows the overpack to deform much further in the side impact without bottoming out onto one of the protuberances on the side wall of the cask (e.g., the tie down lug). The overpack would be expected to act as if it were only 30 inches long on each end for the first 3.5 inches of impact deflection. After that, the additional 10 inches of overpack on each end would begin to be mobilized.

Thirdly, the flat areas on either side of the package will act very little like the cylindrical overpack modeled in SYDROP. Loads and deflections for an impact on the overpack flat areas will be calculated by hand.

Tables 2.7.1-11 through 2.7.1-14 represent the response of 20 and 60 inch long overpacks at  $-20^{\circ}$  and  $109^{\circ}\text{F}$ , the hypothetical accident temperature range for the polyurethane foam. The properties of the foam were degraded 15% from the

expected response at 109°F and were increased 15% from the expected response at -20°F, consistent with previous analyses presented herein.



TABLE 2.7.1-11

SYDROP(SIDE)

NUCLEAR PACKAGING PROPRIETARY  
NUPAC 10/140M COLD FOAM (-20 DEG)

17.47.18

85/06/26

PAGE 5

PACKAGE HEIGHT \* 65000 (LBS)  
 PACKAGE EXTERNAL LENGTH \* 60.00 (IN)  
 PACKAGE EXTERNAL DIAMETER \* 108.00 (IN)  
 PAYLOAD DIAMETER \* 75.00 (IN)  
 DROP HEIGHT \* 30.00 (FT)

## STRAIN VS STRESS TABLE

SYDROP(SIDE)

NUCLEAR PACKAGING PROPRIETARY  
NUPAC 10/140M COLD FOAM (-20 DEG)

17.47.18

85/06/26

PAGE 6

CRUSH DEPTH (IN)	** CRUSH PLANE **		**** IMPACT ****		***** ENERGY *****			DISTRIBUTION OF STRAIN RATIOS BY PERCENT OF CONTACT AREA				
	AREA (IN <sup>2</sup> )	VOLUME (IN <sup>3</sup> )	FORCE (LBS)	ACCEL (G)	POTENTIAL (IN-LB)	STRAIN (IN-LB)	RATIO (SE/PE)	LE.70	GT.70 LE.80	GT.80 LE.90	GT.90 LE.95	GT.95
.25	622.8	104.	201140.	3.1	23416250.	25143.	.001	100.00	0.00	0.00	0.00	0.00
.50	879.8	294.	967642.	8.7	23432500.	121240.	.005	100.00	0.00	0.00	0.00	0.00
.75	1076.2	539.	988617.	15.2	23448750.	315773.	.013	100.00	0.00	0.00	0.00	0.00
1.00	1241.3	829.	1425121.	21.9	23465000.	617490.	.026	100.00	0.00	0.00	0.00	0.00
1.25	1386.2	1158.	1853808.	28.5	23481250.	1027356.	.044	100.00	0.00	0.00	0.00	0.00
1.50	1516.7	1521.	2234554.	34.4	23497500.	1538401.	.065	100.00	0.00	0.00	0.00	0.00
1.75	1636.3	1915.	2570213.	39.3	23513750.	2158997.	.091	100.00	0.00	0.00	0.00	0.00
2.00	1747.2	2338.	2863236.	44.0	23530000.	2818178.	.120	100.00	0.00	0.00	0.00	0.00
2.25	1851.0	2788.	3120706.	48.0	23546250.	3566171.	.151	100.00	0.00	0.00	0.00	0.00
2.50	1948.8	3263.	3356182.	51.6	23562500.	4375782.	.186	100.00	0.00	0.00	0.00	0.00
2.75	2041.5	3762.	3574521.	55.0	23578750.	5242120.	.222	100.00	0.00	0.00	0.00	0.00
3.00	2129.8	4284.	3779292.	58.1	23595000.	6161346.	.261	100.00	0.00	0.00	0.00	0.00
3.25	2214.1	4827.	3973051.	61.1	23611250.	7130389.	.302	100.00	0.00	0.00	0.00	0.00
3.50	2295.0	5391.	4158308.	64.0	23627500.	8146809.	.345	100.00	0.00	0.00	0.00	0.00
3.75	2372.7	5974.	4337166.	66.7	23643750.	9208743.	.389	100.00	0.00	0.00	0.00	0.00
4.00	2447.5	6577.	4511114.	69.4	23660000.	10314778.	.436	100.00	0.00	0.00	0.00	0.00
4.25	2519.8	7198.	4681531.	72.0	23676250.	11463859.	.484	100.00	0.00	0.00	0.00	0.00
4.50	2589.7	7836.	4849708.	74.6	23692500.	12655264.	.534	100.00	0.00	0.00	0.00	0.00
4.75	2657.5	8492.	5016875.	77.2	23708750.	13888587.	.586	100.00	0.00	0.00	0.00	0.00
5.00	2723.2	9165.	5184126.	79.8	23725000.	15163712.	.639	100.00	0.00	0.00	0.00	0.00
5.25	2787.1	9854.	5351775.	82.3	23741250.	16480699.	.694	100.00	0.00	0.00	0.00	0.00
5.50	2849.2	10558.	5521436.	84.9	23757500.	17839851.	.751	100.00	0.00	0.00	0.00	0.00
5.75	2909.7	11278.	5694426.	87.6	23773750.	19241834.	.809	100.00	0.00	0.00	0.00	0.00
6.00	2968.6	12013.	5872159.	90.3	23790000.	20687657.	.870	100.00	0.00	0.00	0.00	0.00
6.25	3026.1	12762.	6056045.	93.2	23806250.	22178682.	.932	100.00	0.00	0.00	0.00	0.00
6.50	3082.3	13526.	6247452.	96.1	23822500.	23716619.	.996	100.00	0.00	0.00	0.00	0.00
6.52	3086.0	13578.	6260869.	96.3	23823596.	23823664.	1.000	100.00	0.00	0.00	0.00	0.00
6.75	3137.1	14303.	6446321.	99.2	23838750.	25303341.	1.061	100.00	0.00	0.00	0.00	0.00
7.00	3190.7	15095.	6632670.	102.3	23855000.	26940690.	1.129	100.00	0.00	0.00	0.00	0.00
7.25	3243.2	15899.	6819676.	105.7	23871250.	28630933.	1.199	100.00	0.00	0.00	0.00	0.00
7.50	3294.5	16716.	7100119.	109.2	23887500.	30377133.	1.272	100.00	0.00	0.00	0.00	0.00
7.75	3344.8	17546.	7347186.	113.0	23903750.	32183046.	1.346	100.00	0.00	0.00	0.00	0.00
8.00	3394.1	18388.	7613574.	117.1	23920000.	34053141.	1.424	100.00	0.00	0.00	0.00	0.00
8.25	3442.4	19243.	7902202.	121.6	23936250.	35992613.	1.504	100.00	0.00	0.00	0.00	0.00
8.50	3489.8	20109.	8206739.	126.3	23952500.	38006231.	1.587	100.00	0.00	0.00	0.00	0.00
8.75	3536.3	20988.	8533378.	131.3	23968750.	40098745.	1.673	100.00	0.00	0.00	0.00	0.00
9.00	3582.0	21878.	8890727.	136.8	23985000.	42276758.	1.763	100.00	0.00	0.00	0.00	0.00
9.25	3626.8	22779.	9286188.	142.9	24001250.	44548873.	1.856	100.00	0.00	0.00	0.00	0.00
9.50	3670.8	23691.	9727536.	149.7	24017500.	46925588.	1.954	100.00	0.00	0.00	0.00	0.00
9.75	3714.1	24614.	10222921.	157.3	24033750.	49419395.	2.056	100.00	0.00	0.00	0.00	0.00
10.00	3756.6	25548.	10781992.	165.9	24050000.	52045010.	2.164	100.00	0.00	0.00	0.00	0.00

TABLE 2.7.1-12

SYDROP(SIDE)

NUCLEAR PACKAGING PROPRIETARY

17.47.18

85/06/26

PAGE 7

NUPAC 10/140M COLD FOAM (-20 DEG)

PACKAGE HEIGHT = 45000. (LBS)  
 PACKAGE EXTERNAL LENGTH = 20.00 (IN)  
 PACKAGE EXTERNAL DIAMETER = 101.00 (IN)  
 PAYLOAD DIAMETER = 75.00 (IN)  
 DROP HEIGHT = 30.00 (FT)

## STRAIN VS STRESS TABLE

SYDROP(SIDE)

NUCLEAR PACKAGING PROPRIETARY

17.47.18

85/06/26

PAGE 8

NUPAC 10/140M COLD FOAM (-20 DEG)

CRUSH DEPTH (IN)	** CRUSH PLANE **		**** IMPACT ****		***** ENERGY *****			DISTRIBUTION OF STRAIN RATIOS BY PERCENT OF CONTACT AREA				
	AREA (IN <sup>2</sup> )	VOLUME (IN <sup>3</sup> )	FORCE (LBS)	ACCEL. (G)	POTENTIAL (IN-LB)	STRAIN (IN-LB)	RATIO (SE/PE)	LE.70	GT.70	GT.80	GT.90	GT.95
.25	200.7	33.	82290.	1.3	23416250.	10286.	.000	100.00	0.00	0.00	0.00	0.00
.50	283.5	95.	226775.	3.5	23432500.	48919.	.002	100.00	0.00	0.00	0.00	0.00
.75	346.8	174.	384167.	5.9	23448750.	125287.	.005	100.00	0.00	0.00	0.00	0.00
1.00	400.0	267.	549475.	8.3	23465000.	240867.	.010	100.00	0.00	0.00	0.00	0.00
1.25	446.7	373.	675248.	10.4	23481250.	392833.	.017	100.00	0.00	0.00	0.00	0.00
1.50	488.7	490.	790424.	12.2	23497500.	576042.	.025	100.00	0.00	0.00	0.00	0.00
1.75	527.2	617.	887284.	13.7	23513750.	785755.	.033	100.00	0.00	0.00	0.00	0.00
2.00	562.8	753.	973238.	15.0	23530000.	1018321.	.043	100.00	0.00	0.00	0.00	0.00
2.25	596.2	898.	1051575.	16.2	23546250.	1271422.	.054	100.00	0.00	0.00	0.00	0.00
2.50	627.7	1051.	1124193.	17.3	23562500.	1543393.	.066	100.00	0.00	0.00	0.00	0.00
2.75	657.5	1212.	1192560.	18.3	23578750.	1832987.	.078	100.00	0.00	0.00	0.00	0.00
3.00	685.9	1380.	1257964.	19.4	23595000.	2139303.	.091	100.00	0.00	0.00	0.00	0.00
3.25	713.0	1555.	1321279.	20.3	23611250.	2461708.	.104	100.00	0.00	0.00	0.00	0.00
3.50	738.9	1736.	1385318.	21.3	23627500.	2799783.	.118	100.00	0.00	0.00	0.00	0.00
3.75	763.9	1924.	1444821.	22.2	23643750.	3153300.	.133	100.00	0.00	0.00	0.00	0.00
4.00	787.9	2118.	1506367.	23.2	23660000.	3522199.	.149	100.00	0.00	0.00	0.00	0.00
4.25	811.1	2318.	1568412.	24.1	23676250.	3906546.	.165	100.00	0.00	0.00	0.00	0.00
4.50	833.5	2524.	1631796.	25.1	23692500.	4306572.	.182	100.00	0.00	0.00	0.00	0.00
4.75	855.2	2735.	1697374.	26.1	23708750.	4722719.	.199	100.00	0.00	0.00	0.00	0.00
5.00	876.4	2951.	1765975.	27.2	23725000.	5155637.	.217	100.00	0.00	0.00	0.00	0.00
5.25	896.8	3173.	1838263.	28.3	23741250.	5606167.	.236	100.00	0.00	0.00	0.00	0.00
5.50	916.7	3400.	1913893.	29.4	23757500.	6075186.	.256	100.00	0.00	0.00	0.00	0.00
5.75	936.1	3631.	1994571.	30.7	23773750.	6563744.	.276	100.00	0.00	0.00	0.00	0.00
6.00	955.0	3868.	2081988.	32.0	23790000.	7073314.	.297	100.00	0.00	0.00	0.00	0.00
6.25	973.4	4109.	2177794.	33.5	23806250.	7605786.	.319	100.00	0.00	0.00	0.00	0.00
6.50	991.4	4354.	2283799.	35.1	23822500.	8163486.	.343	100.00	0.00	0.00	0.00	0.00
6.75	1008.9	4604.	2397962.	36.9	23838750.	8748706.	.367	100.00	0.00	0.00	0.00	0.00
7.00	1026.1	4859.	2523775.	38.8	23855000.	9363923.	.393	100.00	0.00	0.00	0.00	0.00
7.25	1042.8	5117.	2666076.	41.0	23871250.	10012655.	.419	100.00	0.00	0.00	0.00	0.00
7.50	1059.2	5380.	2829438.	43.5	23887500.	10699594.	.448	100.00	0.00	0.00	0.00	0.00
7.75	1075.3	5647.	3018708.	46.4	23903750.	11430613.	.478	100.00	0.00	0.00	0.00	0.00
8.00	1091.1	5918.	3240379.	49.9	23920000.	12212999.	.511	100.00	0.00	0.00	0.00	0.00
8.25	1106.5	6193.	3498872.	53.8	23936250.	13055405.	.545	100.00	0.00	0.00	0.00	0.00
8.50	1121.6	6471.	3796949.	58.4	23952500.	13967383.	.583	100.00	0.00	0.00	0.00	0.00
8.75	1136.4	6753.	4138168.	63.7	23968750.	14959272.	.624	100.00	0.00	0.00	0.00	0.00
9.00	1151.0	7039.	4525164.	69.6	23985000.	16042189.	.669	100.00	0.00	0.00	0.00	0.00
9.25	1165.3	7329.	4952700.	76.2	24001250.	17269922.	.718	88.00	12.00	0.00	0.00	0.00
9.50	1179.3	7622.	5404146.	83.1	24017500.	18521528.	.771	80.67	19.33	0.00	0.00	0.00
9.75	1193.1	7918.	5879880.	90.5	24033750.	19932031.	.829	76.00	24.00	0.00	0.00	0.00
10.00	1206.6	8218.	6378359.	98.1	24050000.	21464311.	.892	72.00	28.00	0.00	0.00	0.00

SYDROP(SIDE)

NUCLEAR PACKAGING PROPRIETARY

17.47.17

85/06/26

PAGE

NUPAC 10/140M HARM FOAM (109 DEG)

PACKAGE HEIGHT \* 65000. (LBS)  
 PACKAGE EXTERNAL LENGTH \* 60.00 (IN)  
 PACKAGE EXTERNAL DIAMETER \* 108.00 (IN)  
 PAYLOAD DIAMETER \* 75.00 (IN)  
 DROP HEIGHT \* 30.00 (FT)

## STRAIN VS STRESS TABLE

SYDROP(SIDE)

NUCLEAR PACKAGING PROPRIETARY

17.47.17

85/06/26

PAGE 2

NUPAC 10/140M HARM FOAM (109 DEG)

CRUSH DEPTH (IN)	** CRUSH PLANE **		**** IMPACT ****		***** ENERGY *****			DISTRIBUTION OF STRAIN RATIOS BY PERCENT OF CONTACT AREA				
	AREA (IN2)	VOLUME (IN3)	FORCE (LBS)	ACCEL. (G)	POTENTIAL (IN-LB)	STRAIN (IN-LB)	RATIO (SE/PE)	LE.70	GT.70	GT.80	GT.90	GT.95
.25	622.8	104.	106858.	1.6	23416250.	13357.	.001	100.00	0.00	0.00	0.00	0.00
.50	879.8	294.	301575.	4.6	23432500.	64411.	.003	100.00	0.00	0.00	0.00	0.00
.75	1076.2	539.	521999.	8.0	23448750.	167358.	.007	100.00	0.00	0.00	0.00	0.00
1.00	1241.3	829.	719806.	11.1	23465000.	322583.	.014	100.00	0.00	0.00	0.00	0.00
1.25	1386.2	1158.	881782.	13.6	23481250.	522782.	.022	100.00	0.00	0.00	0.00	0.00
1.50	1516.7	1521.	1023191.	15.7	23497500.	740903.	.032	100.00	0.00	0.00	0.00	0.00
1.75	1636.3	1915.	1152768.	17.7	23513750.	1032898.	.044	100.00	0.00	0.00	0.00	0.00
2.00	1747.2	2338.	1269326.	19.5	23530000.	1335660.	.057	100.00	0.00	0.00	0.00	0.00
2.25	1851.0	2788.	1375572.	21.2	23546250.	1666272.	.071	100.00	0.00	0.00	0.00	0.00
2.50	1948.8	3263.	1475793.	22.7	23562500.	2022693.	.086	100.00	0.00	0.00	0.00	0.00
2.75	2041.5	3762.	1571417.	24.2	23578750.	2403594.	.102	100.00	0.00	0.00	0.00	0.00
3.00	2129.8	4284.	1663517.	25.6	23595000.	2807961.	.119	100.00	0.00	0.00	0.00	0.00
3.25	2214.1	4827.	1752885.	27.0	23611250.	3235011.	.137	100.00	0.00	0.00	0.00	0.00
3.50	2295.0	5391.	1840002.	28.3	23627500.	3684122.	.156	100.00	0.00	0.00	0.00	0.00
3.75	2372.7	5974.	1925130.	29.6	23643750.	4154788.	.176	100.00	0.00	0.00	0.00	0.00
4.00	2447.3	6577.	2009393.	30.9	23660000.	4646629.	.196	100.00	0.00	0.00	0.00	0.00
4.25	2519.8	7198.	2092634.	32.2	23676250.	5159382.	.218	100.00	0.00	0.00	0.00	0.00
4.50	2589.7	7836.	2175469.	33.5	23692500.	5692895.	.240	100.00	0.00	0.00	0.00	0.00
4.75	2657.5	8492.	2258295.	34.7	23708750.	6247116.	.263	100.00	0.00	0.00	0.00	0.00
5.00	2723.2	9165.	2341435.	36.0	23725000.	6822082.	.288	100.00	0.00	0.00	0.00	0.00
5.25	2787.1	9854.	2424593.	37.3	23741250.	7417835.	.312	100.00	0.00	0.00	0.00	0.00
5.50	2849.2	10558.	2508517.	38.6	23757500.	8034474.	.338	100.00	0.00	0.00	0.00	0.00
5.75	2909.7	11278.	2593850.	39.9	23773750.	8672270.	.365	100.00	0.00	0.00	0.00	0.00
6.00	2968.6	12013.	2681212.	41.2	23790000.	9331653.	.392	100.00	0.00	0.00	0.00	0.00
6.25	3026.1	12762.	2771273.	42.6	23806250.	10013214.	.421	100.00	0.00	0.00	0.00	0.00
6.50	3082.3	13526.	2864661.	44.1	23822500.	10717705.	.450	100.00	0.00	0.00	0.00	0.00
6.75	3137.1	14303.	2961196.	45.6	23838750.	11465938.	.480	100.00	0.00	0.00	0.00	0.00
7.00	3190.7	15095.	3060540.	47.1	23855000.	12198655.	.511	100.00	0.00	0.00	0.00	0.00
7.25	3243.2	15899.	3164714.	48.7	23871250.	12976812.	.544	100.00	0.00	0.00	0.00	0.00
7.50	3294.5	16716.	3275249.	50.4	23887500.	13781807.	.577	100.00	0.00	0.00	0.00	0.00
7.75	3344.8	17546.	3393686.	52.2	23903750.	14615424.	.611	100.00	0.00	0.00	0.00	0.00
8.00	3394.1	18388.	3521597.	54.2	23920000.	15479834.	.647	100.00	0.00	0.00	0.00	0.00
8.25	3442.4	19243.	3660639.	56.3	23936250.	16377614.	.684	100.00	0.00	0.00	0.00	0.00
8.50	3489.8	20109.	3808622.	58.6	23952500.	17311271.	.723	100.00	0.00	0.00	0.00	0.00
8.75	3536.3	20988.	3968591.	61.1	23968750.	18283423.	.763	100.00	0.00	0.00	0.00	0.00
9.00	3582.0	21878.	4144598.	63.8	23985000.	19297571.	.805	100.00	0.00	0.00	0.00	0.00
9.25	3626.8	22779.	4340292.	66.8	24001250.	20358183.	.848	100.00	0.00	0.00	0.00	0.00
9.50	3670.8	23691.	4559465.	70.1	24017500.	21470652.	.894	100.00	0.00	0.00	0.00	0.00
9.75	3714.1	24614.	4806042.	73.9	24033750.	22641341.	.942	100.00	0.00	0.00	0.00	0.00
10.00	3756.6	25548.	5081933.	78.2	24050000.	23877337.	.993	100.00	0.00	0.00	0.00	0.00
10.03	3762.2	25674.	5122624.	78.8	24052172.	24052274.	1.000	100.00	0.00	0.00	0.00	0.00
10.25	3798.4	26492.	5386306.	82.9	24066250.	25158867.	1.047	100.00	0.00	0.00	0.00	0.00
10.50	3839.5	27447.	5734166.	88.2	24082500.	26575926.	1.104	100.00	0.00	0.00	0.00	0.00
10.75	3880.0	28412.	6138540.	94.4	24098750.	28060014.	1.164	100.00	0.00	0.00	0.00	0.00
11.00	3919.8	29387.	6618615.	101.8	24115000.	29654659.	1.230	100.00	0.00	0.00	0.00	0.00

TABLE 2.7.1-14

SYDROP(SIDE)

NUCLEAR PACKAGING PROPRIETARY

17.47.17

85/06/26

PAGE 3

NUPAC 10/140M HARM FOAM (109 DEG)

PACKAGE HEIGHT = 65000. (LBS)  
 PACKAGE EXTERNAL LENGTH = 20.00 (IN)  
 PACKAGE EXTERNAL DIAMETER = 101.00 (IN)  
 PAYLOAD DIAMETER = 75.00 (IN)  
 DROP HEIGHT = 30.00 (FT)

## STRAIN VS STRESS TABLE

SYDROP(SIDE)

NUCLEAR PACKAGING PROPRIETARY

17.47.17

85/06/26

PAGE 4

NUPAC 10/140M HARM FOAM (109 DEG)

CRUSH DEPTH (IN)	** CRUSH PLANE **		**** IMPACT ****		***** ENERGY *****		RATIO (SE/PE)	DISTRIBUTION OF STRAIN RATIOS BY PERCENT OF CONTACT AREA				
	AREA (IN <sup>2</sup> )	VOLUME (IN <sup>3</sup> )	FORCE (LBS)	ACCEL. (G)	POTENTIAL (IN-LB)	STRAIN (IN-LB)		LE.70	GT.70	GT.80	GT.90	GT.95
.25	200.7	33.	43717.	.7	25416250.	5465.	.000	100.00	0.00	0.00	0.00	0.00
.50	283.5	95.	120575.	1.9	25432500.	26001.	.001	100.00	0.00	0.00	0.00	0.00
.75	346.8	174.	196237.	3.0	25448750.	65602.	.003	100.00	0.00	0.00	0.00	0.00
1.00	400.0	267.	256009.	3.9	25465000.	122133.	.005	100.00	0.00	0.00	0.00	0.00
1.25	446.7	373.	306600.	4.7	25481250.	192459.	.008	100.00	0.00	0.00	0.00	0.00
1.50	488.7	490.	351600.	5.4	25497500.	274734.	.012	100.00	0.00	0.00	0.00	0.00
1.75	527.2	617.	391205.	6.0	25513750.	367585.	.016	100.00	0.00	0.00	0.00	0.00
2.00	562.8	753.	427799.	6.6	25530000.	469960.	.020	100.00	0.00	0.00	0.00	0.00
2.25	596.2	898.	462368.	7.1	25546250.	581251.	.025	100.00	0.00	0.00	0.00	0.00
2.50	627.7	1051.	495494.	7.6	25562500.	700964.	.030	100.00	0.00	0.00	0.00	0.00
2.75	657.5	1212.	527548.	8.1	25578750.	828844.	.035	100.00	0.00	0.00	0.00	0.00
3.00	685.9	1380.	558784.	8.6	25595000.	964635.	.041	100.00	0.00	0.00	0.00	0.00
3.25	713.0	1555.	589506.	9.1	25611250.	1108172.	.047	100.00	0.00	0.00	0.00	0.00
3.50	738.9	1736.	619973.	9.5	25627500.	1259356.	.053	100.00	0.00	0.00	0.00	0.00
3.75	763.9	1924.	650626.	10.0	25643750.	1418156.	.060	100.00	0.00	0.00	0.00	0.00
4.00	787.9	2118.	681010.	10.5	25660000.	1584586.	.067	100.00	0.00	0.00	0.00	0.00
4.25	811.1	2318.	711742.	10.9	25676250.	1758680.	.074	100.00	0.00	0.00	0.00	0.00
4.50	833.5	2524.	743029.	11.4	25692500.	1940526.	.082	100.00	0.00	0.00	0.00	0.00
4.75	855.3	2735.	775265.	11.9	25708750.	2110113.	.090	100.00	0.00	0.00	0.00	0.00
5.00	876.4	2951.	808822.	12.4	25725000.	2282324.	.098	100.00	0.00	0.00	0.00	0.00
5.25	896.8	3173.	844017.	13.0	25741250.	2534929.	.107	100.00	0.00	0.00	0.00	0.00
5.50	916.7	3400.	880501.	13.5	25757500.	2750493.	.116	100.00	0.00	0.00	0.00	0.00
5.75	936.1	3631.	919225.	14.1	25773750.	2975459.	.125	100.00	0.00	0.00	0.00	0.00
6.00	955.0	3868.	961110.	14.8	25790000.	3210501.	.135	100.00	0.00	0.00	0.00	0.00
6.25	973.4	4109.	1007072.	15.5	25806250.	3456524.	.145	100.00	0.00	0.00	0.00	0.00
6.50	991.4	4354.	1058120.	16.3	25822500.	3714673.	.156	100.00	0.00	0.00	0.00	0.00
6.75	1008.9	4604.	1113644.	17.1	25838750.	3986143.	.167	100.00	0.00	0.00	0.00	0.00
7.00	1026.1	4859.	1175401.	18.1	25855000.	4272274.	.179	100.00	0.00	0.00	0.00	0.00
7.25	1042.8	5117.	1245707.	19.2	25871250.	4574912.	.192	100.00	0.00	0.00	0.00	0.00
7.50	1059.2	5380.	1326804.	20.4	25887500.	4896476.	.205	100.00	0.00	0.00	0.00	0.00
7.75	1075.3	5647.	1421046.	21.9	25903750.	5239958.	.219	100.00	0.00	0.00	0.00	0.00
8.00	1091.1	5918.	1528604.	23.5	25920000.	5608464.	.234	100.00	0.00	0.00	0.00	0.00
8.25	1106.5	6193.	1653928.	25.4	25936250.	6006481.	.251	100.00	0.00	0.00	0.00	0.00
8.50	1121.6	6471.	1805546.	27.8	25952500.	6438915.	.269	100.00	0.00	0.00	0.00	0.00
8.75	1136.4	6753.	1993600.	30.7	25968750.	6913808.	.288	100.00	0.00	0.00	0.00	0.00
9.00	1151.0	7039.	2222738.	34.2	25985000.	7440850.	.310	100.00	0.00	0.00	0.00	0.00
9.25	1165.3	7329.	2487811.	38.3	24001250.	8029669.	.335	88.00	12.00	0.00	0.00	0.00
9.50	1179.1	7622.	2769964.	42.6	24017500.	8686891.	.362	80.67	19.33	0.00	0.00	0.00
9.75	1193.1	7918.	3070463.	47.2	24033750.	9416944.	.392	76.00	24.00	0.00	0.00	0.00
10.00	1206.8	8218.	3388132.	52.1	24650000.	10224269.	.425	72.00	28.00	0.00	0.00	0.00

A conservative estimate of the maximum acceleration experienced by the cask when impacted on the curved sides of the overpack maybe obtained by combining the 60 inch and 20 inch SYDROP runs as follows. Assume that the response of the 60 inch overpack is correct for the first 3.5 inches of deflection, after which the results of the two analyses should be added together to get the combined force and strain energy in the foam. The combined force maybe divided by the package weight to determine the effective acceleration. Clearly, the highest loads will result from the -20°F case, and the table below shows how the data from the two SYDROP runs can be combined from the 60 inch overpack analysis:

Crush Depth	Impact Force	Strain Energy
6.00	5872159	20687567
6.25	6056045	22178682

From the 20 inch overpack length analysis:

Crush Depth	Impact Force	Strain Energy
2.50 (=6.0-3.5)	1124193	1543393
2.75 (=6.25-3.5)	1192560	1832987

Combining the two analyses and comparing with the potential energy of the total drop distance:

Crush Depth	Impact Force	Acceleration	Potential Energy	Strain Energy	Ratio (SE/PE)
6.00	6996352	107.6	23790000.	22231050	.934
6.25	7248605	111.5	23806250.	24011669	1.009

The impact force and crush depth maybe found by interpolation from the combined data:

Crush Depth	Impact Force	Acceleration	Ratio (SE/PE) (By Interpolation)
6.22	7218335	111.1	1.000

Thus, for side impact on the curved portion of the overpack, the maximum acceleration that could be expected would be 111.1 g's, which would occur at -20°F.

The acceleration at the upper temperature extremes maybe determined in the same manner from the analyses using foam properties at 109°F.

From the 60 inch overpack length analysis:

Crush Depth	Impact Force	Strain Energy
9.25	4340292	20358183
9.50	4559465	21470652

From the 20 inch overpack length analysis:

Crush Depth	Impact Force	Strain Energy
5.75(=9.25-3.5)	919225.	2975459
6.00(=9.50-3.5)	961110.	3210501

Combining:

Crush Depth	Impact Force	Acceleration	Potential Energy	Strain Energy	Ratio (SE/PE)
9.25	5259517.	80.9	24001250.	23333642	.972
9.50	5520575.	84.9	24017500.	24681153	1.028

The impact force and crush depth maybe found by interpolation from the combined data:

Crush Depth	Impact Force	Acceleration	Ratio
9.38	5390046.	82.9	1.00

The foam properties used in this 109°F analysis were degraded 15% to account for fabrication variables and thus the crush depth of 9.38 inches is the maximum that might be expected assuming a fully effective overpack. For conservatism, however, the crush depth expected assuming that only the 108 inch diameter portion of the overpack is effective in resisting the impact may be used to determine whether any of the cask protuberances could be hit during impact. The largest protuberance which could be affected is the tie-down lug, which extends 6 inches out from the side of the cask (not including the thermal shield). Since the overpack is 16.75 inches thick on the side, any crush in excess of 10.75 inches would cause the tie-down lug to 'bottom out'. Since SYDROP predicts that under the most unfavorable circumstances the deflection is limited to 10.03 inches, clearly the tie down lug would not be expected to bottom out.

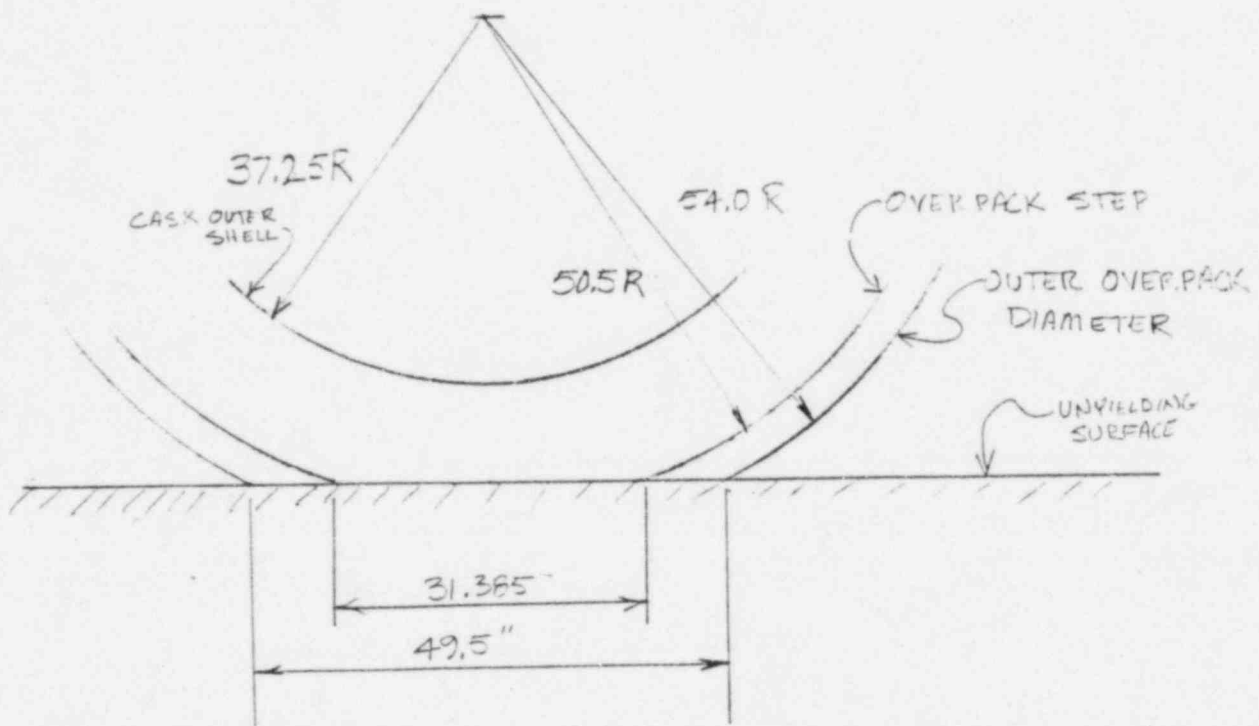
The energy margin of safety on this may be taken directly from the SYDROP output for the energy ratio between the Potential and Strain energies at a deflection of 10.75 inches. SYDROP indicates that the strain energy-potential energy ratio at the deflection which would just cause the lug to touch the impacted surface is 1.164 or a margin of safety on energy of

$$M.S. = 1.164 - 1 = +0.16$$

To summarize, the highest acceleration experienced by the 10/140MB during a flat side impact onto the curved portion of the overpack would not exceed 111.1 g's, while the greatest impact deflection expected would not exceed 10.03 inches and would be closer to 9.38 inches.



As previously stated, impacts on the overpack flat sides cannot be accurately modeled using the program SYDROP. However, the overpack deformations and impact forces may be estimated from hand analyses. A schematic representation of the impact scenario is shown in the Figure below:





An upper bound on overpack deformation maybe calculated by noting that the actual deformation of the overpack will be less than that from a rectangular pad of foam uniformly stressed of dimensions 49.5 inches wide by 60 inches long by 20 inches thick. Such a pad corresponds to the footprint area of the flattened side of the overpack, not considering the outer 10 inches on each end of the overpack as being effective. The thickness corresponds to the maximum thickness of foam actually present behind the footprint area. Thus, the resisting effect of the foam mobilized outside of the initial footprint area is conservatively ignored, and the strains for most of the impact are taken to be less than they would actually be since the curvature of the steel outer shell causes the center of the impact zone to be only about half as thick as the pad is assumed to be. This assumption causes the resistance of impact to be further reduced from what would actually occur.

The table below was developed using hand calculations and the stress-strain relationship for 109°F polyurethane foam. Stresses were assumed to vary linearly between integration points at 0%, 5%, 10%, 30%, 40%, 45%, and 50%.

The columns of the table are related by the following relationships:

Strain = Deflection/20 inches

Stress =  $f(\text{strain})$  where  $f(x)$  is defined by the design stress-strain relationship at this temperature

Force = Stress x 49.5 x 60

The total strain energy is obtained by multiplying the average of the force at the given deflection and the force at the previous deflection by the difference in deflections, and adding this to the total strain energy at the previous deflection.

Deflection (in.)	Strain	Stress (psi)	Force (lbs)	Total Strain Energy (lb-in)
0	0%	0	0	0
1	5%	725	2153250.	1076625.
2	10%	834	2476980.	3391740.
6	30%	974	2892780.	14131260.
8	40%	1122	3332340.	20356380.
9	45%	1270	3771900.	23908500.
10	50%	1438	4270860.	27929880.

The energy the overpack would be required to dissipate from a 30 foot drop onto an unyielding surface assuming 9 inch deflection would be:

$$[(30 \text{ ft})(12 \text{ in/ft}) + 9 \text{ in deflection}] 65,000 = 23.985 \times 10^6 \text{ in-lb.}$$

The energy to dissipate assuming 10 inches of deflection would be  $24.05 \times 10^6$  in-lb. Thus the ratio of strain energy to required energy dissipation at 9 inches of deflection is

$$23908500/2398500 = .997$$

The ratio at 10 inches is

$$27929880./24050000. = 1.161$$

By interpolation, the deflection predicted by this extremely conservative analysis is

$$((1-.997)/(1.161-.997))(10-9) + 9 = 9.02 \text{ inches}$$

Since the flat side of the overpack provides over 10 inches of protection to the side of the cask, clearly the cask will not bottom out.

Forces may be estimated using a similar approach, but assuming a different 'pad' geometry. Since an upper bound on the impact forces is sought, the entire overpack footprint is assumed effective. In addition, the pad is assumed to be only 10.75 inches thick, corresponding to the minimum effective thickness of the overpack. Finally, to account for the additional foam mobilized as the impact deflections proceed, the pad is assumed to be 60 inches wide for 30 inches of length on each end (compared with 49.5 inches actual footprint width at zero deflection) and 40 inches wide for the remaining 10 inches of length on each end (compared with 31.4 inches actual footprint width at zero deflection).

The pad cross-sectional area is then:

$$2((30)(60) + (10)(40)) = 4400 \text{ in}^2.$$

The impact forces will be at a maximum during impacts at  $-20^{\circ}\text{F}$ . The following table may be constructed using the same techniques used above to calculate deflections:

Deflections (in.)	Strain	Stress (psi)	Force (lbs.)	Total Strain Energy (lb.-in.)
0	0%	0	0	0
.538	5%	1416.	6230400.	1675978.
1.075	10%	1968.	8659200.	5677558.
2.150	20%	2015.	8866000.	15097353.
3.225	30%	2108.	9275200.	24848248.

The drop energy to be dissipated by the overpack strain energy at 2.15 inches of deformation is

$$(362.15)(65,000) = 2359750. \text{ lb.-in.}$$

and at 3.225 inches:

$$(363.225)(65000) = 23609625$$

The ratio of strain energy to energy to dissipate at 2.15 inches of deformation is then .641 and at 3.225 inches the ratio is 1.052. The impact force maybe interpolated as follows:

$$\begin{aligned} & ((1-.641)/(1.052-.641))(9275200-8866000)+8866000 = 9223428 \text{ lbs.}, \\ & 9223428/65000 = 141.9 \text{ g's} \end{aligned}$$

Due to the conservative assumptions used in the calculation of this force, the maximum impact acceleration the 10/140MB might experience when striking on the flattened sides of the package from a drop of 30 feet is less than 141.9 g's. The design based on a side acceleration of 141.9 g's will result in calculated stresses higher than those that would be experienced by the package in an actual event.

#### 2.7.1.3.2 Outer Shell Bending Stresses

Because the 10/140MB overpacks extend only 22 inches up the side of the steel and lead radiation shield, the center section of the cask is unsupported during the side impact. A bending moment will develop between the overpacks.

Conservatively assume the cask is simply supported at the ends of the lead and steel cylindrical shell. The shell is 79 inches long. The payload is assumed to be distributed along the middle 73 inches of length, so that the weight per inch is

$$15000/73 = 205 \text{ lb/in.}$$

The shield linear weight can be calculated as follows

$$\begin{aligned} & 0.25\pi[(67.5^2 - 66^2) + (74.5^2 - 72^2)] 490/1728 + .25\pi(72^2 - 67.5^2) 700/1728 \\ & = 126 + 200 = 326 \text{ lb/in} \end{aligned}$$

The total distributed load may be taken as  $205 + 326 = 531$  lb/in which conservatively assumes the payload distributed load extends the entire 79 inches length of the shell. The maximum moment on a simply supported beam with a distributed load is given by:

$$M = WL^2/8 = (141.9)(531)(79)^2/8 = 58.8 \times 10^6 \text{ in-lb}$$

The moment of inertia of the outer A516 Gr. 70 steel shell is given by the formula

$$\begin{aligned} I &= .25\pi (R_o^4 - R_i^4) \\ &= .25(\pi)(37.25^4 - 36.0^4) = 1.93 \times 10^5 \end{aligned}$$

Bending stress is then

$$\begin{aligned} \sigma &= Mc/I \\ &= (58.8)(10^6)(37.25)/(1.93)(10^5) = 11350 \text{ psi} \end{aligned}$$

This is a pure tension and pure compression stress on the extreme fibers of the shell. Simultaneous with this stress, a stress due to the shell's tendency to flatten into an oval shape occurs as a bending stress in the hoop direction of the shell. These stresses may be estimated using Case 19 in Table 17 of Roark, p. 237, which gives the formula for the bending moment at the top of a circular ring loaded by its own weight and supported by tangential shear:

$$\begin{aligned} M &= WgR^2 (1-k_4)/2 \\ g &= \text{acceleration} = 141.9 \end{aligned}$$

Where

$$\begin{aligned} W &= \text{weight per inch of circumference per inch of length} = 531/2\pi R \\ &= 23.07 \text{ lb/in} \end{aligned}$$

$$R = \text{Mean Radius of the shell} = 36.63$$

$$k_4 = k_2/k_1 = .999789$$

$$k_1 = 1+\alpha+\beta = 1.012189$$

$$k_2 = 1-\alpha+\beta = 1.012082$$

$$\alpha = I/AR = .00106$$

$$\beta = FEI/GAR^2 = .01219$$

$$F = 1.2 \text{ (form factor for a rectangular section)}$$

$$I = bh^3/12(1-\mu^2) \text{ (b=1, h=1.25, } \mu=.3)$$

$$= .1789 \text{ in}^4$$

$$A = bh$$

$$= 1.25 \text{ in}^2$$

$$E = 29 \times 10^6 \text{ psi}$$

$$G = E/2(1+\mu) = 11.2 \times 10^6$$

Thus

$$M = (2.307)(141.9)(36.63)^2(1-.999789)/2 = 46.33 \text{ lb. in.}$$

$$I = .1789$$

$$C = .625$$

$$\sigma = Mc/I = (46.33)(.625)/.1789 = 162 \text{ psi}$$

The worst biaxial state of stress may be assumed to occur when the hoop bending stress (ovalty) acts in tension and the longitudinal bending stress acts in compression (as at the inner wall of highest point of the shell during impact). The stress intensity under such conditions can be approximated by the sum of the hoop and longitudinal bending stresses calculated above (under the assumed conditions, there is virtually no shear stress):

$$S.I. = 162 + 11350 = 11512 \text{ psi}$$

The margin of safety is then

$$.7(70,000)/11512 - 1 = + \text{ Large}$$

The bending buckling allowable stress for the outer shell is 32,258 so the margin of safety against buckling is:

$$M.S. = 32,258/11,512 - 1 = +1.80$$

2.7.1.3.3 Side Impact Inner Shell Stresses

During a side impact, the inner shell of the 10/140 MB would be expected to act in conjunction with the outer shell to carry bending load. However it is conservative to assume that the inner shell must support its own weight, the payload weight, and the weight of the lead above it. This load can be calculated as below:

$$.25\pi(67.5^2 - 66^2)(490)/1728 + (.5)(.25)\pi(72^2 - 67.5^2)(700)/1728 \\ = 145 \text{ lb/in}$$

As before, the payload weighs 205 lb./in. so the total load on the inner shell would be 350 lb/in. The maximum moment is:

$$M = WL^2/8 = (141.9)(350)(79)^2/8 = 38.74 \times 10^6 \text{ in-lb.}$$

The moment of inertia of the inner shell is

$$I = .25\pi(33.75^4 - 33^4) = 87,600 \text{ in.}^4$$

The stress in the inner shell, then is

$$\sigma = Mc/I = 38.74(10^6)(33.75)/87600 = 14925 \text{ psi}$$

As in the outer shell, this stress should be combined with the moment in the hoop direction. The following quantities may be calculated using the same method as presented for the outer shell:

$$I = .0386$$

$$A = .75$$

$$\mu = .000046$$

$$\beta = .00482$$

$$k_1 = 1.004861$$

$$k_2 = 1.004769$$

$$k_4 = .999907$$

$$E = 28,000,000$$

$$G = 10,800,000$$

$$W = 350$$

$$R = 33,375$$

$$\begin{aligned} M &= 350(141.9)(1-.999907)(33,375)^2/2 \\ &= 12.14 \text{ lb} - \text{in} \end{aligned}$$

$$\sigma = 12.14(.375)/.0386 = 118 \text{ psi}$$

Adding hoop and longitudinal bending stresses to get the stress intensity:

$$S.I. = 14925 + 118 = 15,043 \text{ psi}$$

The allowable stress is 48,000 psi so the margin of safety in bending is:

$$M.S. = 48,000/15043 - 1 = +2.19$$

For buckling in bending, the allowable is 27,754 psi so the buckling margin of safety is:

$$M.S. = 27,754 \text{ psi} / 15,043 - 1 = +0.84$$

### 2.7.2 Puncture

A 40 inch drop onto a 6 inch diameter pin can occur in three separate regions, e.g., cylindrical body or cask side wall between the overpacks, top and bottom lids inside the overpack center opening, and the overpack itself.



2.7.2.1 Side Wall Puncture Resistance

Using ORNL-NSIC-68 for the side wall evaluation, the required outer shell thickness for puncture integrity can be calculated as:

$$t = (W/S_u)^{.71}$$

Where:  $t$  = Outer Shell Thickness = 1.25 in.

$W$  = Cask Gross Weight = 65,000 lb.

$S_u$  = Outer Shell Ultimate Strength = 70,000 psi (Sect. 2.3)

Realizing that the kinetic energy of the 40 inch drop is:

$$E = h W = 40 W$$

this equation may be rearranged as:

$$E/S_u = 40 t^{1/.71} = 40 t^{1.41}$$

Assuming that the total kinetic energy of the 40 inch drop is absorbed in stressing the outer shell material just to the point of failure, the minimum energy ratio required to preclude puncture is:

$$E/S_u = 40 \text{ in-lb/psi}$$

From the drawings in the Appendix (Section 1.3), it can be seen that the external shell for the NuPac-B 10/140M cask is fabricated from 1.25 in. thick ASTM A516 Gr. 70 alloy steel. Therefore, the drop energy ratio is:

$$E/S_u = (40)(1.25)^{1.41} = 54.77$$

The resulting energy Margin of Safety can be calculated as:

$$M.S. = 54.77/40 - 1 = + 0.37$$

Sakamoto's equation for the side puncture event is:

$$E/S_u = [.003 + .047(t/D) + .002(d/D) + .006(r/d)] \\ t(1.585-.11r)_d(1.465+.077r)$$

Where: d = Puncture Pin Diameter

D = Cask Outside Diameter

both expressed in metric units.

Resolving the equation into English units and utilizing a 6-inch diameter puncture pin yields:

$$E/S_u = [64.30 + 237.4/D + 929.88(t/D)]t^{.8865} \\ = [64.30 + 237.4/74.50 + 929.88(1.25/74.50)](1.25)^{.8865} \\ = 101.26$$

Energy Margin of Safety is:

$$M.S. = 101.26/40 - 1 = + 1.53$$

Similarly, Shieh's equation:

$$\frac{W}{S_u} = \frac{.37[1 + 6/D + (41/D)^2]e^{t/3}t^{1.68}}{1 + .1t^{.87}}$$

can be expressed as:

$$\frac{E}{S_u} = \frac{14.8[1 + 6/D + (41/D)^2]e^{t/3}t^{1.68}}{1 + .1t^{.87}}$$

$$\frac{E}{S_u} = \frac{14.8[1 + 6/74.50 + (41/74.50)^2]e^{1.25/3}(1.25)^{1.68}}{1 + (.1)(1.25)^{.87}}$$

$$= 40.29$$

for a Margin of Safety of:

$$M.S. = 40.29/40 - 1 = + 0.01$$

It is thus evident that the cask side wall is adequate to resist the regulatory puncture impact requirement.

#### 2.7.2.2 Cask Lid Puncture Resistance

Due to the extremely rigorous leak-tightness requirements for this Type B package, it was determined that a finite element analysis would be required to evaluate the structural response due to post impact on the cask lids within the overpack center opening. The secondary lid opening in the top primary lid makes this member the more structurally flexible of the two lids and therefore the more prone to high stresses and permanent deformation leading to loss of seal integrity. It was therefore this structure which was subjected to the the most intensive analysis. The bottom lid (utilized in optional bottom-loading casks) was evaluated rather than the fixed bottom, since it will be more flexible, and therefore more highly stressed, than the rigidly-attached bottom plate of the baseline fixed bottom cask model.

In addition to complying with accident condition stress allowables set out in Regulatory Guide 7.6 and outlined in Section 2.7.1 above, lid deflections were to be limited so that a residual compression would be maintained on at least one of the two sets of EnviroSeal<sup>tm</sup> O-rings at the end of the puncture event. To maintain lid stress levels within regulatory limits while ensuring continued sealing integrity, special lid configurations with integral latching assemblies were developed. These unique designs are shown in the general arrangement drawings in Section 1.3, Appendix.

For the analysis, the ANSYS finite element routine was utilized. The capabilities of the program are outlined in Appendix 2.10.2 and details of the analysis are given in Appendix 2.10.8. All possible worst case conditions for both stress and deflection were evaluated. These included a center-loaded axisymmetric model of the bottom lid to evaluate center impact, and a three-dimensional model of the top lid with post impact at the center, at the secondary seal location (outside diameter of the secondary lid) and at the inside diameter of the overpack center opening.

Material properties for a 200°F temperature condition were used in the analysis. This is conservative, since, from Section 3.0, the maximum anticipated lid temperature for the accident condition drop events is 106°F. Also, the lowest applicable 304 stainless steel material properties from Table 2.3-1 were used to evaluate stress level Margins of Safety.

A summary of analysis results is outlined in Table 2.7.2-1 below. These results indicate that the cask lids are suitably designed to withstand any regulatory puncture event.

#### 2.7.2.3 Overpack Puncture Resistance

Since it has been demonstrated that the unprotected cask will survive a 40 inch drop onto the puncture pin per 10 CFR 71, damage from such a drop impacting the overpacks will be less severe than from the cases already examined.

The above results demonstrate that the NuPac 10/140MB cask will survive a 40 inch drop onto the puncture pin per 10 CFR 71 with no adverse affect on cask sealing and shielding integrity.

TABLE 2.7.2-1

## Summary of Lid Analysis Results

Load Case	Max. Bending Stress (psi) (Margin of Safety)	Max. Membrane Stress (psi) (Margin of Safety)	Min. O-ring Compression- Primary Seal	Min. O-ring Compression- Secondary Seal	Max. Enviro-Lock <sup>tm</sup> Load (lb.) (Margin of Safety)	Max. Bolt Stress (psi) (Margin of Safety)
Center Punch-Bottom Lid	61,703 (M.S. = +0.13)	25,576 (M.S. = +0.88)	18.6%	---	58,606 (M.S. = +1.99)	---
Center Punch-Top Lid	57,231 (M.S. = +0.22)	29,040 (M.S. = +0.65)	19.9%	21.3%	57,270 (M.S. = +2.06)	16,025 (M.S. = +4.46)
Punch at Secondary Lid O.D.	65,810 (M.S. = +0.11)	48,105 (M.S. = +0.49)	18.6%	20.2%	86,070 (M.S. = +1.03)	0
Punch at Overpack I.D.	43,620 (M.S. = +0.60)	42,454 (M.S. = +0.13)	20.1%	17.5%	64,193 (M.S. = +1.73)	8,930 (M.S. = +Large)

### 2.7.3 Thermal

The hypothetical fire transient is analyzed in Section 3.5. From that section, maximum temperatures and pressures are directly available for use.

#### 2.7.3.1 Summary of Pressures and Temperatures

The maximum fire accident condition temperatures for the various cask components are presented in Sections 3.5.3 and 3.5.4. Maximum internal pressure resulting from the fire transient is 24.4 psig.

#### 2.7.3.2 Differential Thermal Expansion

Differential thermal expansions due to the fire accident are of little consequence for the NuPac 10/140MB Cask. All stresses resulting from differential expansions can be classified as secondary, displacement limited stresses. As limits on secondary stresses do not apply for accident conditions (per Section 2.1.2), differential expansions do not compromise the integrity of the cask. Through wall (and through thickness) thermal gradients also result in secondary stresses and again are of little consequence for the cask.

#### 2.7.3.3 Stress Calculations

The concern for accident conditions is with primary, load controlled stresses. The only load controlled stresses during and after the fire transient are those resulting from pressure and dead weight, and are therefore rather modest. Although temperatures associated with the fire transient are typically higher than those associated with other accident conditions, the NuPac 125-B Cask design is considered by inspection to be governed by the significantly more severe drop accident events.

#### 2.7.3.4 Comparison with Allowable Stresses

Based on the discussions presented in Section 2.7.3.1 through 2.7.3.3, it is apparent that large margins of safety exist for the fire transient condition.

#### 2.7.4 Immersion - Fissile Material

This section is not applicable to the NuPac 10/140MB, since only insignificant quantities of fissile material would be transported in it.

#### 2.7.5 Immersion - All Packages

The effect of a 21 psig external pressure due to immersion in 50 feet of water as required by 10 CFR 71.73(c)(5) is analyzed below:

Assuming the pressure is entirely reacted by the outer shell, the component stresses are:

$$\text{Hoop stress} = \sigma_h = pr/t$$

$$\text{Longitudinal stress} = \sigma_L = pr/2t$$

$$\text{Radial Stress} = \sigma_r = p$$

$$\text{where } p = \text{pressure} = 21 \text{ psig}$$

$$r = \text{outer shell radius} = 36.625 \text{ in.}$$

$$t = \text{outer shell thickness} = 1.25 \text{ in.}$$

So,

$$\sigma_h = (21)(36.625)/1.25 = 615 \text{ psi}$$

$$\sigma_L = (21)(36.625)/(2)(1.25) = 308 \text{ psi}$$

$$\sigma_r = 21$$

The maximum stress intensity in the outer shell is then  $615 - 21 = 594$  psi and the margin of safety is very large.



Stresses in the 5.25 inch minimum thickness end plates are similarly trivial and completely bounded by the stresses in the lid from the payload pressure during the 170.8g acceleration from end impact from 30 feet at -20°F.

#### 2.7.6 Summary of Damage

From the analyses presented in Sections 2.7.1 through 2.7.5, it can be shown that the accident test sequence will not result in any significant structural damage to the NuPac 10/140MB Cask. Nearly all permanent damage occurs in the external overpacks as desired. Minor amounts of damage can occur to cask components as follows:

For a 40 inch drop on a 6.0 inch diameter puncture pin, with impact occurring on the side of the cask at midlength, localized cask damage can occur at the impact point, but the outer cask outer shell will not be perforated and the overall bending response of the cask remains elastic. Finally, for a 40 inch drop on a 6.0 inch diameter puncture pin, with impact occurring on the outer cask lid, a very slight permanent bow of the 7.50 inch thick lid may occur.

These permanent deformations are of little consequence for the NuPac 10/140MB Cask as they represent only minor changes in cask geometry. In particular, damage is not sufficient to compromise 'leaktightness' of the containment vessel or cask seals. For these reasons, the integrity of the cask is not considered to be compromised by the accident test sequence set forth in 10 CFR 71.

#### 2.8 Special Form

This section does not apply for the NuPac 10/140MB Cask.

#### 2.9 Fuel Rods

This section does not apply for the NuPac 10/140MB Cask.

APPENDIX 2.10.1  
STABILITY AND BUCKLING DESIGN CRITERIA

### 2.10.1 Stability and Buckling Design Criteria

This appendix defines a stability and buckling criteria for radioactive materials packages consistent with the guidelines of Paragraph C.5, NRC Regulatory Guide 7.6, see reference 2.10.1.5.1. The technical rationale for this criteria is presented and discussed in conjunction with appropriate works in the technical literature. This appendix concludes with an analysis of the inherent factors of safety embodied within this criteria and a comparison of these factors of safety with comparable elements of other established forms of design criteria for stability.

Briefly, the criteria establishes the limit (membrane compression) stress at  $1/5$  or  $1/7.5$  of the elastic buckling (Euler) stress limits for accident and normal conditions of transport, respectively. In the domain where failure is characterized by yielding or plastic flow, rather than instability, the limit stress is further reduced by consideration of physical material limits for yielding and strength. A parabolic curve provides the transition between the physical material property limits and the elastic stability limits.

The boundary between stability and plastic flow or yielding regimes is set at a point where the elastic buckling load exceeds the yield load by a factor of 5. This boundary criterion is taken from the work of Combescure, reference 2.10.1.5.10. Within this stability design criteria, this boundary is implicitly satisfied, for accident conditions, by setting stress limits at  $1/5$  of the elastic buckling stress. The corresponding factor of  $1/7.5$ , applied to normal conditions, is attained by application of the conventional ASME factor of  $2/3$ , representing the ratio of  $(S_m/S_y)$ .

The criteria defined here recognizes that compressively loaded structures behave in different fashions depending upon geometric aspect ratio of the structure. The nature of the criteria is such that the factors of safety vary with this geometric aspect ratio up to asymptotic values of 5 and 7.5, versus elastic buckling stresses, for accident and normal conditions of transport, respectively. These asymptotic factors of safety may be considered

conservative for general use as radioactive materials package design criteria. It should be noted that the general form of the criteria allow adjustment of these asymptotic factors of safety to any values considered appropriate.

#### 2.10.1.1 Criteria Definition

Direct primary compressive membrane stresses,  $S$ , in containment vessels shall be less than the lesser of  $S_e/R_d$  or  $S_j$ .  $S_e$  is defined as the appropriate elastic buckling stress limit considering adjustments resolving theoretical and experimental results, but neglecting plasticity corrections. The reduction coefficient  $R_d$  is to be taken as 7.5 for normal conditions of transport and 5 for accident conditions of transport. This reduction coefficient,  $R_d$ , corresponds to the intended factor of safety of the method at high aspect ratios of the structure.  $S_j$  is a generalized 'Johnson' parabolic transition curve having a value of  $S_s$ , at an aspect ratio,  $G$ , of zero. This parabolic transition curve is also tangent to the expression  $S_e/R_d$  at a stress level of  $2/3 S_s$ . The term  $S_s$  denotes the applicable strength limit of the material --  $S_m$  for normal conditions of transport and  $S_y$  for hypothetical accident conditions, both as defined within reference 2.10.1.5.1. The details of the criteria, in symbolic form are as follows:

Where  $G$  is less than  $G^*$ :

$$S \leq S_j,$$

Where  $G$  is greater than or equal to  $G^*$ :

$$S \leq S_e/R_d.$$

Where:  $S_e$  = The classical elastic buckling stress expression cast in the generalized form:

$$= K/G.$$

- $K$  = A numerical constant unique to each compressive loading mechanism reflecting materials properties ( Young's Modulus, Poisson's ratio) and empirical or theoretical coefficients. See Table 2.10.1.1-1 for a summary versus typical loading mechanisms.
- $G$  = A non-dimensionalized geometric aspect ratio unique to each loading mechanism. See Table 2.10.1.1-1 for a summary versus typical loading mechanisms. For example:
- =  $(L/p)^2$ , for column type loadings [Note:  $p = (I/A)^{1/2}$ ],
- =  $(R/t)$ , for external pressures on long cylinders and axial compression loadings of cylinders.
- $R_d$  = 7.5, for Normal Conditions,  
= 5.0, for Accident Conditions.
- $S_j$  = The parabolic transition from  $S_s$  to  $(S_e/R_d)$ :
- =  $S_s - 4S_s^3 G^2 / [27(K/R_d)^2]$ .
- $G^*$  = The aspect ratio,  $G$ , where the parabola defined by  $S_j$  intercepts and is tangent to the curve defined by  $(S_e/R_d)$ , in other words,  $G^*$  corresponds to the aspect ratio where  $S_j = (S_e/R_d)$ , or:
- =  $(3/2)(K/R_d)/S_s$ .
- $S_s$  =  $S_m$ , for Normal Conditions,  
=  $S_y$ , for Accident Conditions.
- $S_m$  = Design Stress Intensity as used within Section III, ASME Boiler and Pressure Vessels Code.
- $S_y$  = Yield Stress.

TABLE 2.10.1.1-1  
 SUMMARY OF NUMERICAL CONSTANTS AND NON-DIMENSIONAL COEFFICIENTS  
 OF  $S_e = K/G$  VERSUS LOADING CONDITIONS

Loading Mode	$K^{(1)}$	$G^{(3)}$	Reference
<u>Axial Compression</u> <u>and Bending:</u>	Varies:	(R/t)	2.10.1.5.13, pp. 230-5
At (R/t) = 10:	0.5022 E <sup>(2)</sup>		
At (R/t) = 100:	0.3570 E		
<u>Long Column Compression:</u>	4.9348 E	(L/R) <sup>2</sup>	2.10.1.5.13, pp. 231
<u>External Pressure -</u> <u>No External Constraints:</u>			
(1) Moderate Length: ( $L^2 t / R^3 < 11$ )	0.9181 E	( $R^{1/2} L / t^{3/2}$ )	2.10.1.5.13, pp. 236
(2) Long: ( $L^2 t / R^3 > 11$ )	0.2473 E	(R/t) <sup>2</sup>	2.10.1.5.13, pp. 237
<u>External Pressure -</u> <u>External Constraint:</u>			
	.09158 E	$\frac{(R/t)^2}{[6.66(R/t)^{.8}-1]}$	2.10.1.5.17, pp. 342, eq. 47-8

Notes: (1) Poisson's ratio = 0.3 assumed for constant evaluation.  
 (2) E = Modulus of Elasticity.  
 (3) Notation:

R = radius  
 L = length  
 t = thickness

2.10.1.2 Background

NRC Reg Guide 7.6, reference 1, requires that 'buckling of the containment vessel should not occur under normal or accident conditions'. The ASME NUPACK Committee has proposed a series of rules governing buckling and instability, Section NX-3133, reference 2.10.1.5.2. The NUPACK proposed criteria are of two parts. Sections NX-3133.1 to NX-3133.6 employ charts and 'rote' procedures to establish limits for specific geometries and loading conditions -- most not applicable to typical package geometries or loadings. The second part of this NUPACK criteria, Section NX-3133.8 proposes rules more consistent with the 'design by analysis' approach of NRC Reg Guide 7.6. This particular set of provisions is taken directly from ASME Section III, Division 1 Code Case N-47-21 for Class 1 components in elevated temperature service. Within Section NX-3133.8, constant safety factors are proposed for load-controlled and strain-controlled buckling. The proposed NX-3133.3 factors of safety are as follows:

<u>Condition</u>	<u>Load F. S.</u>	<u>Strain F. S.</u>
Normal (Level A):	3.0	1.67
Accident (Level D):	1.5	1.1

Per NX-3133.8, these factors of safety are applied to the 'load (strain) which would cause instant instability at the design (or actual service) temperature'. Application of these proposed rules has proven difficult due to the diversity of opinion concerning the resolution of these issues:

- o 'Instant instability' implies a classic elastic instability failure that is fundamentally inconsistent with the practical geometries of radioactive materials packages. If elastic instability is not of concern for a particular package, are the factors of safety applicable?
- o The applicable instability regime is not defined. Does this imply that all compressive loading states are to be treated as potential instability situations?



- o 'Instant instability' does not characterize the behavior of structures whose failure modes are associated with yielding or plastic flow where no loss of load resistance is experienced. What criteria govern the design of these structures? How do these criteria 'mesh' with stability criteria as the aspect ratios of a structure increase?
- o The single-valued factors of safety appear both potentially low for 'instant instability' associated with true elastic instability and excessively conservative for plastic flow or yielding situations where no loss of load resistance takes place. In fact, the single-valued factors may be appropriate only within some intermediate regime.

Investigations to resolve these issues have lead to the following findings:

1. ASME Code Case N-47-21 is overly conservative for situations were 'instant instability', or buckling does not represent the failure mechanism of the component, references 2.10.1.5.3 and 2.10.1.5.4.
2. For cylindrical shells, as used for containment vessels of radioactive materials packages, there are three characteristic failure mechanisms associated with compressive loadings, references 2.10.1.5.5 and 2.10.1.5.6. Each of these failure mechanisms is controlled by a different priority set of geometric and material properties, references 2.10.1.5.6, 2.10.1.5.7, 2.10.1.5.8, 2.10.1.5.9 and 2.10.1.5.10. The characteristics of the failure, or safety consequence, in each mechanism differ -- ranging from catastrophic collapse, at one extreme, to controlled plastic flow, at the other extreme, reference 2.10.1.5.5. Thus each, can and should possess differing factors of safety. To illustrate, Johnston, reference 2.10.1.5.6, states (page 265): '...formulas to predict the buckling capacity of thick-walled tubular members under axial compression are much more reliable than formulas to predict the capacity of thin-walled shells. [Thus] .... factors-of-safety used in thick-walled member design should be less than those used with thin-walled shells'.



3. The boundaries between each of the three failure mechanisms can be defined with reasonable accuracy. These boundaries typically are defined in terms of the shell aspect ratio and material properties, for example, see reference 2.10.1.5.11, Section 7.5a. A recent French proposal, reference 2.10.1.5.10, suggests definition of these boundaries in terms of the ratio of elastic buckling stress to yield stress. Both approaches give reasonably consistent results. For example, using a cylindrical shell compression case and assuming a steel with a modulus of  $29.5 \times 10^6$  psi and a yield of 30 ksi, reference 2.10.1.5.11 gives the inception of plastic buckling at  $(R/t) = 62$ , whereas the French approach predicts this boundary at  $(R/t) = 70$ .
4. Typical industry design (criteria) codes provide varying factors of safety as a function of aspect ratios, for example, see Paragraph 1.5.1.3 of the AISC Specification, reference 2.10.1.5.12.

The above discussion notes that there are three characteristic failure mechanisms or behavior regimes. They are cataloged below, along with their principal attributes.

o Soft Structures:

- a. Stress Range: Elastic.
- b. Buckling Type: Local buckling, bifurcation buckling, antisymmetric buckling, diamond (shaped) buckling.
- c. Failure Mode: Catastrophic Collapse, oil-canning snap-through.
- d. Predictive Sensitivity: Initial imperfections in geometry and material properties lead to large and random variations observed in buckling tests as compared to theory. Large factors of safety are required, reference 2.10.1.5.6. In this range these factors can range from 3 to 10.

o Intermediate Structures:

- a. Stress Range: Elasto-plastic.
- b. Buckling Type: Equilibrium collapse load buckling, bellows type buckling, full-wall buckling, symmetrical (axisymmetric) buckling.
- c. Failure Mode: Controlled plastic deformation, constant or increasing load resistance (for strain-hardening materials, like stainless steels or aluminum).
- d. Predictive Sensitivity: Primarily dependent upon materials properties in the transition regions between fully-elastic and strain-hardening behavior. Relatively insensitive to geometric imperfections and end conditions. Factors of safety should be somewhat greater than those typically applied to strength designs.

o Hard Structures:

- a. Stress Range: Plastic.
- b. Buckling Type: Generally not considered as a buckling phenomena since no instability (loss of load resistance) occurs for a work-hardened material. Yielding, plastic flow.
- c. Failure Mode: Plastic deformation and flow.
- d. Predictive Sensitivity: Completely dependent upon materials properties and strain-hardening behavior. Totally insensitive to geometric imperfections and end conditions. Factors of safety should not exceed those typically applied to strength design.

Boundaries between these three classes of behavior are described in a variety of formats. The most conventional, separating 'Hard' structures from 'Intermediate' and 'Soft' structures is the conventional distinction between thin shells and thick shells, references 2.10.1.5.7, 2.10.1.5.8, 2.10.1.5.9

and 2.10.1.5.13. This is a relatively imprecise distinction with estimates of  $(R/t)$  values ranging from 20 to greater than 100. With a well behaved stress-strain curve, i.e., a smooth transition and strain hardening, the predictive reliability of this boundary determination increases. Thus, from a stability standpoint, stainless steel and some aluminum alloys, with smooth transitions and strain hardening, are preferable to mild steels, with sharp transitions and minimal strain hardening.

Combesure, reference 2.10.1.5.10, suggests that a ratio of elastic buckling stress to yield stress,  $(S_e/S_y)$ , of 5.0 defines this boundary. Yu, reference 2.10.1.5.11, points out that the AISI Code (Equation 3.8-1), reference 2.10.1.5.14, defines the boundary between 'Hard' (yielding, plastic flow) and 'Intermediate' (plastic buckling) structures at a  $(D/t) = 3300/S_y$ , or approximately 110 for a 30 ksi steel. Yu also notes that for lesser  $(D/t)$  values the design stress need not be reduced below conventional strength allowables. Importantly, the boundary employed by AISI has been developed by extensive tests, references 2.10.1.5.15 and 2.10.1.5.16.

The boundary between 'Intermediate' and 'Soft' structures can be stated in similar terms. For example, Yu gives the AISI boundary estimate as  $(D/t) = 13000/S_y$ , or approximately 430 for a 30 ksi steel.

#### 2.10.1.3 Criteria Rationale

The proposal of Combesure, reference 2.10.1.5.10, have been adopted as the defining boundary between 'Hard' and 'Intermediate' structures. Thus, this boundary is determined at an aspect ratio defined by the stress ratio  $(S_e/S_y) = 5.0$ . This boundary is used to define the intercept of the basic strength limit,  $S_s$ , and the reduced elastic buckling curve,  $(S_e/R_d)$ . Of course, in this region the parabolic transition curve,  $S_j$ , passes below this intercept value. The primary reason for adoption of this method is that it is independent of loading mode whereas all the aspect ratio methods are mode-specific. Importantly, the Combesure method and the more conventional aspect ratio methods, such as references 2.10.1.5.11, 2.10.1.5.15, and 2.10.1.5.16, all give comparable results, as mentioned in Item 3, Section 2.10.1.2.

At lesser aspect ratios, the basic strength allowables are not reduced significantly. At greater aspect ratios, the allowables are governed by a 'degraded' elastic buckling relation,  $(S_e/R_d)$ . Smooth transition from the 'flat-topped' strength limit to the 'degraded' elastic buckling curve is provided by a traditional 'Johnson' parabola.

The principal attributes of the stability design criteria set forth herein are as follows:

1. At high aspect ratios corresponding to 'Soft' structures, the method provides large factors of safety -- 5 for accident conditions, 7.5 for normal conditions. This is significantly greater than as provided within the NUPACK proposed rules and as provided in other stability related design criteria. Importantly, these increased factors of safety provide a 'penalty-function' for use of 'Soft' structures. This has the effect encouraging use of more robust structural forms that behave in a 'Hard' or 'Intermediate' structural fashion. This penalty-function directly supports the philosophy of Reg Guide 7.6 -- 'buckling ... should not occur'.
2. At low aspect ratios, the method implicitly provides a correction to the elastic buckling relation which conservatively envelopes the plasticity correction factor, see reference 2.10.1.5.13. Using the method, there is no need to calculate this plasticity correction factor. This is a desirable feature because the plasticity correction factor must be derived for each specific material given accurate stress-strain data in the transition region from the proportional limit to the strain-hardening tangent. Such data is difficult to obtain for design purposes, is unique to a particular heat of material and cannot be easily verified or checked by review or Regulatory personnel.
3. For normal conditions, no stresses exceed the proportional limit. This guarantees no instabilities and no inelastic behavior that could invalidate structural demonstrations of adequacy. This condition is assured by the limitation of stresses to values below  $S_m$ , which closely approximates the proportional limit stress for all typical package materials.

4. While the bulk of discussion has focused upon axial compressive loadings, it is important to note that the method is fully applicable to column stability and external pressure (these two are mathematically similar). In fact, the method (for normal conditions) precisely duplicates the column design formulas of AISC and the Column Research Council, see page 64, reference 2.10.1.5.6, when  $S_m$  is assumed equal to  $0.6 \cdot S_y$ . In application, this method proves to be considerably more conservative due to the fact that the parabolic transition is tangent to  $(S_e/R_d)$  whereas the AISC and CRC parabolic transitions are tangent to  $S_e$  itself. Clearly, the reduction factor,  $R_d$ , forces a significant and predictable additional measure of conservatism.

#### 2.10.1.4 Safety Analysis

The characteristics of the recommended criteria are analyzed within this section. Three basic loading conditions are examined in a parametric fashion: axial loadings, external pressure loadings and finally, column-type loadings. The analyses are conducted in a parametric fashion, examining results as a function of appropriate aspect ratio. For each examination, two plots are provided. The first is a non-dimensionalized stress plot versus aspect ratio, normalized by yield stress. Shown on this plot is the basic elastic buckling stress with experimental/theoretical corrections,  $(S_e/S_y)$ , the buckling stress as determined by 'modern' analysis methods including plasticity corrections, Chapter 10, reference 2.10.1.5.13,  $(S_{cr}/S_y)$ , and finally the stress limits  $(S_{ai}/S_y)$  proposed within this criteria,  $S_{ai} = S_j$  where  $G < G^*$  and  $S_{ai} = (S_e/R_d)$  elsewhere, where the subscript 'i' = 'n', for normal conditions and 'i' = 'a', for accident conditions. The second companion plot presents the distribution of the resultant factor of safety (of this method), plasticity correction factor from 'modern' theory, and approximate plasticity correction provided by this method.

Within each of the following paragraphs, the particular characteristics of the inputs to the analysis are described. Resultant output is discussed, where appropriate. For calculation purposes, material properties of 304 stainless at 212 °F are utilized.

2.10.1.4.1 Axial Compression Behavior

The relations given by Baker, reference 2.10.1.5.13, page 230, are used for this demonstration and comparison analysis. In the Baker relation an experimental correction coefficient is applied to the basic (Euler) elastic buckling stress value. This coefficient ranges from 0.83 at an aspect ratio,  $G = (R/t) = 10$ , to 0.59 at an aspect ratio of 100. For these two aspect ratios, sample criteria evaluation and analysis is provided below (notation follows Section 2.10.1.1).

PARAMETER	Symbol		
Aspect Ratio:	$G$	10	100
Numerical Coefficient:	$K$	13910000	9888000
Euler Buckling Stress:	$S_e = K/G$	1391000	98880
Plasticity Factor	-	46.57	4.214
Baker Limit Stress:	$S_{cr}$	29869	23465
Reduction Factors: (from elastic buckling)	$R_d$		
Normal		7.5	7.5
Accident		5	5
Strength Limits:	$S_s$		
Normal	$S_m$	20000	20000
Accident	$S_y$	24700	24700
Intercept Aspect Ratio:	$G^*$		
Normal		139.1	98.9
Accident		168.9	120.1
Criteria Stress Limit:	$S_{ai}$		
Normal	$S_{an}$	19966	13184
Accident	$S_{aa}$	24671	18992



PARAMETER	Symbol		
<hr/>			
Factors of Safety:			
Normal	$S_{cr}/S_{an}$	1.50	1.78
Accident	$S_{cr}/S_{aa}$	1.21	1.24

Comprehensive comparison data is graphically provided in Figures 2.10.1.4-1 and 2.10.1.4-2 for a full range of aspect ratios. The conservatism of the proposed criteria for 'Intermediate' and 'Soft' structures is readily apparent. The graphs are largely self-explanatory, however the difference between normal condition limits and AISI design values requires discussion. For all construction industry codes, including AISI, the working stress limit,  $F$ , is set as  $3/5$  of yield,  $S_y$ . The criteria proposed here, sets the normal, or working stress limits at  $S_m$ . Normally this provides a value approximating  $2/3$  of yield,  $S_y$ . For the comparison shown in these Figures, data corresponds to properties at 212 °F. At this temperature, yield is degraded from the room temperature value of 30 ksi to about 24.7 ksi whereas the value  $S_m$  remains constant. Room temperature comparisons would have shown both the proposed criteria and AISI nearly coincident, 0.6 versus 0.67, at low aspect ratios.

The Figures clearly show the conservative impact of limiting high-aspect ratio stresses to  $(S_e/R_d)$  rather than a constant factor offset ( $3/5$ ) from  $S_e$ , as done by AISI. Figure 2.10.1.4-2 graphically shows how the resultant factors of safety asymptotically approach 7.5 and 5, at high aspect ratios, for normal and accident conditions, respectively. Of note, the plotted plasticity correction shown on this Figure is simply the inverse of that used by Baker, reference 2.10.1.5.13.

FIGURE 2.10.1.4-1

## AXIAL COMPRESSION CRITERIA

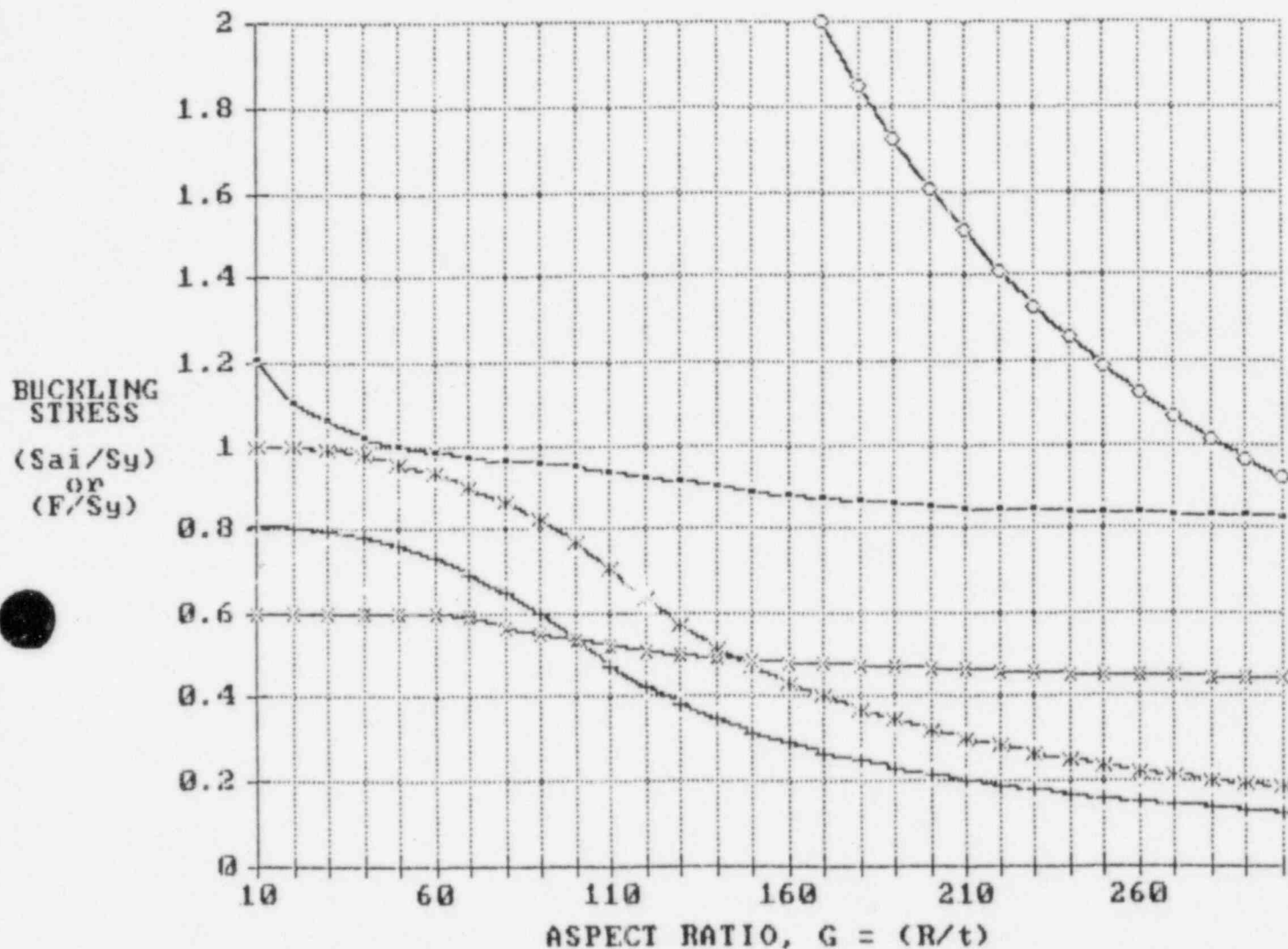
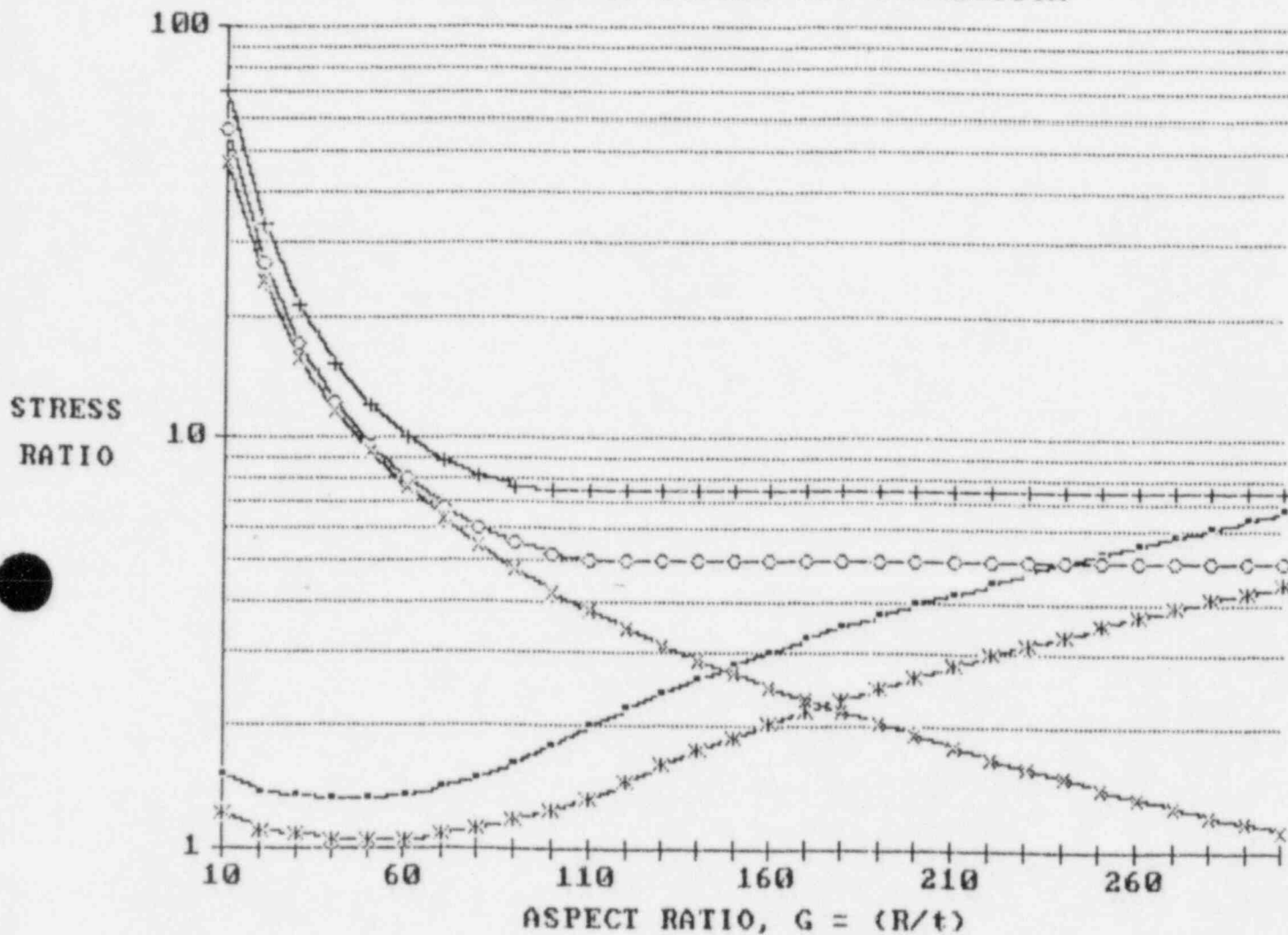




FIGURE 2.10.1.4-2

# AXIAL COMPRESSION CRITERIA FACTORS OF SAFETY AND CORRECTION



\* ACCIDENT FACTOR  
OF SAFETY  
( $S_{cr}/S_{aa}$ )

- NORMAL FACTOR OF  
SAFETY  
( $S_{cr}/S_{an}$ )

◇ ACCIDENT METHOD  
CORRECTION  
( $S_e/S_{aa}$ )

+ NORMAL METHOD  
CORRECTION  
( $S_e/S_{an}$ )

\* PLASTICITY  
CORRECTION  
( $S_e/S_{cr}$ )

#### 2.10.1.4.2 External Pressure Behavior

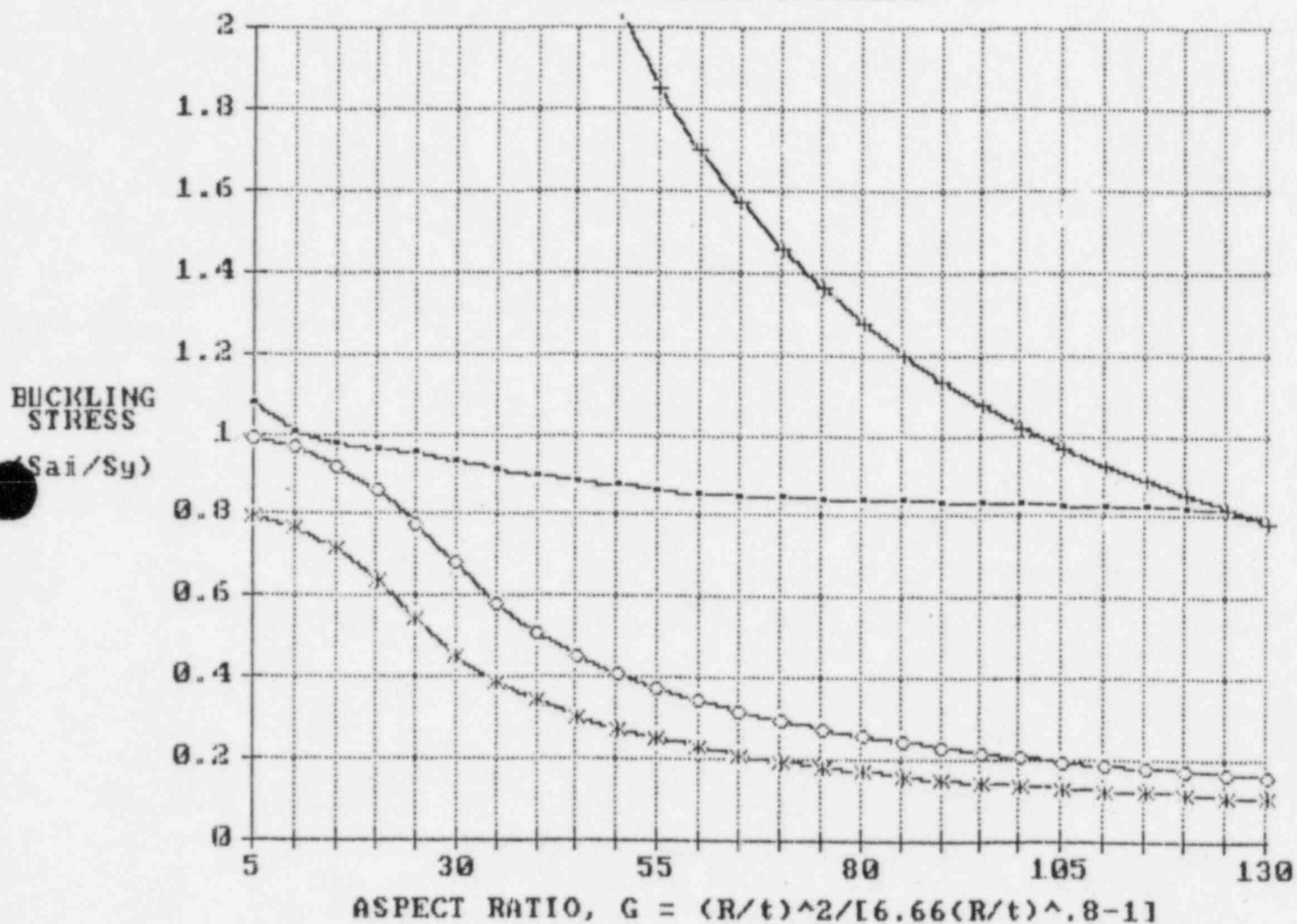
These results, Figures 2.10.1.4-3 and 2.10.1.4-4, are essentially identical in form and significance to those discussed for axial compression behavior.

#### 2.10.1.4.3 Column Behavior

Once again, Figures 2.10.1.4-5 and 2.10.1.4-6, display results comparable to the axial compression behavior. The conventional AISC column design formula is shown. For  $(L/R)$  values in excess of approximately 60 this design criteria limits stresses to less than 40-60% of the allowable AISC values. This impact is a direct result of the intended high reduction factor, or safety factor of 7.5 and 5 for normal and accident conditions, respectively. This criteria also provides a more sharply defined 'cut-off' of permissible stresses, at the plastic instability boundary ('Hard' to 'Intermediate' structures), due to the fact that the parabolic transition is mapped in the transformed 'G' coordinate system, not the conventional  $(L/R)$  coordinate system, as used by AISC. In the case of the column equations this coordinate transformation is given as,  $G = (L/R)^2$ .

FIGURE 2.10.1.4-3

# CONSTRAINED EXTERNAL PRESSURE BUCKLING CRITERIA



--- PLASTIC BUCKLING  
STRESS ( $S_{cr}/S_y$ )

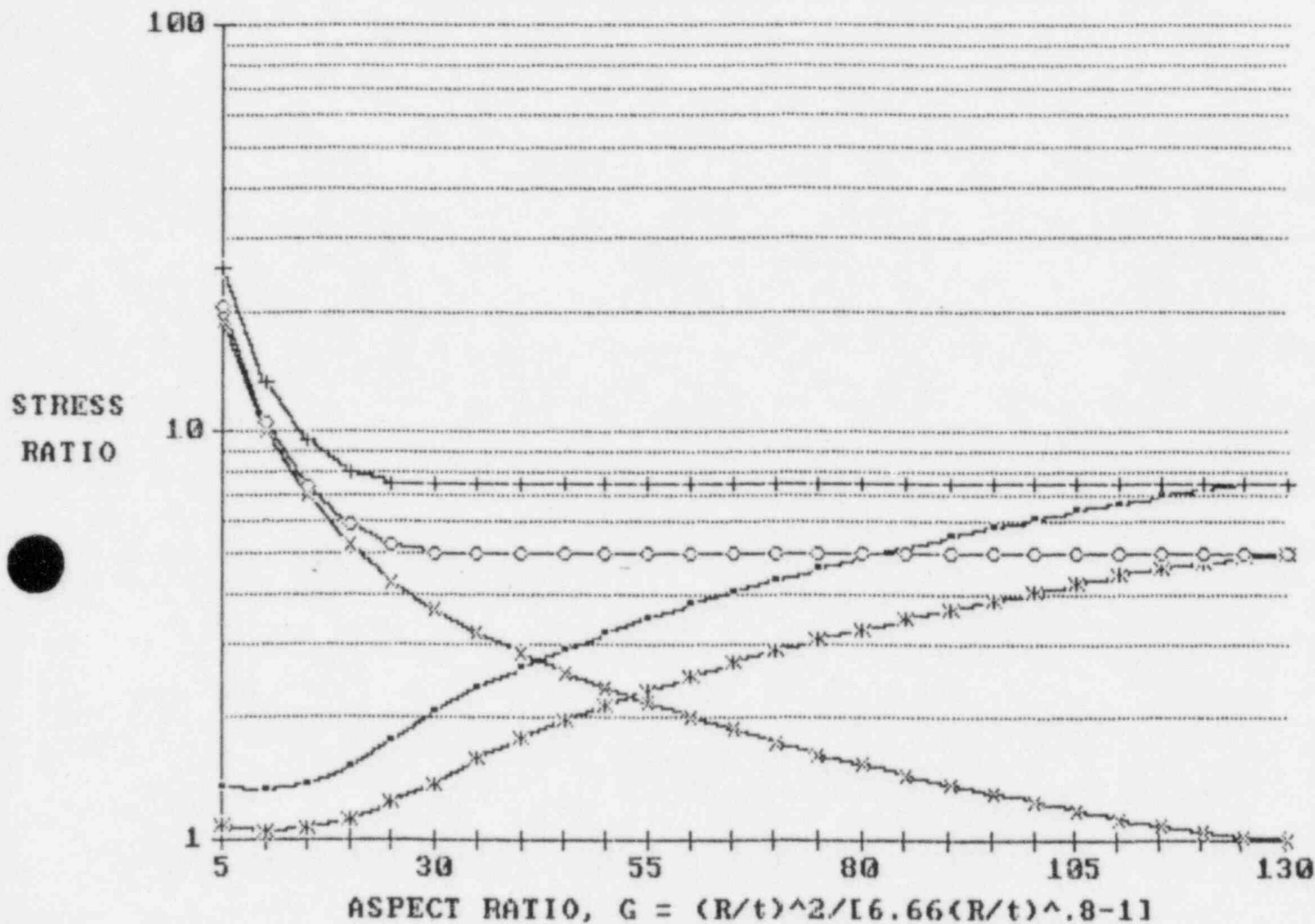
\* NORMAL LIMITS  
( $S_{an}/S_y$ )

+ ELASTIC BUCKLING  
ESTIMATE  
( $S_e/S_y$ )

○ ACCIDENT LIMITS  
( $S_{aa}/S_y$ )

FIGURE 2.10.1.4-4

# CONSTRAINED EXTERNAL PRESSURE CRITERIA FACTORS OF SAFETY AND CORRECTION



-- NORMAL FACTOR  
OF SAFETY  
( $S_{cr}/S_{an}$ )

+ NORMAL METHOD  
CORRECTION  
( $S_e/S_{an}$ )

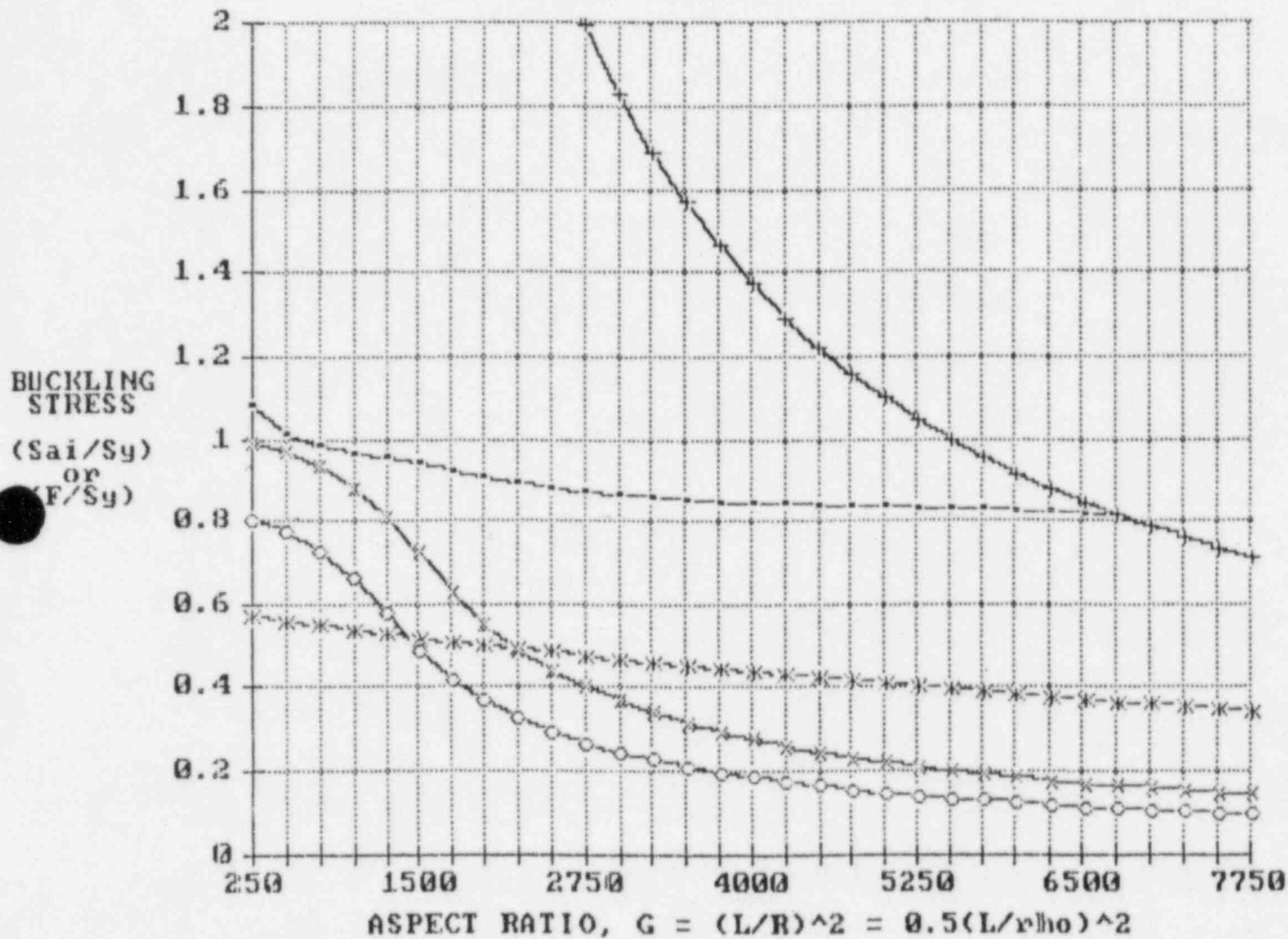
\* ACCIDENT FACTOR  
OF SAFETY  
( $S_{cr}/S_{aa}$ )

◇ ACCIDENT METHOD  
CORRECTION  
( $S_e/S_{aa}$ )

\* PLASTICITY  
CORRECTION  
( $S_e/S_{cr}$ )

FIGURE 2.10.1.4-5

## COLUMN BUCKLING CRITERIA



-- PLASTIC BUCKLING STRESS ( $S_{cr}/S_y$ )

+ ELASTIC BUCKLING ESTIMATE ( $S_e/S_y$ )

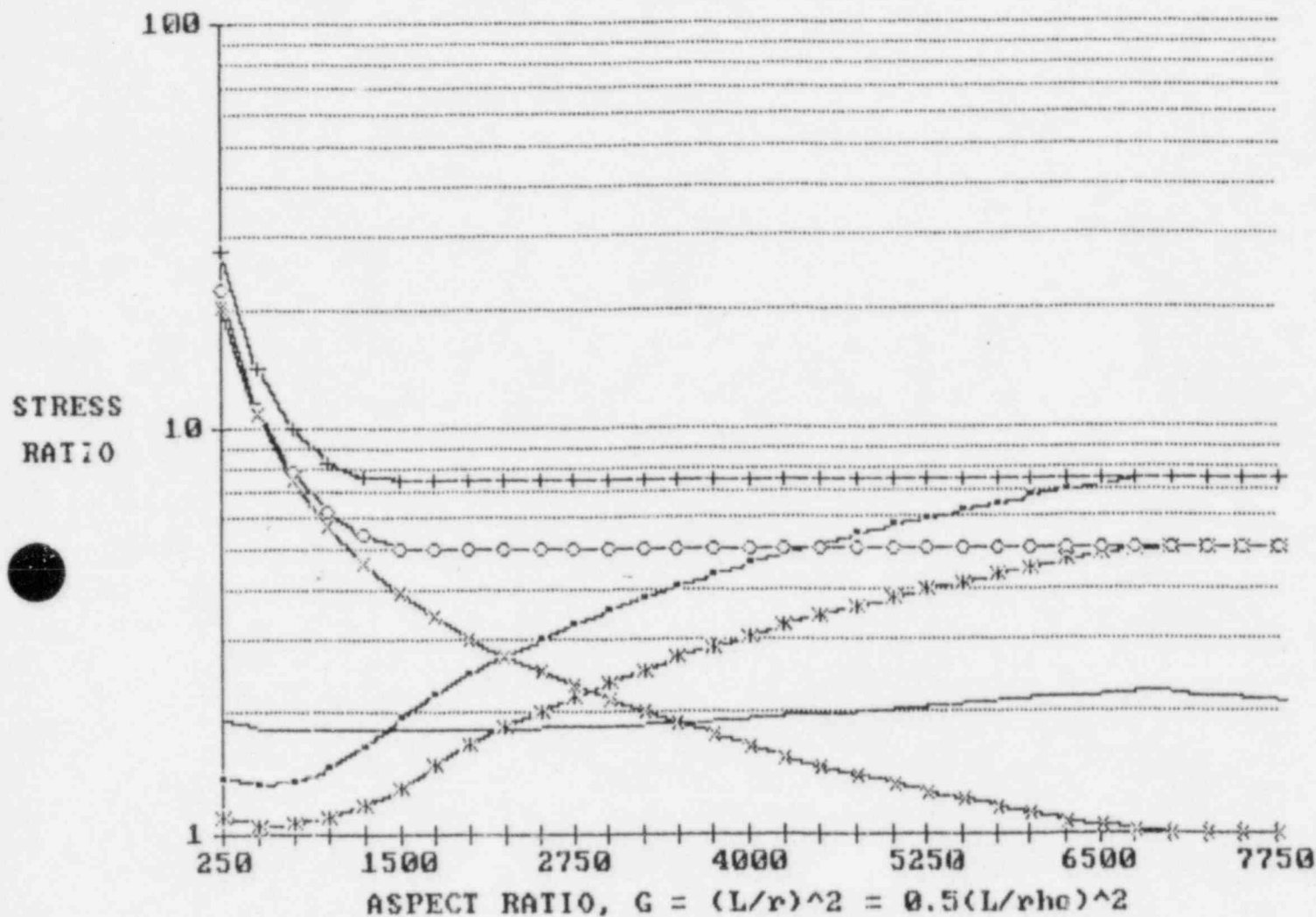
\* AISC COLUMN RULES ( $F/S_y$ )

◇ NORMAL LIMITS ( $S_{an}/S_y$ )

\* ACCIDENT LIMITS ( $S_{aa}/S_y$ )

FIGURE 2.10.1.4-6

# COLUMN BUCKLING CRITERIA FACTORS OF SAFETY AND CORRECTION



○ ACCIDENT METHOD  
CORRECTION  
( $S_e/S_{aa}$ )

\* PLASTICITY  
CORRECTION  
( $S_e/S_{cr}$ )

— AISC FACTOR  
OF SAFETY  
( $S_{cr}/F$ )

-- NORMAL FACTOR  
OF SAFETY  
( $S_{cr}/S_{an}$ )

+ NORMAL METHOD  
CORRECTION  
( $S_e/S_{an}$ )

\* ACCIDENT FACTOR  
OF SAFETY  
( $S_{cr}/S_{aa}$ )

2.10.1.5 References

- 2.10.1.5.1 U.S. Nuclear Regulatory Commission Regulatory Guide 7.6, Design Criteria for the Structural Analysis of Shipping Cask Containment Vessels, Revision 1, March 1978.
- 2.10.1.5.2 Design Task Group, ASME Committee on Containment Systems for Nuclear Spent Fuel and High-Level Waste Transport Packagings (NUPACK).
- 2.10.1.5.3 Personal communications with Code Case N-47-21 Committee member, Dr. Donald Griffin, Westinghouse, Madison, Pennsylvania to Dr. Howard C. Merchant (NuPac consultant).
- 2.10.1.5.4 Personal communications with Code Case N-47-21 Committee member, Mr. Al W. Dalcher, General Electric, (408) 738-7605 to Dr. Howard C. Merchant (NuPac consultant).
- 2.10.1.5.5 Bushnell, D., 'Static Collapse: A Survey of Methods and Modes of Behavior', Collapse Analysis of Structures, PVP-Vol.84, ASME, 1984, pp. 7-50.
- 2.10.1.5.6 Johnston, Bruce G., Editor, Guide to Stability Design Criteria for Metal Structures, Third Edition, John Wiley and Sons, New York, 1976.
- 2.10.1.5.7 Batterman, S. C., 'Plastic Buckling of Axially Compressed Cylindrical Shells', AIAA Journal, Volume 3, No. 2, January 1965, pp. 316-325.
- 2.10.1.5.8 Gerard, George, 'On the Role of Initial Imperfections in Plastic Buckling of Cylinders Under Axial Compression', Journal of Aerospace Sciences, Vol. 29, June 1962, pp.744-745.



- 2.10.1.5.9 Sobel, L. H., S. Z. Newman, 'Plastic Buckling of Cylindrical Shells Under Axial Compression', Journal of Pressure-Vessel Technology, Vol. 102, February 1980, pp. 40-44.
- 2.10.1.5.10 Combescure, A., 'Design Against Elasto-Plastic Buckling of Shells: Proposition of a Methodology', Recent Advances in Nuclear Component Testing and Theoretical Studies on Buckling, PVP-Vol. 89, ASME, 1984, pp 137-155.
- 2.10.1.5.11 Yu, Wei-Wen, Cold-Formed Steel Structures -- Design, Analysis, Construction, McGraw-Hill Book Company, New York, 1973.
- 2.10.1.5.12 Manual of Steel Construction, 6th Edition, American Institute of Steel Construction Inc. (AISC), 1963.
- 2.10.1.5.13 Baker, E. H., L. Kovalevsky and F. L. Rish, Structural Analysis of Shells, Robert E. Krieger Publishing Company, 1981.
- 2.10.1.5.14 Cold-Formed Steel Design Manual, 1983 Edition, American Iron and Steel Institute (AISI).
- 2.10.1.5.15 Plantema, F. J., 'Collapsing Stresses in Circular Cylinders and Round Tubes', Report S.280, 1946, Nat. Luchtvaartlaboratorium, Amsterdam, Netherlands.
- 2.10.1.5.16 Wilson, W. M., and N. M. Newmark, 'The Strength of Thin Cylindrical Shells as Columns', University of Illinois Engineering Experimental Station Bulletin No. 255, 1933.
- 2.10.1.5.17 Cheney, James A., Pressure Buckling of Ring Incased in a Cavity, ASCE EM Journal, April, 1971, Vol. 97, EM2.



APPENDIX 2.10.2

ANSYS Program Description

The ANSYS computer program is a large-scale, general purpose computer program for the solution of several classes of engineering analyses. Analysis capabilities include static and dynamic; elastic, plastic, creep and swelling; buckling; small and large deflections; steady state and transient heat transfer, fluid and current flow.

The matrix displacement method of analysis based upon finite element idealization is employed throughout the program. The library of finite elements available numbers more than forty for static and dynamic analyses, and twenty for heat transfer analyses. This variety of elements gives the ANSYS program the capability of analyzing two- and three-dimensional frame structures, piping systems, two-dimensional plane and axisymmetric solids, three-dimensional solids, flat plates, axisymmetric and three-dimensional shells and nonlinear problems including interfaces and cables.

Loading on the structure may be forces, displacements, pressures, temperatures or response spectra. Loadings may be arbitrary functions of time for linear and nonlinear dynamic analyses. Loadings for heat transfer analyses include internal heat generation, convection and radiation boundaries, and specified temperatures or heat flows.

The ANSYS program uses the wave-front (or "frontal") direct solution method for the system of simultaneous linear equations developed by the matrix displacement method, and gives results of high accuracy in a minimum of computer time. The program has the capability of solving large structures. There is no limit on the number of elements used in an analysis. There is no "band width" limitation in the analysis definition; however, there is a "wave-front" restriction. The "wave-front" restriction depends on the amount of core storage available for a given problem. Up to 2000 degrees of freedom on the wave-front can be handled in a large core. For extremely large analyses, an out-of-core wave-front procedure (which effectively removes the "wave-front" limit with an increased run time penalty) is available.

The input data for the ANSYS program has been designed to make it as easy as possible to define the analysis to the computer. A preprocessor (PREP7) contains powerful mesh generation capability as well as being able to define all other analysis data (real constants, material properties, constraints, loads, etc.). Geometry plotting is available for all elements in the ANSYS library, including isometric, perspective, section, edge, and hidden-line plots of three-dimensional structures.

ANSYS has the capability of generating substructures (or superelements). These substructures may be stored in a library file for use in other analyses. Substructuring portions of a model can result in considerable computer-time savings for nonlinear analyses.

Postprocessing routines are available for algebraic modification, differentiation, and integration of calculated results. Root-sum-square operations may be performed on seismic modal results. Response spectra may be generated from dynamic analysis results. Results from various loading modes may be combined for harmonically loaded axisymmetric structures. Post routines also plot distorted geometries, stress contours, safety factor contours, temperature contours, mode shapes, time history graphs, and stress-strain curves.

Details of the types of finite elements used in the various analyses of NuPac 10/140MB components can be found in the ANSYS Users Manual, Revision 4.1, Volumes I and II, Swanson Analysis Systems, Inc., Houston, Penn., 1983.

APPENDIX 2.10.3

TIEDOWN LUG LOAD AND STRESS ANALYSIS

THIS SECTION IS PROPRIETARY

APPENDIX 2.10.4

ENVIROLOCK<sup>™</sup> STRUCTURAL ANALYSIS

THIS SECTION IS PROPRIETARY

APPENDIX 2.10.5

DESCRIPTION OF NUPAC

PROPRIETARY DROP PROGRAMS

### 2.10.5 Description of NuPac Proprietary Drop Programs

This section briefly documents the methodology employed by the NuPac proprietary computer programs which are used to demonstrate compliance of the package with applicable provisions of 10 CFR 71 for normal and hypothetical accident conditions. The first two subsections deal with the calculation of external and internal forces imposed upon the package, when subjected to drop events. A sample problem is then presented and the NuPac computer code quality assurance program is briefly discussed. These subsections describe techniques and computer programs developed by Nuclear Packaging, Inc. of Federal Way, Washington, as follows:

- o 2.10.5.1: Describes derivation of energy absorbing overpack load-deflection relations.
- o 2.10.5.2: Describes the methods to evaluate the dynamic behavior of oblique impacts and the associated internal forces generated within the cask body.
- o 2.10.5.3: Describes a sample problem, and input and output for each of the four computer codes (EYDROP, SYDROP, CYDROP, and OBLIQUE) discussed in this section.
- o 2.10.5.4: Describes the quality assurance program utilized to maintain NuPac computer codes.

#### 2.10.5.1 Overpack Deformation Behavior

The package is protected by foam-filled, energy-absorbing end buffers, called overpacks. For purposes of analysis, the overpacks are assumed to absorb, in plastic deformation of foam, the potential energy of the drop event. That is, the analyses assume that none of the drop potential energy is transferred to kinetic or strain energy of the target (the unyielding surface assumption of 10 CFR 71), nor strain energy in the package body itself.

There are three orientations of the package where the potential energy of a drop is assumed totally absorbed by plastic deformations of the overpacks. At other orientations, where rotational effects are important, the methods outlined in Section 2.10.5.2 are employed. The three orientations where rotational (or pitch) motions play no role in the evaluation of the impact event are:

- o End Drop - on the circular end surface of the overpack.
- o Side Drop - on the cylindrical side surfaces of the overpacks.
- o Corner Drop - with package center of gravity directly above the struck corner of the overpack.

For these three orientations, the prediction of overpack behavior can be approached from straightforward energy balance principles:

$$E = W(h + \delta) = \int_0^{\delta} F_x dx \quad (1)$$

Where:

$W$  = package weight

$h$  = drop height

$\delta$  = maximum overpack deformation

$F_x$  = force imposed upon target and package by  
the overpack at a deflection equal to  $x$ .

The left-hand term represents the potential energy of the drop. The right hand term represents the strain energy of the deformed overpack.

Each of these three orientations is treated by an individual computer program reflecting the differing geometry characteristics of each event. All three computer programs employ common energy balance techniques to assess maximum overpack deformations, including utilizing a common description of the crushable energy absorbing foam. The foam typically exhibits a stress-strain



plateau of nearly constant stress up to a total strain of 40-60%. Above this strain value, pronounced strain hardening effects commence which reflect the collapse or consolidation of the entrapped bubbles within the foam. Accordingly, a tabular definition of foam stress-strain relations is employed in each of the three computer programs. This tabular definition is taken directly from measured properties and accurately reflects the strain hardening behavior of the foam up to strains of about 80%.

The following discussion of these three computer programs proceeds from the geometrically simplest (end drop) to the most complex (corner drop).

#### 2.10.5.1.1 End Drop (EYDROP)

EYDROP performs the calculations outlined in Equations (1), (2), and (3) for a trial range of deformation values,  $\delta$ . For each trial value of total deformation, the energy balance of Equation (1) is monitored and reported. Solution for total overpack deformation is found by an interpolated balance of Equation (1). EYDROP assumes a constant foam strain across the crush area, neglecting the affects of any unbacked areas. A sample problem input and output for EYDROP may be found in Section 2.10.5.3.1.

The force produced by the overpack is simply:

$$F_x = A\sigma_\varepsilon \quad (2)$$

Where:

$A = \pi D^2/4$ , the end area of the package

$D$  = effective diameter of package

$$\sigma_\varepsilon = \xi[\varepsilon], \text{ the foam crush stress at a strain of } \varepsilon \quad (3)$$

$\xi[\varepsilon]$  = the tabular definition of foam stress strain properties

$$\varepsilon = x/x_u$$

$x$  = deformation

$x_u$  = end thickness of overpack

### 2.10.5.1.2 Side Drop (SYDROP)

SYDROP differs from the end drop solution only in the fact that both deformation and strain vary from point to point and total force, at a given crush depth, must be found by geometric integration over these points. The details on this geometry are found in Figure 2.10.5.1-1. SYDROP assumes all foam is backed, exhibiting homogeneous properties along the package length. A sample problem input and output for SYDROP may be found in Section 2.10.5.3.2.

For each trial deformation value, the force is found as:

$$F_{\delta} = 2L \int_0^{x_{\max}} \sigma_{ex} dx$$

Where:

$L$  = effective length of the overpack

$$x_{\max} = [r_o^2 - (r_o - \delta)^2]^{0.5}$$

$\sigma_{ex} = \zeta[\epsilon_x]$ , tabular definition of foam stress-strain properties

$\epsilon_x$  = foam strain at location 'x'

Referring to Figure 2.10.5.1-1, the strain at a point 'x' is found by:

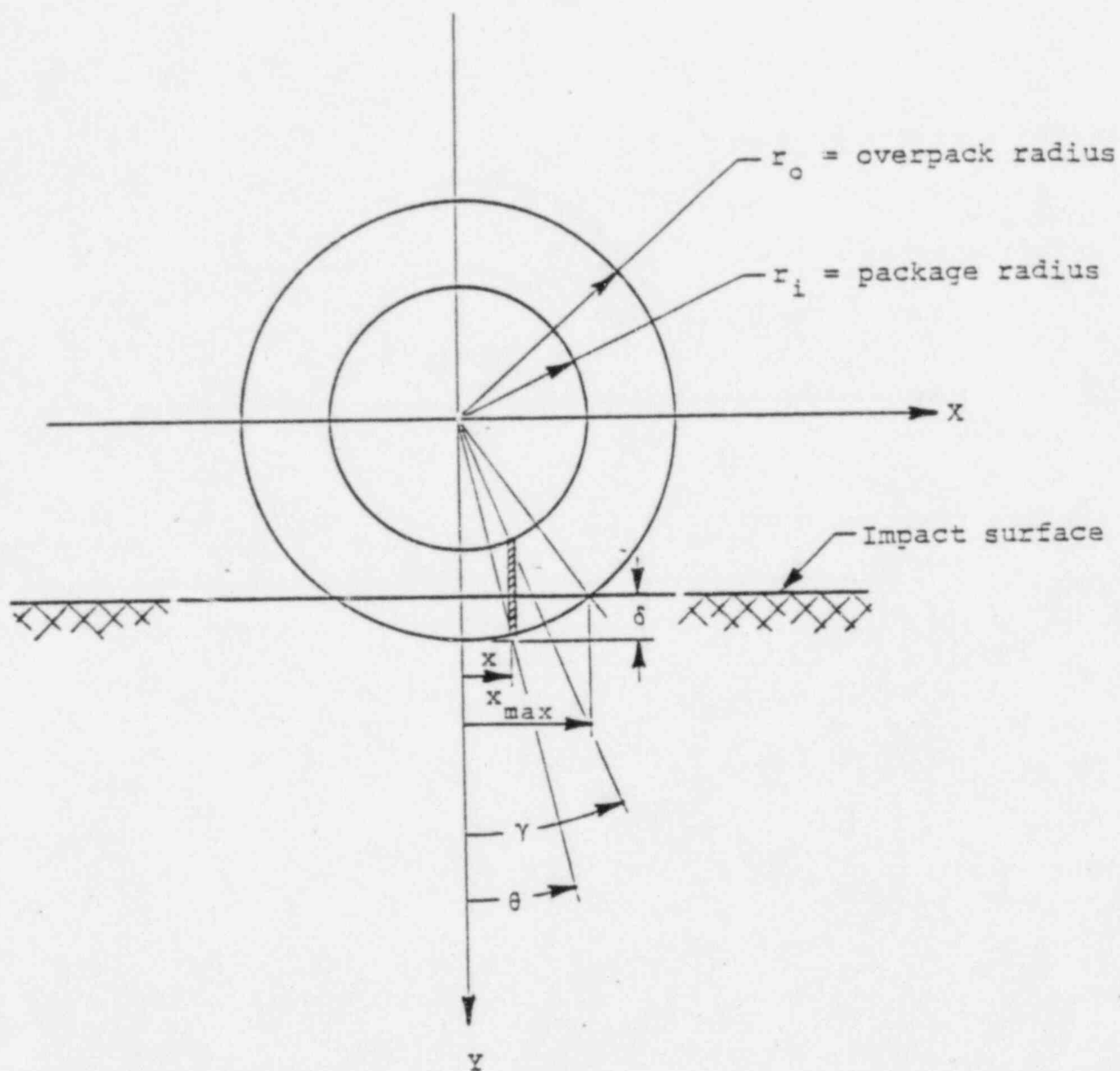
$$\epsilon_x = [\delta - r_o(1 - \cos \theta)] / [r_o(\cos \theta) - r_i(\cos \gamma)]$$

Where:

$$\theta = \sin^{-1}(x/r_o)$$

$$\gamma = \sin^{-1}(x/r_i)$$

FIGURE 2.10.5.1-1  
Side Impact Geometry (SYDROP)



2.10.5.1.3 Corner Drop (CYDROP)

CYDROP is similar to SYDROP, excepting that a two dimensional geometric integration is required to assess the overpack crush force at each deformation. A sample problem input and output for CYDROP may be found in Section 2.10.5.3.3.

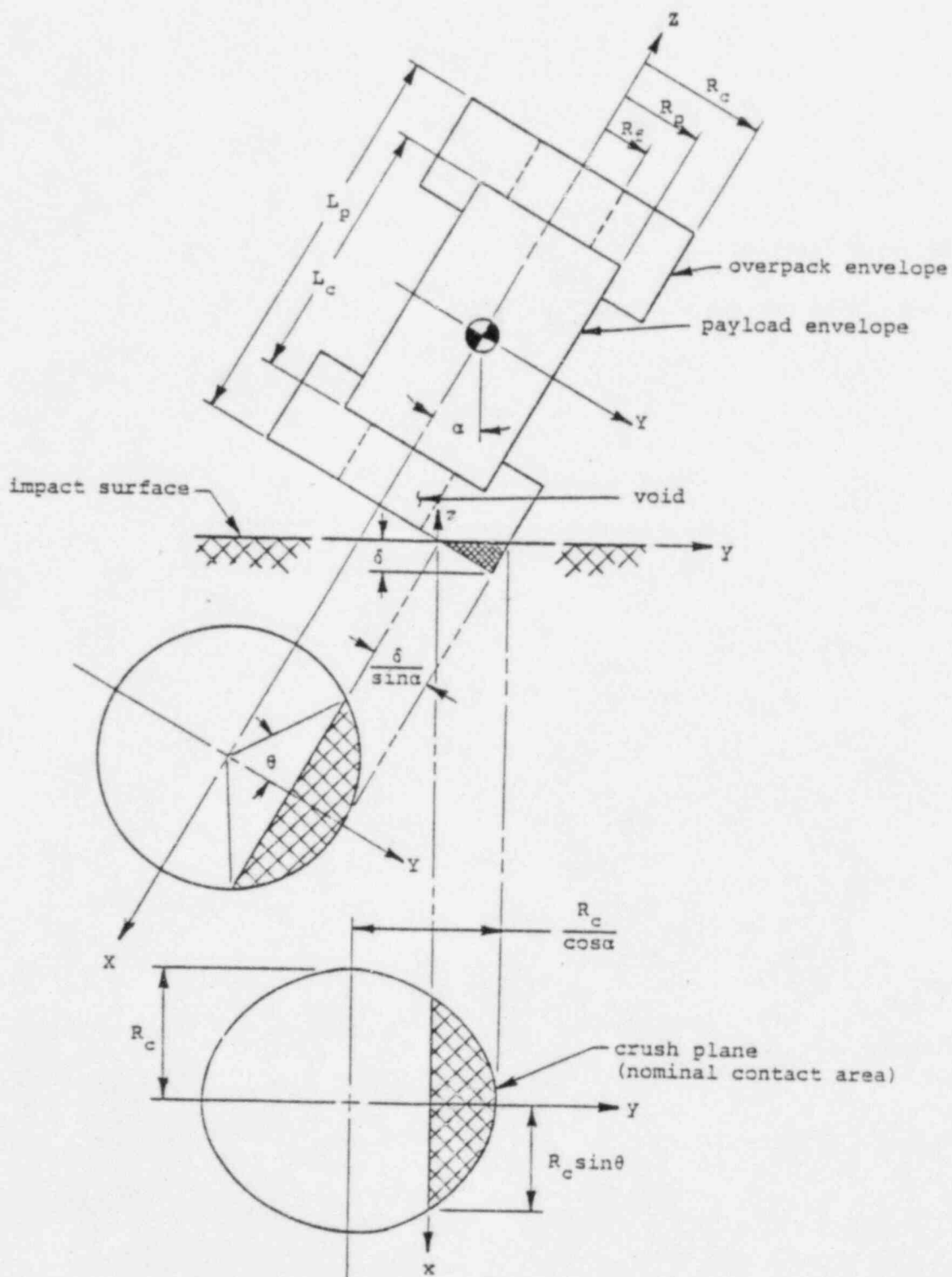
CYDROP treats the corner impact of a cylindrical package upon an unyielding surface. The package itself consists of a cylindrical payload portion surrounded by a larger cylindrical column composed of a crushable media. So long as the deformations of the crushable media are modest, the problem may be approximately solved by assuming a uniform crush stress exists over the elliptical surface of the crush plane (contact surface). CYDROP was developed specifically to address problems of large deformations of this crushable media and to treat geometries where the cylindrical overpack envelope possesses axisymmetric cylindrical voids (e.g., does not completely cover the cylindrical ends of the payload package).

The large deformation behavior of the crushable media is accommodated by determining the actual strain of the crushable media at a point. This strain is used to determine the corresponding stress from an implicit tabular definition of media stress-strain characteristics. The total crush force is found by a double integration over the contact area of the crush plane.

Strain energy absorbed by the crushable media is determined by integrating the crush force and its associated deformation. The package is assumed to be at rest when the computed strain energy value equals the applied drop energy.

The geometric calculations for the contact surface and the associated strains are carried out using a moving (x, y, z) coordinate system in which the x-y plane corresponds to the crush plane, as illustrated in Figure 2.10.5.1-2. The crush plane itself represents a segment of an ellipse. The contact area is this ellipse segment, provided no cylindrical end void exists. When a cylindrical end void exists, the contact area of the crush plane is reduced by the removal of a second elliptical region associated with the projection of this void into the contact plane.

FIGURE 2.10.5.1-2  
Corner Impact Geometry (CYDROP)



Calculation of strain is somewhat more complex. In principle, the distance from point (x, y) in the crush plane to the payload is found and denoted,  $Z_{top}$ . Similarly, the distance to the undeformed external overpack envelope is found and denoted,  $Z_{bot}$ . The strain represents deformation divided by original thickness, or:

$$\epsilon = Z_{bot} / (Z_{bot} + Z_{top})$$

At any point (x, y), the calculation of  $Z_{top}$  may follow three branches, according to location. The three possible branches relate to the payload surface intercepted. They are the circular bottom of the payload, the cylindrical surface of the payload, and the unbacked regions, each of which are separately addressed below:

#### The Circular Bottom of the Payload:

The bottom of the payload cylinder describes an ellipse in the crush plane. If point (x, y) is inside this ellipse, the point is considered backed by the bottom of the payload. An exception to this general statement is noted in the discussion of the unbacked region, below.

#### The Cylindrical Surface of the Payload:

The cylindrical surface of the payload describes a rectangular region tangent to the payload bottom ellipse at its major axes. If point (x, y) is outside the bottom ellipse yet possesses an x-coordinate less than the radius of the payload bottom, the point is considered backed by the payload cylinder.

#### Unbacked Regions:

Unbacked regions are of two forms - those associated with the cylindrical end void and those near the external surface of the overpack. The unbacked region associated with the end void is a point in the crush plane which lies within the ellipse defined by the void circle lying in the plane of the payload

bottom. The unbacked region associated with points near the overpack extremities is defined by those points (x, y) where the x-coordinate exceeds the radius of the payload volume. Points which are unbacked employ a nominal crush stress for force integration purposes.

The calculation of  $Z_{\text{bot}}$ , the distance to the undeformed overpack envelope, may follow two branches. These branches correspond to intercepts with either the cylindrical surface of the overpack or the circular end of the overpack.

The analytics describing the geometry discussed above, consists of the sequential application of a series of geometric transformations of surfaces described in the coordinates of the cylindrical package (X, Y, Z) to the coordinates of the contact plane (x, y, z). The surfaces in package coordinates are:

Overpack Cylinder:	$X^2 + Y^2 = R_c^2$
Overpack Bottom Circle:	$X^2 + Y^2 = R_c^2$ $Z = -L_c/2$
Payload Cylinder:	$X^2 + Y^2 = R_p^2$
Payload Bottom Circle:	$X^2 + Y^2 = R_p^2$ $Z = -L_p/2$
Void Circle at Payload:	$X^2 + Y^2 = R_f^2$ $Z = -L_p/2$
Void Circle at Overpack Exterior:	$X^2 + Y^2 = R_f^2$ $Z = -L_c/2$

CYDROP also performs a sensitivity analysis to determine the amount of unbacked foam at each incremental crush depth. Additionally, this calculation is carried over to the impact force and strain energy. The code automatically prints a warning message if the foam strain exceeds 80% and the ratio of foam strain energy to kinetic energy is less than one ( $SE/KE < 1$ ).

2.10.5.2 Oblique Impact Dynamic Analysis

Impacts at arbitrary orientation angles differ in two major respects from those that occur at angles corresponding to stable or neutral equilibrium (end, side, and center of gravity over struck corner). In the neutral and stable equilibrium conditions, the entire initial kinetic energy of drop is transformed into strain energy associated with plastic deformation of the overpack. At arbitrary orientation angles, only a portion of this kinetic energy is transformed into strain energy at the impacted end. The remainder of this kinetic energy becomes rotational motion of the package. The solution approach must properly reflect the continually changing transformation of initial translational kinetic energy into rotational kinetic energy and plastic deformation of the overpack energy absorber.

The second major difference between neutral equilibrium impacts and arbitrary angle impacts relates to the rather different load-deflection behavior of the overpacks at low angle ( $<30^\circ$  from horizontal) orientations. Under neutral equilibrium conditions, a major portion of the crush footprint is backed by the cylindrical body of the package, allowing strain hardening effects to stiffen the overpack load-deflection relation. At low angle orientations ( $<30^\circ$  from horizontal), much of the overpack crush footprint is unbacked. Thus, the low angle load-deflection relations are initially quite soft, then abruptly harden as portions of the crush footprint grow into backed regions. As these low angle orientations approach horizontal attitudes, this terminal stiffening phenomena becomes more pronounced.

There are two potential solution paths to problems of this nature - a momentum formulation or a direct solution of the equations of motion. The momentum approach provides an easy and simple means to assess the transformation of translational initial velocities into rotary velocities, hence, total plastic strain energy absorbed by the overpack energy absorber. Unfortunately, this momentum formulation does not produce intermediate values of crush force and crush deformation needed to assess overpack attachment forces, nor does it conveniently provide a means to incorporate the varying load-deflection relationships of the overpack as a function of orientation angle. Thus, a direct solution of the equations of motion was selected.



The three key problem variables, crush force,  $F$ , crush depth,  $\delta$ , and orientation angle,  $\theta$ , all vary with time,  $t$ , for a given initial orientation angle,  $\theta_0$ . The crush force is assumed to act at the centroid of the elliptical crush footprint. For the model illustrated in Figure 2.10.5.2-1, three independent second order differential equations of motion can be formed:

$$M(\partial^2 X / \partial t^2) = F_x$$

$$M(\partial^2 Y / \partial t^2) = F_y - Mg$$

$$I(\partial^2 \theta / \partial t^2) = \{[\delta(a - c)/c(\sin \theta) + T_B + L/2](\sin \theta)\}F_x \\ + \{\bar{x} - [\delta(a - c)/c(\sin \theta) + T_B + L/2](\cos \theta)\}F_y$$

Where:

$M$  = the package mass =  $\rho L$

$F$  = the crush force

$g$  = the gravitational constant =  $386.4 \text{ in/sec}^2$

$I$  = the rotational mass moment of inertia (as input)

$r_0$  = the radius of the body

$L$  = the length of the body

$T_B$  = overpack bottom thickness

$\theta$  = the instantaneous orientation angle of the package with respect to the horizon

$\rho$  = the mass per unit length

$\bar{x}$  = distance to centroid of footprint

$a, c$  = geometric quantities defined in Figure 2.10.5.2-2

FIGURE 2.10.5.2-1  
Oblique Impact Geometry

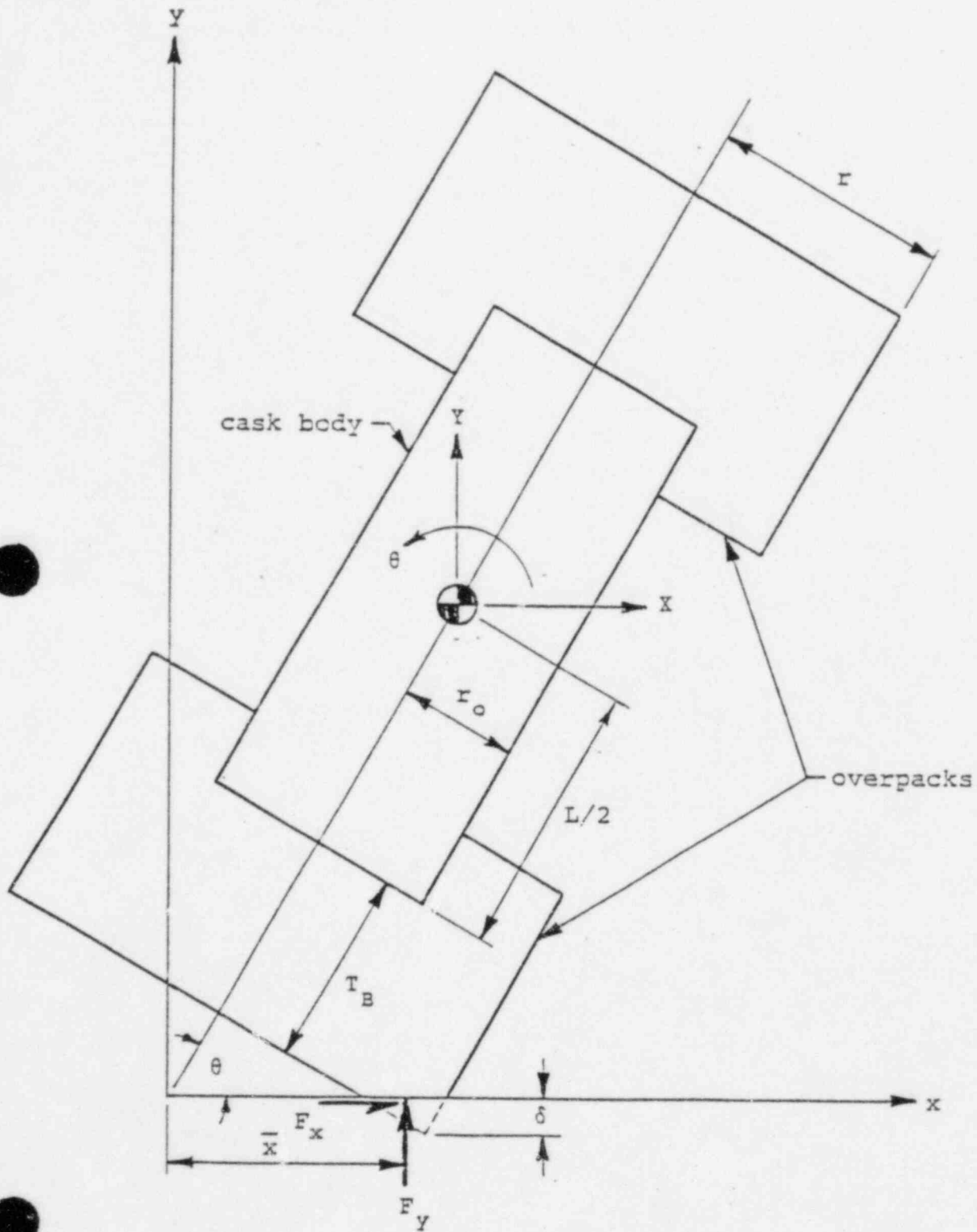
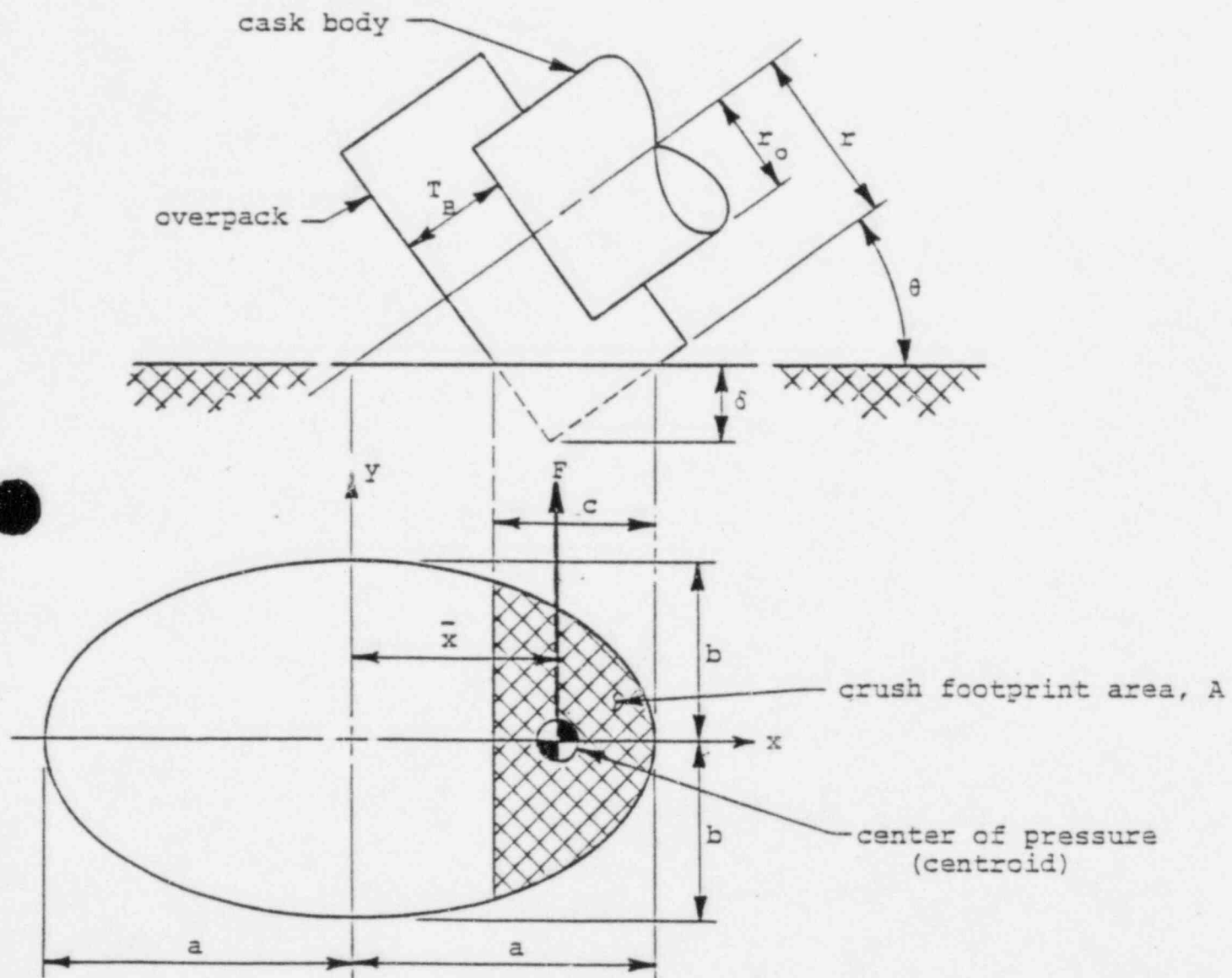


FIGURE 2.10.5.2-2  
Elliptical Footprint Geometry



These differential equations are integrated subject to initial conditions, associated with the moment of impact when time,  $t$ , equals zero, of:

$$X = 0$$

$$Y = 0$$

$$\theta = \theta_0$$

$$\partial X / \partial t = \partial X_0 / \partial t$$

$$\partial Y / \partial t = \partial Y_0 / \partial t$$

$$\partial \theta / \partial t = \partial \theta_0 / \partial t$$

Where:

$$\theta_0 = \text{impact angle (varies with time, } t)$$

$$\partial Y_0 / \partial t = (2gh)^{0.5}$$

$$h = \text{drop height}$$

Each of the above differential equations requires a continuously updated value of the force,  $F$ , reflecting both crush depth and package orientation, or:

$$F = \xi(\delta_y, \theta)$$

This continuously updated value of the force,  $F$ , is supplied to the integration process by means of a two dimensional Lagrangian interpolation of crush depth,  $\delta_y$ , and orientation angle,  $\theta$ . The tabular data used in this interpolation consist of a series of complete force-deflection relations for separate orientation angles developed via the CYDROP computer program, described in Section 2.10.5.1.3. The deflection,  $\delta_y$ , is expressed in terms of problem variables as:

$$\delta_y = L(\sin \theta - \sin \theta_0)/2 + r_0(\cos \theta - \cos \theta_0) - Y$$

The foregoing analysis process for evaluating impacts at oblique orientations was consolidated in a NuPac developed computer program, OBLIQUE. OBLIQUE integrates the equations of motion for each value of orientation angle versus time, until maximum values are found for crush force, crush deformation, shear, and body bending moment. At each incremental time step (incremental crush deformation), overpack attachment moments are computed, scanned for maximum values and output. By sweeping through a series of initial orientation angles, the maximum values of all internal loads are found. At each specified initial orientation angle, a solution is realized when all internal forces, moments, and deflection have reached a maximum value. Note that these internal forces, moments, and deflections do not necessarily happen at the same instantaneous angle,  $\theta$ .

#### 2.10.5.2.1 Overpack Force Analysis

This section treats both external and internal forces imposed upon the package. Key to the treatment of external force application locations is an understanding of crush footprint geometry.

The crush footprint is a sector of the ellipse, as illustrated in Figure 2.10.5.2-2. The location of the centroid,  $\bar{x}$ , is calculated relative to the ellipse origin. The geometric properties of the elliptical crush footprint are:

$$a = r / \sin \theta$$

$$b = r$$

$$c = \delta / [(\sin \theta)(\cos \theta)]$$

The area,  $A$ , and the centroidal offset,  $\bar{x}$ , of the crush footprint are derived as:

When  $c \leq a$ :

$$A = 2 \int_{(a-c)}^c y \, dx$$

Where:

$$y = b(a^2 - x^2)^{0.5}/a$$

Then,

$$A = (2b/a) \int_{(a-c)}^c (a^2 - x^2)^{0.5} \, dx$$

Solving,

$$A = (b/a) \{ (\pi a^2/2) - (a-c)(2ac - c^2)^{0.5} - a^2 \sin^{-1}[(a-c)/a] \}$$

The center of pressure,  $\bar{x}$ , is:

$$A\bar{x} = (2b/a) \int_{(a-c)}^c x(a^2 - x^2)^{0.5} \, dx$$

Then,

$$\bar{x} = \{2b[(2ac - c^2)^{1.5}]/3a\}/A$$

When  $a < c \leq 2a$ :

$$A = \pi ab - A'$$

$$\bar{x} = (A'\bar{x}')/A$$

Where  $A'$  and  $\bar{x}'$  are as defined for  $A$  and  $\bar{x}$ , except that  $c'$  replaces  $c$ . The value of  $c'$  is:

$$c' = 2a - c$$

When  $a > 2a$ :

$$A = \pi ab$$

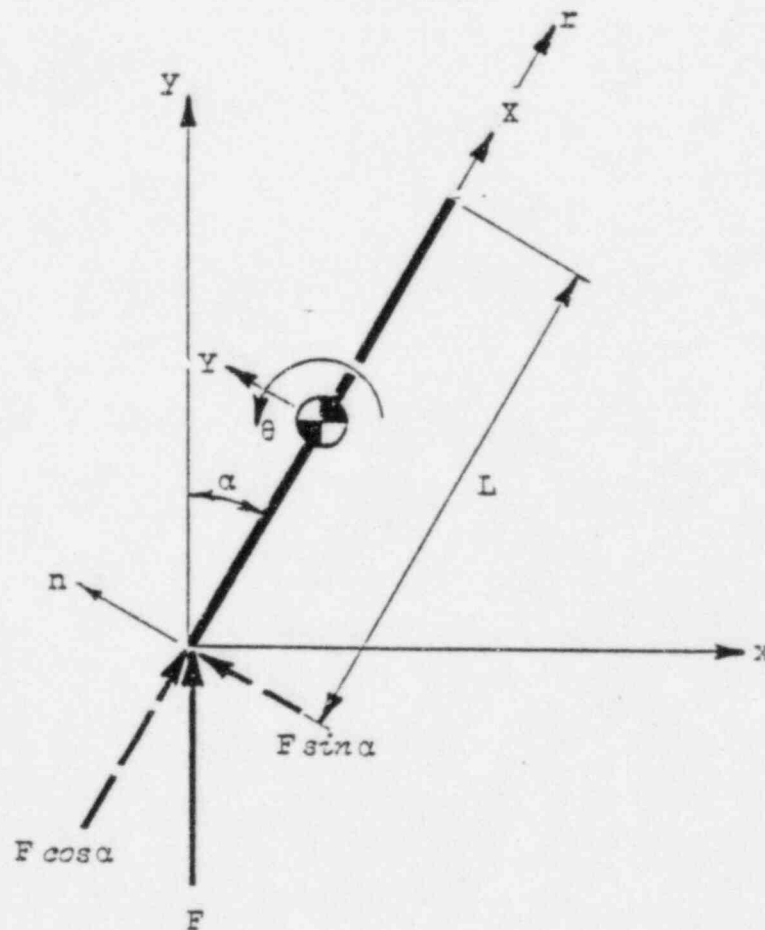
$$\bar{x} = 0$$

2.10.5.2.2 Overpack Attachment Forces

Overpack attachment forces are calculated by POSTOB, a post-processor for the OBLIQUE program. POSTOB's analytic technique includes the effects of inertia in calculating the attachment forces, and thus represents an improvement in the accuracy of this calculation. See Section 2.10.5.2.4 below for details.

2.10.5.2.3 Internal Forces

The package is idealized as a beam impacting on the lower end. The equations of motion are formed and used to define station-wise accelerations. These accelerations, in conjunction with the unit mass of the package, form forces which vary along the length of the package. When integrated, these forces provide a complete definition of internal thrusts, shears, and moments for the package as a function of total impact force and orientation angle.





For a planar rigid body system, the behavior is totally defined by a solution of the three equations of equilibrium written at the center of gravity of the rigid body. In the preceding figure, local coordinates are defined at the center of gravity, with axes parallel and normal to the beam. The end impact force is resolved into components parallel to these local axes. Summation of forces at the center of gravity leads to three rigid body equations of motion:

$$\text{Sum of Lateral Forces} - M(\partial^2 Y / \partial t^2) = F(\sin \alpha)$$

$$\text{Sum of Longitudinal Forces} - M(\partial^2 X / \partial t^2) = F(\cos \alpha)$$

$$\text{Sum of Moments} - I(\partial^2 \theta / \partial t^2) = -FL(\sin \alpha)/2$$

Where:

$M = \rho L$ , the mass of the body

$I = \rho L^3 / 12$ , the mass moment of inertia of the body

$\rho$  = the mass per unit length of the body

$\alpha$  = the orientation angle with respect to vertical

Note that the mass moment of inertia term given above is valid only for infinitely slender beams of mass. A more accurate mass moment approximation is provided by the equation:

$$I = \rho L(3R^2 + L^2)/12$$

Where:

$R$  = the radius of the cylindrical cask

This increased mass moment of inertia demonstrably decreases the internal moment. Thus, all moments calculated using the slender body approximation are conservative in proportion to the degree with which the cask is not slender. A very squat cask would have an internal moment predicted by OBLIQUE considerably higher than reality.

Substituting for the mass and inertia terms:

$$\partial^2 Y / \partial t^2 = F(\sin \alpha) / \rho L$$

$$\partial^2 X / \partial t^2 = F(\cos \alpha) / \rho L$$

$$\partial^2 \theta / \partial t^2 = -6F(\sin \alpha) / \rho L^2$$

The lateral and longitudinal accelerations at a point 'r' are:

$$\begin{aligned} \partial^2 S_n / \partial t^2 &= \partial^2 Y / \partial t^2 + [r - (L/2)](\partial^2 \theta / \partial t^2) \\ &= [F(\sin \alpha) / \rho L^2] [L - 6[r - (L/2)]] \\ &= [2F(\sin \alpha) / \rho L^2] (-3r + 2L) \end{aligned}$$

$$\partial^2 S_r / \partial t^2 = \partial^2 X / \partial t^2 = F(\cos \alpha) / \rho L$$

The lateral inertial force acting on the body at the  $r^{\text{th}}$  location is:

$$\partial V_r / \partial r = -\rho(\partial^2 S_n / \partial t^2)$$

The corresponding expression for shear is found by integrating this lateral force from the free end to the  $r^{\text{th}}$  location, or:

$$\begin{aligned} V_r &= [-2F(\sin \alpha) / L^2] \int_L^r (-3r + 2L) dr \\ &= [-2F(\sin \alpha) / L^2] \{-3(r^2 - L^2)/2 + 2L(r - L)\} \end{aligned}$$

Rearranging,

$$\begin{aligned} V_r &= [-2F(\sin \alpha) / L^2] \{-3r^2/2 + 3L^2/2 + 2Lr - 2L^2\} \\ &= [F(\sin \alpha) / L^2] [3r^2 - 4Lr + L^2] \end{aligned}$$

Similarly, the corresponding moment is found by integration of the shear expression:

$$\partial M_r / \partial r = V_r$$

$$\begin{aligned} M_r &= [F(\sin \alpha) / L^2] \int_L^r \{3r^2 - 4Lr + L^2\} dr \\ &= [F(\sin \alpha) / L^2] \{(r^3 - L^3) - 2L(r^2 - L^2) + L^2(r - L)\} \end{aligned}$$

Rearranging,

$$\begin{aligned} M_r &= [F(\sin \alpha) / L^2] \{r^3 - L^3 - 2Lr^2 + 2L^3 + L^2r - L^3\} \\ &= [F(\sin \alpha) / L^2] \{r^3 - 2Lr^2 + L^2r\} \end{aligned}$$

In order to verify these expressions for shear and moment, they are evaluated at the boundaries,  $r = 0$  and  $r = L$ :

At  $r = 0$ :

$$\begin{aligned} V_r &= [F(\sin \alpha) / L^2] [3r^2 - 4Lr + L^2] \\ &= [F(\sin \alpha) / L^2] [L^2] = F(\sin \alpha) \\ M_r &= [F(\sin \alpha) / L^2] [r^3 - 2Lr^2 + L^2r] = 0 \end{aligned}$$

At  $r = L$ :

$$\begin{aligned} V_r &= [F(\sin \alpha) / L^2] [3r^2 - 4Lr + L^2] \\ &= [F(\sin \alpha) / L^2] [3L^2 - 4L^2 + L^2] = 0 \\ M_r &= [F(\sin \alpha) / L^2] [r^3 - 2Lr^2 + L^2r] \\ &= [F(\sin \alpha) / L^2] [L^3 - 2L^3 + L^3] = 0 \end{aligned}$$

The maximum moment occurs where the shear,  $V_r$ , equals zero. For this to occur, the quadratic term in the shear equation must be solved.

$$0 = 3r^2 - 4Lr + L^2$$

$$r = \{4L \pm [16L^2 - 4(3)L^2]^{0.5}\}/6$$

$$= (4L \pm 2L)/6 = L, L/3$$

The maximum moment is found at  $r = L/3$ , or

$$M_{\max} = [F(\sin \alpha)/L^2][L^3/27 - 2L^3/9 + L^3/3]$$

$$= 4FL(\sin \alpha)/27 \quad \text{at } r = L/3$$

The minimum shear occurs where the lateral force equals zero. For this to occur, the linear term in the lateral force equation must be solved.

$$\partial V_r / \partial r = [-2F(\sin \alpha)/L^2][-3r + 2L] = 0$$

$$r = 2L/3$$

The magnitude of the axial (thrust) force can be found as a function of location as:

$$\partial T / \partial r = -\rho(\partial^2 S_r / \partial t^2)$$

$$T = -\rho(\partial^2 S_r / \partial t^2) \int_L^r dr = -\rho(\partial^2 S_r / \partial t^2)(r - L)$$

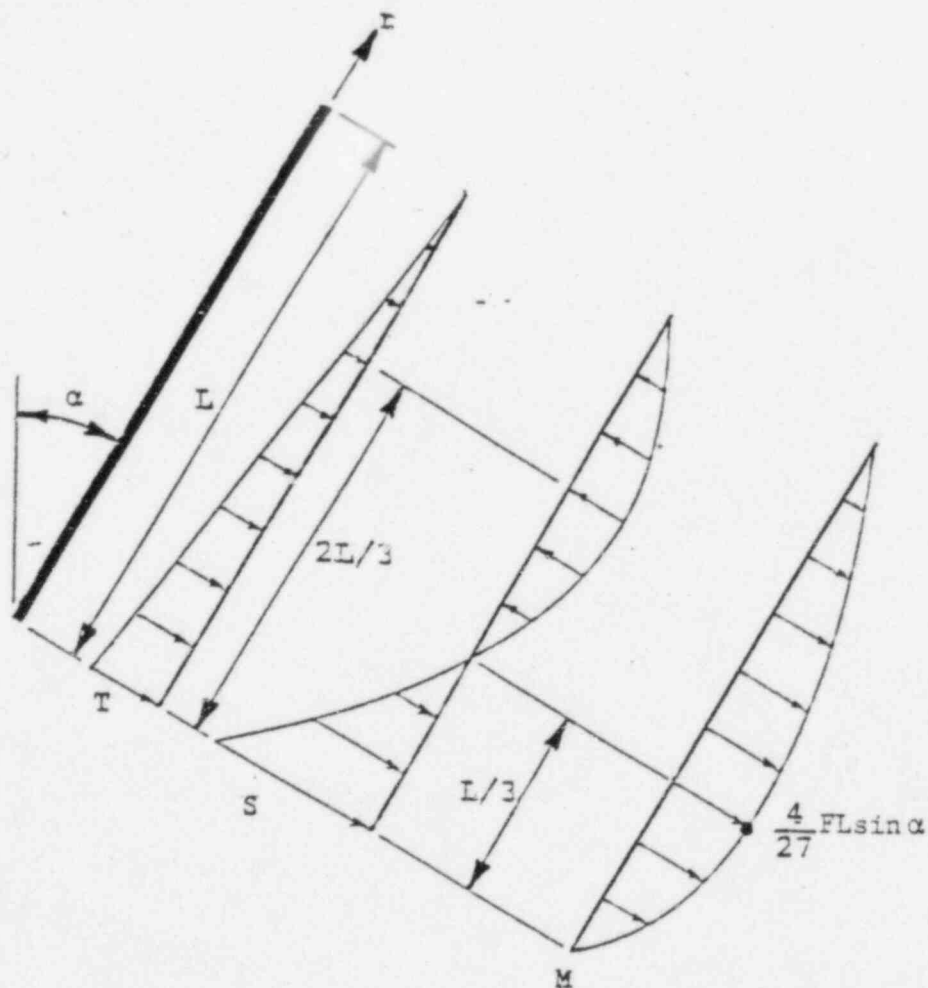
Then,

$$T = F(\cos \alpha)[1 - (r/L)]$$

For convenience, the package internal forces are summarized below:

PARAMETER	EQUATION	MAXIMUM	MINIMUM
Thrust	$F(\cos \alpha)[1 - (r/L)]$	$F(\cos \alpha)$ ( $r = 0$ )	0 ( $r = L$ )
Shear	$F(\sin \alpha)[3r^2 - 4Lr + L^2]/L^2$	$F(\sin \alpha)$ ( $r = 0$ )	0 ( $r = L/3, L$ )
Moment	$F(\sin \alpha)[r^3 - 2Lr^2 + L^2r]/L^2$	$4FL(\sin \alpha)/27$ ( $r = L/3$ )	0 ( $r = 0, L$ )

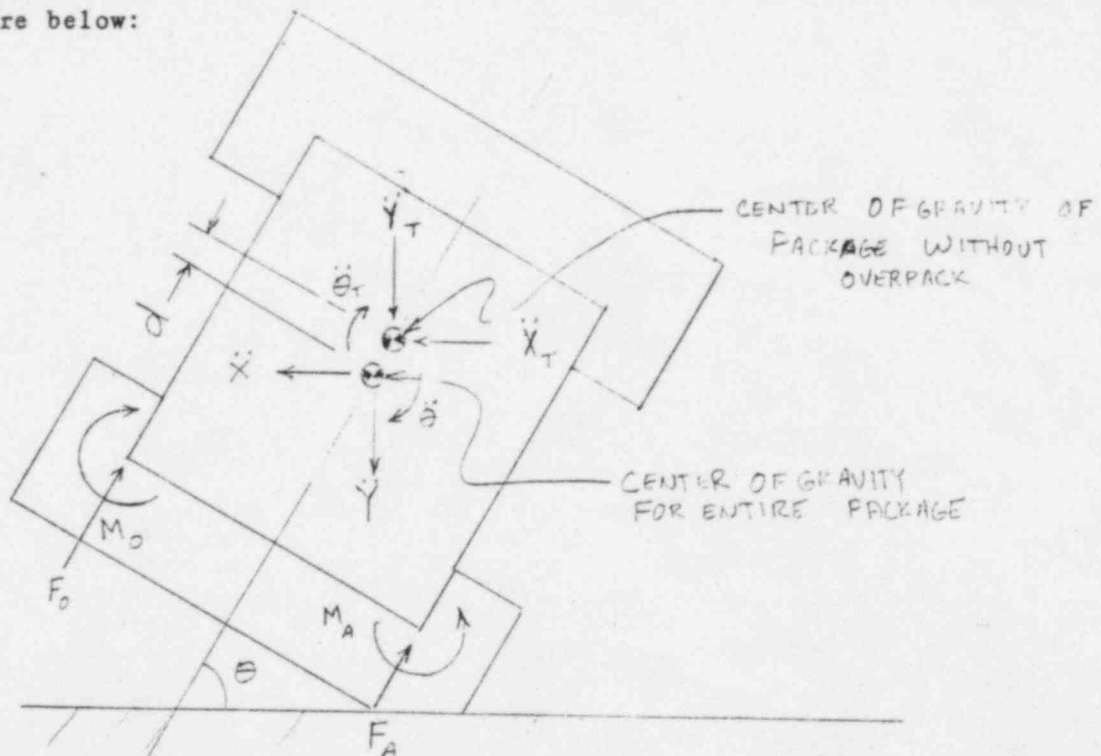
These forces are graphically illustrated below:



#### 2.10.5.2.4 POSTOB Post-processor for OBLIQUE

Overpack attachment forces predicted by OBLIQUE as described in Section 2.10.2.2.2 above are valid and conservative for impact angles near horizontal and near vertical, but recent tests indicate that the overpack attachment forces near c.g. over struck corner are underestimated by the OBLIQUE algorithm. POSTOB was written to more adequately model the physical and inertial forces on the package during impact and to thereby determine the internal forces required to hold the overpack in place throughout the event.

To achieve this, POSTOB calculates the rigid body acceleration of the package center of gravity from the time history of component velocities calculated by OBLIQUE. These accelerations are then translated to the center of gravity of the package without the overpack (and lid if the lid and overpack are restrained by the same load path). The overpack attachment forces are represented as a force and moment acting on the package-overpack interface. See the figure below:



The figure above shows the inertial accelerations at the package c.g. calculated from OBLIQUE data ( $\ddot{X}$ ,  $\ddot{Y}$ , and  $\ddot{\theta}$ ), as well as the inertial accelerations of the package at the center of gravity of the package without the overpack ( $\ddot{X}_T$ ,  $\ddot{Y}_T$  and  $\ddot{\theta}_T$ ).

These values are related by the following equations:

$$\ddot{X}_T = \ddot{X} - d\ddot{\theta}\sin\theta$$

$$\ddot{Y}_T = \ddot{Y} + d\ddot{\theta}\cos\theta + g$$

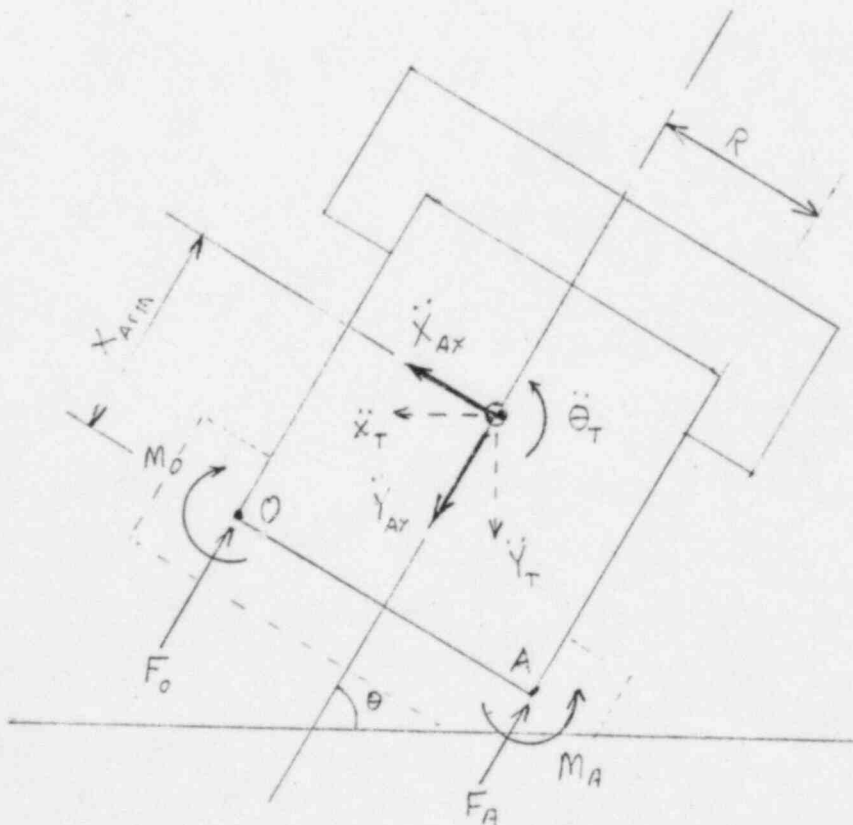
$$\ddot{\theta}_T = \ddot{\theta}$$

Note that gravity acts on the package in the same direction as the inertial acceleration.

These inertial accelerations may be resolved in the package frame of reference by the following equations (see sketch):

$$\ddot{Y}_{AX} = \ddot{Y}_T \sin\theta + \ddot{X}_T \cos\theta$$

$$\ddot{Y}_{AY} = \ddot{X}_T \sin\theta - \ddot{Y}_T \cos\theta$$



To determine the inertial forces at the c.g. of the package without the overpack, some assumptions regarding how the payload reacts must be made. POSTOB conservatively assumes that the inertial force of the payload in the axial direction is entirely reacted by the separation moment, while the payload rotational inertia and lateral inertial forces are reacted by the package sidewalls. Thus, the forces on the package from the overpack may be calculated using standard force and moment balance methods.

As stated above, POSTOB assumes that the attachment forces may be represented as a moment about the corner of the package. In the sketches above, a force and moment around either corner is shown. In reality, only one set of these forces will occur at a time, depending on the geometry of impact. POSTOB calculates the value of the moment required at either point A or point O to balance the inertial forces on the package without the overpack. When both moments calculate to be negative, there is no net force in the attachments. It is physically impossible for both moments to be positive.

The equations for the moment may be obtained by summing the moments around the appropriate point on the package:

$$M_A = I_T \ddot{\theta} - (M_T - M_P) \ddot{Y}_{AXR} - M_T \ddot{X}_{AX} X_{ARM}$$

$$M_O = M_T \ddot{X}_{AX} X_{ARM} - I_T \ddot{\theta}_T - (M_T - M^P) \ddot{Y}_{AXR}$$

Where:

$M_A$  = moment about corner adjacent to impact

$M_O$  = moment about corner opposite impact

$I_T$  = mass moment of inertia of package without overpack but including payload

$M_T$  = mass of package without overpack but including payload

$R$  = radius of cask without overpack



$X_{ARM}$  = distance from overpack point of rotation (either point A or O)  
to center of gravity of package without overpack

Input to POSTOB is of two forms - the first is the actual time history of the impact, output from OBLIQUE by selecting the appropriate print-out option. This output contains velocity and coordinate data for the total package as a function of time after the initial impact. From this information, the accelerations of the package c.g. are easily calculated. The other input file consists only of the following information:

1. The distance the center of gravity of the package is from the center of gravity of the package without the overpack.
2. Mass moment of inertia of the package without overpack but including the payload.
3. Mass of the package without overpack but including payload.
4. Mass of the payload.
5. Location of the attachment interface relative to the end of the package without overpacks. This is essentially the thickness of lid overhanging the sides of the package when the attachment interface is between the lid and the sides of the package rather than between the end of the package and the inside surface of the overpack.
6. Package radius without overpacks.
7. Package length without either overpack.
8. The acceleration of gravity in units consistent with the OBLIQUE output.

Note that POSTOB calculates  $X_{ARM}$  in the equations above as Item 1 plus one-half Item 7 minus Item 5 in the list above.

2.10.5.3 Sample Program Input and Output

This section contains sample input and output tables for the computer codes EYDROP, SYDROP, CYDROP and OBLIQUE. As a descriptive illustration, assume a package with the geometry described below in Figure 2.10.5.3-1.

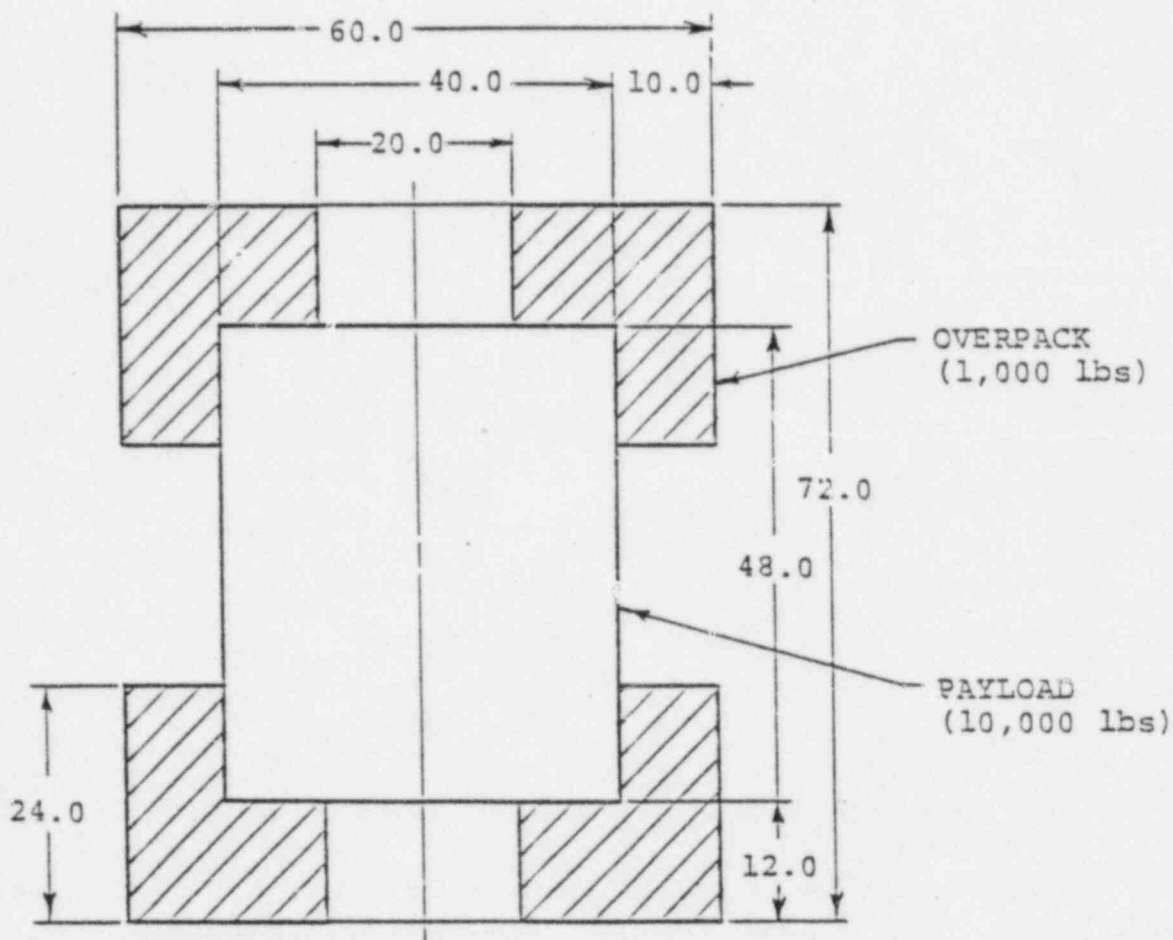


FIGURE 2.10.5.3-1  
Sample Problem Package Geometry

2.10.5.3.1 End Drop Sample Problem

Table 2.10.5.3-1 contains the data input to EYDROP for the above geometry.

PROGRAM EYDROP, VERSION 2, DATE 5/11/81

```

1234567890123456789012345678901234567890123456789012345678901234567890
  V      V      V      V      V      V      V      V      V      V
EYDROP (END DROP) SAMPLE RUN, 20 PCF FOAM OVERPACKS
12000.   60.   20.   12.   30.
   .2     3.     .2
17
0.00     0.00
0.05     668.00
0.10     1337.00
0.15     1345.00
0.20     1315.00
0.25     1347.00
0.30     1411.00
0.35     1507.00
0.40     1673.00
0.45     1901.00
0.50     2206.00
0.55     2523.00
0.60     3283.00
0.65     4242.00
0.70     5908.00
0.75     9058.00
0.80    15322.00

```

TABLE 2.10.5.3-1  
EYDROP Input Table

A summary of each card is as follows:

- Card 1     Problem Title
- Card 2     Package weight   package diameter, overpack hole diameter,  
             overpack end thickness, drop height.
- Card 3     Starting crush depth iteration, ending iteration, increment.
- Card 4     Number of foam curve data points.
- Card 5-N   Foam strain, foam crush stress.

All the required input parameters are straightforward. Table 2.10.5.3-2 contains the sample problem output. Information from this table is essentially self-explanatory. A solution is determined when the kinetic energy of the drop is equal to the strain energy ( $SE/KE = 1$ ) from crushing the foam overpacks.

EYDROP(END)

EYDROP (END DROP) SAMPLE RUN, 20 PCF FOAM OVERPACKS

PACKAGE WEIGHT = 12000. (LBS)  
 PACKAGE DIAMETER = 60.00 (IN)  
 HOLE DIAMETER = 20.00 (IN)  
 OVERPACK DEPTH = 12.00 (IN)  
 DROP HEIGHT = 30.00 (FT)

CRUSH DEPTH (IN)	STRAIN	++++ IMPACT +++++		++++++ ENERGY ++++++		
		FORCE (LBS)	ACCEL. (G)	KINETIC (IN-LB)	STRAIN (IN-LB)	RATIO (SE/KE)
.20	.017	456640.	38.1	4322400.	45664.	.011
.40	.033	1036803.	86.4	4324800.	195008.	.045
.60	.050	1678367.	139.9	4327200.	466575.	.108
.80	.067	2321210.	193.4	4329600.	866583.	.200
1.00	.083	2902211.	241.9	4332000.	1383925.	.321
1.20	.100	3360248.	280.0	4334400.	2015171.	.465
1.40	.117	3474214.	289.5	4336800.	2698617.	.622
1.60	.133	3461585.	288.5	4339200.	3392197.	.782
1.80	.150	3380354.	281.7	4341600.	4076391.	.939
2.00	.167	3353421.	279.5	4344000.	4749769.	1.093
2.20	.183	3325186.	277.1	4346400.	5417629.	1.246
2.40	.200	3304955.	275.4	4348800.	6080643.	1.398
2.60	.217	3318173.	276.5	4351200.	6742956.	1.550
2.80	.233	3345913.	273.8	4353600.	7409365.	1.702

TABLE 2.10.5.3-2

EYDROP Output

In this case, a linear interpolation of the SE/KE ratio results in a crush depth of approximately 1.88 inches and an acceleration of almost 281 g's. Equations for EYDROP are discussed in Section 2.10.5.1.1.

2.10.5.3.2 Side Drop Sample Problem

Table 2.10.5.3-3 contains the data input to SYDROP for the sample problem package geometry.

PROGRAM SYDROP, VERSION 3, DATE 1/28/85

123456789012345678901234567890123456789012345678901234567890  
 V V V V V V V V  
 SYDROP (SIDE DROP) SAMPLE RUN, 20 PCF FOAM OVERPACKS  
 12000. 48. 60. 40. 30.

17  
 0.00 0.00  
 0.05 668.00  
 0.10 1337.00  
 0.15 1345.00  
 0.20 1315.00  
 0.25 1347.00  
 0.30 1411.00  
 0.35 1507.00  
 0.40 1673.00  
 0.45 1901.00  
 0.50 2204.00  
 0.55 2623.00  
 0.60 3288.00  
 0.65 4242.00  
 0.70 5908.00  
 0.75 9058.00  
 0.80 15322.00  
 150 .25 6.0 .25

TABLE 2.10.5.3-3  
 SYDROP Input Table

A summary of each card is as follows:

Card 1 Problem Title

Card 2 Package weight, overpack length, package diameter, payload diameter, drop height.

Card 3 Number of foam curve data points.

Card 4-N Foam strain, foam crush stress

Card N+1 Number of integration points, starting crush depth iteration,  
ending iteration, increment.

As with the end drop problem, all required input parameters are straightforward. The chosen number of integration points (150) is based upon previous parametric study for the side drop geometry. Increasing the number will alter the end results by only a fraction of one percent. As with EYDROP, a solution is determined when the kinetic energy of the drop is equal to the strain energy from crushing the foam overpacks. Table 2.10.5.3-4 contains the SYDROP output. Equations for SYDROP are discussed in Section 2.10.5.1.2.

TABLE 2.10.5.3-4

## SYDROP Output

SYDROP(SIDE)      NUCLEAR PACKAGING PROPRIETARY      18.09.59      85/03/16      PAGE 1

SYDROP (SIDE DROP) SAMPLE RUN, 20 PCF FOAM OVERPACKS

PACKAGE HEIGHT      = 12000. (LBS)  
 PACKAGE EXTERNAL LENGTH      = 48.00 (IN)  
 PACKAGE EXTERNAL DIAMETER      = 60.00 (IN)  
 PAYLOAD DIAMETER      = 40.00 (IN)  
 DROP HEIGHT      = 30.00 (FT)

## STRAIN VS STRESS TABLE

PT	STRAIN	STRESS
1	0.00	0.00
2	.05	668.00
3	.10	1337.00
4	.15	1345.00
5	.20	1315.00
6	.25	1347.00
7	.30	1411.00
8	.35	1507.00
9	.40	1673.00
10	.45	1901.00
11	.50	2204.00
12	.55	2623.00
13	.60	3288.00
14	.65	4242.00
15	.70	5908.00
16	.75	9058.00
17	.80	15322.00

SYDROP(SIDE)      NUCLEAR PACKAGING PROPRIETARY      18.09.59      85/03/16      PAGE 2

SYDROP (SIDE DROP) SAMPLE RUN, 20 PCF FOAM OVERPACKS

CRUSH DEPTH (IN)	++ CRUSH PLANE ++		++++ IMPACT ++++		***** ENERGY *****		RATIO (SE/PE)	DISTRIBUTION OF STRAIN RATIOS BY PERCENT OF CONTACT AREA				
	AREA (IN <sup>2</sup> )	VOLUME (IN <sup>3</sup> )	FORCE (LBS)	ACCEL. (G)	POTENTIAL (IN-LB)	STRAIN (IN-LB)		LE.70	GT.70	GT.80	GT.90	GT.95
.25	371.0	62.	82479.	6.9	4323000.	10310.	.002	100.00	0.00	0.00	0.00	0.00
.50	523.6	175.	232610.	19.4	4326000.	49671.	.011	100.00	0.00	0.00	0.00	0.00
.75	639.9	321.	449672.	37.5	4329000.	134931.	.031	100.00	0.00	0.00	0.00	0.00
1.00	737.4	493.	675582.	56.3	4332000.	275588.	.064	100.00	0.00	0.00	0.00	0.00
1.25	822.7	688.	857486.	71.5	4335000.	467222.	.108	100.00	0.00	0.00	0.00	0.00
1.50	899.3	904.	989341.	82.4	4338000.	698075.	.161	100.00	0.00	0.00	0.00	0.00
1.75	969.3	1138.	1096877.	91.4	4341000.	958852.	.221	100.00	0.00	0.00	0.00	0.00
2.00	1034.0	1388.	1191399.	99.3	4344000.	1244887.	.287	100.00	0.00	0.00	0.00	0.00
2.25	1094.3	1654.	1281336.	106.8	4347000.	1553979.	.357	100.00	0.00	0.00	0.00	0.00
2.50	1151.0	1935.	1370454.	114.2	4350000.	1885452.	.433	100.00	0.00	0.00	0.00	0.00
2.75	1204.6	2229.	1459288.	121.6	4353000.	2239170.	.514	100.00	0.00	0.00	0.00	0.00
3.00	1255.4	2537.	1549023.	129.1	4356000.	2615209.	.600	100.00	0.00	0.00	0.00	0.00
3.25	1303.8	2857.	1640286.	136.7	4359000.	3013873.	.691	100.00	0.00	0.00	0.00	0.00
3.50	1350.0	3189.	1735198.	144.6	4362000.	3435808.	.788	100.00	0.00	0.00	0.00	0.00
3.75	1394.3	3532.	1837541.	153.1	4365000.	3882401.	.889	100.00	0.00	0.00	0.00	0.00
4.00	1436.8	3886.	1949171.	162.4	4368000.	4355740.	.997	100.00	0.00	0.00	0.00	0.00
4.01	1437.8	3895.	1952158.	162.7	4368074.	4368082.	1.000	100.00	0.00	0.00	0.00	0.00
4.25	1477.7	4250.	2070772.	172.6	4371000.	4858233.	1.111	100.00	0.00	0.00	0.00	0.00
4.50	1517.1	4624.	2203828.	183.7	4374000.	5392558.	1.233	100.00	0.00	0.00	0.00	0.00
4.75	1555.2	5008.	2349512.	195.8	4377000.	5961725.	1.362	100.00	0.00	0.00	0.00	0.00
5.00	1592.0	5402.	2510461.	209.2	4380000.	6569222.	1.500	100.00	0.00	0.00	0.00	0.00
5.25	1627.6	5804.	2688622.	224.1	4383000.	7219107.	1.647	100.00	0.00	0.00	0.00	0.00
5.50	1662.1	6216.	2890243.	240.9	4386000.	7916465.	1.805	100.00	0.00	0.00	0.00	0.00
5.75	1695.5	6635.	3125496.	260.5	4389000.	8668433.	1.975	100.00	0.00	0.00	0.00	0.00
6.00	1728.0	7063.	3401972.	283.5	4392000.	9484366.	2.159	100.00	0.00	0.00	0.00	0.00



2.10.5.3.3 Corner Drop Sample Problem

Table 2.10.5.3-5 contains the data input to CYDROP for the sample problem package geometry.

PROGRAM CYDROP, VERSION 3, DATE 2/07/84

```

123456789012345678901234567890123456789012345678901234567890
  V          V          V          V          V          V          V
CYDROP (CORNER DROP) SAMPLE RUN, 20 PCF FOAM OVERPACKS
12000.      72.      60.      48.      40.      20.      24.
  30.      39.8
1100.      17
  0.00      0.00
  0.05      668.00
  0.10      1337.00
  0.15      1345.00
  0.20      1315.00
  0.25      1347.00
  0.30      1411.00
  0.35      1507.00
  0.40      1673.00
  0.45      1901.00
  0.50      2204.00
  0.55      2623.00
  0.60      3288.00
  0.65      4242.00
  0.70      5908.00
  0.75      9058.00
  0.80      15322.00
25 25.512 15.37 .512

```

TABLE 2.10.5.3-5  
CYDROP Input Table

A summary of each card is as follows:

Card 1 Problem Title

Card 2 Package weight, package length, package diameter, payload length, payload diameter, overpack hole diameter, overpack length.

Card 3 Drop height, angle from vertical.



Card 4     Unbacked foam crush stress, number of foam curve data points.

Card 5-N   Foam strain, foam crush stress.

Card N+1   Number of integration points along crush plane semi-minor ellipse axis, number of integration points along crush plane semi-major ellipse axis, starting crush depth iteration, ending iteration, increment.

The angle from vertical to execute a center of gravity over struck corner impact is calculated as:

$$\theta = \tan^{-1}(60.0/72.0) = 39.8^{\circ}$$

The unbacked foam crush stress is the foam compressive yield strength, about 1,100 psi for the 20 pcf foam. Program default for this entry is to assume the foam crush stress at 10% strain, a value usually close to the plateau compressive strength.

Similar to SYDROP, the number of integration points chosen for CYDROP (25) have been determined from a parametric evaluation. Additional points are unnecessarily time consuming and provide very little change in the end results.

Table 2.10.5.3-6 contains the CYDROP output for the sample problem. CYDROP also calculates the percentage of foam in the crush area less than and greater than 80% foam strain in the backed and unbacked regions. The foam data used in the drop analyses provide accurate empirical relationships to 80% strain. This calculation is carried into the force and strain energy results to provide the program user with information on solution reliability.

Energy equilibrium for the sample problem may be linearly interpolated to a crush depth of about 10.6 inches and an acceleration of 106.5 g's. The distribution of strain energy ratios for this problem indicate the foam stress data interpolated from the input file never exceeded 70% strain.

Linear interpolation of the sensitivity analysis shows approximately 24.5% of the total crush area was unbacked. Additionally, further interpolation shows the unbacked foam accounted for about 17.5% of the total force and 8.7% of the strain energy at  $SE/KE = 1$ . Equations for CYDROP are discussed in Section 2.10.5.1.3.

CYDROP(CORNER)

NUCLEAR PACKAGING PROPRIETARY

10.11.19

84/02/14

PAGE 1

## CYDROP (CORNER DROP) SAMPLE RUN. 20 PCF FOAM OVERPACKS

PACKAGE WEIGHT \* 12000. (LBS)  
 PACKAGE EXTERNAL LENGTH \* 72.00 (IN)  
 PACKAGE EXTERNAL DIAMETER \* 60.00 (IN)  
 PACKAGE EXTERNAL HOLE DIA \* 20.00 (IN)  
 PAYLOAD ENVELOPE LENGTH \* 48.00 (IN)  
 PAYLOAD ENVELOPE DIAMETER \* 40.00 (IN)  
 OVERPACK LENGTH \* 24.00 (IN)

DROP HEIGHT \* 30.00 (FT)  
 ORIENTATION ANGLE \* 39.800 (DEGREES WRT TO VERTICAL)

PLATEAU CRUSH STRESS \* 1100.00 (PSI)  
 (DEFAULT TAKEN AT 10 PCT STRAIN)

STRESS/STRAIN EVALUATED IN 1/2 CRUSH PLANE ELLIPSE AT:  
 NX \* 25 POINTS PARALLEL TO SEMI-MINOR ELLIPSE AXIS  
 NY \* 25 POINTS PARALLEL TO SEMI-MAJOR ELLIPSE AXIS

## EXPERIMENTAL STRAIN-VS. STRESS VALUES

PT	STRAIN	STRESS
1	0.00	0.00
2	.05	668.00
3	.10	1337.00
4	.15	1345.00
5	.20	1315.00
6	.25	1347.00
7	.30	1411.00
8	.35	1507.00
9	.40	1673.00
10	.45	1901.00
11	.50	2204.00
12	.55	2625.00
13	.60	3258.00
14	.65	4242.00
15	.70	5908.00
16	.75	9058.00
17	.80	15322.00

TABLE 2.10.5.3-6

CYDROP Output

CYDROP(CORNER)

NUCLEAR PACKAGING PROPRIETARY

10.11.20

84/02/14

PAGE 2

## CYDROP (CORNER DROP) SAMPLE RUN, 20 PCF FOAM OVERPACKS

CRUSH DEPTH (IN)	** CRUSH PLANE **		*** IMPACT ***		***** ENERGY *****			DISTRIBUTION OF STRAIN RATIOS BY PERCENT OF CONTACT AREA				
	AREA (IN <sup>2</sup> )	VOLUME (IN <sup>3</sup> )	FORCE (LBS)	ACCEL. (G)	KINETIC (IN-LBS)	STRAIN (IN-LBS)	RATIO (SE/KE)	LE.70 LE.80	GT.70 LE.90	GT.80 LE.95	GT.90 LE.95	GT.95 LE.95
.51	9.6	2.	1386.	.1	4326144.	355.	.000	100.00	0.00	0.00	0.00	0.00
1.02	26.3	12.	8775.	.7	4332288.	2956.	.001	100.00	0.00	0.00	0.00	0.00
1.54	49.3	31.	25334.	2.1	4338432.	11688.	.003	100.00	0.00	0.00	0.00	0.00
2.05	74.9	63.	51131.	4.3	4344576.	31263.	.007	100.00	0.00	0.00	0.00	0.00
2.56	103.9	109.	83257.	6.9	4350720.	65666.	.015	100.00	0.00	0.00	0.00	0.00
3.07	135.6	170.	119934.	10.0	4356864.	117683.	.027	100.00	0.00	0.00	0.00	0.00
3.58	169.6	248.	160452.	13.4	4363008.	189462.	.043	100.00	0.00	0.00	0.00	0.00
4.10	205.7	344.	204557.	17.0	4369152.	282904.	.065	100.00	0.00	0.00	0.00	0.00
4.61	243.6	459.	252250.	21.0	4375296.	399847.	.091	100.00	0.00	0.00	0.00	0.00
5.12	283.1	594.	304305.	25.4	4381440.	542325.	.124	100.00	0.00	0.00	0.00	0.00
5.63	324.1	749.	361485.	30.1	4387584.	712767.	.162	100.00	0.00	0.00	0.00	0.00
6.14	366.4	926.	422256.	35.2	4393728.	913405.	.208	100.00	0.00	0.00	0.00	0.00
6.66	409.8	1123.	490795.	40.9	4399872.	1147146.	.261	100.00	0.00	0.00	0.00	0.00
7.17	454.3	1366.	568073.	47.3	4406016.	1418216.	.322	100.00	0.00	0.00	0.00	0.00
7.68	499.7	1590.	648625.	54.1	4412160.	1729691.	.392	100.00	0.00	0.00	0.00	0.00
8.19	545.9	1858.	736216.	61.4	4418304.	2084210.	.472	100.00	0.00	0.00	0.00	0.00
8.70	592.8	2149.	826311.	68.9	4424448.	2484217.	.561	100.00	0.00	0.00	0.00	0.00
9.22	640.2	2465.	927107.	77.3	4430592.	2933092.	.662	100.00	0.00	0.00	0.00	0.00
9.73	688.2	2805.	1046738.	87.2	4436736.	3438397.	.775	100.00	0.00	0.00	0.00	0.00
10.24	736.6	3170.	1181164.	98.4	4442880.	4008740.	.902	100.00	0.00	0.00	0.00	0.00
10.75	785.3	3560.	1322256.	110.2	4449024.	4649615.	1.045	100.00	0.00	0.00	0.00	0.00
11.26	834.2	3974.	1483405.	123.6	4455168.	5367864.	1.205	99.33	.67	0.00	0.00	0.00
11.78	883.3	4414.	1678677.	139.9	4461312.	6177357.	1.385	98.69	1.31	0.00	0.00	0.00
12.29	932.4	4879.	1920373.	160.0	4467456.	7098714.	1.589	96.31	3.69	0.00	0.00	0.00
12.80	981.5	5369.	2246590.	187.2	4473600.	8165457.	1.825	95.07	4.49	.44	0.00	0.00
13.31	1030.5	5884.	2652834.	221.1	4479744.	9419709.	2.103	92.95	5.75	1.30	0.00	0.00
13.82	1079.4	6426.	3155349.	262.9	4485888.	10906604.	2.431	91.07	6.12	2.82	0.00	0.00
14.34	1128.0	6989.	3762296.	313.5	4492032.	12677521.	2.822	88.97	6.72	4.09	.22	0.00
14.85	1176.2	7579.	4496986.	374.7	4498176.	14791897.	3.288	87.74	6.26	4.70	1.30	0.00
15.36	1224.0	8193.	5345237.	445.4	4504320.	17311506.	3.843	85.38	6.02	6.15	1.07	.87

CYDROP(CORNER)

NUCLEAR PACKAGING PROPRIETARY

10.11.27

84/02/14

PAGE 3

## CYDROP (CORNER DROP) SAMPLE RUN, 20 PCF FOAM OVERPACKS

## SENSITIVITY ANALYSIS OF STRAIN ASSUMPTIONS

CRUSH DEPTH (IN)	**** CRUSH AREA ****				**** IMPACT FORCE ****				**** STRAIN ENERGY ****				STRAIN TO KINETIC ENERGY RATIO
	TOTAL AREA (IN <sup>2</sup> )	PCT DISTRIBUTION BACKED		MAX STRAIN	TOTAL FORCE (LBS)	PCT DISTRIBUTION BACKED		MAX STRAIN	TOTAL ENERGY (IN-LBS)	PCT DISTRIBUTION BACKED		MAX STRAIN	
		UN- BACKED	LT	GT		UN- BACKED	LT	GT		UN- BACKED	LT	GT	
.51	10.	0.0	100.0	0.0	1386.	0.0	100.0	0.0	355.	0.0	100.0	0.0	0.000
1.02	27.	0.0	100.0	0.0	8775.	0.0	100.0	0.0	2956.	0.0	100.0	0.0	.001
1.54	49.	0.0	100.0	0.0	25334.	0.0	100.0	0.0	11688.	0.0	100.0	0.0	.003
2.05	76.	0.0	100.0	0.0	51131.	0.0	100.0	0.0	31263.	0.0	100.0	0.0	.007
2.56	105.	0.0	100.0	0.0	83257.	0.0	100.0	0.0	65666.	0.0	100.0	0.0	.015
3.07	135.	0.0	100.0	0.0	119934.	0.0	100.0	0.0	117683.	0.0	100.0	0.0	.027
3.58	173.	0.0	100.0	0.0	160452.	0.0	100.0	0.0	189462.	0.0	100.0	0.0	.043
4.	211.	0.0	100.0	0.0	204557.	0.0	100.0	0.0	282904.	0.0	100.0	0.0	.065
4.61	250.	0.0	100.0	0.0	252250.	0.0	100.0	0.0	399847.	0.0	100.0	0.0	.091
5.12	292.	.3	99.7	0.0	304305.	.3	99.7	0.0	542325.	0.0	100.0	0.0	.124
5.63	335.	1.0	99.0	0.0	361485.	1.0	99.0	0.0	712767.	.2	99.8	0.0	.162
6.14	380.	1.5	98.5	0.0	422256.	1.5	98.5	0.0	913405.	.4	99.6	0.0	.208
6.66	427.	2.9	97.1	0.0	490795.	2.7	97.3	0.0	1147146.	.8	99.2	0.0	.261
7.17	475.	5.5	94.5	0.0	568073.	5.0	95.0	0.0	1418216.	1.4	98.4	0.0	.322
7.68	524.	7.2	92.8	0.0	648625.	6.4	93.6	0.0	1729691.	2.2	97.8	0.0	.392
8.19	575.	10.6	89.4	0.0	736216.	9.1	90.9	0.0	2084210.	3.1	96.7	0.0	.472
8.70	626.	12.4	87.6	0.0	826311.	10.3	89.7	0.0	2484217.	4.2	95.8	0.0	.561
9.22	679.	14.7	85.3	0.0	927107.	11.9	88.1	0.0	2933092.	5.3	94.7	0.0	.662
9.73	733.	19.0	81.0	0.0	1046738.	14.6	85.4	0.0	3438397.	6.4	93.6	0.0	.775
10.24	788.	22.7	77.3	0.0	1181164.	16.7	83.3	0.0	4008740.	7.8	92.2	0.0	.902
10.75	844.	25.3	74.7	0.0	1322256.	17.8	82.2	0.0	4649615.	9.1	90.9	0.0	1.045
11.26	900.	30.3	69.7	0.0	1483405.	20.2	79.8	0.0	5367864.	10.4	89.6	0.0	1.205
11.78	957.	32.2	67.8	0.0	1678677.	20.2	79.8	0.0	6177357.	11.7	88.3	0.0	1.385
12.29	1015.	36.4	63.6	0.0	1920373.	21.2	78.8	0.0	7098714.	12.9	87.1	0.0	1.589
12.80	1074.	37.0	62.6	.4	2246590.	19.4	77.2	3.3	8165457.	13.5	85.9	.2	1.825
13.31	1131.	38.6	60.1	1.3	2652834.	18.1	71.6	10.3	9419709.	14.5	84.4	1.2	2.103
13.82	1183.	42.0	55.2	2.8	3155349.	17.3	62.0	20.7	10906604.	14.9	81.9	3.2	2.431
14.34	1237.	43.9	51.8	4.3	3762296.	15.9	53.7	30.4	12677521.	15.1	78.5	6.4	2.822
14.85	1289.	44.1	49.9	6.0	4496986.	13.9	46.8	39.3	14791897.	15.1	74.4	10.5	3.288
15.36	1343.	45.4	46.3	6.1	5345237.	12.5	38.3	48.9	17311506.	14.8	69.7	15.4	3.843

CYDROP Output

(continued)

2.10.5.3.4 Oblique Impact Sample Input

Table 2.10.5.3-7 contains the data input to OBLIQUE for the sample problem package geometry. Equations for OBLIQUE are discussed in Section 2.10.5.2.

PROGRAM OBLIQUE VERSION 7, DATE 9/15/83

12345678901234567890123456789012345678901234567890123456789012345678901234567890
V          V          V          V          V          V          V          V
OBLIQUE SAMPLE RUN, 20 PCF FOAM OVERPACKS
48.      20.      24.      10.      12.
31.056     12574.     386.4
.25      12.      .25      10.      10.
5.      10.      20.      30.      40.      50.
60.      70.      80.      85.
-527.45     85.      5.      -5.      0.      3.

TABLE 2.10.5.3-7  
OBLIQUE Input Table

A summary of each card is as follows:

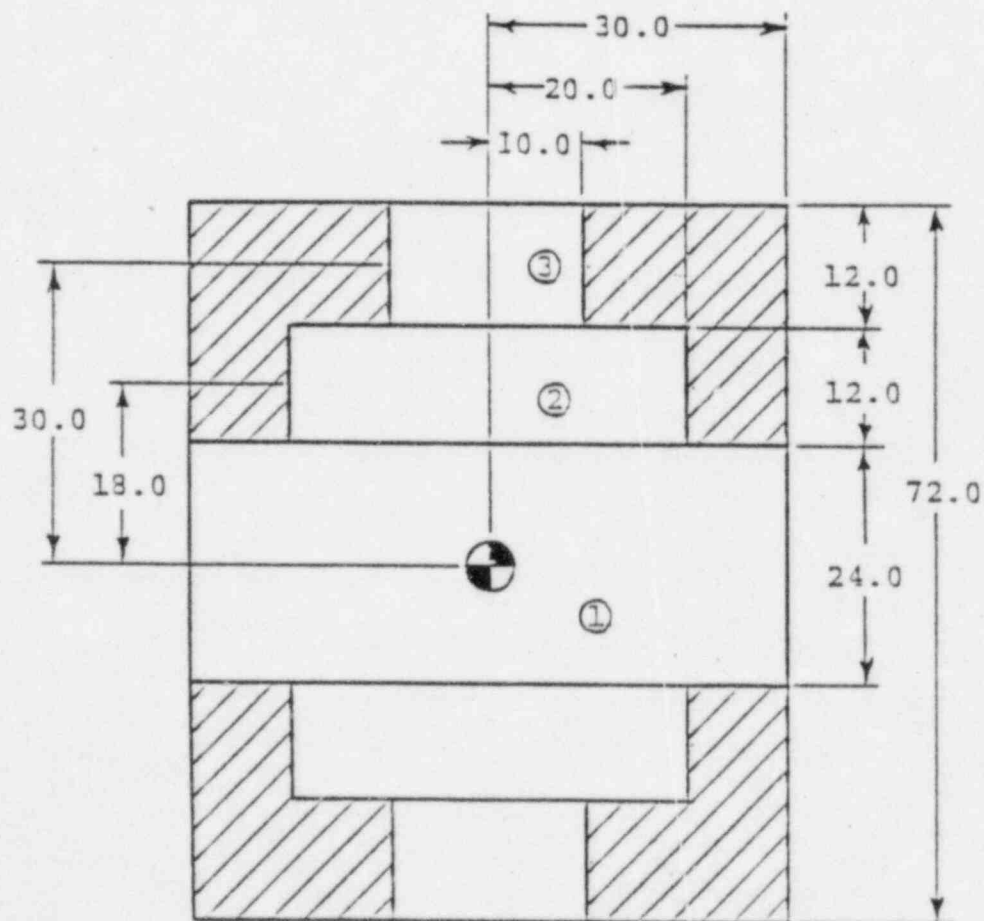
- Card 1    Problem title
- Card 2    Payload length, payload radius, overpack length, overpack side thickness, overpack end thickness.
- Card 3    Package mass, radial mass moment of inertia about the center of gravity, gravitational acceleration.
- Card 4    Starting deflection, ending deflection, deflection increment, number of angles, print control.
- Card 5-N   Angles (6 per card, 24 maximum)

Card N+1 Package free-fall velocity, output starting angle, output ending angle, angle increment, friction coefficient, estimated deflection, package translational velocity, package rotational velocity.

The package mass, assuming a gravitation acceleration of  $386.4 \text{ in/sec}^2$ , is:

$$m = 12,000/386.4 = 31.056 \text{ lb-sec}^2/\text{in}$$

The radial mass moment of inertia of the system is calculated, knowing the payload and overpack weights, using composite sections:



For the Payload:

$$I_p = m(R^2 + L^2/3)/4$$

Where:

$$m = 10,000/386.4 = 25.88 \text{ lb-sec}^2/\text{in}$$

$$R = 40.0/2 = 20.0 \text{ in}$$

$$L = 48.0 \text{ in}$$

Then,

$$\begin{aligned} I_p &= 25.88[(20.0)^2 + (48.0)^2/3]/4 \\ &= 7,557 \text{ lb-in-sec}^2 \end{aligned}$$

For the overpacks:

$$\begin{aligned} I_{op} &= m[R^2 + (L^2/3)]/4 - m_1[R_1^2 + (L_1^2/3)]/4 - 2m_2[R_2^2 \\ &\quad + (L_2^2/3)]/4 - 2m_2d_2^2 - 2m_3[R_3^2 + (L_3^2/3)]/4 - 2m_3d_3^2 \end{aligned}$$

Where:

$$m = \bar{m}\pi R^2 L$$

$$\bar{m} = W_{op}/(386.4)V_{op}$$

$$W_{op} = 1,000 \text{ lbs}$$

$$\begin{aligned} V_{op} &= \pi[(30.0)^2 - (20.0)^2]24.0 + \pi[(20.0)^2 - (10.0)^2]12.0 \\ &= 49,009 \text{ in}^3 \end{aligned}$$

$$\bar{m} = 1,000/[(386.4)49,009] = 5.28(10)^{-5} \text{ lb-sec}^2/\text{in}^3$$

$$R = 30.0 \text{ in}$$

$$L = 72.0 \text{ in}$$

$$m = [5.28(10)^{-5}] \pi (30.0)^2 (72.0) = 10.75 \text{ lb-sec}^2/\text{in}$$

$$m_1 = \bar{m} \pi R_1^2 L_1$$

$$R_1 = 30.0 \text{ in}$$

$$L_1 = 24.0 \text{ in}$$

$$m_1 = [5.28(10)^{-5}] \pi (30.0)^2 (24.0) = 3.583 \text{ lb-sec}^2/\text{in}$$

$$m_2 = \bar{m} \pi R_2^2 L_2$$

$$R_2 = 20.0 \text{ in}$$

$$L_2 = 12.0 \text{ in}$$

$$m_2 = [5.28(10)^{-5}] \pi (20.0)^2 (12.0) = 0.7962 \text{ lb-sec}^2/\text{in}$$

$$m_3 = \bar{m} \pi R_3^2 L_3$$

$$R_3 = 10.0 \text{ in}$$

$$L_3 = 12.0 \text{ in}$$

$$m_3 = [5.28(10)^{-5}] \pi (10.0)^2 (12.0) = 0.1991 \text{ lb-sec}^2/\text{in}$$

$$d_2 = 18.0 \text{ in}$$

$$d_3 = 30.0 \text{ in}$$

Then,

$$\begin{aligned}
 I_{op} &= 10.75[(30.0)^2 + (72.0)^2/3]/4 - 3.583[(30.0)^2 + (24.0)^2/3]/4 \\
 &\quad - 2(0.7962)[(20.0)^2 + (12.0)^2/3]/4 - 2(0.7962)(18.0)^2 \\
 &\quad - 2(0.1991)[(10.0)^2 + (12.0)^2/3]/4 - 2(0.1991)(30.0)^2 \\
 &= 5,017 \text{ lb-in-sec}^2
 \end{aligned}$$

Finally,

$$I = 7,557 + 5,017 = 12,574 \text{ lb-in-sec}^2$$

The starting deflection, ending deflection, and deflection increment are values set to build a uniform force/deflection table for use by OBLIQUE. Prior to use of OBLIQUE, a tape holding force/deflection data (Table 2.10.5.3-8) over the range of angles from  $5^\circ$  to  $85^\circ$  is created by CYDROP. OBLIQUE, in turn, reads the tape and converts the force/deflection data to a uniform table for each specified angle. Note that the angles specified in OBLIQUE are with respect to horizontal whereas CYDROP references vertical. The magnitude of the ending deflection must be chosen such that it is greater than the maximum deflection expected in OBLIQUE, yet need not exceed the maximum possible deflection in the corner drop evaluation.

The print control determines whether the output will be a tabular summary or a time history table.

Package free-fall velocity is based on the drop height. From the equations of motion:

$$V = -(2gh)^{0.5}$$

Where:

$$g = 386.4 \text{ in/sec}^2$$

$$h = 30 \text{ ft} = 360 \text{ in}$$



TABLE 2.10.5.3-8  
CYDROP Force/Deflection Data

12345678901	2345678901	2345678901	2345678901	2345678901	2345678901	2345678901	2345678901	2345678901	2345678901
V	V	V	V	V	V	V	V	V	V
.55	11.01	.55							
32367.	128991.	205207.	334008.	477903.	583552.	677442.	758737.		
845422.	934841.	1038385.	1135477.	1268206.	1515395.	1751333.	2111306.		
2821622.	3527691.	5437239.	8027229.						
.60	11.93	.60							
18240.	67473.	121760.	173898.	258462.	368714.	504353.	634713.		
743455.	842066.	941411.	1049548.	1178914.	1320453.	1509786.	1859217.		
2337319.	3044434.	4269526.	6258679.						
.67	13.49	.67							
12193.	56671.	91499.	113057.	156188.	229526.	313617.	404088.		
501563.	609987.	733768.	880232.	1023819.	1173033.	1357047.	1585754.		
1992534.	2555789.	3396621.	4655222.						
.73	14.65	.73							
5028.	21986.	51813.	100182.	163505.	232741.	304621.	381703.		
465956.	560855.	668431.	792142.	937642.	1114234.	1326595.	1593802.		
1971609.	2595205.	3524784.	4638336.						
.77	15.39	.77							
3109.	20093.	57039.	108821.	168429.	234305.	311057.	394634.		
486876.	592357.	705257.	841422.	999463.	1197891.	1441110.	1764085.		
2248183.	2989067.	4003001.	5295208.						
.78	15.63	.78							
4255.	26380.	68840.	123526.	187139.	259087.	340108.	434086.		
543328.	667914.	804180.	958380.	1156760.	1371183.	1650632.	2040733.		
2621016.	3413833.	4478667.	5815325.						
.77	15.39	.77							
4057.	26494.	76869.	148989.	234326.	330652.	436820.	555823.		
687002.	828086.	979995.	1150114.	1341620.	1566648.	1844710.	2230726.		
2842792.	3730696.	4961650.	6537525.						
.73	14.69	.73							
13772.	68814.	132583.	236890.	366604.	500474.	640691.	801924.		
979105.	1151239.	1316710.	1487169.	1694739.	1946953.	2263342.	2722947.		
3482689.	4608111.	6214733.	8341342.						
.63	13.55	.63							
52820.	216804.	345960.	547724.	819178.	1093308.	1315683.	1515427.		
1750771.	1988978.	2293295.	2677752.	3097958.	3572765.	4040177.	4728886.		
6012544.	8077597.	10828178.	14261926.						
.64	12.83	.64							
132903.	468917.	829010.	1274790.	1673088.	2085488.	2617955.	3024971.		
3080822.	3176792.	3326468.	3552364.	3876190.	4362971.	5134758.	6525535.		
9073079.	12696963.	17334716.	22304149.						

Then,

$$V = -[2(386.4)(360)]^{0.5} = -527.45 \text{ in/sec}$$

The output starting angle, ending angle, and angle increment specify the OBLIQUE analysis package angles of impact with respect to the horizon. The sample problem specified solutions at angles of  $5^\circ$  to  $85^\circ$  in  $5^\circ$  increments. The friction coefficient is usually set to zero. Package translational and rotational velocities are parameters specified to study the effects of secondary impacts.

The sample problem output for OBLIQUE is found in Table 2.10.5.3-9. For each specified angle of impact the magnitude of FMAX is determined as the maximum value of the vector summation of the thrust and shear forces at some instantaneous package angle during the analysis. Note that the maximum value of the package internal forces, moments, and deflections do not necessarily happen at the same instantaneous angle. When all parameters have achieved a maximum value, the problem terminates for that specified angle of impact. OBLIQUE continues the analysis at each angle of impact.

Additionally, OBLIQUE utilizes the methods delineated in Section 2.10.5.2.2 to determine the maximum overpack separation moments about the opposite and adjacent corners in the overpack. As before, a solution occurs when the maximum value is found for each moment at some instantaneous angle, not necessarily the same instantaneous angle for each moment. A negative moment denotes overpack compression and a positive moment overpack separation.

TABLE 2.10.5.3-9

## OBLIQUE Output

## NUPAC OBLIQUE ANALYSIS-OBLIQUE SAMPLE RUN, 20 PCF FOAM OVERPACKS

PACKAGE GEOMETRY-  
 LENGTH = 48.000  
 RADIUS = 20.000  
 OVERPACK LENGTH = 24.000  
 OVERPACK SIDE THICKNESS = 10.000  
 OVERPACK BOTTOM THICKNESS = 12.000  
 PACKAGE MASS PROPERTIES-  
 MASS = 31.056  
 MASS MOMENT OF INERTIA = 12574.000  
 GRAVITATIONAL CONSTANT = 336.400  
 SOLUTION CHARACTERISTICS-  
 IMPACT VELOCITY (YDOT) = -527.450  
 (XDOT) = 0.000  
 (THETADOT) = 0.000  
 FRICTION COEFFICIENT = 0.000  
 ESTIMATED CRUSH DEPTH = 3.000

THETA0	FMAX	SHEAR	THRUST	MOMENT	DEFLECTION	CLEARANCE
85.0000	1730212.	114405.	1727493.	813544.	3.30	9.23
80.0000	1330952.	137346.	1319863.	1335795.	4.81	8.56
75.0000	1240256.	266731.	1213409.	1897113.	6.56	7.23
70.0000	1181325.	352957.	1130530.	2509913.	7.43	6.95
65.0000	1166252.	447335.	1073325.	3184961.	8.70	6.20
60.0000	1240943.	592237.	1091295.	4211462.	9.62	5.70
55.0000	1231335.	736041.	1049450.	5234069.	10.29	5.27
50.0000	1270203.	845096.	948232.	6009575.	10.57	5.04
45.0000	1130439.	879539.	739060.	6254501.	10.55	4.91
40.0000	1054731.	854279.	622354.	6074872.	10.24	4.90
35.0000	940457.	811764.	482942.	5772543.	9.73	4.96
30.0000	847985.	766511.	372050.	5450742.	9.06	5.03
25.0000	795536.	745525.	233112.	5301510.	8.26	5.26
20.0000	723357.	693598.	209484.	4932252.	7.32	5.63
15.0000	641400.	623733.	136961.	4471579.	5.92	6.19
10.0000	310749.	305405.	109797.	5727323.	5.81	5.47
5.0000	579215.	577510.	44411.	4106735.	3.28	7.62

2.10.5.4 NuPac Computer Code Quality Assurance

NuPac computer analysis programs are maintained in accordance with a formal quality assurance program approved by the Nuclear Regulatory Commission under certificate number 0192 that complies with ANSI N45.2. These provisions are applied to both NuPac authored software and vendor supplied software. Vendors of computer services, such as Boeing Computer Services, have demonstrated that their quality standards are in accordance with the provisions of ANSI N45.2. Documentation of such compliance is maintained in NuPac Quality Assurance files.

The requirements of ANSI N45.2 are interpreted to impose the following stipulations upon computing software:

## ANSI N45.2

SectionRequirement

4.3

The supplier shall require the identification and performance of verification/qualification evaluations which demonstrate that computer codes are capable of producing information of sufficient accuracy to satisfy design requirements.

All calculations and computer input data shall receive documented, independent, in-house verification.

7.0

The supplier shall establish responsibilities and procedures relating to computer code configuration identification and configuration control.

NOTE:

Configuration identification is the establishment and use of a unique identifier for a code version. Configuration control includes the documentation and preservation of a code version to assure its retrievability and includes similar preservation of input for computer runs to assure that output results can subsequently be reconstructed.

A valid computer solution requires that each of the following tests be satisfied:

- o Does the analytic method accurately represent the modeled physical processes?
- o Does the computer code fully and accurately implement the analytic method?
- o Does the input problem data accurately reflect the physical properties of the situation being analyzed?
- o Can the resultant output data be uniquely identified as resulting from a particular input data set?

NuPac procedures assure that each of the above questions is answered in an affirmative fashion. These procedures include the following configuration control elements.

1. Each safety analysis report or design analysis summary provides a complete description of appropriate analysis methods implemented in NuPac developed software.
2. Version identification for each run of the computer code is maintained by the automatic appearance of current code revisions numbers and dates in both output headers and day file listings.
3. All superseded versions of codes are maintained on file.
4. All input data are automatically echoed on output for verification and checking purposes.
5. All output data, including plots, are labeled with a machine generated name, time and date corresponding to the run which generated the reported engineering results.

Verification of methodology and code accuracy involves one or more of the following steps:

1. End-to-end experiments:

These experiments simultaneously test the accuracy of both methodology and code implementation of methodology. For example, a full scale series of 30' drop tests conducted in September, 1980 on the Chem-Nuclear Systems, Inc. CNSI-13C (II) package demonstrated that the overall predictive error of NuPac impact dynamics software is about 6%. (Reference page 2-91, Section 2.7.1.2 of CNSI-13C (II) S.A.R.)

2. Comparison with Alternative Methods:

The method of comparison varies with the particular technology involved. Two examples are described below.

a. Impact Analyses:

Alternative energy balance and momentum methods are used to check-point time history impact dynamics solutions. These end-to-end checks have been performed at three orientations where the dynamic equations of motion become simplified: end, side and center of gravity over struck corner. At other orientations, the impact dynamic solution method has been verified by momentum techniques combined with idealized perfectly plastic energy absorber assumptions.

b. Thermal Analyses:

Steady state solutions are checked by independent iteration methods and a careful check of model heat flow balances (equilibrium). Transient analyses are independently checked by Schmidt plot graphical analysis methods.

### 3. Hand Checks of Code:

Hand checks have been performed to assure that:

- o Equilibrium is always satisfied. Both thermal and all impact solutions have been so tested.
- o Force or heat transfer between points, or nodes, obey the assumptions of the analysis model.
- o Analytic geometry calculations obey the model assumptions. These features have been checked by both descriptive geometry constructions and mathematical checks of the algorithms.
- o Interpolations of non-linear tabular data are correctly performed.
- o Numerical integrations are properly performed.

APPENDIX 2.10.6

INNER SHELL BUCKLING ANALYSIS

THIS SECTION IS PROPRIETARY



APPENDIX 2.10.7

END DROP LID ANALYSIS

THIS SECTION IS PROPRIETARY

APPENDIX 2.10.8

LID PUNCTURE ANALYSIS

THIS SECTION IS PROPRIETARY

APPENDIX 2.10.9

ANSYS MICROFICHE

THIS SECTION IS PROPRIETARY

### 3.0 THERMAL EVALUATION

This section identifies and describes the principal thermal engineering design aspects of the NuPac Model 10/140MB shipping cask important to safety and compliance with the performance requirements of 10 CFR 71.

#### 3.1 Discussion

The NuPac Model 10/140MB Cask is designed with a totally passive thermal system. As seen from Figure 2, the principal physical components of this thermal system consist of a single thickness thermal fire shield surrounding the cask sides, a single thickness thermal fire shield partially covering the cask end plate, and an insulated panel partially covering the cask lid. Additional thermal protection is achieved by the polyurethane foam overpacks. Together, these various protective devices completely cover the cask, such that the entire exterior of the cask is protected against direct exposure to external conditions (assuming that no damage has occurred).

The cylindrical cask wall consists of a 1.25 inch thick carbon steel plate outer shell, a 2.25 inch thick lead shield, and a 0.75 inch thick stainless steel plate inner shell. The cask end plate is fabricated from 6.5 inch thick stainless steel. The cask lid is fabricated from a 5.25 inch thick stainless steel plate. Accidental impact protection is provided by 20 lb/cubic foot polyurethane foam overpacks covering each end of the cask.

Four principal heat transfer analyses were run utilizing the Martin Marietta computer thermal network analyzer program, MITAS II: 1) steady-state analyses at an ambient temperature of 100°F with solar insolation as prescribed by NRC 10CFR71, 2) steady-state analysis at 100°F ambient and no solar insolation, 3) a transient analysis for an undamaged condition with an exposure to an ambient temperature of 1,475°F for thirty minutes followed by exposure to 100°F ambient air to simulate a hypothetical fire accident condition, and 4) the same fire accident condition for a hypothetical damaged

cask configurations. The following table presents the maximum temperatures determined by each of these analyses for selected major components of the cask. Details of the analyses and additional temperature levels are presented in Sections 3.4 and 3.5.

Maximum Temperature (<sup>o</sup>F)

<u>Location</u>	<u>Steady-State</u>		<u>Transient</u>		
	(w/ Solar)	(w/o solar)	(No Damage)	(Corner Drop)	Pin Drop)
Cask Inner Shell	123	105	487	503	487
Lead Shield	123	105	483	509	494
Cask Outer Shell	123	104	496	523	513
Thermal Shield	120	103	1084	1094	1084
Overpack Shell	160	100	1423	1420	1423
Overpack Foam	157	105	160	155	162
Inner Lid Closure Seal	132	106	230	230	264
Outer Lid Closure Seal	124	105	212	270	220
Cask Bottom Seal	121	105	220	223	220
Cask End Plate	123	107	252	252	252
Tie-Down Lug	118	104	1074	1045	1045

These results are based on a maximum internal decay heat load of 95 watts.

### 3.2 Summary Of Thermal Properties Of Materials

The NuPac Model 10/140MB Cask is fabricated primarily of stainless steel, carbon steel, lead, and polyurethane foam. The void spaces within the package are assumed to be filled with air. Air also fills the gap between the cask exterior and the thermal shields. The following table documents the thermal properties used in the model and the sources from which they were obtained.

Material	<u>Property</u>		<u>Specific</u>	
	Conductivity (BTU/hr-ft-°F)	Density (Lb/ft <sup>3</sup> )	Heat	Ref.
<hr/>				
Stainless Steel				
Type 304	10 at 300°F	488	0.11	3.7.1
Carbon Steel	24.5 at 300°F	487	0.113	3.7.1
Lead	18.8 at 300°F	710	0.031	3.7.1
Polyurethane	0.025 at 75°F	20	0.30	3.7.2
Air	see below	0.071	0.240	3.7.3

The thermal conductivity of air varies significantly with temperature as shown in the following table:

<u>Properties of Air</u>		
Temperature (°F)	Conductivity (BTU/hr-ft-°F)	Density (Lb/ft <sup>3</sup> )
32	.0140	.081
100	.0154	.071
300	.0193	.052
500	.0231	.0412
700	.0268	.0341
1000	.0319	.0271
1500	.0400	.0202

Radiation Properties

<u>Component</u>	<u>Material</u>	<u>e</u>	<u>Conditions</u>	<u>Ref.</u>
Cask I.D.	S. Steel	0.5	All	3.7.4
Cask O.D.	Carbon Steel	0.8	All	3.7.5
Overpack Shell	S. Steel	0.8	Fire	3.7.6
		0.5	Normal	3.7.4
Thermal Shield	S. Steel	0.8	Fire	3.7.6
		0.5	Normal	3.7.4

3.3 Technical Specifications Of Components

The O-rings used at the closure seals of the cask are the most temperature sensitive material within the package. The O-rings are made of neoprene and have an extended exposure allowable temperature range of -40 to 250°F (Reference 3.7.7). However, Figure 3-1, taken from Reference 3.7.7, indicates the O-rings can withstand much higher temperatures during short term exposures.

The stainless steel used in the construction of the cask meets the specifications for ASTM A320 304, while the carbon steel meets ASTM A516 Gr. 70. The melting temperatures for lead, carbon steel, and stainless steel are 620, 2750, and 2600°F, respectively. The thermal properties are given in Section 3.2.

The foam stock used in the overpacks is a rigid polyurethane foam produced under the direction of Nuclear Packaging, Inc. of Federal Way, WA. The foam is fire resistant and has been demonstrated to not support a flame. All other technical specifications are given in Reference 3.7.2.

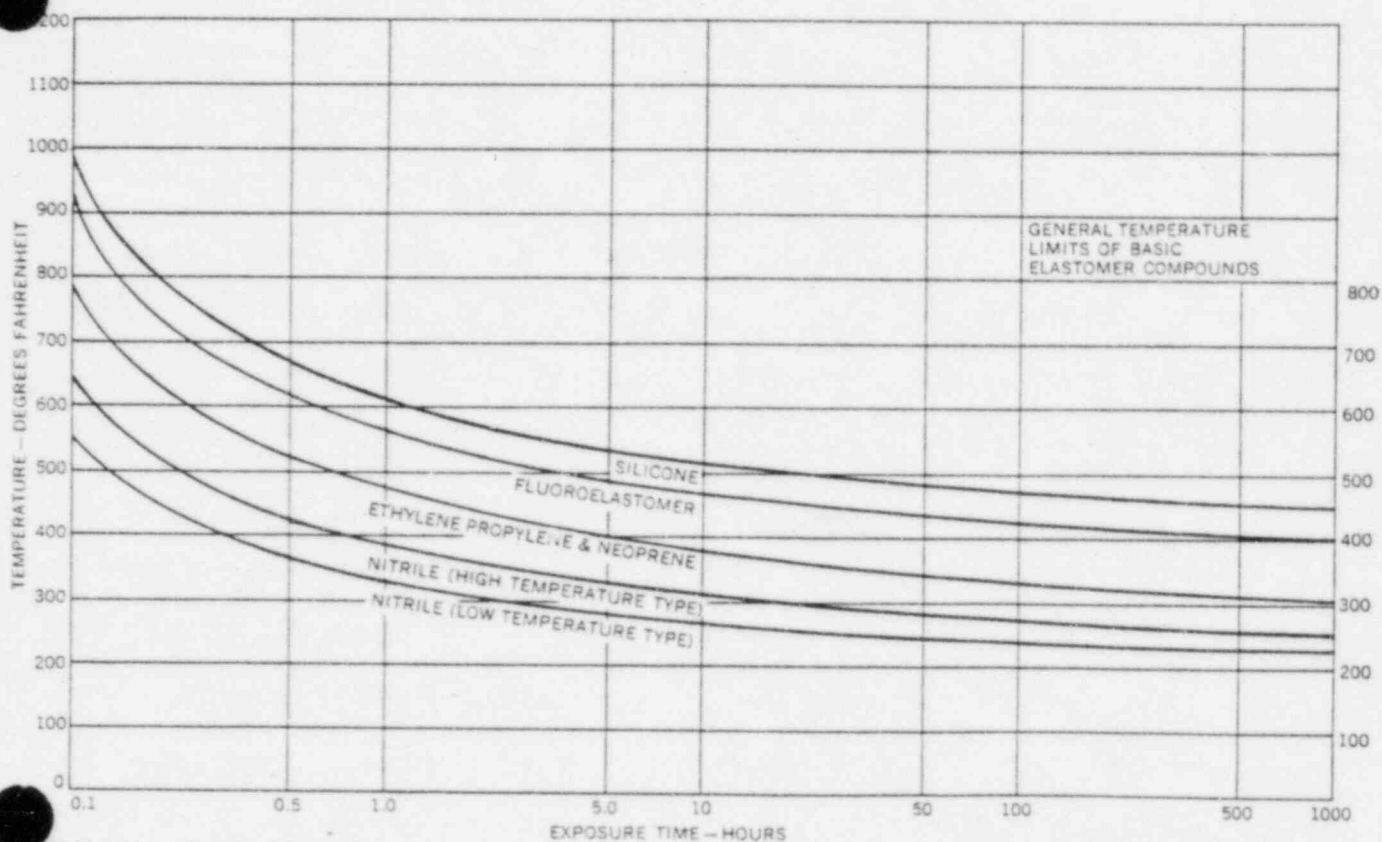


FIGURE A3-6 SEAL LIFE AT TEMPERATURE

FIGURE 3-1

### 3.4 Thermal Evaluation For Normal Conditions Of Transport

This section presents the thermal analyses of the NuPac Model 10/140MB cask for normal conditions of transport. The thermal conditions considered are those specified in 10 CFR 71.71. Per 71.71 (c)(1), a 100°F ambient temperature and the solar insolation values given in the table below are to be used for thermal boundary conditions. An assumed solar absorptivity of 0.5 for the stainless steel overpack shells and heat shields was used with these solar insolation values.

A 95 watt payload internal heat load was also assumed for the normal transport thermal model.



SOLAR INSOLATION

Form and Location of Surface	Total Insolation for a 12-Hour Period (g cal/c <sup>2</sup> )
Flat surfaces transported	
horizontally	
- Base	None
- Other surfaces	800
Flat surfaces not transported	
horizontally	200
Curved surfaces	400

An additional steady-state case was run using an external ambient temperature of 100°F with internal heat generation, but without solar insolation. This case is to be considered as the initial condition for the hypothetical accident conditions. A final, rather trivial case of -20°F ambient air with no solar insolation and no internal heat generation is also considered herein as another extreme initial condition for other events.

3.4.1 Thermal Model3.4.1.1 Analytical Model

Figure 3-2 illustrates the location of the 71 nodes used in the analytical model. The location and the number of nodes were chosen to permit accurate determination of the temperature distribution in the major cask components. The model utilized the different thermal properties presented in Section 3.2. For simplicity's sake, a fixed value of thermal conductivity and specific heat was used for the metals and polyurethane insulation since

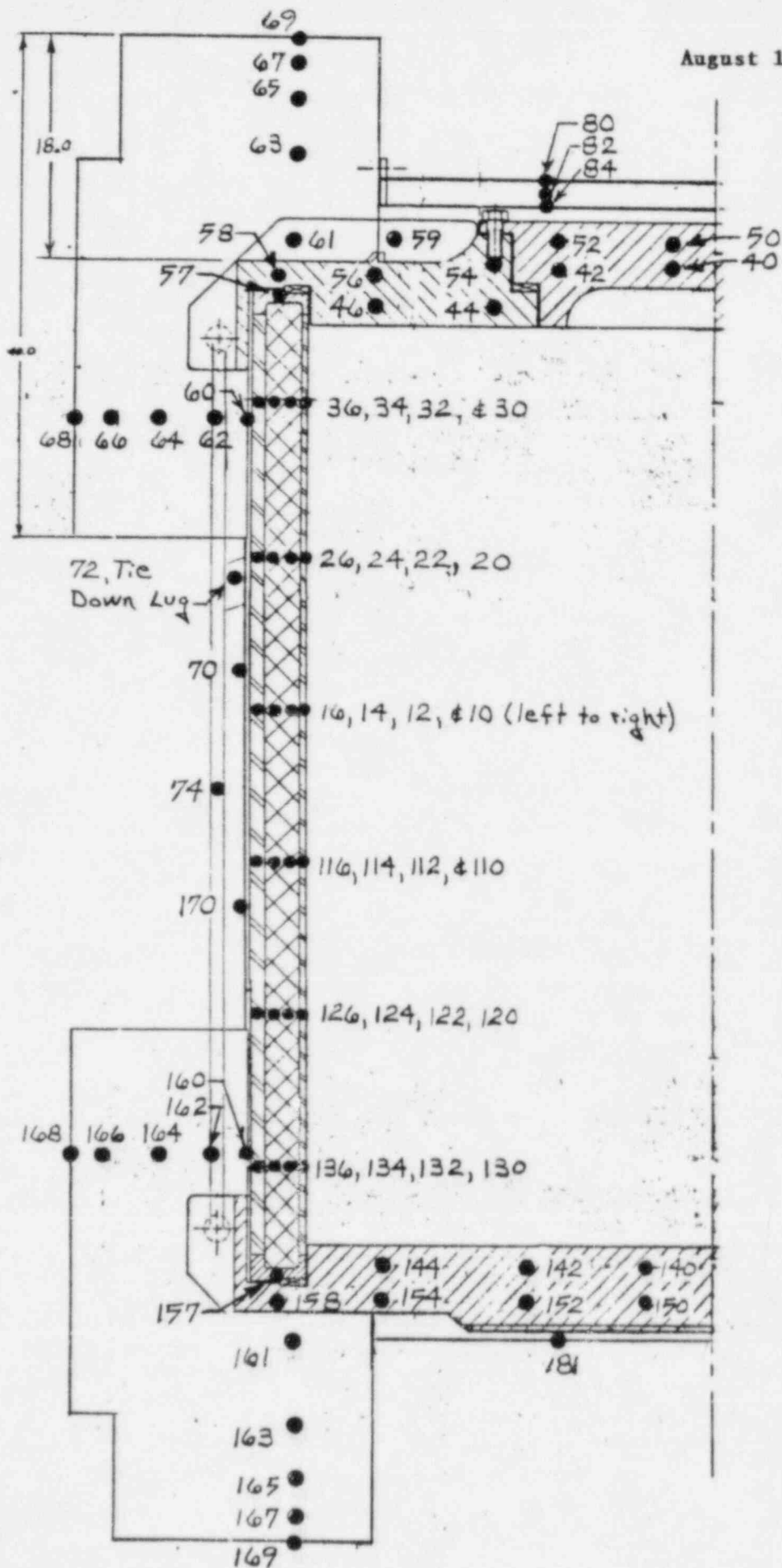


FIGURE 3-2 THERMAL MODEL NODE LOCATION

their change with temperature is small over the temperature range seen. In contrast, the thermal conductivity of air was computed as a function of temperature since its conductivity variation with temperature is significant.

The thermal model represents an axisymmetric segment of the cask. The analysis assumes that the cask is in its normal upright shipping position and that the end of the cask sees an adiabatic surface. It is further assumed that the fuel loading within the cask is evenly distributed. The relatively low assumed decay heat rate of 95 watts means that a change in this assumption will not have a serious effect on the peak temperature distributions.

The internal structure within the package was not modeled. Instead, the transfer of heat from the payload to the inner wall of the cask was modeled as a simple heat input to the interior wall nodes.

Heat transfer through all other portions of the cask structure was calculated using a combination of conduction and 'gray body' radiation heat transfer. The heat transfer across the air gaps within the cask (e.g. between the thermal shield and the cask, cask lid, etc.) was treated as radiation plus pure conduction since the Grashof number is below that for which free convection occurs. An exception occurs for the air gap between the cask lid and the thermal shield (i.e. node 84) when the cask is in a horizontal orientation such as occurs for the hypothetical accident scenario (see Section 3.5). Under these conditions the heat transfer across the gap consists of radiation and free convection.

The free convection of heat from the exterior surfaces was computed as a function of temperature and orientation of the surface using standard equations for free convection from cylinders, and vertical or horizontal surfaces. See Section 3.6 for the specific equations used in each case.

3.4.1.2 Test Model: Not applicable as no thermal testing is performed for the NuPac Model 10/140MB.

### 3.4.2 Maximum Temperatures

The maximum temperatures noted for normal conditions of transportation (i.e. 100°F ambient temperature, solar insolation, and 95 decay heat loading) are presented in the following table for the major components of the cask. See Figure 3-2 for the location of the various nodes. A complete listing of nodal temperatures is provided in the appendix, Section 3.6.

A point for consideration when reviewing the temperature levels in the table below is that the relatively long time constant of the foam overpacks (i.e. 50+ hours) means that the steady-state temperatures are conservatively high. This is due to the fact that the overpacks will isolate the cask components from the effects of solar insolation such that the cask temperatures will not reach a steady-state condition during the typical daily ambient thermal cycle.

## Max. Temperatures For NuPac Model 10/140MB

Normal Conditions

<u>Location</u>	<u>Node #</u>	<u>Temperature °F</u>
Cask Inner Shell	10	121
	30	123
	130	121
Lead Shield	14	121
	34	123
	134	121
Cask Outer Shell	16	121
	36	123
	136	121
Cask Lid	40	132
	46	128
Cask End Plate	140	123
	144	122
Seals - Lid	42	132
- Cover Plate	58	124
- End Plate	158	121
Thermal Shield	70	120
	80	172
	181	123
Overpack Shell	69	160
	68	113
Overpack Foam	67	157
	65	151
	63	140
	61	129
	66	113
	64	117
	62	121
	72	118
Tie Down Lug	72	118

### 3.4.3 Minimum Temperatures

The minimum temperature distribution for the NuPac Model 10/140MB cask will occur with no decay heat load and an ambient air temperature of  $-40^{\circ}\text{F}$  (per 10 CFR 71.71 (c)(2)). Since the steady state analysis of these conditions represents a trivial case, no computerized thermal calculations were performed. Instead, it was assumed that all cask components would reach the  $-40^{\circ}\text{F}$  temperature under steady state conditions. This temperature is within the allowable range of all cask components. As a further potential initial condition for normal or accident events, a  $-20^{\circ}\text{F}$  minimum uniform temperature was also considered per 10 CFR 71.71(b).

### 3.4.4 Maximum Normal Condition Internal Pressure

Internal pressures in the NuPac 10/140MB are affected by three physical effects. First, gas laws predict that pressures in a fixed volume are proportional to the absolute temperature of the gas. Second, some anticipated payloads which would be shipped in the 10/140MB exhibit some gas evolution when subjected to a gamma flux. Finally, a change in temperature would change the vapor pressure of water, so that if small amounts of water are present in the package, the internal pressure would increase accordingly.

From the data presented above, it can be seen that the highest inner surface temperature predicted on the lid of the cask is  $132^{\circ}\text{F}$  (node 40) while the remainder of the cask inner surface averages about  $122^{\circ}\text{F}$ . A weighted average of the inner surface temperature can be taken as a means of determining the gas law and vapor pressure effects on the internal pressure.

The inner surface area of the lid can be approximately as:

$$\pi(33)^2 = 3421 \text{ in.}^2$$

The remainder of the internal surface area is:

$$\pi(33)^2 + 2\pi(66)(73) = 18557 \text{ in}^2$$

So, the average temperature:

$$(132(3421)+122(18557))/(3421+18557) = 124^{\circ}\text{F}$$

Some assumption regarding the amount of free space present in a loaded container must be made. A typical payload configuration involves a inner waste container (most likely a High Integrity Container, or HIC) filled as much as practical with ion exchange resins. Operational requirements dictate that the HIC may be filled no more than 8 to 10 inches from the top. In addition, the HIC typically is designed with at least 1 inch of clearance on the sides and 2 inches between the top of the HIC and the top of the 10/140MB. For purposes of calculating the internal pressure, assume a void space equivalent to the sum of an 8 inch high cylinder the entire diameter of the cavity, and a one inch thick cylindrical shell the length of the remainder of the cavity:

$$V_{\text{void}} = \pi((33)^2(8)+(73-8)(33^2-32^2))/1728 = 23.52 \text{ ft}^3$$

This volume conservatively ignores the interstitial volume inherent in the waste form, dewatering plumbing internal volume, and the volume of the domed secondary lid design.

The amount of gas generated may be estimated by assuming that the entire volume of the 10/140MB not counted as void space is filled with ion-exchange resins. BNL-NUREG-51565, p. 27, indicates that the gas generation rate of a typical ion-exchange media exposed to a gamma flux is  $1.595 \times 10^{-8} \text{ cm}^3/\text{gram-Rad}$ . Conservatively assume an average gamma flux through the resin of 300 R/hr (see Section 5).

The volume of the 10/140MB cavity is:

$$\pi (33)^2 73 / 1728 = 144.53 \text{ ft}^3$$

So the volume of resin is:

$$144.53 - 23.52 = 121.01 \text{ ft}^3$$

The resins may be assumed to be 60 lbs./ft.<sup>3</sup> in density so the gas generation rate given above can be converted to British units:

$$(1.595 \times 10^{-8} \text{ cc/gram-Rad})(453.6 \text{ g/lb.}) 60 \text{ lb./ft}^3 = 4.341 \times 10^{-4} \text{ cc/ft}^3\text{-Rad}$$

$$(4.341 \times 10^{-4} \text{ cc/ft}^3\text{-Rad})(3.5315 \times 10^{-5} \text{ ft}^3/\text{cc}) = 1.533 \times 10^{-8} \text{ ft}^3/\text{ft}^3\text{-Rad}$$

The gas generated assuming a 300 R/hr flux for one year can then be calculated:

$$(1.533/10^{-8} \text{ ft}^3/\text{ft}^3\text{-Rad})(121.01 \text{ ft}^3)(300 \text{ R/hr})(24 \text{ hr/day})(365 \text{ day/yr}) \\ = 4.88 \text{ ft}^3$$

So, applying the prefect gas law:

$$P_i V_i / T_i = P_f V_f / T_f$$

$$P_i = 14.7 \text{ psi}$$

$$V_i = 23.52 + 4.88 = 28.4 \text{ ft}^3$$

$$T_i = 70^\circ\text{F} = 530^\circ\text{R}$$

$$V_f = 23.52 \text{ ft}^3$$

$$T_f = 124^\circ\text{F} = 584^\circ\text{R}$$

Solving for  $P_f$ :

$$P_f = P_i V_i T_f / V_f T_i$$

$$P_f = (14.7)(28.4)(584) / (23.52)(530) = 19.6 \text{ psia} \\ = 4.9 \text{ psig}$$

Any water vapor present may be assumed to condense on the lowest surface temperature present in the cavity. This temperature will be conservatively taken as 130°F. The internal pressure will increase when water is present by the difference in vapor pressure between maximum normal conditions and the conditions at closure. Since the vapor pressure at 70°F is 0.36 psi and at 130°F it is 2.23 psi, the pressure increase due to vapor pressure is 2.23 - 0.36 = 1.87 psi. Therefore, the total pressure increase, assuming a typical payload, is:



$4.9 + 1.87 = 6.8$  psig, maximum normal condition internal pressure.

#### 3.4.5 Thermal Stresses

An examination of the predicted temperatures in the large steel numbers of the 10/140MB Cask reveals that through wall thermal gradients are virtually non-existent. Because of this, and because the overall temperature change from the upper to lower temperature limits is very much less than from the lead pour fabrication temperature to the lowest service temperature, it seems clear that thermal stresses per se are negligible under normal conditions.

#### 3.4.6 Evaluation Of Package Performance For Normal Conditions Of Transport

The component temperatures found for both the maximum and minimum normal temperature distributions, as described in Sections 3.4.2 and 3.4.3 above, were all well within the allowable limits for the respective material (see Section 3.3). As input to Section 2.6, the minimum temperature for any cask component is taken as  $-20^{\circ}\text{F}$ , and the maximum temperature as  $123^{\circ}\text{F}$  for the cask cylindrical outer wall, and as  $157^{\circ}\text{F}$  for the overpack foam.

### 3.5 Hypothetical Accident Thermal Evaluation

This section presents the thermal analyses of the NuPac Model 10/140MB cask for the hypothetical fire accident condition specified in 10 CFR 71.73 (c)(3). The initial temperature distribution in the cask prior to the fire is taken as that corresponding to the 100°F steady state condition without solar insolation as discussed in Section 3.4. This is in accordance with 10 CFR 71.73 (b) and represents the most unfavorable initial condition for determining the maximum cask temperatures.

To determine the effect of a hypothetical accident involving a fire, the cask is exposed to a 1475°F flame having an emissivity of 0.90 for a half hour. After this time period, the thermal boundary conditions are returned to 100°F ambient air with no sun. The transient is then continued for a time sufficient for all temperatures within the cask to reach their maximum values. All thermal boundary conditions meet those specified in 10 CFR 71.73 (c)(3).

#### 3.5.1 Thermal Model

##### 3.5.1.1 Analytical Model

The analytical model used to evaluate the hypothetical accident conditions was identical to that described in Section 3.4.1.1 except that the cask is assumed to have been dislodged from its normal upright shipping position and to be resting horizontally at the start of the accident transient. This assumption implies that the cask end is now exposed to the fire conditions as opposed to the adiabatic conditions seen in the cask's normal shipping orientation. This assumption also affects the free convection equations used for each surface. The thermal model also conservatively assumes that the fire conditions will exist around the entire surface of the cask. An emissivity of 0.80 was used for all external surfaces.

The overpack polyurethane foam is assumed to begin to char at temperatures in excess of 400°F. However, since the foam will not support a flame, a basic assumption for this analysis is that, although some foam in the direct vicinity of the metal surfaces will be lost, the bulk of the foam will remain intact. For conservatism, the thermal model assumes that three inches of foam is lost due to charring and that the burned foam is replaced with an equivalent three inch air gap.

In addition to these assumptions, minor thermal model modifications were incorporated to account for any hypothetical accident condition damage. The details of this damage are discussed in Section 3.5.2.

3.5.1.2 Test Model: Not applicable as no thermal testing is performed for the NuPac Model 10/140MB cask.

### 3.5.2 Package Conditions and Environment

Three hypothetical package conditions were examined for the accident thermal environment. The first condition represents an undamaged cask. This condition serves as a reference against which to judge the sensitivity of the cask to the damage condition discussed below.

The second condition evaluated was for a corner drop which results in the O.D. of the overpack covering the lid end of the cask being crushed inward by approximately 12 inches. This would reduce the normal separation distance between the I.D. and O.D. of the overpack from 15.5 inches to a minimum of 3.5 inches at the centerline of the impact zone. Due to this narrow distance, it is conservatively assumed that the polyurethane foam in the impact zone would be completely charred away during a fire transient. For modeling purposes, the charred foam is replaced with air. It is further assumed that, following the free drop, the cask would roll over and expose the damaged portion of the overpack to the fire conditions.

The third condition represents a hypothetical pin drop damage to the thermal shield covering the cask lid. The location of the damage was chosen to be adjacent to the I.D. of the overpack. This site was selected since the 4+ inch space below the thermal shield in this area would promote the greatest damage. The projected extent of the damage consists of a 9-inch O.D. hole through the shield. However, for reasons of conservatism and to offset the effects of the axisymmetric model, the area of damage used in the thermal model is 2.6 sq. feet. The cask is again assumed to be resting horizontally prior to the start of the fire transient and the foam in the lid thermal shield (node #82) to be completely charred away.

### 3.5.3 Package Temperatures

The maximum temperatures noted for the hypothetical accident conditions described above are presented in the following table for the major components of the cask. In addition, the initial condition for the transients, as described in Section 3.5, is also given. A complete listing of nodal temperatures is provided in Section 3.6.2. In addition, Figures 3-3, 3-4 and 3-5 illustrate the temperature time histories for typical cask locations for each accident condition. The initial accident condition temperatures were used in Section 2.7 as design temperatures in the analysis of the accident events. Specifically, the cask walls are assumed to be no more than 105°F, and the overpack foam is taken to be less than 109°F.

Max. Temperatures For NuPac Model 10/140 M CaskFire Accident

<u>Location</u>	<u>Node #</u>	<u>Temperature (F)</u>			
		<u>Initial</u>	<u>No</u>	<u>Corner</u>	<u>Pin</u>
		<u>Cond.</u>	<u>Damage</u>	<u>Drop</u>	<u>Drop</u>
Inner Shell	10	104	487	503	487
	30	105	227	314	232
	130	105	227	230	227
Lead Shield	14	104	483	509	494
	34	104	227	314	232
	134	105	227	230	227
Outer Shell	16	104	496	523	513
	36	104	227	314	232
	136	105	227	230	227
Cask Lid	40	106	215	215	245
	46	105	173	198	189
End Plate	140	107	252	252	252
	144	106	201	202	201
Seals					
- Lid	42	106	230	230	264
- Cover Plate	57	105	212	270	220
- End Plate	157	105	220	223	220
Thermal Shield	70	103	1084	1094	1084
	80	101	1269	1269	1296
	181	107	1155	1155	1155
Overpack Shell	69	100	1420	1420	1420
	68	100	1423	1385	1423
Overpack Foam	67	101	---	---	---
	65	101	150	149	149
	63	103	106	106	106
	61	105	138	155	146
	66	100	---	---	---
	64	102	107	---	107
	62	104	160	---	162
	72	104	1045	1074	1045

\* - Missing Nodes Represent Charred Foam

#### 3.5.4 Maximum Internal Pressure

As calculated in Section 3.4.4 above, the maximum normally occurring internal pressure is 6.8 psig. Assuming the entire internal volume is at the highest temperature predicted for any node on the inner cask surface (503°F at node 10), the internal pressure may be calculated using the perfect gas law:

$$P_1/T_1 = P_2/T_2$$

Assuming the initial temperature is 70°F, the internal pressure may be calculated:

$$(14.7 + 6.8)/(460 + 70) = P_2/(460 + 503)$$

$$\begin{aligned} P_2 &= 39.1 \text{ psia} \\ &= 24.4 \text{ psig} \end{aligned}$$

So, the maximum internal pressure which could occur during the hypothetical accident fire transient is 24.4 psig. -

#### 3.5.5 Maximum Thermal Stresses

Through-wall temperature gradients during the accident thermal transient event are never more than about 50°F from the inner steel shell to the outer shell in the center of the cask side wall. Further, the higher temperature shell is the outer shell, so the shells would tend to move apart relative to each other, such that no thermal stresses would arise due to the interaction of the inner and outer shell.

In any case, thermal stresses associated with the fire transient can be classified as secondary, displacement limited stresses. As limits on secondary stresses do not apply for accident conditions (per Section 2.1.2), the magnitude of thermal stresses during the fire transient are of little consequence and are not specifically determined herein.

### 3.5.6 Evaluation of Package Performance for the Hypothetical Accident Thermal Conditions

Of the component temperatures noted from the transient analyses for the undamaged cask condition, none exceeded the temperature limitations of the respective materials as defined in Section 3.3. The highest lead temperature noted is 140°F below the melting point, while the highest seal temperature noted is 20°F below the recommended 250°F extended exposure operating limit of neoprene.

Similar results were seen for the corner drop case with the one notable exception of the temperature for the cover plate seal (i.e. node 57). This temperature reached a peak of 270°F, or 20°F over manufacturer's extended exposure limitation. However, as indicated in Figure 3-4, this peak temperature will last only a couple of hours before declining below the 250°F extended exposure limit. Per the information seen in Figure 3-1, this transient is within the limit of the O-rings. In addition, this predicted temperature level is excessively conservative since the use of an axisymmetric thermal model results in the damage being modeled as if it had occurred over the entire circumference of the overpack and not just at one point. For this same reason, the temperature noted for the lead shield at node #14 will actually be below the indicated 509°F and, thus, provide an even greater margin below the melting point of lead.

The results for the case with pin drop damage to the cask lid thermal shield are similar. In this case, the peak seal temperature was noted for the cask lid (node #42). Again, the conservatively predicted temperature of 264°F together with the time of exposure indicates that the seal will not be adversely affected.

In conclusion, all analyses indicate that no loss of shielding or loss of containment will occur as a result of the fire transient for either the undamaged or the damaged conditions examined under this study.



FIGURE 3-3 HYPOTHETICAL FIRE  
ACCIDENT TRANSIENT  
- UNDATED CASK

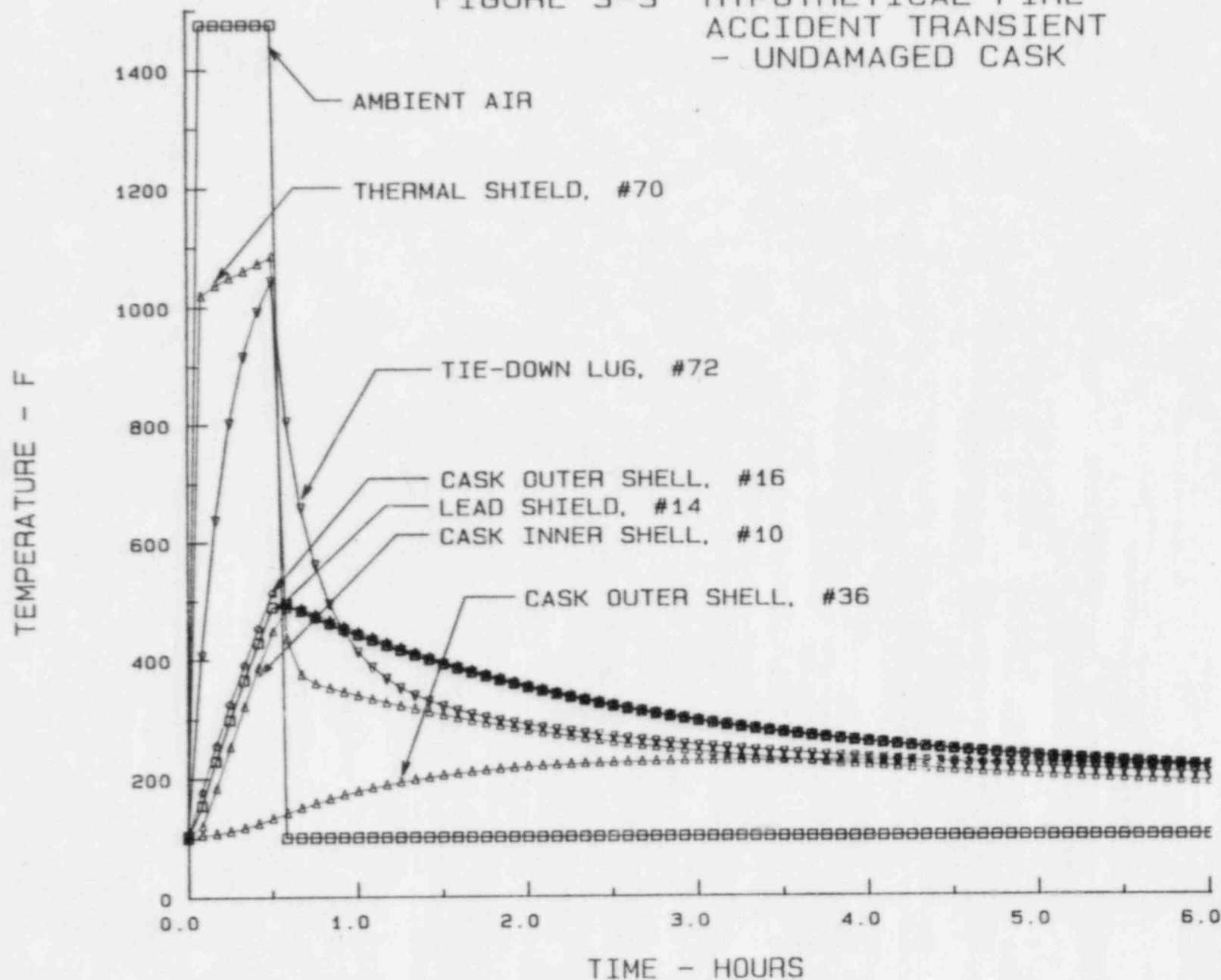


FIGURE 3-3 HYPOTHETICAL FIRE  
ACCIDENT TRANSIENT  
- UNDAMAGED CASK

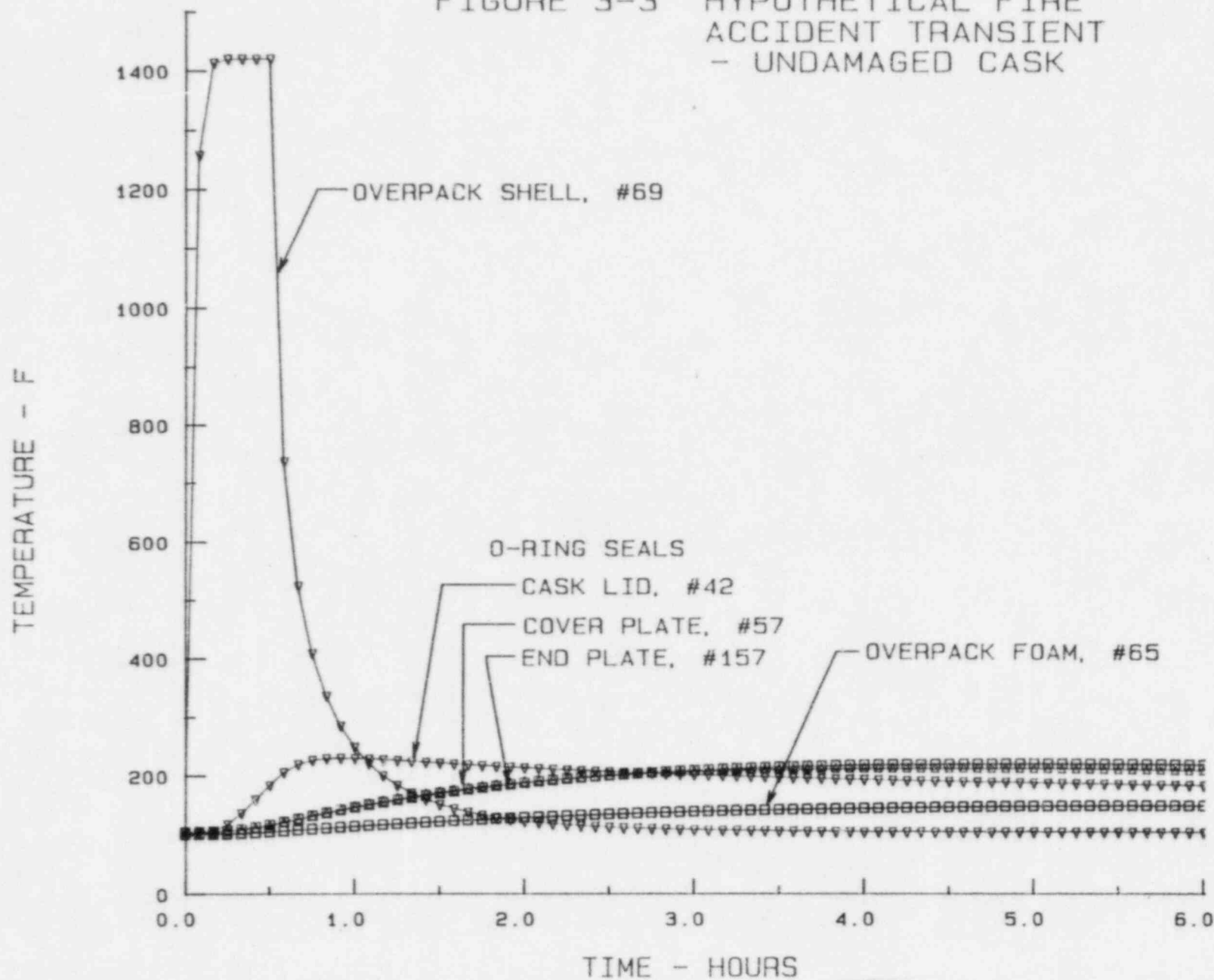


FIGURE 3-4 HYPOTHETICAL FIRE  
ACCIDENT TRANSIENT  
- OVERPACK CORNER DROP

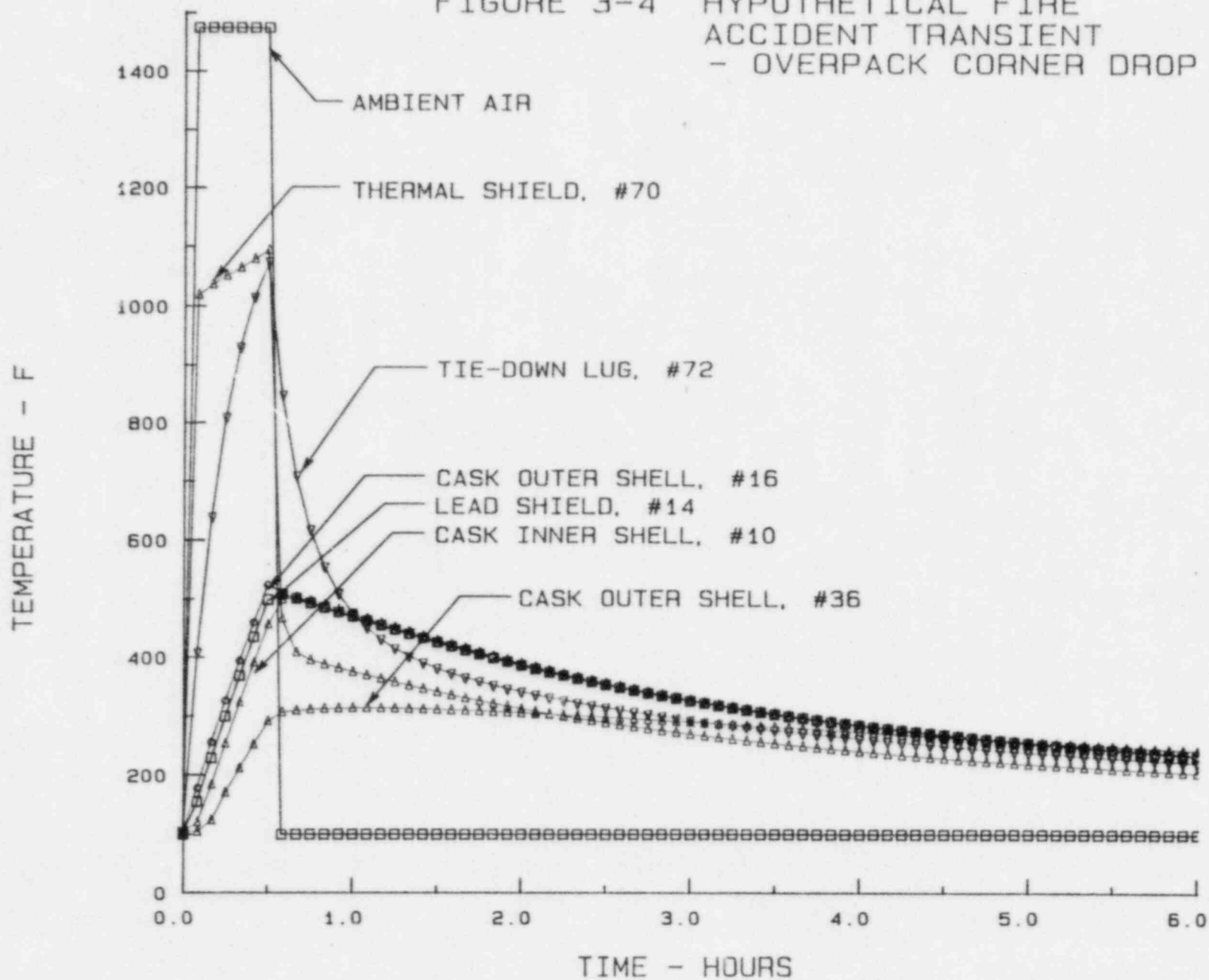


FIGURE 3-4 HYPOTHETICAL FIRE  
ACCIDENT TRANSIENT  
- OVERPACK CORNER DROP

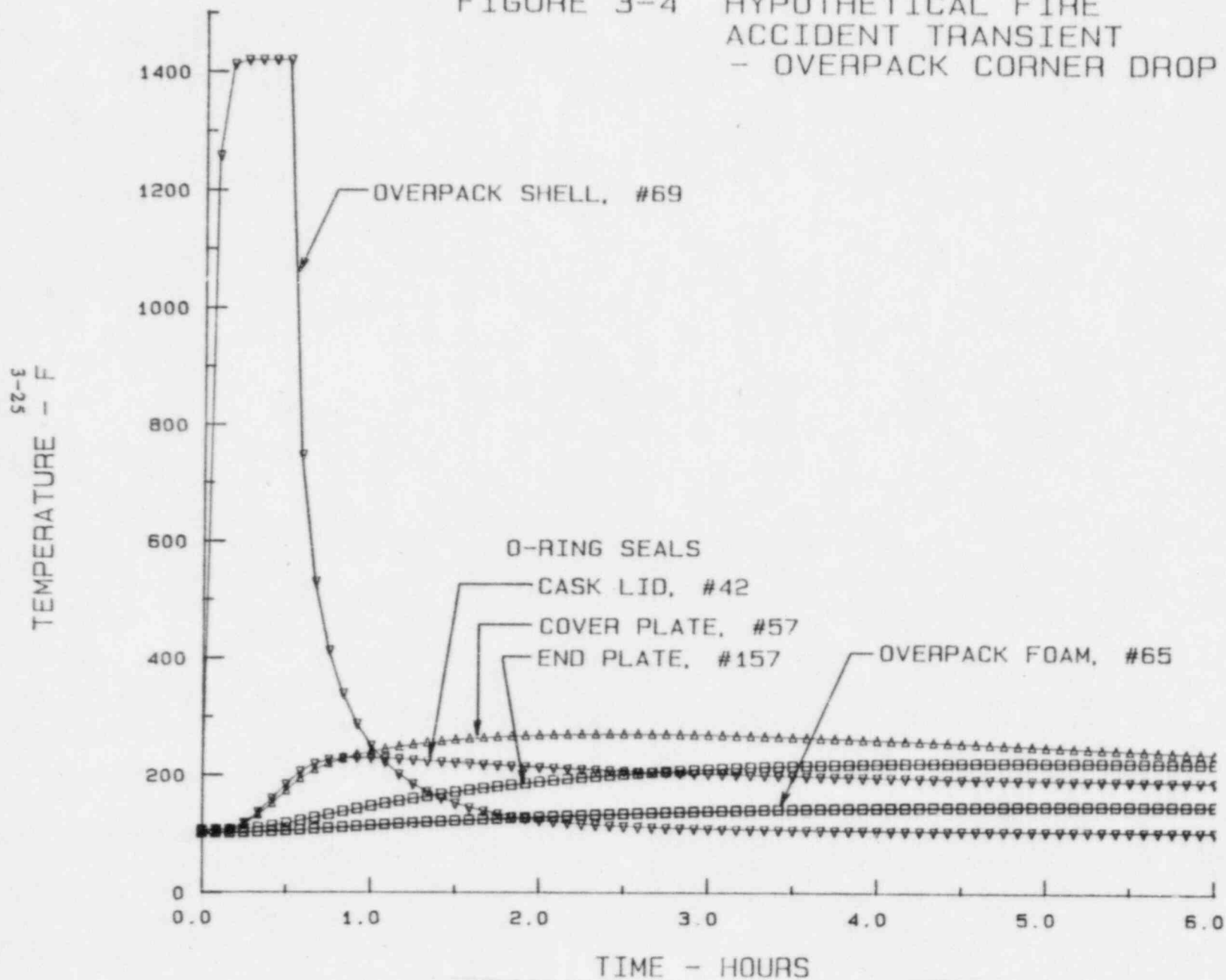


FIGURE 3-5 HYPOTHETICAL FIRE  
ACCIDENT TRANSIENT  
- PINDROP DAMAGE

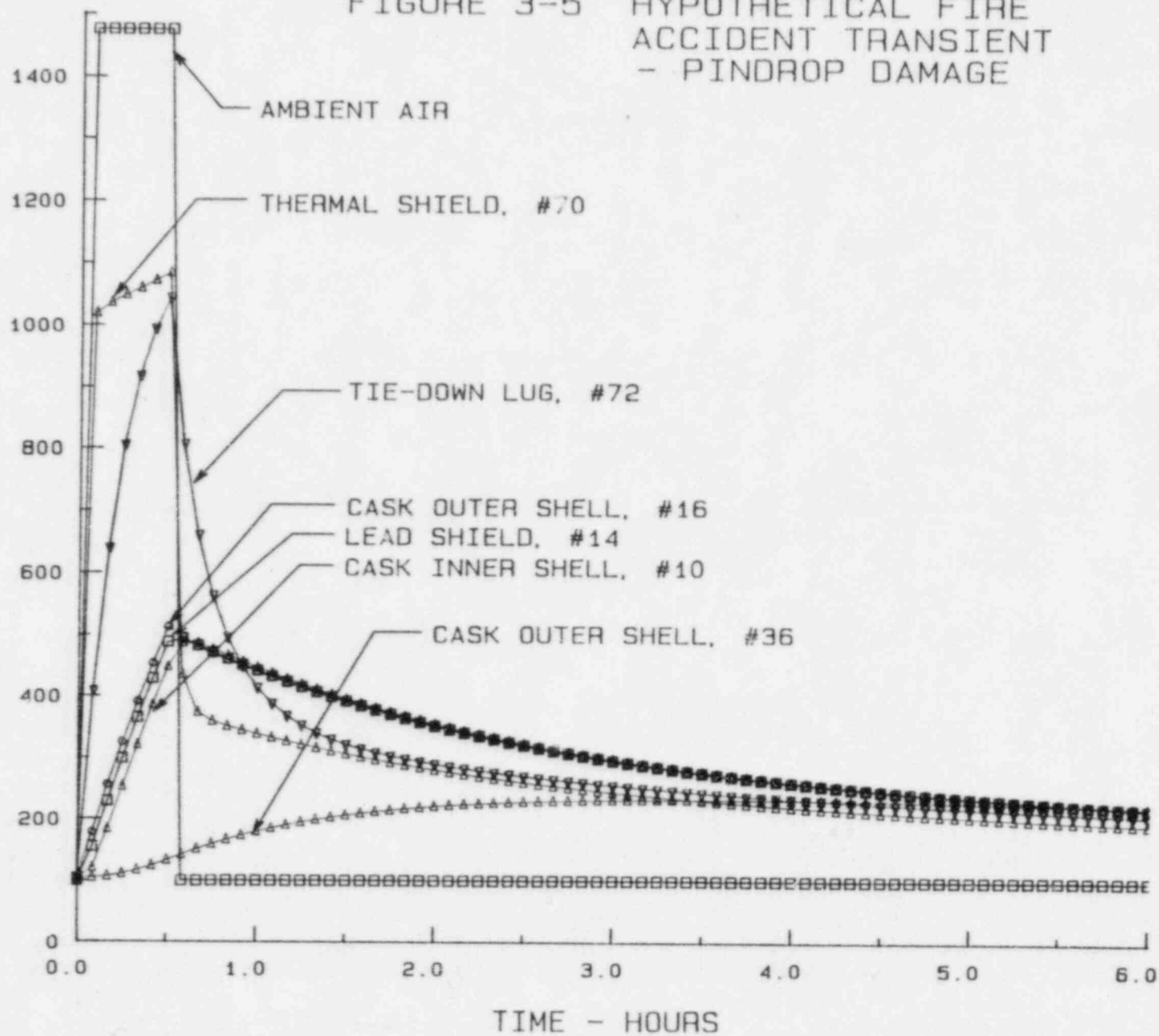
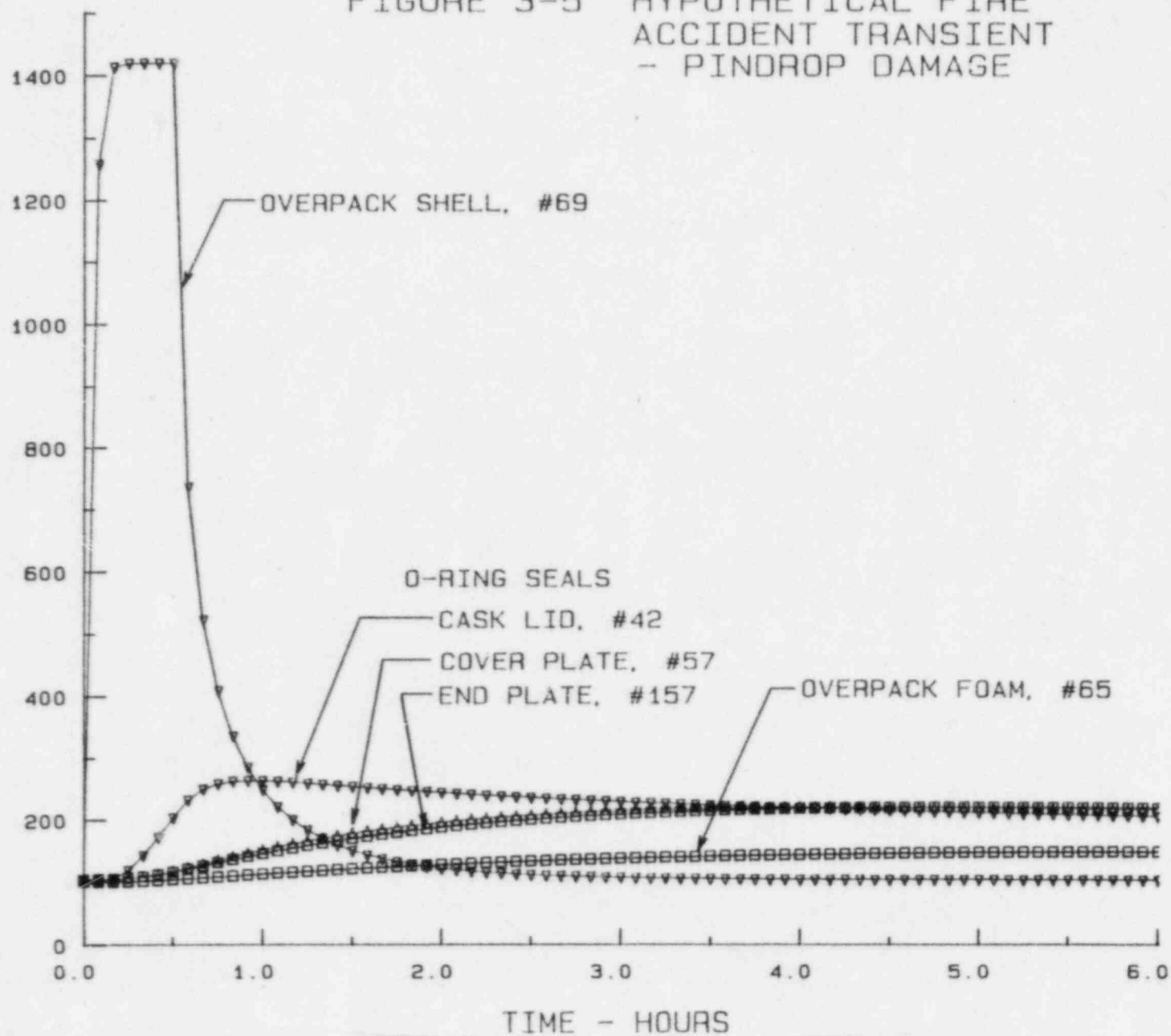


FIGURE 3-5 HYPOTHETICAL FIRE  
ACCIDENT TRANSIENT  
- PINDROP DAMAGE



### 3.7 REFERENCES

1. Rohsenow and Hartnett, Handbook of Heat Transfer, 1973, McGraw-Hill, Table 28.
2. Product Brochure for 'LAST-A-FOAM', General Plastics Manufacturing Company, Tacoma, WA.
3. Frank Kreith, Principles of Heat Transfer, 3rd Edition, McGraw-Hill, Table A-3.
4. J.P. Holman, Heat Transfer, McGraw-Hill, 1963, Table A- 10, gives values of 0.54 to 0.63. F. Kreith, Radiation Heat Transfer, International Textbook Co., 1962, Table 2[5], gives values of 0.43 to 0.78.
5. J.P. Holman, Heat Transfer, McGraw-Hill, 1963, Table A- 10, gives values of 0.31 to 0.80. For conservatism during fire exposure the high value of 0.8 is used.
6. Nuclear Regulatory Commission, 10 CRF Part 71.73.
7. Parker O-Ring Handbook, ORD 5700, 1982, P.A3-35

APPENDIX 3.6

THERMAL ANALYSIS MODELLING NOTES

THIS SECTION IS PROPRIETARY



## 4.0 CONTAINMENT

### 4.1 Containment Boundary

#### 4.1.1 Containment Vessel

The containment boundary of NuPac 10/140MB is formed by an inner 0.75 inch stainless steel cylindrical shell, with ends formed from a varying thickness of heavy stainless steel forged plate. The upper end plate as well as optionally the lower end plate form removable lids for loading and unloading. The upper end plate features a large secondary lid designed to allow loading without removing the shielding capability of the primary lid.

#### 4.1.2 Containment Penetrations

For models without the bottom loading capability afforded by a removable lower end plate, a testable drain port is provided to facilitate decontamination and other cleaning activities.

#### 4.1.3 Seals and Welds

Each of the closures are equipped with NuPac's EnviroSeal<sup>™</sup> (for which patent protection is being pursued), which provide a very high degree of sealing capability while preventing damage from loading and unloading operations in the field. Each EnviroSeal<sup>™</sup> consists of a metallic ring, with four O-ring grooves cut into it, two on each side of the ring. Between the inner and outer O-rings on each side, large holes allow the free passage of gasses from either side of the ring. The ring is fixed in place by screws through the ring. Because the seal is fixed in place, the sealing surfaces on the lower half of the ring are protected from possible damage by the ring itself, while the grooves on the top surface are protected by the O-ring itself. The seal surface on the upper lid is in a relatively inaccessible location on the underside of the upper lid, protected from accidental damage by the presence of the overpack. For the optional removable lower lid, the EnviroSeal<sup>™</sup> stays with the lower lid, and the seal on the bottom of the side wall is protected

by administrative controls requiring that the side wall seal be kept from bearing against any surface except the seal on the lower lid.

The seals are protected from the effects of normal and hypothetical accident thermal conditions by thick sections of self-extinguishing polyurethane foam. The seal on the secondary lid is protected by a removable thermal shield/pad and the primary lid seals are protected by the overpacks. The seals are tested using helium mass spectroscopy to prove that the seals do not exceed a leak rate of  $1 \times 10^{-7}$  standard cubic centimeters per second. The design of the seals is such that a redundant seal is always present. Therefore, the seals provide an unprecedented level of security against leakage.

Prior to first use, the containment vessel welds are radiographed to show their integrity. Also prior to first use, the containment vessel is pressure tested to 1.5 times its design basis pressure per the requirements of ASME Boiler and Pressure Vessel Code Section III.

#### 4.1.4 Closure

Closure of the containment vessel is effected by a combination of eight EnviroLock<sup>™</sup> closure devices on each removable end, and eight ASME A320 Grade L43 bolts securing the secondary lid in the center of the upper primary lid. These devices provide for quick and secure closure of the containment vessel.

### 4.2 Requirements for Normal Conditions of Transport

Prior to each shipment of radioactive material not classified as a Type A quantity or Low Specific Activity (LSA), an assembly leak test meeting the requirements of ANSI N14.5 shall be performed to demonstrate proper assembly of seals. Because the NuPac 10/140MB cask may be used to ship particulate and semi-liquid payloads such as dewatered ion exchange resins, ANSI N14.5 may require that the cask be capable of being sealed to a 'leak tight' condition, or less than  $1 \times 10^{-7}$  standard cubic centimeters per second. This capability shall be demonstrated annually, or whenever the O-rings, EnviroSeal<sup>™</sup> ring or other seal elements are changed or reworked.

#### 4.2.1 Release of Radioactive Material

Section 2.6 above demonstrates that normal conditions of transport do not impart loads on any part of the containment vessel in excess of the Regulatory Guide 7.6 design criteria. Because the containment vessel is equipped with NuPac EnviroSeals<sup>tm</sup>, which allow for minor flexure of the seal without loss of containment, there shall be no release of radioactive material to the environment in excess of the tested leak rate of the seals. This leak rate, deemed to constitute 'leak tight' conditions per ANSI N14.5, is extremely insignificant. Assuming a pressure gradient of one atmosphere (14.7 psi), this leak rate would result less than four liters of leakage in 300 years.

#### 4.2.2 Pressurization of Containment Vessel

Section 2.6.3 addresses the structural capability of the NuPac 10/140MB cask for normal pressure. That section demonstrates that the pressures present for normal conditions will not reduce the effectiveness of the package design.

#### 4.2.3 Coolant Contamination

There are no coolants in the NuPac 10/140MB package design, so this section is not applicable.

#### 4.2.4 Coolant Loss

There are no coolants in the NuPac 10/140MB package design, so this section is not applicable.

### 4.3 Containment Requirements for the Hypothetical Accident Conditions

Section 2.7 above demonstrates that in all hypothetical accident conditions, no significant permanent deformation of the package would be experienced, assuring that the EnviroSeals<sup>tm</sup> remain compressed. Because of the Enviro-Seal<sup>tm</sup>'s double sided seal design, the seal can tolerate an extraordinary amount of seal distortion without significantly affecting the effectiveness of

the seal to remain within ANSI N14.5 limits defining leak-tightness. This is well in excess of the leak requirements of ANSI N14.5 accident criteria for any possible payload.

#### 4.3.1 Fission Gas Products

The NuPac 10/140MB package will normally contain negligible quantities of fission gas products.

#### 4.3.2 Releases of Contents

Because the residual seal effectiveness following a hypothetical accident is the same as for normal conditions of transport, there can be no release of radioactive materials in excess of the limits defined in 10 CFR 71.

## 5.0 SHIELDING EVALUATION

This chapter will describe and quantify the shielding capabilities of the NuPac 10/140MB cask. This is provided as a means for users to select the appropriate package for their particular needs. In all cases, a radiation survey will be made prior to the release of a particular cask for shipment to verify that external radiation dose rates fall below the limits set by 10 CFR 71.

### 5.1 Discussion and Results

Because each shipment may include an indeterminate quantity of various isotopes, it is not possible to fully assess the external dose rate from every possible payload isotope content and distribution. In many cases it is difficult to determine this information even for specific shipments. As a result, shielding calculations have been performed assuming that the source consists entirely of Cobalt-60, an isotope commonly found in power plant waste streams. The use of  $^{60}\text{Co}$  as a benchmark case for shielding is justified, since in most shipments, it is the presence of this isotope which controls the external dose rate.

Table 5.1-1 presents the estimated surface dose limits of typical liners filled with dewatered resins loaded to the maximum distributed quantity of  $^{60}\text{Co}$  which would remain below 10 CFR 71 limits. In other words, a liner loaded with  $^{60}\text{Co}$  resin showing a surface dose rate of that indicated would cause a dose rate at the surface of the 10/14MB cask would not exceed 200 mr/hr. and the dose rate 2 meters from the side of the conveyance would not exceed 10 mr/hr.

TABLE 5.1-1

Total $^{60}\text{Co}$ Curies	Center of Liner	Dose (R/hr)			
		At Liner Surface	At Cask Side	2M From Side of Conv.	Top Surface
160.5*	471.5	76.0	0.060	0.010	0.182

\* 160.5 Ci of  $^{60}\text{Co}$  is equivalent to 2.5 watts

## 5.2 Source Specification

### 5.2.1 Gamma Source

The point-kernel method of calculating shielding effectiveness was used to generate the data presented in Table 5.1-1. It was assumed that the gamma source was  $^{60}\text{Co}$  uniformly distributed within a bed of dewatered resins completely filling a typical Enviroalloy<sup>tm</sup> High Integrity Container sized specifically for the NuPac 10/140MB model cask. The  $^{60}\text{Co}$  source is assumed to emit two gamma photons per disintegration, one of approximately 1.17 MeV and the other at approximately 1.332 MeV. The quantity of  $^{60}\text{Co}$  was determined by scaling a unit quantity by that required to remain within the 10 CFR 71 limits. Self-shielding is accounted for by assuming that the resin exhibits approximately the same attenuation properties as water.

### 5.2.2 Neutron Source

Since only negligible quantities of neutron emitters would be shipped within the Series B casks, no neutron sources were assumed for this shielding evaluation.

## 5.3 Model Specification

### 5.3.1 Description of the Radial and Axial Shielding Configuration

#### 5.3.1.1 Radial Shielding

The radial shielding of the NuPac 10/140MB consists of a 0.75 inch inner stainless steel shell, a varying lead thickness dependent on the particular model, and a 1.25 inch thick outer shell. For the purposes of Table 5.1-1, the 0.375 inch thick wall of the Enviroalloy<sup>tm</sup> High Integrity Container was included in the shielding model, as well as the 0.50 inch thick top plate. This additional element of shielding is considered to be part of a typical configuration. Figure 5.3.1-1 shows schematically how the radial shielding is modeled.

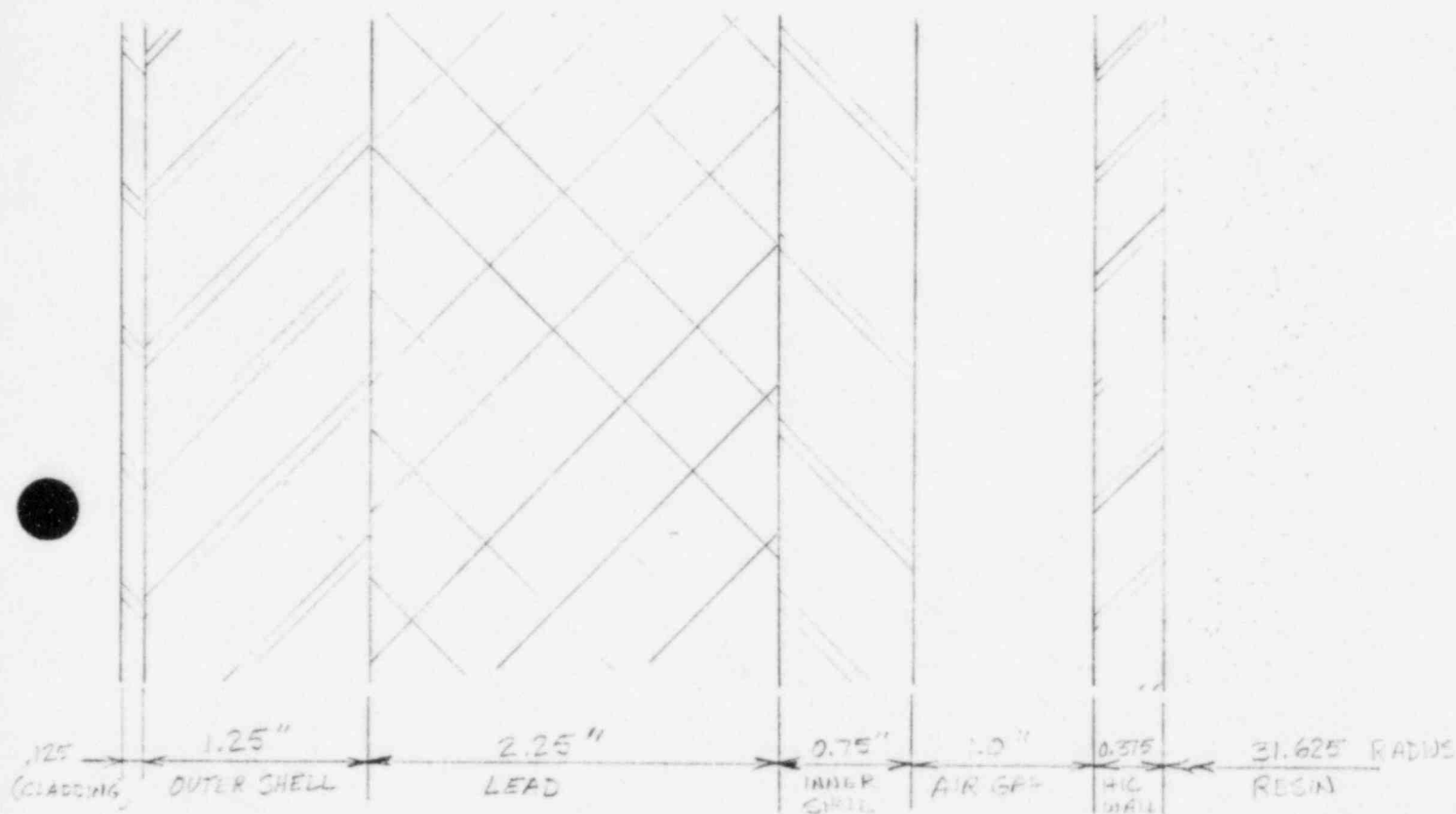


FIGURE 5.3.1-1

Radial Shielding Model Diagram



### 5.3.1.2 Axial Shielding

Axial shielding in the NuPac 10/140MB cask is provided by thick stainless steel plates on each end. The plates have been sized such that the payload source which would just meet the 10 CFR 71 requirements for radial external dose rates would cause an external dose rate through the end of the cask at or below 200 mr/hr at the package top surface.

### 5.3.2 Package Regional Densities

The calculational method used for this analysis requires that the mass densities and mass attenuation coefficients for the various regions of the shield be known. The point-kernel build-up factors are also required.

Mass attenuation coefficients and build-up factors are taken from Reactor Handbook, Volume III, Part B, Second Edition. Following the recommendation of N. M. Schaeffer in Reactor Shielding for Engineers, the outermost material greater than two mean free paths thick is used to calculate the build-up factor.

The mass attenuation coefficients and build-up factors for stainless steel were taken to be the same as iron. The properties of water were substituted in regions designated as resin.

The density of stainless steel is assumed to be 490 lbm/ft.<sup>3</sup> while lead is assumed to be 700 lbm/ft.<sup>3</sup>. Resin is assumed to be 62.4 lbm/ft.<sup>3</sup>. The attenuation of air is conservatively neglected.

#### 5.4 Shielding Evaluation

The data presented in Table 5.1-1 above was generated using standard point-kernel techniques on a very simplified model of a possible payload. Because of the uncertainty inherent in the payload to be shipped in this type of cask, the data presented in that table should be considered as reference only. To assure compliance with the requirements of 10 CFR 71, a radiation survey is taken prior to each shipment. The following is a description of the technique used to develop the table.

A computer program was developed by Nuclear Packaging, Inc. to apply these techniques in an iterative fashion to the unique geometric constraints of a right circular cylindrical shield. The program, referred to as 'SAP' for Shielding Analysis Program, breaks up the source term into discrete elements each treated as point sources with no self-shielding. The attenuation of other elements of the source is not ignored, however. The attenuation of photons emanating from each discrete element is calculated, and the dose from all elements are integrated (summed) to arrive at the total dose rate at a given distance from the outside of the shield. To speed calculations, the contribution to the dose rate of elements of source farther than a specified number of mean free paths from the outside of the source are ignored. For the purposes of Table 5.1-1, elements more than 5 mean free paths from the source surface are ignored, since they do not contribute significantly to the total external dose rate at the point in question.

The relative size of the elements of source is controlled by the user. In general, the smaller the elements, the more accurate the results, as in any numerical integration procedure. However, because self-shielding is ignored within calculation of the dose contribution of each individual element, the dose rate calculated is conservatively predicted regardless of the size of the elements.

The program evaluates the expression:

$$\phi_A = S B \exp(-\sum \mu t) 4\pi R^2$$

where

- $\phi_A$  = Photon flux at the point in question
- S = Photon Generation Rate
- B = Dose Build-up Factor
- $\mu t$  = Number of mean free paths through material of mass attenuation coefficient  $\mu$  and thickness  $t$
- R = Distance from source element to point in question

for each element of the source and each source photon energy and generation rate. A running total of the contributions to the photon flux at the dose point is kept for all elements less than 5 mean free paths from the edge of the source. From the above expression, it is clear that the other elements will contribute very little to the total flux at the dose point.

The total photon flux from each gamma energy level is then converted to dose rate by means of a standard flux-dose relation from the Reactor Handbook.

The program allows either cylindrical or infinite slab shields to be modeled as well as cylindrical or rectangular source volumes. It allows point and line source calculations as well.

The program has been benchmarked against ANYSN and QAD calculations as well as actual measurements, with good results. Comparisons show the SAP output to be within 10% of other calculational methods, which is well within the accuracy of the point-kernel technique.

As stated in Section 5.1 above, these calculations are presented as a means of comparing the shielding capability of the Series B casks. In every case, the cask should be surveyed to determine that the regulatory dose rate limits are not exceeded prior to delivery of the package to a carrier for transport. The dose rates and contents limits suggested by Table 5.1-1 are not intended to be used as administratively controlled limits, since many parameters not modeled may affect the actual measured dose rate and permissible radioisotope quantities within any given shipment.

## 6.0 CRITICALITY

### 6.1 Discussion and Results

Because the NuPac 10/140MB package will not contain significant quantities of fissile material, this section is not applicable.

## 7.0 OPERATING PROCEDURES

This section describes the general procedures to be used for loading and unloading the various configurations of the NuPac 10/140MB packaging.

### 7.1 Procedures for Loading the Package

The following procedure assumes that the cask is in the loading area assembled in its over-the-road configuration. The cask may or may not be on the vehicle used to transport the cask over public roads.

#### 7.1.1

Remove the Thermal Shield Cover from the top of the package. Loosen and stow the EnviroLock<sup>tm</sup> closure devices which secure the primary lid.

#### 7.1.2

Remove the lid by attaching suitable hooks to the primary lid lifting lugs. Care should be taken during the operation so as not to damage the lid to body interface seal while setting the lid down. Inspect the EnviroLock<sup>tm</sup> devices for signs of damage or wear.

#### 7.1.3

Inspect the inside of the shielded cask to assure there are no loose articles within the packaging. Inspect seal surfaces on underside of lid and clean if necessary. Carefully clean the primary lid seal. Replace O-ring seals upon signs of wear or deterioration. Required spare parts may be obtained from Nuclear Packaging, Inc., Federal Way, WA (206) 874-2235.

7.1.4

Place the disposable steel liner into the cask. If the liner is significantly smaller than the internal cavity of the particular NuPac Series B model being used, sufficient shoring and/or bracing shall be provided to insure the payload will not shift significantly during shipment.

7.1.5

Replace lid and secure it to the body using the EnviroLocks<sup>tm</sup>. Torque EnviroLocks<sup>tm</sup> to 500±20ft-lb torque.

7.1.6

If any loading of material is to be done through any of the secondary openings in the upper lid of the cask, the secondary lid nuts should be removed and Steps 7.1.7 through 7.1.10 shall be performed.

7.1.7

The lug in the center of the secondary lid may be used to remove the secondary lid from the cask. Care should be taken to avoid damage to the sealing surface on the lip of the secondary lid.

7.1.8

Inspect secondary lid studs, bolts and nuts for signs of wear. Damaged threads and excessive corrosion shall be cause for replacement of these items. Measures should be taken to protect the EnviroSeal<sup>tm</sup> in the secondary lid opening from damage during loading operations.

7.1.9

Load cask through secondary lid. Replace secondary lid and torque bolts to 375±15 ft.-lbs. Install a tamper-indicating seal on the secondary lid.

7.1.10

Survey the loaded cask to assure compliance with 10 CFR 71.47. Inspect for surface contamination per the requirements of 10 CFR 71.81(i).

7.1.11

If the contents is not classified as Low Specific Activity material, an assembly verification leak-test per 8.2.5.1 or 8.2.5.2 shall be performed as required by ANSI N14.5. Undisturbed seals (those which have not been opened since their most recent leak test) need not be tested. This assembly verification test shall demonstrate that all tested seals exhibit leak rates less than  $1 \times 10^{-3}$  standard cubic centimeters per second, and any leak actually detected is less than  $1 \times 10^{-7}$  standard cubic centimeters per second. The sensitivity of this test shall be at least  $5 \times 10^{-4}$  scc/sec.

7.1.12

Inspect the package for proper labeling necessary to meet all applicable regulations.

7.1.13

Using suitable material handling equipment, transfer the package to the transport vehicle, if it is not already on the vehicle. Replace the Auxiliary Impact Limiter.

7.1.14

Check to see that the Thermal Shield Cover lifting lug is covered for transit.

7.1.15

Install a tamper-indicating seal on the EnviroLocks<sup>tm</sup>.



7.1.16

Secure package to the transport vehicle using the appropriate tie down devices, if it is not already. If the cask had been previously secured to the vehicle, re-check all tie-down devices for proper security.

7.1.17

NuPac 10/140MB packages may be equipped with bottom loading capability to facilitate remote loading operations in fuel pools or other waste storage facility. The procedures for such operations are similar to those for top loading in steps 7.1.16.

7.2 Procedures for Unloading the Package7.2.1

The requirements of 10 CFR 20.205 shall be followed whenever greater than Type A quantities of RAM are received.

7.2.2

Move the unopened package to the appropriate unloading area. Place it in a suitable unloading attitude.

7.2.3

Perform an external inspection of the unopened package. Record any significant or potentially significant observations.

7.2.4

Remove tamper-indicating seals from EnviroLocks<sup>tm</sup>.

7.2.5

Repeat steps 7.1.1 and 7.1.2 in Section 7.1, above, for removing the overpack lid.

7.2.6

Remove the disposable steel liner.

7.2.7

After unloading the entire package, the interior and exterior shall be visually inspected to assure that it has not been significantly damaged i.e., no cracks, punctures, holes or broken welds.

7.2.8

The following configuration checks shall be performed after unloading and prior to any loading activity:

7.2.8.1 Exterior nameplates, stencils, placards and other required identification is in place and legible.

7.2.8.2 Latch pins, ratchet binders and gaskets are in place and in good operating condition and free of defects.

7.2.8.3 All required documentation is completed and retained/displayed as specified by the regulatory authority and the user.

## 8.0 ACCEPTANCE TESTS AND MAINTENANCE PROGRAM

### 8.1 Acceptance Tests

The NuPac 10/140MB packaging shall be inspected and released for use by responsible operation personnel prior to loading. The following items shall be included in such inspection:

#### 8.1.1

Before first use, the 10/140MB package shall be subjected to the leak test as described below in section 8.2.5.

#### 8.1.2

All configuration checks described in Section 7.2.8 above.

#### 8.1.3

The cask shall be pressure tested to 1.5 times the normal operating pressure of the cask. This is taken as the pressure given for the Normal Conditions of Transport in Section 3.4.4. In that section, the pressure is given as 6.8 psig, so this test shall be carried out at least 10.2 psig.

#### 8.1.4

The integrity of the shield shall be demonstrated by means of a gamma scan performed on the lead-filled cylinder during the fabrication process, as described in Appendix 8.3.1 below.

## 8.2 Maintenance Program

### 8.2.1

A good sound industrial maintenance program should be followed to assure the integrity of the NuPac 10/140MB packaging. Components such as O-ring seals, latch pins, nuts, studs, bolts, and ratchet binders, shall be inspected prior to each use and repaired or replaced as necessary. A leak test shall be performed when seals are replaced or when damaged seals are suspected. The test shall be performed in accordance with Section 8.2.5 below.

### 8.2.2

As a minimum, O-ring seals shall be replaced with new O-rings meeting the description in the drawings shown in Appendix 1.3 every twelve (12) months (sooner if visible wear is detected).

### 8.2.3

'EnviroLock'<sup>tm</sup> primary lid closure binders must operate freely and easily. They shall be lubricated as required and replaced if necessary.

### 8.2.4

Any damaged or lost fasteners shall be replaced with equivalent grade and strength as shown on the drawings in Appendix 1.3.

### 8.2.5

Before first use and whenever the O-ring seals are replaced, a leak test shall be conducted (see below). Regardless of condition, all O-ring seals shall be replaced every twelve (12) months.

8.2.5.1 The package shall be leak tested utilizing a Mass Spectrometer Leak Detector (MSLD) type test in accordance with ANSI N14.5, Section A3.8. The helium test gas shall be introduced to the fully assembled package through appropriate fittings.

8.2.5.2 The leak test described in section 8.2.5.1 shall be performed at the Primary and Secondary seals and at all ports as appropriate for the particular 10/140MB cask configuration. The acceptance criterion shall be  $10^{-7}$  std cm<sup>3</sup>/s. Test sensitivity shall be approximately  $10^{-8}$  std cm<sup>3</sup>/s.

APPENDIX 8.3.1

GAMMA SCAN

### 8.3 APPENDIX

#### APPENDIX 8.3.1 DISCUSSION OF GAMMA SCAN PROCEDURE

Lead shielding integrity shall be confirmed via gamma scanning. There are two gamma scan techniques utilized. The main difference is in the method utilized to determine acceptance criteria.

Both Gamma Scan Techniques are exactly the same in all other respects and are conducted as follows.

An Eberline EI20 probe or equivalent is used to scan the outer surface of the cask while an Iridium 192 or Cobalt 60 source of sufficient strength is present in the center of the cask. The source is first placed on the bottom of the cask while the surface is scanned around its circumference parallel to the source. The source is then moved up a pre-determined distance and the circumference scanned again. This sequence is repeated until the entire cask surface is scanned.

For these tests, the cask surface is gridded (in this case the grid consists of 4 inch squares) and a chart is made to reflect the gridded cask surface. Readings are taken from each grid square by scanning every point in the grid and recording the maximum reading in the corresponding grid on the chart. This data then serves as the raw gamma scan results. All readings are in Milliroentgens (MR).

The readings are evaluated by comparing them to predetermined MR values for nominal, or as designed, lead thickness and nominal -10% lead thickness.

The two different methods utilized to determine acceptance criteria are discussed below.

The Laboratory Calibration Method (NuPac Procedure GS-001) utilizes test blocks of the cask wall made up of lead and steel sheets. The test blocks simulate nominal or as designed and -10% lead thicknesses. The source is placed behind the test block at a distance equal to the inside radius of

the cask. The probe is then placed on the outside of the test block and readings are taken. This sequence is repeated on the nominal and -10% test blocks and the data is recorded.

The resultant values are then averaged. A ratio of the values is also developed. Then the average value is multiplied by the ratio. The value so derived is the maximum acceptable value for the shielding to be inspected.

An optional Laboratory Calibration Method can be utilized in lieu of the lead/steel calibration mockup method. In that case, calculations are run to establish acceptance criteria.

To do this, compiled source power data and attenuation characteristics data for steel, lead and distance through air are utilized to calculate the expected readings at the cask surface. The calculations allow for different source powers and are corrected for nominal and -10% shielding configurations.

The following excerpt from NuPac Gamma Scan Procedure No. GS-001 is provided to illustrate the calculation Method of Laboratory Calibration:

1.1 The nominal and -10% shielding calibration MR readings may be obtained via calculation as an option. These calculations shall be performed as follows:

1.1.1 Data and transmission charts found in the Tech/Ops Gamma Radiography Radiation Handbook shall be utilized. Copies of the handbook can be obtained from:

Tech/Ops, Inc.  
Radiation Products Division  
40 North Avenue  
Burlington, Mass. 01803



- 1.2.2 Attachment A, Table 2, 'Selected Radioisotope Data' from the handbook shall be utilized to obtain source power data. (Copy of Table 2 included as Attachment A.)
- 1.2.3 Attachment B figures of the handbook shall be utilized to determine the attenuation of Gamma Rays in the shielding materials utilized in the cask to be inspected. (Copy of typical figures included as Attachment B.)
- 1.2.4 The following is an example of the calculated calibration method using Cobalt 60:

EXAMPLE

Cask O.D. 48 in. Cask I.D. 36 in. I.D. Wall 0.50 in. O.D. Wall 0.50 in. FE

Lead Shielding = 5.0 in. Less 10% lead shielding = 4.5 in.

Total FE shielding = 1.0 in.

Source Cobalt 60 strength 15 curies  $\times$  14.0 = 210 R/Hr at 12 in. (using Attachment A).

210 R/Hr at 12 in. = 52.5 R/Hr at 24 in. This would be the outer surface of the cask.

52.5 R/hr at 24 in.  $\times$  reduction factor for 1.0 in. FE 0.58 = 30.45 R/Hr.

30.45 R/Hr at 24 in.  $\times$  reduction factor for 5.0 Pb 0.0009 = 27.4 Mr/Hr.

30.45 R/Hr at 24 in.  $\times$  reduction factor for 4.5 in Pb 0.000185 = 56.3 Mr/Hr (using Attachment B).

Design thickness reading at cask surface = 27.4 Mr/Hr.

Design thickness reading less 10% Pb = 56.3 Mr/Hr.

The following is an example of the calculated calibration method using Iridium 192:

EXAMPLE

Cask O.D. 48 in. Cask I.D. 46 in. I.D. Wall 0.25 in. FE O.D. Wall 0.25 in. FE

Lead Shielding = 1.5 in less 10% lead = 1.35 in.

Total FE Shielding 0.50 in.

Source Iridium 192 50 curies  $\times 5.9 = 295$  R/hr at 12 in. (using Attachment A).

295 R/Hr. at 12 in. = 73.75 R/Hr at 24 in. This would be the outer surface of the cask.

73.75 R/Hr at 24 in.  $\times$  Reduction Factor for 0.50 in. FE 0.55 = 40.5625 R/Hr.

40.5625 R/Hr.  $\times$  Reduction Factor for 1.50 Pb. 0.0024 = 0.09735 R/hr.

40.5625 R/Hr.  $\times$  Reduction Factor for 1.35 in. Pb. 0.004 = 0.16225 R/Hr. (using Attachment B.)

Design thickness reading at cask surface = 97.35 Mr/Hr.

Design thickness reading less 10% of Pb = 162.2 Mr/Hr.

The calculation values and methods are based on data developed during approximately 300 actual calibrations utilizing the lead sheet/steel plate sandwich technique described in Rev. 4 of the referenced procedure.

Additional correlation has been provided by the use of established attenuation values obtained from the various figures found in the Tech/Ops Radiation Safety Handbook. This reference source is a recognized standard document utilized throughout the NDE industry. This information, together with NuPac's, extensive laboratory data enabled NuPac to develop the current optional calculation method of laboratory calibration for gamma scan.

The calculation method provides a greater degree of accuracy and correlation to the actual gamma scan conditions present in a typical cask than the lead and steel plate setup used in the past. It also reduces operator exposure during the calibration phase. The resultant calibration values for acceptance of the lead shield are, in fact, slightly more conservative and therefore assure a greater margin of safety for the shield.

The resultant improvement in the calibration of gamma scan acceptance criteria provides greatly improved accuracy and repeatability.

To illustrate this accuracy, correlation and conservativeness, the calibration data for a typical NuPac OH-142 (C of C No. 9073) gamma scan was rerun using the calculation method of Laboratory Calibration. The original calibration technique for this cask had been the lead and steel setup method.

The correlation between the two Laboratory Calibration methods is essentially identical. The variance in the acceptance criteria between the two methods is from .3 MR in the nominal to .1 MR in the -10% values. This equals to more than 2% variance between the Pb/FE and calculation methods of Laboratory Calibration. The difference in percentage (DIFF, %) between the nominal and -1-% values for the two calibrations is also very close with the Pb/FE at 64% and the Calc at 63%. The calibration results follow:

## SUMMARY OF GAMMA SCAN ACCEPTANCE VALUES - NuPac OH-142 (C of C No. 9073)

Source Type	Source Strength (curies)	Calib Type (1)	Nominal Value (MR) (2)	-10% Value (MR) (3)	Diff (%) (4)
Co 60	11	Pb/FE	21.5	33.5	64%
Co 60	11	Calc	21.2	33.4	63%

## NOTES:

1. Pb/FE = Laboratory Calibration using lead and steel sheets to simulate the cask wall. Calc = Laboratory Calibration using the calculation method.
2. Nominal Values is the calibrated acceptance value expected if the lead and steel thickness meet the design requirements.
3. The -10% value is the calibrated gamma reading expected if the lead thickness is 10% less than that required by the design. The steel thickness is assumed to be at the nominal. This reading will be larger than the nominal reading. No reading above this value during actual gamma scan inspection is acceptable.
4. DIFF (%) refers to the percentage of difference between the Nominal and -10% values. A variance of approximately 5 to 6% between the nominal and -10% values of separate calibrations is normal. This is attributable to differences in lead density (cast vs. rolled sheet), accuracy of meters and related equipment, as rolled steel thickness variables, etc.

The Field Calibration Method (NuPac Procedure GS-002) utilizes a specially fabricated test lid which incorporates a holder for various lead and steel sheet thicknesses. This fixture is installed onto the cask to be scanned. The test lid is then set up to simulate the nominal lead thickness, the source is placed below the test lid in the cask at a distance equal to the inside radius of the cask. Readings are then taken. The test lid is then set up to recreate the -10% lead thickness configuration, and readings are again taken.

Other readings are then taken in 1/8 inch lead thickness increments between and beyond the two base readings until four to eight readings are obtained. The data is then plotted on a chart of readings versus lead thickness. The value for nominal lead -10% is then utilized as the maximum acceptable reading during the actual gamma scan.

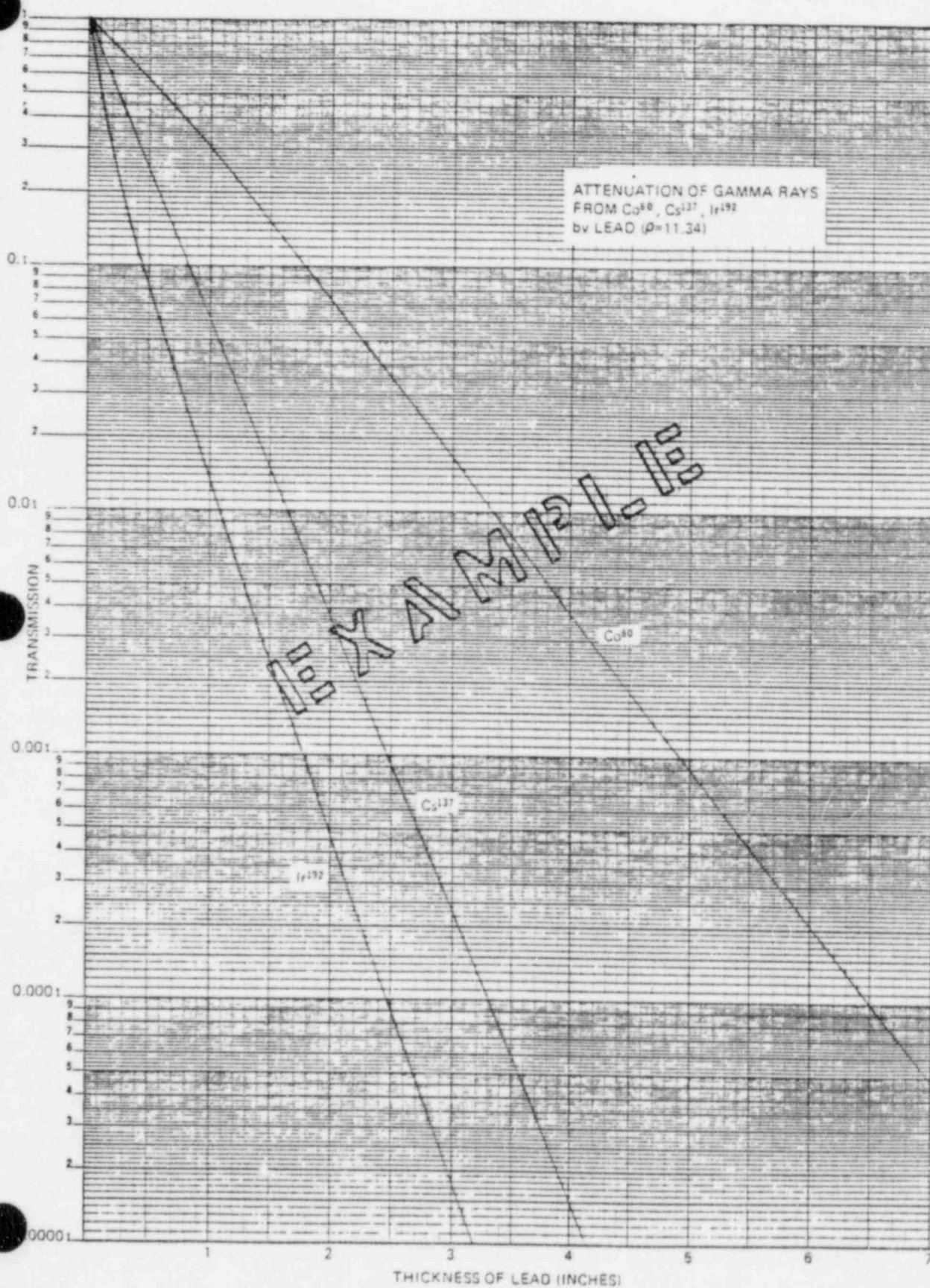
GS - 001 - ATTACHMENT A

TABLE 2  
SELECTED RADIOISOTOPE DATA

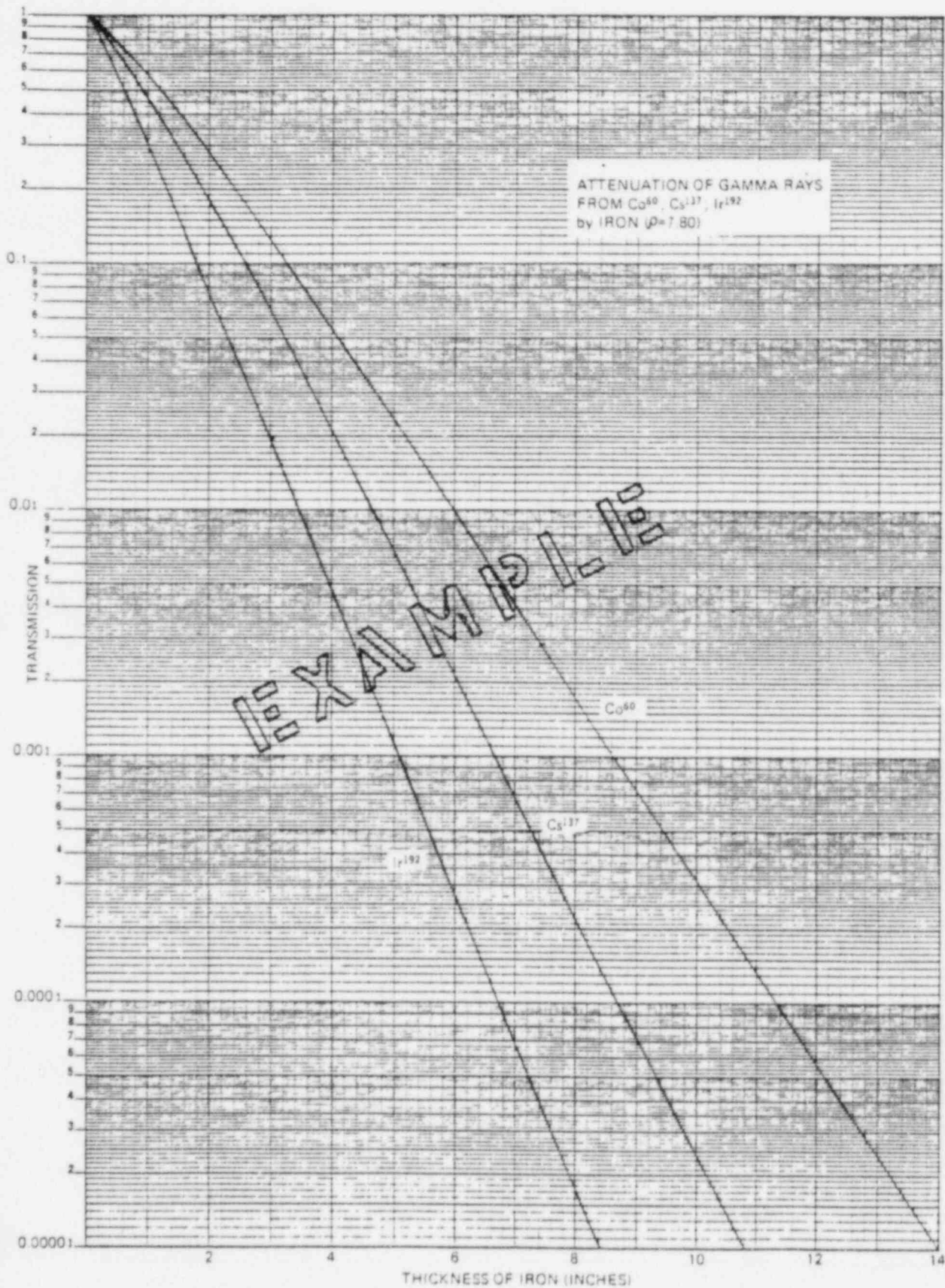
Radioisotope	Half-life	Principal Photon Energies (keV)	Specific Gamma Ray Constant R/hr per curie	
			at 1 foot	at 1 meter
Cesium <sup>137</sup>	30y	662	3.4	0.32
Cobalt <sup>60</sup>	5.3y	1173, 1332	14.0	1.30
Iridium <sup>192</sup>	74d	311, 468, 603	5.9	0.55*
Thulium <sup>170</sup>	134d	84.6 keV - x-rays	0.015	0.0014
Ytterbium <sup>169</sup>	32d	63, 110, 131 177, 198, 308 Tm x-rays	1.35	0.125

\*American National Standards Institute Standard N432 has proposed a value of 0.48R-m<sup>2</sup>/hr-Ci for the specific gamma ray constant for Iridium 192.

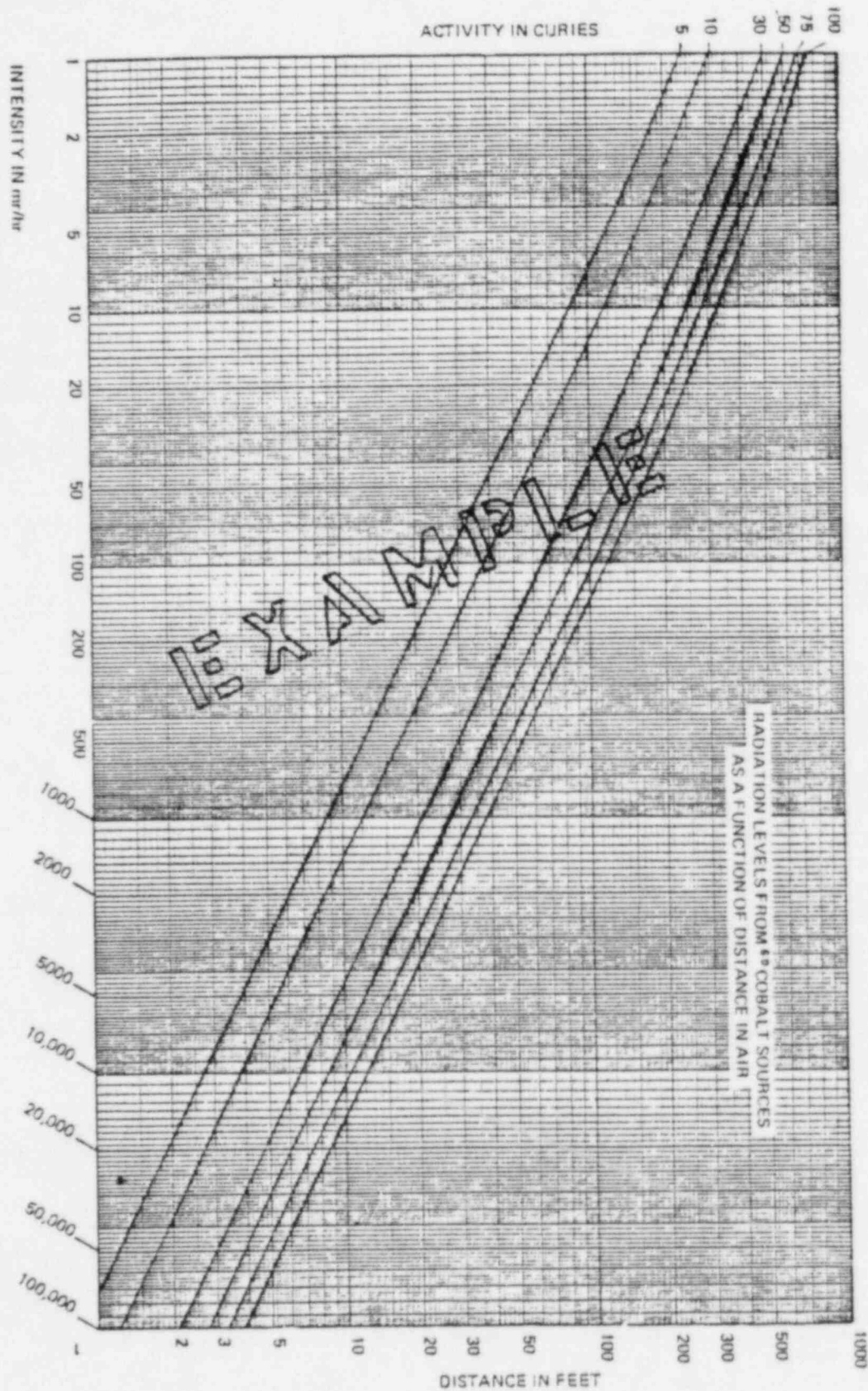
GS - 001 - ATTACHMENT B

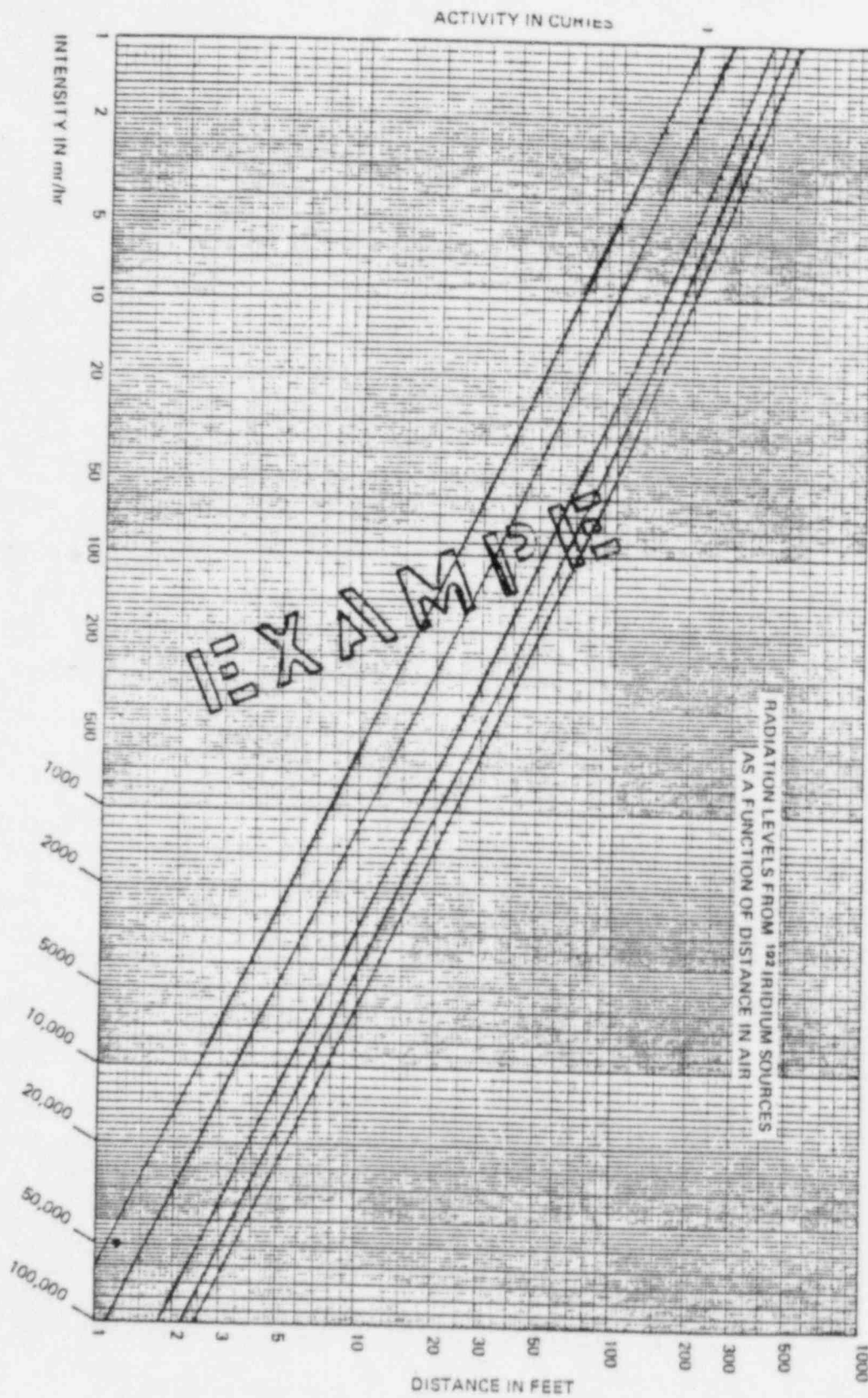












APPENDIX 8.3.2

HELIUM LEAK TESTING

The NuPac 10/140MB shielded shipping cask is designed to the Type B criteria of 10 CFR 71. The criteria also places certain requirements for acceptance of the cask during fabrication and after in-service seal maintenance. A major requirement pertains to acceptable leakage past the cask seals. The acceptable leak rate for the seal integrity test is  $10^{-7}$  atm-cm<sup>3</sup>/s or less based on dry air at 25°C. The requirement is delineated in detail in ANSI N14.5, Leakage Tests on Packages for Shipment of Radioactive Materials.

The accepted method for ascertaining leak rates in the  $10^{-7}$  range is via a Helium Mass Spectrometer Sniffer or Spray test. This test is described in ANSI N14.5 and is utilized for all seal integrity acceptance tests on the 10/140MB cask prior to first use and after any seal maintenance or replacement after the cask is in service.

The test utilizes helium gas as the detector medium and a calibrated helium sniffer or probe as the detector. The helium sniffer or probe is calibrated against a standard leak simulator that produces a known leak rate. This device is traceable to the National Bureau of Standards.

The interior cavity or seal area between the redundant seals is evacuated to an indicated pressure below one atmosphere (vacuum). A special test port tool is utilized for the evacuation. After the evacuation, the special test port tool is adjusted to allow the helium sniffer or probe to monitor the evacuated area between the seals. The exterior of the cask seal area is then loosely enveloped to trap helium gas injected into the enclosed area. If any leaks are present greater than  $10^{-7}$  atm-cm<sup>3</sup>/sec, they will allow the helium to migrate from the positive exterior pressure to the negative interior pressure. This leak will allow the helium to then be monitored by the helium leak probe. The equipment which monitors the probe's input will indicate when the leak rate exceeds the preset acceptance level. Additionally, the seal in the 10/140MB test ports are also tested to  $1 \times 10^{-7}$  atm-cm<sup>3</sup>/sec or less. This is done after the main cask seals are tested. The void between the main seals is flooded with helium at one atmosphere pressure and the test port is then

## 9.0 QUALITY ASSURANCE

The NuPac 10/140MB Cask has been designed and will be fabricated by Nuclear Packaging, Inc., (NuPac) Federal Way, Washington. The Quality Assurance Program used for the design, fabrication, assembly, testing, use and maintenance of the NuPac 10-140 cask satisfies the eighteen (18) criteria of 10 CFR 71, Subpart H in its entirety. NuPac's Quality Assurance Program meeting these criteria has been submitted to the United States Nuclear Regulatory Commission and has been awarded Approval Number 0192, Revision 1.

In addition, the QA program and the implementation of it during the design and fabrication phases will adhere to NuReg CR-3854, Category III requirements.

A synopsis of the Pacific Nuclear Systems, Inc./Nuclear Packaging, Inc. Quality Assurance Program follows:

### 9.1 Introduction

Pacific Nuclear Systems, Inc. (PNSI) has developed a quality program to (1) assure traceability, and (2) control the quality of all materials and processes utilized in the production of radioactive shielding, casks, containers, and other equipment pertaining to shipping packages for irradiated fuel, high level waste, and plutonium.

A Quality Manual delineates requirements and procedures necessary to exercise control over design, documentation, procurement, material, fabrication, inspection, operational testing, equipment operation and use, maintenance, repair, modification, inventory, shipment and quality data retention.

The PNSI Quality Program is implemented by Quality Procedures which are designed and administered to meet the 18 criteria of 10 CFR 71, Subpart H. The Quality Program is implemented throughout the company and its subsidiaries. The Subsidiaries include: Pacific Nuclear Systems, Inc., Nuclear Packaging, Inc., NuPac Leasing, Inc., and Pacific Nuclear Systems and Services, Inc.

## 9.2 Description of the PNSI, 10 CFR 71, Subpart H Quality Program

### 9.2.1 Organization

Full responsibility for the Quality Assurance (QA) Program adherence to 10 CFR 71, Subpart H criteria rests with PNSI. Quality Program activities include calibration of measuring equipment, non-destructive examination (NDE), and materials testing. PNSI surveys and qualifies all organizations performing these services to assure adherence to the 18 criteria prior to their use. All other quality activities are performed by PNSI quality personnel. However, the responsibility of the control of quality in the other organizations continues to rest with PNSI.

PNSI's President has full authority over all functions of the company, and delegates authority and responsibility for selected functions to other personnel within the company.

The administrative function includes financial, legal, and marketing activities.

Procurement department personnel perform purchasing activities and maintain supplier performance records. The Engineering Department is responsible for research and development of shipping container technology, design of casks for licensing and fabrication, and design documentation.

The PNSI Quality Department has sufficient authority and organizational freedom to identify quality programs, implement corrective action, and verify corrective action effectiveness.

Additionally, the Quality Department is independent from other organizations within PNSI and reports directly to the President of PNSI. The Quality Department is headed by the Corporate Quality Director who is responsible for the development, implementation, and administration of the entire PNSI Quality



Program. He must have sufficient expertise in the entire field of Quality to enable him to direct the entire quality function in close adherence to the 18 criteria of 10 CFR 71 and the PNSI Quality Manual. Responsibility for development of quality acceptance requirements, inspections, and NDE activities rests with the Corporate Quality Director. It is his responsibility to delegate and evaluate the performance of all quality related tasks for PNSI through the authority of the president.

It is delineated in writing through the Corporate Quality Director that designated QA personnel have the authority to prevent the continued processing, fabrication, installation, or delivery of unsatisfactory work.

This authority also extends to the quality monitoring of special processes utilizing PNSI equipment, personnel and procedures such as waste processing, in-service inspections, etc.

Production responsibilities include scheduling or in-service inspection and administration of all fabrication activities, both within PNSI and at qualified suppliers. The shipping and receiving function is also the responsibility of the Production Department.

On-site activities such as waste processing, in-service inspections, etc. are administered as a joint effort of the operations and engineering personnel. Quality supports these activities with written procedures that provide methods, process controls and check points. Inspection personnel perform monitoring activities and verifications of regulatory, contractual, and technical requirements during these operations.

The Corporate Quality Director and all other quality personnel and/or organizations within, or utilized by PNSI, are fully qualified for their quality responsibilities. Qualification records are maintained in the PNSI Quality Record File.

### 9.2.2 Quality Assurance Program

PNSI has established and implemented a QA Program for the control of quality in the design, fabrication, operation, and maintenance of shipping containers for nuclear products. Training and/or evaluation of personnel qualifications are required for all QA functions in accordance with written procedures and are approved by the Quality Manager. The QA Program assures that all quality requirements, engineering specifications, and specific provisions of any package design approval are met. Those characteristics critical to safety are emphasized.

The President of PNSI regularly evaluates the PNSI QA program for adherence to the 18 criteria in scope, implementation, and effectiveness. Further, the President requires that the Quality System, including the QA Manual Policies and Procedures, be implemented and enforced on all applicable programs at PNSI.

A Material Review Board, consisting of Engineering, Procurement Production, and Quality Personnel has been established to resolve all discrepancies or disagreements pertaining to the acceptability of material, hardware, or safety related operations. Their dispositions are final and binding.

### 9.2.3 Design Control

PNSI Quality Procedures (QP's) have been developed, approved, and implemented to control design review in such a manner to assure that the following occur:

- 9.2.3.1 Design activity is planned, controlled, and documented.
- 9.2.3.2 Regulatory and design requirements are correctly translated into specification, drawings, and procedures.
- 9.2.3.3 Design documents contain quality requirements.
- 9.2.3.4 Deviations from quality requirements are controlled.



- 9.2.3.5 Design verification is performed by Quality Assurance personnel independent of the design activity. These verifications may include tolerance studies, alternate calculations or tests. Qualification tests are conducted in accordance with approved test programs and procedures
- 9.2.3.6 Interface control is established and adequate.
- 9.2.3.7 Design and specification changes are reviewed and approved by the same organization(s) as the original issue.
- 9.2.3.8 Design errors and deficiencies are documented and corrective action is taken to prevent recurrence.
- 9.2.3.9 Design organization(s) and their responsibilities and authorities are delineated and controlled via written procedure.

#### 9.2.4 Procurement Document Control

The PNSI QA Program assures that all purchased material, components, equipment, and services adhere to design specifications.

Supplier evaluation and selection, objective evidence of supplier quality, assignment of quality requirements to procurement documents and related design documents, and source, in-process, and receiving inspections are all administered and controlled in accordance with approved PNSI QA procedures.

All procurement activity is performed in accordance with written procedures delineating requirements for preparation, review, approval, and control of procurement documentation. Particular emphasis is placed on assuring that revisions to procurement documentation are reviewed and approved by the same cognizant groups as the original.

Quality Assurance clause sheets are included with all request for quotes and purchase orders. Quality Assurance personnel assign clauses from the sheets to the procurement document referencing 10 CFR 71, Subpart H requirements appropriate to the contract. In addition, material information including grade, type, size, and special physical or chemical data requirements is included on the procurement documents. Other documentation and information such as drawings, procedures, inspection and test requirements, hold points, welding and other process qualification requirements are delineated on the procurement documents by the Quality Assurance personnel as appropriate to the contract.

Quality Assurance personnel assure that requirements for acceptance of hardware and documentation appropriate to the contract are included in procurement documentation.

PNSI Quality Assurance personnel maintain the right of access to all supplier facilities and documentation for source inspection and/or audit activities. A statement to this effect is included on procurement documentation when it is appropriate to the contract.

#### 9.2.5 Instruction, Procedures and Drawings

Quality planning is developed by qualified Quality Engineers (QE's) for all activities requiring quality participation in accordance with approved PNSI QA procedures and is approved by the Corporate Quality Director.

All design documents (i.e., drawings, specifications, special processes, etc.) affecting quality are reviewed by the Quality Department and referenced in quality planning as necessary to assure adherence to package design approvals and the applicable criteria of 10 CFR 71, Subpart H.

All instructions, procedures, and drawings are developed, reviewed, approved, utilized, and controlled in accordance with the requirements of written quality assurance procedures.

9.2.6 Document Control

Policy and procedure for review, approval, release and change control of all controlled, quality related documents are delineated in approved PNSI QA Procedures. Provisions are provided in the QA Procedures for identification of individuals/organizations responsible for review, approval, and issuance of documents. Document control responsibilities, facilities, and distribution requirements are also addressed.

Controlled documents include, but are not limited to:

- (a) Design specifications
- (b) Design manufacturing drawings
- (c) Special process specifications and procedures
- (d) Procurement documents
- (e) QA Procedures and manuals
- (f) Quality Planning for receiving, in-process, source and in-service inspections
- (g) Source surveillance and evaluation reports
- (h) Test procedures
- (i) Audit reports
- (j) Operational test procedures and data.

When revised documents appear in other documents as references, supplements, or exhibits, appropriate revisions are made to those documents prior to the release of the basic approved change.

Documentation listings are maintained delineating the title, number and current revision for all drawings, procedures, specifications, and purchase orders.

The Quality Personnel assure that all required support documentation is available at the work area prior to the initiation of the work effort.

9.2.7 Control of Purchased Materials, Parts and Components

Procurement documents are reviewed for acceptability of suggested suppliers based on the PNSI approved supplier lists.

In addition, and as required, supplier surveys are conducted by qualified PNSI personnel to further assure supplier acceptability. These evaluations are based on one or all of the following criteria:

- (a) The supplier's capability to comply with the requirements of 10 CFR 71, Subpart H, that are applicable to the contract.
- (b) A review of previous records and performance of the supplier.
- (c) A survey of the supplier's facilities and QA program to determine his capability to supply a product which meets the design, manufacturing, and quality requirements.

Results of all supplier evaluations are recorded on Supplier Evaluation forms and are retained in the Quality Data File.

Quality requirements and standard clauses are added to procurement documents to require suppliers to identify material, provide test reports, control special processes, certify equipment and personnel, etc. As a minimum, requirements are imposed on suppliers to identify materials, specific codes, specifications and/or design not adhered to during fabrication. Justifications for 'accept-as is' or 'repair' dispositions are also required to be submitted to the Material Review Board for review and acceptance.

Quality planning is prepared and approved by the Quality Department for performance of all source, test, shipping and/or receiving inspections in accordance with approved design requirements, applicable 10 CFR 71 criteria, procurement document requirements, and contract specifications.

Receiving inspection is performed to determine that the following, as appropriate to the contract, are assured:

- (a) The material, component, or equipment is properly identified and corresponds with the identification on receiving documentation.
- (b) Material, components, equipment, and acceptance records are inspected and are acceptable in accordance with inspection instructions, prior to installation or use.
- (c) Inspection records and/or certificates of conformance attesting to the acceptance of material and components are available prior to installation or use.
- (d) Items accepted and released are identified as to their inspection status prior to forwarding them to a controlled storage area or releasing them for further work.

All described activities are delineated in approved PNSI QA procedures.

#### 9.2.8 Identification and Control of Materials, Parts, and Components

The identification and control of materials, parts, components, and completed and in-process assemblies is administered by the Quality Department in accordance with approved PNSI QA Procedures. These procedures address quality status tags, maintenance of material identification and traceability, part identification, and related documentation. Some of the details of these procedures follow:

- (a) Material identification procedures included in inspection planning and fabrication drawings require that identification of material, components, and/or hardware be maintained on the item or in traceable records to prevent use of incorrect or defective items.

- (b) When appropriate, due to contractual or safety related concerns requiring specific identification and Material Review Board action, Quality Assurance personnel assure that identification of materials, components, specifications, procurement documentations, manufacturing, and inspection records, discrepancy reports, and material test data is provided and is complete.
- (c) Quality Assurance personnel assure, via drawings and inspection planning requirements, that identification locations do not affect the fit-up, interfacing capability, performance or overall quality of the finished product. Identification, in accordance with drawings and inspection planning requirements, is verified prior to releasing the item for further processing or delivery.

#### 9.2.9 Control of Special Processes

PNSI approved QA Procedures delineate the policies and procedures established to control such special processes as: welding, heat treating, lead pouring, non-destructive examination, waste processing, etc. in accordance with applicable codes, standards, specifications, 10 CFR 71 criteria, and other requirements. Special processes developed by PNSI suppliers and by PNSI are documented.

All procedures for special processes and the personnel required to perform them are qualified under the cognizance of the Quality Department in accordance with applicable codes, standards, specifications, and contract requirements.

All qualification records and support data are retained in the Quality Data file, and are maintained in a current status by Quality Assurance personnel.

These documents are controlled as delineated in Section 9.2.6 of this Quality System description.

#### 9.2.10 Inspection

All receiving, source, in-process, and in-service inspection activities are performed in accordance with approved PNSI QA procedures. All inspection personnel and/or organization qualifications are reviewed and accepted by the Quality Manager prior to inspection activity. The inspection activity is performed in strict accordance with approved quality planning prepared by qualified QA personnel (See also Section 9.2.5 discussion).

Quality Inspection personnel are independent from all other organizations within PNSI and report directly to the Corporate Quality Director or the Subsidiary Quality Manager.

Inspection personnel qualifications are based on their capability to perform the required inspection functions in accordance with applicable codes, standards, professional society programs such as the ASQC quality technician certification, and PNSI training programs. Qualification reviews are performed periodically to maintain personnel proficiency and assure current qualification.

Mandatory hold points, inspection equipment requirements, accept reject criteria, personnel requirements, characteristics to inspect, variable/attributes recording instructions, reference documentation, and other requirements are included in the inspection planning.

The Quality Assurance department assures that any replacements, modifications, or repairs performed after final acceptance of material, components or hardware are inspected in accordance with the original inspection planning or new planning prepared as appropriate.

#### 9.2.11 Test Control

A test control program, as it applies to quality, is addressed in approved PNSI QA Procedures and assures, via required planning, that all required testing, such as proof and acceptance tests, are identified and performed in accordance with test procedures, design requirements, and limitations.

Prerequisites, accept/reject criteria, data recording criteria, instrumentation calibration, environmental conditions, documentation and evaluation requirements, etc. are delineated in the test procedures. Changes to the test procedures are required to be reviewed/approved by the same organization(s) as the original issue.

Whenever equipment, components, and/or assemblies require modification, repairs, or replacement which could result in requirements for re-test or additional testing, Quality Assurance personnel assure, as appropriate, that original or new test inspection planning is prepared and adhered to.

In any case, test results are documented, evaluated, and accepted by qualified personnel as required by the test inspection plan prepared for the test under the cognizance of Quality Assurance personnel.

#### 9.2.12 Control of Measuring and Testing Equipment

Administration of the calibration of measuring equipment and instrumentation is performed by the Quality Department in accordance with approved PNSI QA Procedures. The calibration system assures that all standard measuring instruments (SMI) used in the acceptance of material, equipment, and assemblies are calibrated and properly adjusted at specified intervals to maintain accuracy within pre-determined limits. Calibration is performed using equipment traceable to national standards. All calibrated equipment is identified and is traceable to the calibration test data.

Whenever SMI are found to be out of calibration during or immediately after use, all items inspected during that period are rejected by inspection and are submitted to review action for possible re-inspection or other appropriate corrective action.



#### 9.2.13 Handling, Storage, and Shipping

PNSI approved QA Procedures require that handling, storage, and shipping requirements adherence verification criteria be included in quality planning. These requirements are designed to prevent damage or deterioration of material and equipment. Information pertaining to shelf life, environment, packaging, temperature, cleaning, handling, preservation, etc., is included as required to meet design, NRC package approval and/or U.S. Department of Transportation shipping requirements.

Shipping documentation preparation, departure and arrival time, and destination data recording are also addressed in the planning, when applicable. Shipping requirements in quality planning must be met prior to release for shipment.

#### 9.2.14 Inspection, Test and Operating Status

The use of inspection status tags, quality inspection stamps, and other means to indicate inspection and test status at, or for, PNSI are delineated in approved PNSI QA Procedures.

The clarity of the status indication, prevention of inspection, and/or test step by-passing, and prohibition of removal or modification of status indications, except with Quality Department approval/Material Review disposition, is assured via these procedures. The Quality Assurance Department assures via Quality Procedure, interoffice memoranda, training sessions, and audit that all PNSI personnel are aware of and understand the meaning and uses of status tags on all hardware, material, and test set-ups (see also Section 9.2.15 discussion).

9.2.15 Non-conforming Material, Parts, or Components

PNSI approved QA Procedures require that material, components, and equipment that do not conform to requirements are controlled to prevent their inadvertent use. Identification, segregation, discrepancy reporting, disposition of non-conformances by authorized individuals, and re-inspection activities are performed and controlled in strict accordance with these procedures.

Quality Discrepancy Reports (QDR) are utilized by the PNSI quality department to identify discrepant items, describe the discrepancy, and provide disposition and re-inspection requirements. The signatures of authorized cognizant personnel are placed on the QDR to signify approval of the disposition. These personnel must be approved by the Corporate Quality Director and President and must be from the same groups approving the original design. In conjunction with repair or re-work dispositions, quality assurance personnel provide supplemental inspection planning to verify proper implementation of the QDR disposition. This assures that the item is re-tested and/or re-inspected to a degree at least equal to the original acceptance activity.

9.2.16 Corrective Action

Failures, malfunctions, and deficiencies in material, components, equipment, and services are identified and reported to the Corporate Quality Director and the President. The cause of the condition and corrective action necessary to prevent recurrence is identified, implemented and then followed up to verify corrective action effectiveness. All reporting requirements of applicable contractual and regulatory specifications and regulations are adhered to as part of any corrective action activity. Detail requirements for this activity are delineated in approved PNSI QA Procedures.

9.2.17 Quality Assurance Records

A quality records system is in effect at PNSI and is administered in accordance with approved PNSI QA procedures. The purpose of the quality record system is to assure that documented evidence pertaining to quality related activities is maintained and available for use by PNSI, its customers, and/or regulatory agencies as applicable. Quality Records include, but are not limited to, inspection and test records, audit reports, quality personnel qualifications, design reviews, quality related procurement data, supplier evaluation reports, etc. All records are identified by work order number, part number, contract number, or drawing number as appropriate to the record type. A complete list of all quality records is maintained and provides cross reference between the different identity methods described above and pinpoints the record location.

Design related records such as calculations, drawings, research and development test reports, etc., are retained in the Quality Assurance records system for the life of the shipping package. All other quality related records are retained for the life of the shipping package in accordance with 10 CFR 71.91(c) unless otherwise specified in related contractual or regulatory requirements.

Inspection records retained in the Quality Assurance records system provide the following data when applicable:

- (a) Inspection type, i.e., in-process, in-service, testing, receiving, and shipping.
- (b) Evidence of completion and verification of manufacturing, inspection, or test operation.
- (c) The date and results of the inspection or test.
- (d) Information related to noted discrepancies.

(e) Inspector or data recorder identification.

(f) Evidence of acceptance.

#### 9.2.18 Audits

Quality program audits are performed on a periodic, scheduled basis by personnel without direct responsibilities in the areas being audited. Audit personnel are certified quality assurance lead auditors who have met all requirements of ANSI N 45.2.23. Written planning sheets and check lists are utilized. Audit results and corrective action activity are reported to management, in writing, and are retained in the quality assurance record file. Responsible management personnel are required to respond to audit findings with the necessary action to correct the noted deficiencies. Current PNSI practice is to audit all quality functions on an annual basis. Areas found deficient during audits are reaudited on a first priority basis to verify corrective action implementation and effectiveness. Details of the PNSI Audit System are delineated in approved PNSI QA Procedures.

#### 9.3 References

- 9.3.1 Title 10, Code of Federal Regulations, Part 71 (10 CFR 71), Subpart H, Criteria 1-18 dated August 24, 1983, Quality Assurance Criteria for Shipping Packages for Radioactive Material.
- 9.3.2 PNSI Corporate Quality Manual, dated August 13, 1984